INTERROGATING A ROLE FOR TUMOUR NECROSIS FACTOR ALPHA IN CD4^{+} T CELL METABOLISM IN HEALTH AND INFLAMMATORY DISEASE

By

EMMA LOUISE BISHOP

A thesis submitted to the University of Birmingham

For the Degree of DOCTOR OF PHILOSOPHY

Institute of Immunology and Immunotherapy

College of Medical and Dental Sciences

University of Birmingham

January 2023

ABSTRACT

Upon activation, $CD4^+$ T cells undergo substantial metabolic reprogramming to support clonal expansion and effector function, largely promoted by T cell receptor (TCR) and CD28 signalling. Whether T cell-derived inflammatory cytokines, such as tumour necrosis factor alpha (TNF-α), amplify this process is not well understood but could be pertinent in chronic inflammatory diseases, such as rheumatoid arthritis (RA), where abundant TNF-α expression and dysregulated $CD4^+$ T cell metabolic phenotypes are present. TNF-α has been previously identified to act as a co-stimulatory signal upon T cell activation, increasing proliferation and cytokine production. Yet, whether TNF-α controls $CD4^+$ T cell metabolism has not been interrogated. Here, it was shown that blocking T cell-derived TNF-α supressed the activation of naïve $CD4^+$ T cells and impaired their upregulation of glycolysis, amino acid uptake, and mitochondrial oxidation of glutamine. Conversely, addition of TNF-α was able to increase glycolysis in these cells. Interrogation of downstream signalling pathways identified that TNF-α drives these changes not through NFκB, which is most commonly reported to be downstream of TNF-α, but through the PI3K/Akt/mTOR pathway. T cell-derived TNF-α signalling was also shown to be involved in driving inflammatory T helper (Th)1 and Th17 cell differentiation in a partially Akt-dependent manner, whilst little effect on regulatory T cell (Treg) differentiation was observed. Finally, to interrogate a role for this TNF-α/PI3K/Akt metabolic axis in chronic inflammatory disease, peripheral blood $CD4^+$ T cells from RA patients and healthy controls were analysed by flow cytometry. RA $CD4^+$ T cells exhibited higher levels of membrane-bound TNF-α, mitochondrial mass, and Akt phosphorylation. These data implicate TNF-α signalling via PI3K/Akt in the dysregulated metabolic phenotype of RA $CD4^+$ T cells.

ACKNOWLEDGEMENTS

I would first like to thank Dr Sarah Dimeloe for her unfaltering support and guidance over the past 4 years. I have thoroughly enjoyed this project and could not have imagined a better supervisor; I truly appreciate the time and effort she has put into helping me develop both personally and as a scientist.

I am extremely grateful to have had such a fun and supportive lab group during this project. Thank you for all your help in the lab, your company, and the weekly supply of cake! In particular, I would like to thank Dr Nancy Gudgeon who has been there for me from the start and has endured all my queries with unrelenting patience and generosity.

Thank you to my co-supervisor Professor Martin Hewison for always being available with advice throughout my studies. I would like to thank the other Fellows labs who have created such a uniquely considerate and collaborative environment which has been an invaluable source of support during my PhD. I also express my gratitude to Professor David Withers who drove my initial interest in immunology during my undergraduate degree and gave me the confidence to apply for this PhD. Thank you to the Wellcome Trust MIDAS programme for allowing me this opportunity and for all the support along the way.

I would like to thank my friends and family, especially my parents who have always supported me in every aspect of my life. Finally, thank you to my partner Greg who has shown me unwavering support, advice, and encouragement throughout the good times, the tougher times, and a global pandemic.

TABLE OF CONTENTS

LIST OF FIGURES

LIST OF TABLES

LIST OF ABBREVIATIONS

1,3-BPG	1,3-bisphosphoglycerate
ABCB1	ABC transporter protein 1
ACPA	anti-citrullinated protein antibodies
αKG	alpha-ketoglutarate
Akti	Akt inhibitor
AMP	adenosine monophosphate
AMPK	AMP-activated protein kinase
ANOVA	analysis of variance
AP-1	activator protein 1
APC	antigen presenting cell
ASCT2	alanine/serine/cysteine-preferring transporter 2
ATM	ataxia telangiectasia mutated
ATP	adenosine triphosphate
BCH	2-Amino-2-norbornanecarboxylic acid
BCR	B cell receptor
BSA	bovine serum albumin
CCL	CC-chemokine ligand
CCR	CC-chemokine receptor
CD	cluster of differentiation
CD62L	CD62 ligand
CoA	coenzyme A
CRAC	calcium release activated Ca^{2+} channels
CXCL	CXC-chemokine ligand
CXCR	CXC-chemokine receptor
DC	dendritic cell
DEG	differentially expressed gene
DHAP	dihydroxyacetone phosphate
dH_2O	deionised water
DMARD	disease-modifying antirheumatic drug
DMSO	dimethyl sulfoxide
DNA	deoxyribonucleic acid
ECAR	extracellular acidification rate
EDTA	ethylenediaminetetraacetic acid
ELISA	enzyme-linked immunosorbent assay
ER	endoplasmic reticulum
ETC	electron transport chain
F16BP	fructose-1,6-bisphosphate
F6P	fructose-6-phosphate
FACS	fluorescent-activated cell sorting
FAD	flavin adenine dinucleotide
FADD	FAS-associated death domain
FAO	fatty acid oxidation

FAS	fatty acid synthesis
FBS	foetal bovine serum
FCCP	carbonyl cyanide 4-(trifluoromethoxy) phenylhydrazone
FLS	fibroblast-like synoviocyte
FoxP3	forkhead box P3
FSC-A/H	forward scatter area/height
G6P	glucose-6-phosphate
GAP	glyceraldehyde-3-phosphate
GAPDH	glyceraldehyde-3-phosphate dehydrogenase
GATA3	GATA binding protein 3
GC-MS	gas chromatography-mass spectrometry
GLUT1	glucose transporter 1
h	hour(s)
H3K27Ac	acetylation of histone H3 at lysine 27
HBSS	Hank's Balanced Salt Solution
HC	healthy control(s)
HEV	high endothelial venule
HIF1α	hypoxia inducible factor 1 alpha
HLA	human leukocyte antigen
IFN	interferon
IFN-γ	Interferon gamma
Ig	immunoglobulin
IL	interleukin
IL-7R	IL-7 receptor
iTreg	induced Treg
IU/U	international units/units
LAG-3	lymphocyte activation gene 3
LAT	linker for activation of T cells
LAT1	large amino acid transporter 1
LCK	lymphocyte-specific protein tyrosine kinase
LDH	lactate dehydrogenase
MACS	magnetic-activated cell sorting
MAPK	mitogen activated protein kinase
Max.	maximal
MFI	mean fluorescence intensity
MHCI/II	major histocompatibility complex I/II
MID	mass isotopomer distribution
min	minute
MMP	matrix metalloproteinase
mRNA	messenger RNA
MS	multiple sclerosis
MSO	MitoSpy Orange
mTNF-α	membrane-bound TNF-α

mTOR	mammalian target of rapamycin
mTORC1/2	mTOR complex 1/2
MVG	MitoView Green
n/µ/mM	nano/micro/millimolar
NA	non-activated
NAD	nicotinamide adenine dinucleotide
NFAT	nuclear factor of activated T cells
NFκB	nuclear factor kappa B
nm	nanometre(s)
NMT1	N-myristoyltransferase 1
°C	degrees Celsius
OCR	oxygen consumption rate
OXPHOS	oxidative phosphorylation
p-	phosphorylated
p/n/µ/mg	pico/nano/micro/milligram(s)
P/S	penicillin/streptomycin
PBMC	peripheral blood mononuclear cell
PBS	phosphate buffered saline
PCA	principal component analysis
PEP	phosphoenolpyruvic acid
Perm Buffer	permeabilisation buffer
PFK1	6-phosphofructo-1-kinase
PFKFB3	6-phosphofructo-2-kinase/fructose-2,6-biphosphatase 3
phospho-flow	flow cytometry of phosphorylated proteins
PI3K	phosphoinositide 3-kinase
PMA	phorbol 12-myristate-13-acetate
PPARγ	proliferator-activated receptor gamma
PPP	pentose phosphate pathway
PRR	pattern recognition receptor
RA	rheumatoid arthritis
RANK	receptor activator of NF-κB
RANKL	RANK ligand
redox	reduction/oxidation
RF	rheumatoid factor
rh	recombinant human
RM	repeated measures
RNA	ribonucleic acid
RNA-seq	RNA-sequencing
RORγt	retinoic acid receptor-related orphan receptor gamma
ROS	reactive oxygen species
rpm	rotations per minute
RPMI	Roswell Park Memorial Institute 1640 Medium
RT	room temperature

s	second(s)
S1P	sphingosine-1-phosphate
S6K	S6 kinase
SD	standard deviation
SDH	succinate dehydrogenase
SF	synovial fluid
SLC	system L amino acid transporter
SLE	systemic lupus erythematosus
SLO	secondary lymphoid organ
SRC	spare respiratory capacity
SSC-A	side scatter area
sTNF-α	soluble TNF-α
TACE	TNF-α converting enzyme
TCA	tricarboxylic acid
T_{CM}	central memory T cell
T_{CONV}	conventional T cell
TCR	T cell receptor
T_{eff}	effector T cell
T_{EM}	effector memory T cell
TF	transcription factor
TGF-β	tumour growth factor beta
Th	T helper
Th1	T helper 1
Th2	T helper 2
Th17	T helper 17
Th17.1	T helper 17.1
TNF-α	tumour necrosis factor alpha
TNFR1/2	TNF receptor 1/2
Treg	regulatory T cell
T_{RM}	tissue-resident memory T cell
tTregs	thymic-derived Treg
µ/ml	micro/millilitre(s)
v	version
x g	times gravity
XF	extracellular flux
Zap70	zeta-chain-associated protein kinase 70

CHAPTER 1: INTRODUCTION

1.1 THE IMMUNE SYSTEM

The immune system is a complex combination of cells, inflammatory mediators, and biological processes. In order to fulfil its role in protecting the body from invading pathogens, the immune system has evolved two main branches, the innate and adaptive. These distinct systems work in collaboration to discriminate between antigens of the body, termed “self”, and those which have come from a foreign source, termed “non-self” (Iwasaki and Medzhitov, 2015). Once recognised as non-self-antigens, invaders are effectively cleared. However, in some cases this process can go awry, and the immune system attempts to eliminate a self-antigen, a process called autoimmunity (Szekanecz *et al.*, 2021; Weyand and Goronzy, 2021). The innate immune system is the initial line of defence encountered by a pathogen, made up of barrier sites and a range of effector cells. As part of this response, cells release a spectrum of chemical mediators and cytokines which promote inflammation (Paludan *et al.*, 2021). Inflammation is characterised by redness, swelling, heat, and loss of tissue function. In the acute phase, this is crucial for the removal of the harmful stimuli and is able to promote healing once resolved. However, long-term induction of inflammation can result in excessive tissue damage (Medzhitov, 2008; Szekanecz *et al.*, 2021). Occasionally, the innate immune system is able to effectively eliminate the pathogen alone, but in cases where this is not achieved the adaptive immune system becomes engaged. Adaptive immunity encompasses a range of immune cells which defend in an antigen-specific manner (Medzhitov, 2008;

Domínguez-Andrés *et al.*, 2019). Additionally, cells of the adaptive immune system can form memory, enabling a more rapid response upon re-infection with a specific pathogen (Iwasaki and Medzhitov, 2015; Domínguez-Andrés *et al.*, 2019). In autoimmune diseases, the persistence of the adaptive immune response drives chronic inflammation to cause pain and tissue destruction (Szekanecz *et al.*, 2021; Weyand and Goronzy, 2021).

1.1.1 Innate immune system

The innate immune system reacts non-specifically to harmful stimuli and is unable to form immunological memory. First, barrier sites, such as the gut, skin, and lungs, provide a physical and chemical boundary to invading pathogens. Production of antimicrobial peptides and mucus by the epithelial cell layer work in combination with the microbiota to ward off potential breaches of the barrier (Guillot *et al.*, 2013; Takiishi *et al.*, 2017; Harris-Tryon and Grice, 2022). Cells of the innate immune system recognise non-self, highly conserved, pathogen associated molecular patterns (PAMPs) of bacteria, viruses, and fungi through pattern recognition receptors (PRRs) (Medzhitov, 2008; Iwasaki and Medzhitov, 2015; Paludan *et al.*, 2021). In addition, danger associated molecular patterns (DAMPs), such as adenosine triphosphate (ATP) and mitochondrial DNA, from cells in distress can be detected by PRRs on the surface of innate immune cells (Paludan *et al.*, 2021). Specific to each cell type, triggering of a PRR induces a cascade of signalling pathways to promote phagocytosis, and the release of antimicrobial and inflammatory molecules (Iwasaki and Medzhitov, 2015; Paludan *et al.*, 2021).

1.1.1.1 The inflammatory response

A fundamental part of an effective inflammatory response involves recruitment of immune cells from the blood to the site of injury. To elicit this, stromal cells, such as endothelial cells, and immune cells release a range of cytokines and chemokines. These act in an autocrine or paracrine manner, with cytokines able to modify the function and behaviours of the responding cell whilst chemokines induce migration of cells down a gradient to the site of release. During an inflammatory response a large cytokine and chemical milieu exists in the local microenvironment, each with a unique role in modulating immunity. Pro-inflammatory cytokines tumour necrosis factor alpha (TNF-α) and interleukin (IL)-6 drive endothelial cells to upregulate adhesion molecules whilst chemical mediators such as histamine, released by mast cells, promote vascular permeability (Griffin *et al.*, 2012; Newton and Dixit, 2012; Ashina *et al.*, 2015). Chemokines such as CC-chemokine ligand (CCL)2 and CCL7 support the migration of innate effector cells, including dendritic cells (DCs) and monocytes (Shi and Pamer, 2011; Crowley, Buckley and Clark, 2018; Németh, Nagy and Pap, 2022). Once at the site of inflammation, these recruited immune cells then produce their own cytokines and chemokines, perpetuating the cycle. Cytokines are important for the activation, maturation, and differentiation of multiple innate immune cells (Bernink *et al.*, 2015; Lusty *et al.*, 2017). For example, macrophages are often described to have two main phenotypes, referred to as M1-like and M2-like. M1-like macrophages are pro-inflammatory and induced by cytokines such as TNF-α and interferon gamma (IFN-γ), whereas pro-resolution M2-like macrophages are induced by anti-inflammatory cytokines such as IL-10 and tumour growth factor beta (TGF-β) (Martinez and Gordon, 2014; Yao *et al.*, 2019). This dichotomy is representative of the

self-perpetuating inflammatory environment until a switch is made to pro-resolution, healing mechanisms. Dysregulation of this balance leading to chronic inflammation.

1.1.1.2 Tumour necrosis factor alpha

One of the principal inflammatory cytokines, TNF-α is produced by cells of both the innate and adaptive immune system, including macrophages and cluster of differentiation (CD)4^+ T helper (Th) cells. To exert its effects, TNF-α can act in an autocrine or paracrine manner on cells through binding to one of its two receptors, TNF receptor 1 (TNFR1) or TNFR2. TNF-α exists first as a transmembrane protein, membrane-bound TNF-α (mTNF-α), which is then cleaved into its soluble form (sTNF-α) by TNF-α converting enzyme (TACE; also called A disintegrin and metalloprotease 17 (ADAM17)) (Yang *et al.*, 2018; Wajant and Siegmund, 2019). Both forms have biological activity when bound to either TNFR1 or TNFR2, although reports have suggested a higher affinity for mTNF-α bound to TNFR2 and sTNF-α to TNFR1 (Grell *et al.*, 1995; Fischer *et al.*, 2017; Su *et al.*, 2022). TNFR1 is ubiquitously expressed on most cells and has its main role in controlling apoptosis. Upon ligation, TNFR1 interacts with TNFR type 1-associated death domain (TRADD) to recruit TNF receptor-associated factor 2 (TRAF2) and receptor interacting protein-1 (RIP-1), this complex is then able to activate the nuclear factor kappa B (NFκB) signalling pathway which drives inflammation. However, association of this complex is transient. Upon dissociation, TNFR1 binds Fas-associated death domain protein (FADD) and activates the downstream caspase cascade, inducing apoptosis (Yang *et al.*, 2018; Wajant and Siegmund, 2019). Alternative activation of this pathway can also drive necroptosis, a form of inflammatory cell death (He *et al.*, 2009). In comparison, TNFR2 is selectively expressed on certain immune cells including T cells and macrophages, and stromal

cells such as fibroblasts. The signalling pathways engaged by TNFR2 are less clear, although there is evidence to suggest interactions with the NFκB and phosphoinositide 3-kinase (PI3K)/protein kinase B (PKB; here referred to as Akt) pathways, drivers of inflammation and metabolism respectively (Yang *et al.*, 2018; Wajant and Siegmund, 2019).

1.1.2 Adaptive immune system

The adaptive immune system is comprised of T and B cells, both able to exert antigen-specific responses and form immunological memory. In order to recognise all self and non-self-antigens, T and B cells exhibit an extremely broad repertoire of T cell receptors (TCRs) and B cell receptors (BCRs) respectively. This is achieved through recombination of the variable (V), diversity (D), and joining (J) regions of the TCR or BCR by recombination activating genes (RAG) proteins early in development, with somatic hypermutation in B cells further diversifying the repertoire (Briney and Crowe, 2013). To protect against autoimmunity, any cells with a receptor recognising a self-antigen are removed by negative selection in the thymus (Nemazee, 2017; Takaba and Takayanagi, 2017). B cells promote T cell responses through their role as antigen presenting cells (APCs) and produce antigen-specific antibodies to neutralise pathogens. T cells develop in the thymus as either CD4 or CD8 positive. $CD8^+$ T cells express a range of cytotoxic granules which they release upon activation along with cytokines, such as IFN-γ. This cytotoxic activity is critical to their role in defence against intracellular infections and cancer (Collier *et al.*, 2021; Raskov *et al.*, 2021). Additionally, $CD8^+$ T cells can exert these cytotoxic effects against self-antigens, contributing to autoimmunity (Collier *et al.*, 2021). This thesis will focus on $CD4^+$ T cells and their role in chronic inflammatory disease.

1.2 CD4$^+$ T CELLS

CD4$^+$ T cells are crucial for defence against pathogens and cancer, largely exerted through their release of certain cytokines. However, when dysregulated, CD4$^+$ T cells are also instrumental in the pathogenesis of autoimmune diseases, including rheumatoid arthritis (RA) and systemic lupus erythematosus (SLE) (Park *et al.*, 2005; Katsuyama, Tsokos and Moulton, 2018; Chemin, Gerstner and Malmström, 2019; Kato *et al.*, 2019).

1.2.1 Naïve CD4$^+$ T cells

Following development in the thymus, naïve CD4$^+$ T cells circulate the blood and secondary lymphoid organs (SLOs), such as lymph nodes and tonsils, surveying for cognate antigen. To enable this movement, naïve CD4$^+$ T cells express CC-chemokine receptor (CCR)7 which binds CCL19 and CCL21, chemokines present throughout lymphatic vessels and high endothelial venules (HEVs), leading to SLOs. In addition, naïve cells express CD62 ligand (CD62L) which binds specialised glycoproteins on HEVs to further mediate trafficking (Yang *et al.*, 2011; Belikan *et al.*, 2018; van den Broek *et al.*, 2018). Within specialised T cell zones of SLOs, naïve CD4$^+$ T cells encounter APCs, most commonly DCs (Jenkins *et al.*, 2001; Saxena *et al.*, 2019). APCs are able to phagocytose pathogens and cell debris which they then process and present on major histocompatibility complex (MHC) molecules on their surface (Neefjes *et al.*, 2011; Tai *et al.,*2018). MHC class I molecules (MHCI) are present on nucleated cells and platelets and are able to bind CD8$^+$ T cells through interaction with CD8. In comparison, MHC class II (MHCII) molecules are mainly restricted to expression on APCs and are able to bind CD4$^+$ T cells via CD4 (Wieczorek *et al.*, 2017). Binding of an antigen-specific naïve CD4$^+$ T cell TCR to its

corresponding antigen presented by MHCII on an APC triggers a cascade of signalling pathways to induce T cell activation (Tai *et al.*, 2018; Shyer, Flavell and Bailis, 2020).

1.2.2 $CD4^+$ T cell activation

1.2.2.1 Signal 1 – T cell receptor signalling

Naïve $CD4^+$ T cell activation requires signalling through three major mechanisms, termed signal 1-3 (Figure 1.1). To initiate signal 1, the TCR which exists in a complex with CD3, binds its relevant MHCII-bound antigen on an APC with CD4 also docking on the MHCII molecule. Ligation of the TCR complex drives lymphocyte-specific protein tyrosine kinase (LCK) to phosphorylate zeta-chain-associated protein kinase 70 (Zap70) which then phosphorylates linker for activation of T cells (LAT), a substrate for the binding of multiple signalling molecules. From LAT, the main downstream pathways of TCR ligation are engaged, including mitogen activated protein kinase (MAPK), NFκB, phospholipase C gamma (PLCγ), and nuclear factor of activated T cells (NFAT) (Gaud *et al.*, 2018; Bhattacharyya and Feng, 2020; Hwang *et al.*, 2020). TCR triggering also induces the mobilisation of intracellular calcium (Ca^{2+}) stores, which subsequently promotes Ca^{2+} entry into the cell through calcium release activated Ca^{2+} channels (CRAC) (Fracchia *et al.*, 2013). Mitochondria then localise to the cellular point of contact with the APC, termed the immunological synapse, and are able to increase Ca^{2+} uptake by preventing inactivation of the CRAC (Schwindling *et al.*, 2010; Fracchia *et al.*, 2013). Ca^{2+} is a crucial signalling molecule required throughout the cell for processes including metabolism, activation, and proliferation, often mediated through interactions with calcineurin (Fracchia *et al.*, 2013; Trebak and Kinet, 2019). Ca^{2+} and calcineurin are essential for NFAT signalling, promoting its localisation to the nucleus. Additionally, several enzymes in the tricarboxylic

acid (TCA) cycle are Ca^{2+}-dependent (Fracchia *et al.*, 2013). Ca^{2+} is also required for activation of NFκB and activator protein 1 (AP-1), a transcription factor (TF) of the MAPK pathway (Feske *et al.*, 2001; Fracchia *et al.*, 2013). These pathways, NFκB, NFAT, and MAPK mediated through TFs JUN, FOS, and AP-1, interact to promote cell growth, survival, and gene expression for effector function in activated $CD4^+$ T cells (Gaud *et al.*, 2018; Trebak and Kinet, 2019; Bhattacharyya and Feng, 2020). The strength of a TCR signal is graded and can have differential effects on cell fate, exhaustion, metabolism, and expression of effector molecules based on the stability and persistence of the interaction (Allison *et al.*, 2016; Snook *et al.*, 2018; Elliot *et al.*, 2021; Trefzer *et al.*, 2021).

1.2.2.2 Signal 2 – Co-stimulatory molecules

Alongside the TCR, co-stimulatory molecules, referred to as signal 2, are able to lower the threshold for TCR activation. This results in increased proliferation and cytokine production in response to lower affinity antigens that would otherwise drive anergy, a state of inactivity in the cell (Janardhan *et al.*, 2011; Chen and Flies, 2013; Ross and Cantrell, 2018). The most important of these molecules for T cell activation is CD28 which binds CD80/86 on an APC. However, the exact contribution of CD28 signalling to this process remains to be fully elucidated, with varied reports on its relative importance in naïve and memory cells and in the induction of different downstream pathways (Kane *et al.*, 2001; Garçon *et al.*, 2008; Xia *et al.*, 2018; Glinos *et al.*, 2020). In essence, CD28 contains a direct binding site for PI3K. Activation of the PI3K/Akt pathway then exerts effects on metabolism, survival, and effector function (Boomer and Green, 2010; Chen and Flies, 2013). Although the PI3K/Akt pathway has also been reported as downstream of TCR signalling, the CD28 pathway is essential in driving its

activity to a sufficient level for $CD4^+$ T cell activation (Harada *et al.*, 2001; Kane *et al.*, 2001; Frauwirth *et al.*, 2002; Buckler *et al.*, 2006). CD28 also directly binds growth factor receptor-bound protein 2 (Grb2) able to activate downstream NFκB, NFAT, and MAPK signalling pathways (Janardhan *et al.*, 2011; Chen and Flies, 2013). Moreover, other co-stimulatory molecules, such as inducible T cell co-stimulator (ICOS), CD40 ligand (CD40L), and OX40, are able to signal these pathways to mediate effects on cell survival, proliferation, and effector function (Croft, 2003; Chen and Flies, 2013; Ward-Kavanagh et al., 2016). Co-stimulation also induces the production of IL-2, an important regulator of $CD4^+$ T cell activation, metabolism, and proliferation (Janardhan et al., 2011; Chen and Flies, 2013; Ross and Cantrell, 2018).

TNF-α signalling through TNFR2 has been suggested to act as a co-stimulatory molecule on $CD4^+$ T cells. Early studies showed a requirement for TNF:TNFR2 interactions to promote T cell proliferation and survival upon activation (Yokota *et al.*, 1988; Tartaglia *et al.*, 1991, 1993). Alongside its main role in apoptosis (Micheau and Tschopp, 2003; Kumar *et al.*, 2022), some studies have also reported a role for TNFR1 as a co-stimulatory molecule on T cells (Church *et al.*, 2005; Evangelidou *et al.*, 2010), potentially due to impacts on Ca^{2+} signalling (Church *et al.*, 2005). However, this observation is contradicted in other reports which show no effect of TNFR1 on T cell activation (Tartaglia *et al.*, 1991, 1993; Aspalter *et al.*, 2003). TNFR2-mediated co-stimulation is described to act similarly to CD28, exerting effects on cytokine production and proliferation. Yet, CD28 was unable to fully recapitulate the effects of TNFR2 signalling in $CD4^+$ and $CD8^+$ T cells (Kim and Teh, 2001, 2004; Aspalter *et al.*, 2003, 2007). TNF-α has been shown to directly downregulate CD28 expression on $CD4^+$ T cells (Bryl *et al.*, 2001). In addition, chronic TNF-α stimulation over several (8-17) days *in vitro* was shown to have inhibitory

effects on T cell activation, through impairment of TCR/CD28 signalling (Bryl *et al.*, 2001; Isomäki *et al.*, 2001; Aspalter *et al.*, 2005) and release of IL-2 and IL-10 (Aspalter *et al.*, 2003). In these studies, NFκB signalling is the most commonly reported downstream mechanism of TNFR2-mediated co-stimulation (Aspalter *et al.*, 2003, 2007; Kim and Teh, 2004; Banerjee *et al.*, 2005). Although, there is some evidence for the involvement of PI3K/Akt and MAPK pathways (Aspalter *et al.*, 2003; Kim and Teh, 2004). Collectively, these studies highlight a unique and non-redundant role for both CD28 and TNF-α as co-stimulatory molecules in T cell activation.

1.2.2.3 Signal 3 – Cytokine-mediated $CD4^+$ T cell differentiation

Following activation, naïve $CD4^+$ T cells require cytokine signals to polarise them towards different Th cell subsets, each subset with a unique role in immunity (Sckisel *et al.*, 2015). These determining cytokines are largely provided by APCs, consequently APCs can bias $CD4^+$ T cell differentiation by altering cytokine production (Jong *et al.*, 2002; Ferreira *et al.*, 2014; Hafkamp *et al.*, 2022). This control of Th cell fate is a key mechanism in promoting the appropriate response to invading pathogens (Zhu and Paul, 2010). However, a dysregulated balance of inflammatory cell subsets such as T helper 1 (Th1) and T helper 17 (Th17) cells, to regulatory T cells (Tregs) is often a hallmark of chronic inflammatory disease (Niu *et al.*, 2012; Lee, 2018). Th cell subsets and their polarising cytokines are discussed below.

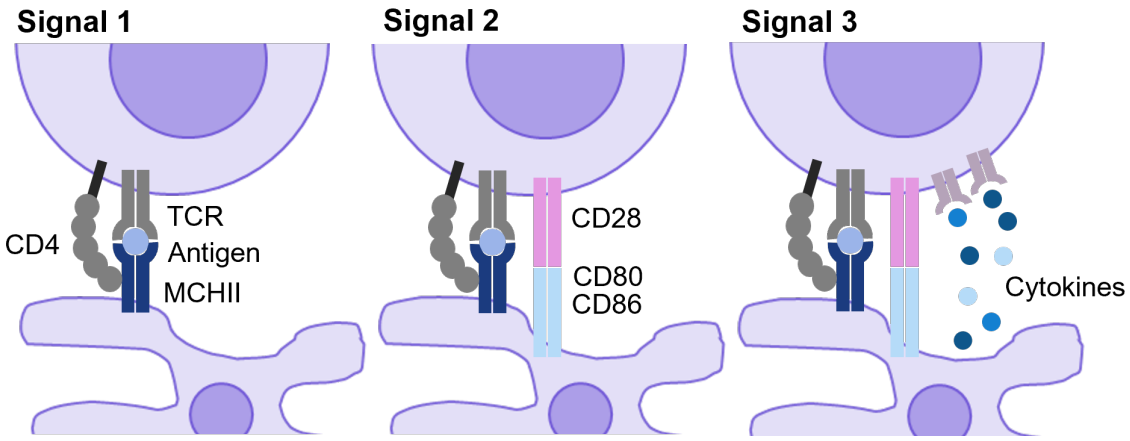

Figure 1.1 The 3 signals of CD4⁺ T cell activation

Three signals are required for activation of CD4⁺ T cells. The antigen-specific T cell receptor (TCR) with associated CD4 molecule bound to an MHC class II (MHCII) molecule presenting the relevant antigen constitutes signal 1. Signal 2 refers to co-stimulatory molecules, commonly on CD4⁺ T cells this is CD28 which binds to a CD80/CD86 complex on the antigen presenting cell (APC). Once activated by these two signals, CD4⁺ T cells are differentiated into a CD4⁺ T cell subset through cytokine signalling, termed signal 3.

1.2.3 CD4⁺ T helper cell subsets

In peripheral immune responses, four main Th cell subsets are currently described, Th1, T helper 2 (Th2), Th17, and Treg cells (Figure 1.2) (Zhu and Paul, 2010). Although, other subsets such as T helper 9 (Th9) and T helper 22 (Th22) cells have been suggested based on unique cytokine profiles (Veldhoen et al., 2008; Eyerich et al., 2009). Increasing evidence for Th cell plasticity has also introduced subsets such as T helper 17.1 (Th17.1) cells, also known as ex-Th17 cells (Hirota et al., 2011; Basdeo et al., 2017). In addition, T follicular helper (Tfh) cells are a specialised subset present in SLOs to aid B cell responses (Crotty, 2019).

1.2.3.1 Th1 and Th2 cells

Identified by Mosmann *et al.* in 1986, Th1 and Th2 cells were the first Th cell subsets to be recognised (Mosmann *et al.*, 1986). Th1 cells are characterised by the expression of the TF T-bet and production of IFN-γ (Szabo *et al.*, 2000). A predominant Th1 cell response is essential for the eradication of intracellular pathogens, mediated largely through IFN-γ driving the activation of M1 macrophages and increasing phagocytosis, antigen-presentation, and the release of inflammatory mediators (Ivashkiv, 2018; Wang *et al.*, 2018; Jorgovanovic *et al.*, 2020). Additionally, IFN-γ is a potent anti-tumour cytokine, selectively promoting apoptosis in tumour cells and enhancing anti-tumour activity of $CD8^+$ cytotoxic T cells (Ni *et al.*, 2013; Bhat *et al.*, 2017; Jorgovanovic *et al.*, 2020). In an autoimmune context, dysregulation of these IFN-γ-mediated effects instead cause excessive tissue damage and exacerbate the pro-inflammatory environment (Leung *et al.*, 2010; Luo *et al.*, 2022). Th1 cells are polarised by IL-12 with IFN-γ able to synergise this effect (Hsieh *et al.*, 1993; Smeltz *et al.*, 2002). Th2 cells are important mediators of anti-helminth immunity, B cell responses, and allergy through their expression of signature cytokines IL-4, IL-5, and IL-13. Pathogenically, a dysregulated Th2 cell response is implicated in asthma, atopic dermatitis, and ulcerative colitis (Heller *et al.*, 2005; Tokura *et al.*, 2018; León and Ballesteros-Tato, 2021). A Th2 transcriptional programme is induced by IL-4 and regulated by TF GATA binding protein 3 (GATA3) (Noben-Trauth *et al.*, 2002; Zhu *et al.*, 2004).

1.2.3.2 Th17 cells

Several years after the discovery of Th1 and Th2 cells, the Th17 cell subset was identified (Harrington *et al.*, 2005; Park *et al.*, 2005). In health, Th17 cells accumulate largely at mucosal

sites and are characterised by the expression of retinoic acid receptor-related orphan receptor gamma (RORγt) and the production of IL-17, both IL-17A and IL-17F (Harrington *et al.*, 2005; Park *et al.*, 2005; Ruan *et al.*, 2011). Th17 cells also express IL-22, which promotes mucosal immunity through induction of antimicrobial peptide and cytokine release by epithelial cells (Ouyang and Valdez, 2008; Lo *et al.*, 2019). Additionally, IL-17 mediates the protective effects of Th17 cells by indirectly promoting activation and migration of neutrophils (Pelletier *et al.*, 2010; Griffin *et al.*, 2012). Consistent with their protective role, Th17 cell differentiation has also been shown to be promoted by segmented filamentous bacteria in the gut (Ivanov *et al.*, 2009; Goto *et al.*, 2014). Multiple autoimmune diseases, including RA and SLE, attribute Th17 cells to pathogenesis due to the production of inflammatory cytokines such as IL-17 and TNF-α (Manara and Sinigaglia, 2015; Hirota *et al.*, 2018; Taams, 2020; Koga *et al.*, 2021). Indeed, Th17 cells migrate towards and accumulate in the inflamed synovium of RA patients via a CCL20 gradient and expression of CCR6 (Hirota *et al.*, 2007; Church *et al.*, 2010). TGF-β, IL-6, IL-23, and IL-1β are all necessary for optimal Th17 cell differentiation (Manel *et al.*, 2008; Volpe *et al.*, 2008). Perhaps due to their complex differentiation requirements, Th17 cells are prone to conversion to a Th1-like phenotype by IL-12, a process termed plasticity (Lee *et al.*, 2009). These cells are named ex-Th17 or Th17.1 cells (from here referred to as Th17.1 cells) and are characterised by the expression of both IFN-γ and IL-17, and both T-bet and RORγt (Lee *et al.*, 2009; Hirota *et al.*, 2011; Basdeo *et al.*, 2017). Th17.1 cells are considered potent drivers of inflammation based on their high expression of cytokine, and have been implicated in the pathogenesis of chronic inflammatory diseases including RA, and multiple sclerosis (MS) (Basdeo *et al.*, 2017; van Hamburg and Tas, 2018; van Langelaar *et al.*, 2018).

1.2.3.3 Regulatory T cells

Tregs develop in the thymus during negative selection from T cells with TCRs that bind with intermediate strength (too high resulting in apoptosis, and appropriately low resulting in positive selection) to the corresponding antigen-presenting MHC molecule, referred to as natural or thymic-derived (n/t)Tregs (here tTregs). Additionally, Tregs can be generated in the periphery during naïve $CD4^+$ T cell activation by TGF-β and IL-2, named induced (i)Tregs (Schmitt and Williams, 2013). Tregs are potently anti-inflammatory, employing direct and indirect mechanisms to restrict $CD4^+$ Th cell function. Suppressive mechanisms include production of anti-inflammatory cytokines such as IL-10 and TGF-β, sequestration of IL-2, and production of inhibitory cyclic adenosine monophosphate (cAMP) (Tamir *et al.*, 1996; Schmidt *et al.*, 2012; Schmitt and Williams, 2013). In addition, co-inhibitory receptors such as cytotoxic T-lymphocyte associated protein 4 (CTLA-4) and lymphocyte activation gene-3 (LAG-3) bind T cells to suppress function or bind APCs via co-stimulatory molecules, which reduces their availability to T cells (Schmitt and Williams, 2013). Treg differentiation in the periphery is driven by TGF-β and IL-2, promoting the master regulator forkhead box P3 (FoxP3) and expression of IL-10. However, this method of FoxP3 induction in iTregs is less stable than in tTregs (Baron *et al.*, 2007; Floess *et al.*, 2007; Q. Chen *et al.*, 2011). TNF-α, through binding of TNFR2, has been shown to have both suppressive and permissive effects on Treg function. Several studies on human and murine Tregs have shown TNF-α signalling through TNFR2 to inhibit Treg function and decrease FoxP3 expression (Zanin-Zhorov *et al.*, 2010; Zhang *et al.*, 2013). Notably, two studies investigating this effect in the context of RA suggested anti-TNFα treatment could rescue this suppression (Valencia *et al.*, 2006; Nie *et al.*, 2013). However, several studies have also suggested that TNFR2 signalling improves Treg function and FoxP3

expression (Nagar *et al.*, 2010; Chen *et al.*, 2013; Zaragoza *et al.*, 2016; S. Yang *et al.*, 2019; de Kivit *et al.*, 2020). One study highlighting this to be driven by TNFR2 preventing methylation of the *Foxp3* promoter (Tseng *et al.*, 2019). Additionally, blockade of TNFR2 *in vivo* was shown to abrogate the suppressive effects of Tregs in a model of graft-versus-host disease (Leclerc *et al.*, 2016). A subsequent study was then able to improve responses by driving TNFR2 signalling, suggesting this as a viable therapeutic target (Moatti *et al.*, 2022). Taken together, these studies show that further work is required to fully understand the role of TNF-α on Treg function. However, the effects are likely highly context dependent on factors such as other cytokines in the local microenvironment, relative stability of the Treg phenotype, and concentration of TNF-α. Reports on Treg function and development in autoimmunity are inconsistent (Miyara *et al.*, 2011). Taking RA as an example, there are studies showing reduced numbers (Lawson *et al.*, 2006; Kawashiri *et al.*, 2011; Niu *et al.*, 2012), increased numbers (van Amelsfort *et al.*, 2004; Pandya *et al.*, 2017; Takeshita *et al.*, 2019; Zhang *et al.*, 2022), and several showing their numbers to be unchanged in peripheral blood compared to controls (Liu *et al.*, 2005; Möttönen *et al.*, 2005). Furthermore, the balance between more resistant to suppression $CD4^+$ Th cells and more suppressive Tregs in inflammatory conditions is hard to determine (van Amelsfort *et al.*, 2004; van Roon *et al.*, 2010). Nevertheless, an overall defect in the Treg response is clear.

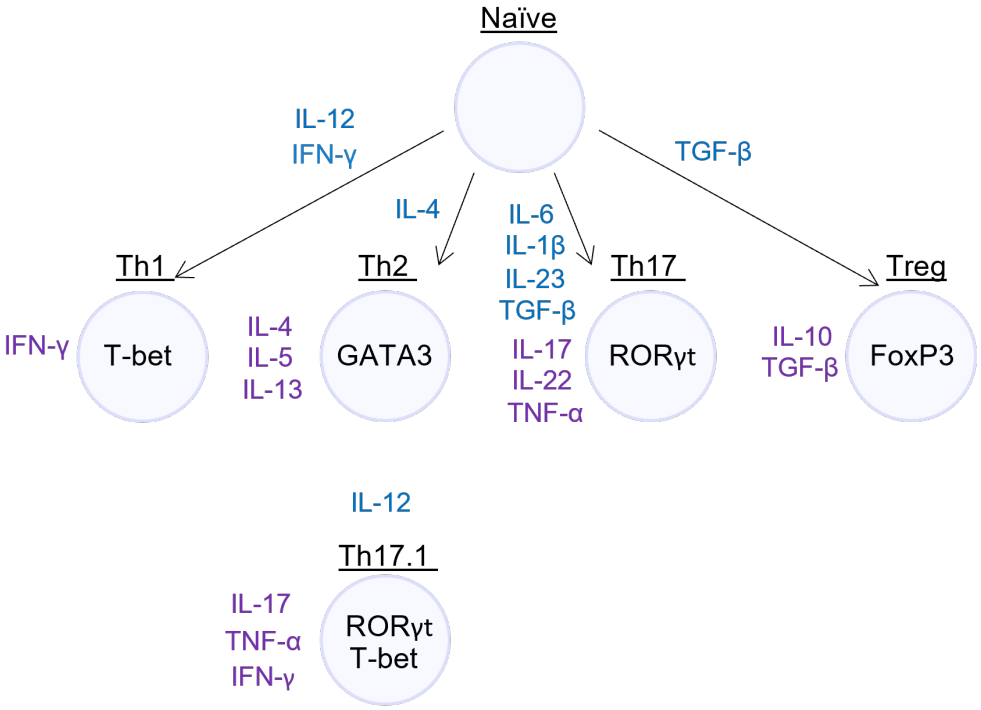

Figure 1.2 CD4⁺ T helper cell subsets

Naïve CD4⁺ T cells are differentiated into CD4⁺ T cell subsets through unique combinations of cytokine signalling. Th1 cells, characterised by expression of T-bet and production of IFN-γ, are polarised by IL-12 with IFN-γ also able to promote differentiation. Th2 cells express GATA3 and cytokines IL-4, IL-5, and IL-13 and are induced by IL-4. Th17 cells can be identified by expression of RORγt and cytokines IL-17 and IL-22. Th17 cells also produce high levels of TNF-α and can be polarised by a combination of IL-6, IL-1β, IL-23, and TGF-β. Th17 cells have been reported to undergo plasticity in presence of IL-12, adopting a more Th1-like phenotype, resulting a subset of cells termed Th17.1 cells which express both RORγt and T-bet and produce cytokines including IL-17, TNF-α, and IFN-γ. Finally, naïve CD4⁺ T cells can be differentiated into induced (i)Tregs by TGF-β, expressing master regulator FoxP3 and regulatory cytokines IL-10 and TGF-β.

1.2.4 Memory CD4$^+$ T cells

During an immune response, large numbers of CD4$^+$ T cells are generated by clonal expansion. Following resolution of the infection, the majority of these cells undergo apoptosis (MacLeod *et al.*, 2009). Those remaining become memory CD4$^+$ T cells, characterised by expression of CD45RO. Memory cells can be further subdivided into central (T_{CM}), effector (T_{EM}), tissue-resident (T_{RM}), and effector re-expressing CD45RA (T_{EMRA}) memory cells, each with unique roles (MacLeod *et al.*, 2009; Nguyen *et al.*, 2019). T_{CM} cells express CCR7 and CD62L, which enable their migration through the blood and SLOs for continued surveillance of re-exposure to known pathogens. T_{EM} cells, lacking CCR7 and CD62L expression, patrol the peripheral circulation and tissue, primed for rapid expression of effector cytokines such as IFN-γ and TNF-α upon activation (MacLeod *et al.*, 2009). T_{RM} cells are recently identified as another memory cell subset also unable to migrate through SLOs, instead remaining in tissues to aid with tissue homeostasis and defence of barrier sites (Beura *et al.*, 2019; Nguyen *et al.*, 2019). Lastly, a subset of terminally differentiated memory cells can be defined by their re-expression of CD45RA, termed T_{EMRA} (Sallusto *et al.*, 1999; Tian *et al.*, 2017). Although more commonly found as a CD8$^+$ T cell subset, CD4$^+$ T_{EMRA} cells have been detected in human peripheral blood and are associated with increased numbers in individuals infected with cytomegalovirus and dengue virus (Harari *et al.*, 2004; Libri *et al.*, 2011; Weiskopf *et al.*, 2015; Burel *et al.*, 2017; Tian *et al.*, 2017).

The generation of memory cells is an area of keen interest due to their protective roles following vaccination and in cancer immunotherapy (Liu *et al.*, 2020; Loyal *et al.*, 2021; Rostamian *et al.*, 2021). IL-2 drives production of memory T cells by promoting expression of IL-7 receptor (IL-7R), IL-7 signalling then promotes the maintenance of cellular metabolism for

long-term memory cell survival (Kondrack *et al.*, 2003; Dooms *et al.*, 2007; Jacobs *et al.*, 2010; Li *et al.*, 2022). Additionally, the strength of a TCR signal and engagement of specific co-stimulatory molecules, such as OX40, have been implicated in determining the generation and differentiation of memory T cell subsets (Soroosh *et al.*, 2007; Keck *et al.*, 2014; Snook *et al.*, 2018). Having already undergone naïve $CD4^+$ T cell activation, memory cells are able to activate rapidly upon TCR/CD28 engagement. Indeed, memory cells are known to require CD28 signalling for optimal activation (Ndejembi *et al.*, 2006); one study suggesting their sensitivity to CD28 to be even higher than naïve cells (Glinos *et al.*, 2020). Memory cells demonstrate a wide range of epigenetic modifications compared to naïve cells (Bevington *et al.*, 2016, 2021; Barski *et al.*, 2017). Acetylation and methylation of specific histones promote open chromatin regions, which allow TF binding and result in the rapid transcription of effector molecules such as IFN-γ and IL-17. Conversely, methylation can also suppress chromatin accessibility preventing transcription of genes (Fields *et al.*, 2002; Morinobu *et al.*, 2004; Renaude *et al.*, 2020). Additionally, memory $CD4^+$ T cells demonstrate metabolic alterations, such as increased mitochondrial content, which promotes increased metabolic capacity upon activation (Dimeloe *et al.*, 2016).

1.3 CELLULAR METABOLISM

Cellular metabolism comprises the biochemical pathways in a cell responsible for the breakdown of metabolic substrates to generate ATP and biosynthetic intermediates which support effector function, growth, and survival. The metabolic requirements of a cell are tightly linked to its function; anabolic, biosynthesis pathways driving cell growth and catabolic pathways maintaining homeostasis in quiescent cells (Pearce, 2010). In T cells, the metabolic

pathways most well described to support function are glycolysis and oxidative phosphorylation (OXPHOS). Multiple other pathways such as fatty acid oxidation (FAO), the pentose phosphate pathway (PPP), and glutaminolysis feed into and derive from these (Figure 1.3) (Tang and Mauro, 2017; Martínez-Reyes and Chandel, 2020).

1.3.1 Glycolysis

Glucose is a primary substrate utilised by cells to generate ATP and biosynthetic intermediate molecules. Glucose is taken up into cells by a glucose transporter (GLUT), predominantly GLUT1 on $CD4^+$ T cells (Macintyre *et al.*, 2014), and converted to glucose-6-phosphate (G6P) by hexokinase (HK) in the initial step of glycolysis. G6P is then converted to fructose-6-phosphate (F6P) which in turn is phosphorylated by 6-phosphofructo-1-kinase (PFK1) to become fructose-1,6-bisphosphate (F16BP) (Tang and Mauro, 2017; Zuo *et al.*, 2021). Alternatively at this point, the enzyme 6-phosphofructo-2-kinase/fructose-2,6-biphosphatase 3 (PFKFB3) converts F6P into fructose-2,6-bisphosphate (F26BP), an allosteric activator of PFK1 essential for driving sufficient glycolysis in $CD4^+$ T cells (Z. Yang *et al.*, 2013). F16BP is then converted to glyceraldehyde-3-phosphate (GAP) or dihydroxyacetone phosphate (DHAP) by aldolase, with DHAP able to covert to GAP and vice versa via enzyme triose phosphate isomerase. Following this, GAP is converted to 1,3-bisphosphoglycerate (1,3-BPG) by glyceraldehyde-3-phosphate dehydrogenase (GAPDH). Further steps convert 1,3-BPG to 3-phosphoglycerate, generating an ATP molecule, and then 2-phosphoglycerate which is converted to phosphoenolpyruvate (PEP) by enzyme enolase. The final step, pyruvate kinase converting PEP to pyruvate, generates an additional ATP molecule. Instead of progressing though glycolysis, G6P can also be shunted into the PPP for the synthesis of

precursor molecules to nucleotides and amino acids (Z. Yang *et al.*, 2013; Salmond, 2018). Pyruvate can then be utilised to generate acetyl-coenzyme A (CoA) for incorporation into the TCA cycle (Martínez-Reyes and Chandel, 2020). Usually in the absence of oxygen, pyruvate is converted to lactate by lactate dehydrogenase (LDH), in a process termed anaerobic glycolysis (Tang and Mauro, 2017). However, more relevant to T cells, it was first observed in cancer cells that pyruvate was also converted to lactate when oxygen was present, referred to as aerobic glycolysis, or the Warburg effect. Aerobic glycolysis is beneficial to rapidly proliferating cells due to its quick production of ATP and propensity for biosynthesis via the PPP (Vander Heiden *et al.*, 2009; Salmond, 2018).

1.3.2 Oxidative phosphorylation

OXPHOS refers to the production of ATP by ATP-synthase which requires a proton gradient (i.e. mitochondrial membrane potential) that is generated through activity of the electron transport chain (ETC). This process is tightly coupled to the TCA cycle by the reduction-oxidation (redox) of nicotinamide adenine dinucleotide (NAD)H and flavin adenine dinucleotide (FAD)H_2, which in turn provide electrons to the ETC (Martínez-Reyes and Chandel, 2020). OXPHOS is required in cells for the production of large amounts of ATP, generation of reactive oxygen species (ROS) by the ETC, and production of TCA cycle intermediates used for epigenetic modifications and cellular biosynthesis (Sena *et al.*, 2013; Peng *et al.*, 2016; Bailis *et al.*, 2019). In the TCA cycle, acetyl-CoA, as derived from pyruvate following glycolysis but also from fatty acids, amino acids, ketone bodies, or lactate, combines with oxaloacetate to form citrate (Tang and Mauro, 2017; Raud *et al.*, 2018; Pucino *et al.*, 2019; Martínez-Reyes and Chandel, 2020; Kaymak *et al.*, 2022; Luda *et al.*, 2022). Citrate is

converted to isocitrate, then to alpha-ketoglutarate (αKG) generating NADH. This is followed by the conversion of αKG to succinate, again reducing NAD^+ to generate NADH which is then oxidised by complex I of the ETC. Here, glutamine can be converted to glutamate and then αKG via the glutaminolysis pathway to provide additional fuel for the TCA cycle (Clerc *et al.*, 2019). Next, succinate is converted to fumarate in a succinate dehydrogenase (SDH; complex II) -mediated reaction coupled to the redox of $FADH_2$. Subsequent generation of malate from fumarate is then converted to oxaloacetate which completes the cycle (Martínez-Reyes and Chandel, 2020). ROS are generated by the ETC, particularly at complex III (Sena *et al.*, 2013; Yarosz and Chang, 2018). Mitochondrial dysfunction is described to drive excessive ROS production with damaging effects on DNA, metabolic enzymes, and cell signalling. One study linking these effects to T cell exhaustion (Scharping *et al.*, 2021). Despite this, ROS have also been described to be essential for T cell activation and differentiation, driving NFAT activity and IL-2 production, and supporting other metabolic pathways (Sena *et al.*, 2013; Abimannan *et al.*, 2016; Bailis *et al.*, 2019).

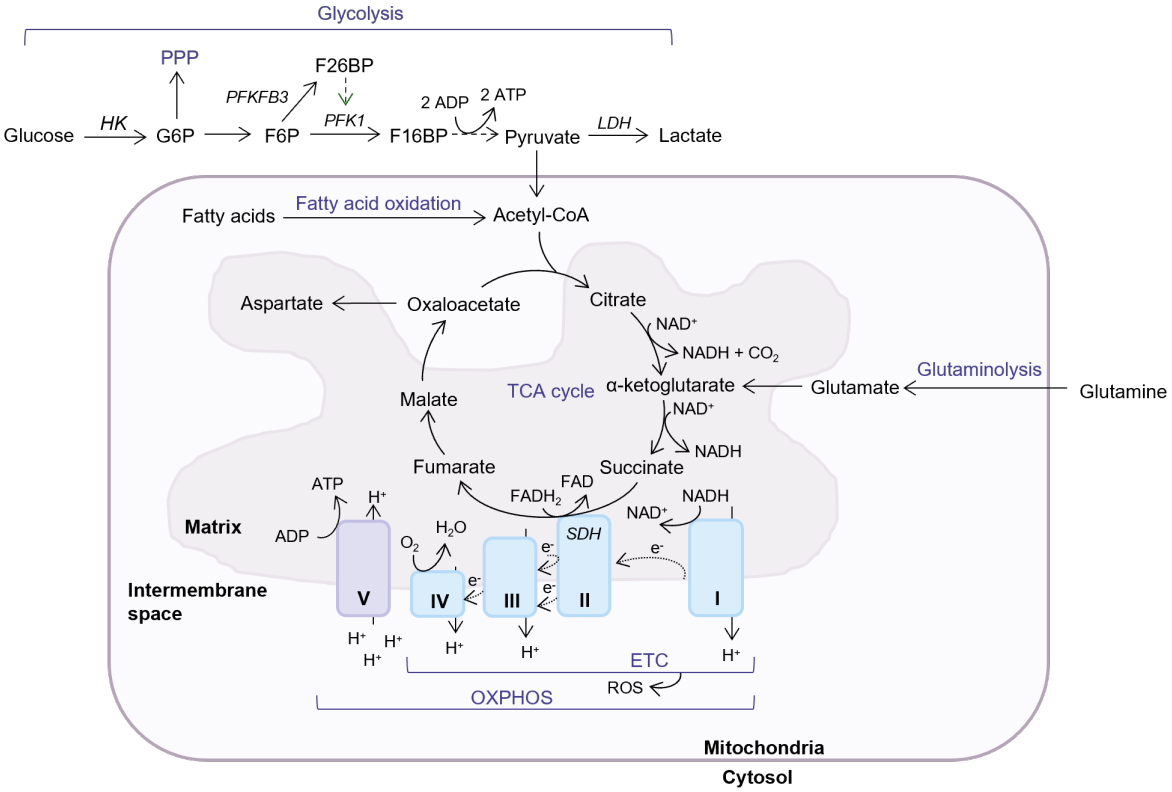

Figure 1.3 Metabolic pathways in T cells

Glycolysis and oxidative phosphorylation (OXPHOS) comprise the central metabolic pathways in $CD4^+$ T cells. Glucose in the cytosol is converted into glucose-6-phosphate (G6P) by hexokinase (HK), here, G6P can also fuel the pentose phosphate pathway (PPP). G6P is then converted to fructose-6-phosphate (F6P) before conversion to fructose-1,6-bisphosphate (F16BP) by phosphofructokinase 1 (PFK1). Alternatively, F6P can be converted to fructose-2,6-bisphosphate (F26BP) by 6-phosphofructo-2-kinase/fructose-2,6-biphosphatase 3 (PFKFB3). F26BP is an allosteric activator of PFK1 crucial for glycolysis in $CD4^+$ T cells. F16BP is then converted to pyruvate, generating net 2 ATP molecules. Pyruvate can be converted to lactate by lactate dehydrogenase (LDH) in aerobic glycolysis or converted to acetyl-CoA to drive the tricarboxylic acid (TCA) cycle. Here, fatty acid oxidation can also fuel the TCA cycle through acetyl-CoA production. Acetyl-CoA is combined with oxaloacetate to form citrate which is then converted into α-ketoglutarate (αKG), generating NADH and CO_2. At this point, glutamine can also feed into the TCA cycle in a process termed glutaminolysis, where glutamine is converted into glutamate and then αKG. Following this, αKG is converted to succinate, which generates NADH. NADH is oxidised by the electron transport chain (ETC), which generates electrons to pass down the chain and protons to efflux from the matrix creating membrane potential. Succinate is then converted to fumarate by complex II of the ETC, succinate dehydrogenase (SDH), this also involves the oxidation of $FADH_2$ again donating electrons to the ETC. Fumarate is further converted to malate, then oxaloacetate to restart the cycle. Oxaloacetate can also be converted to aspartate outside of the TCA cycle. The proton gradient generated by the ETC then drives ATP production by activity of complex V ATP-synthase, which utilises oxygen.

1.4 CD4$^+$ T CELL METABOLISM

Distinct subsets of T cells exhibit unique metabolic activity, influenced by activation status and stimuli from the local microenvironment (Munford and Dimeloe, 2019; Bishop *et al.*, 2021). Resting naïve CD4$^+$ T cells rely on a catabolic metabolism, breaking down substrates such as glucose and glutamine to drive OXPHOS. This homeostatic metabolism is maintained by IL-7 signalling which drives Akt to promote GLUT1 expression in support of low-level glucose uptake (Wofford *et al.*, 2008; Jacobs *et al.*, 2010). Moreover, a baseline level of mammalian target of rapamycin (mTOR) signalling downstream of Akt is essential for maintaining resting metabolism in naïve CD4$^+$ T cells (Myers *et al.*, 2019). Sphingosine-1-phosphate (S1P), a signalling molecule released by endothelial cells, has also been shown to be required in maintaining naïve CD4$^+$ T cell mitochondrial fitness (Mendoza *et al.*, 2017). Although not directly linked in this study, S1P is known to drive Akt/mTOR signalling, likely the mechanism by which it exerts effects on metabolism (Schieke *et al.*, 2006; Liu *et al.*, 2009; Mendoza *et al.*, 2017). Similarly, resting memory T cells have a predominant dependence on OXPHOS, CD8$^+$ T cells engaging IL-7 which promotes triacylglycerol synthesis to fuel FAO and the TCA cycle (Cui *et al.*, 2015). CD4$^+$ memory T cells have been shown to rely on Notch signalling to drive Akt and GLUT1 expression (Maekawa *et al.*, 2015). In addition, resting memory T cells exhibit higher basal respiration levels, mitochondrial content, and ETC expression than naïve CD4$^+$ T cells (Dimeloe *et al.*, 2016; Jones *et al.*, 2019). Memory cells also have a higher expression of glycolytic enzymes, GLUT1, and permissive epigenetic modifications on key metabolic genes providing them the capacity to engage metabolic upregulation rapidly upon reactivation (Dimeloe *et al.*, 2016; Barski *et al.*, 2017; Jones *et al.*, 2019).

1.4.1 Metabolic reprograming

Upon activation $CD4^+$ T cells undergo a significant shift in metabolism in order to meet the energy demands of effector function (Figure 1.4) (Shyer *et al.*, 2020). As described above, the TCR and CD28 collectively induce a range of signalling pathways to promote activation. Most importantly for metabolism is PI3K/Akt/mTOR, predominantly driven by CD28 but also by IL-2 (Frauwirth *et al.*, 2002; Jacobs *et al.*, 2008; Ray *et al.*, 2015). Although metabolic reprogramming in naïve $CD4^+$ T cells involves upregulation of both OXPHOS and glycolysis, effector T (T_{eff}) cells are characterised by their shift towards a reliance on aerobic glycolysis from the prevailing OXPHOS dependence of naïve cells, converting glucose-derived pyruvate to lactate (Michalek *et al.*, 2011; Sena *et al.*, 2013; Macintyre *et al.*, 2014). Critical for the growth and survival of activated T cells, glucose uptake is increased by Akt-dependent GLUT1 recruitment to the cell surface. (Frauwirth *et al.*, 2002; Jacobs *et al.*, 2008). To support heightened metabolic demands, T_{eff} cells also increase amino acid uptake through upregulation of multiple amino acid transporters, including alanine/serine/cysteine-preferring transporter 2 (ASCT2; system L amino acid transporter family 1 member 5 (SLC1A5)) and large amino acid transporter 1 (LAT1; SLC7A5). Glutamine, taken up by ASCT2, is essential for the activation and proliferation of T_{eff} cells through glutaminolysis and its direct incorporation into the TCA cycle to fuel OXPHOS (Carr *et al.*, 2010; Wang *et al.*, 2011). Furthermore, glutamine has been shown to indirectly influence mTOR activity through its role in leucine uptake (Wang *et al.*, 2011; Nakaya *et al.*, 2014). LAT1 forms a complex with CD98 to enable amino acid uptake (e.g. leucine) coupled with glutamine efflux. Studies have shown that leucine is essential for mTOR activity, acting through suppression of the mTOR inhibitor Sestrin2 (Wolfson *et al.*, 2016). In T_{eff} cells, studies reported that leucine activates mTOR via an Akt-independent

mechanism and that deletion of LAT1 prevented cells from metabolically reprogramming upon activation (Nicklin *et al.*, 2009; Wang *et al.*, 2011; Sinclair *et al.*, 2013). Indeed, mTOR is a major regulator of metabolic reprogramming, driving upregulation of glycolytic enzymes and glucose flux through glycolysis (Shi *et al.*, 2011; K. Yang *et al.*, 2013; Salmond, 2018). In order to mediate these effects, mTOR increases expression of the TFs c-Myc and hypoxia inducible factor 1 alpha (HIF1α). Through its deletion, one study showed the absolute dependence of T cells on c-Myc for upregulation of glycolysis and glutaminolysis in metabolic reprogramming. Genes including *Glut1*, *Slc7a5*, *Pfkfb3*, and *Ldha* (encoding lactate dehydrogenase) were all suppressed in the absence of c-Myc resulting in poor growth and proliferation (Wang *et al.*, 2011). This was further confirmed by another study showing that the c-Myc-induced proteome includes multiple metabolic regulators, including LAT1, which then promotes leucine uptake and mTOR activity to sustain c-Myc in a positive feedback loop (Marchingo *et al.*, 2020). Of note, c-Myc has a quick turnover in T cells due to its persistent targeting for degradation. This enables careful control of c-Myc responses, as a cell must maintain sufficient amino acid uptake for continued protein synthesis (Preston *et al.*, 2015). HIF1α was shown to be indispensable for metabolic reprogramming in T cells (Wang *et al.*, 2011). However, its role in driving glycolysis was essential for promoting Th17 cell differentiation over generation of Tregs (Shi *et al.*, 2011). In addition, mTOR drives upregulation of TF proliferator-activated receptor gamma (PPARγ), required for fatty acid metabolism and mitochondrial biogenesis to support OXPHOS (Angela *et al.*, 2016). To prevent aberrant aerobic glycolysis, particularly in environments of low-nutrient availability, adenosine monophosphate (AMP)-activated protein kinase (AMPK) senses increasing ratios of AMP:ATP and acts to restore its balance. AMPK promotes glutamine metabolism through the TCA cycle to drive OXPHOS and

reciprocally inhibits mTOR activity. Limiting ROS was shown to impair mTOR-driven glycolytic flux upon CD4$^+$ T cell activation through the upregulation of AMPK (Previte *et al.*, 2017). This self-regulation of T cell metabolism shown to be required for optimal T cell responses in mouse models of inflammation (Gwinn *et al.*, 2008; Blagih *et al.*, 2015; Mayer *et al.*, 2021).

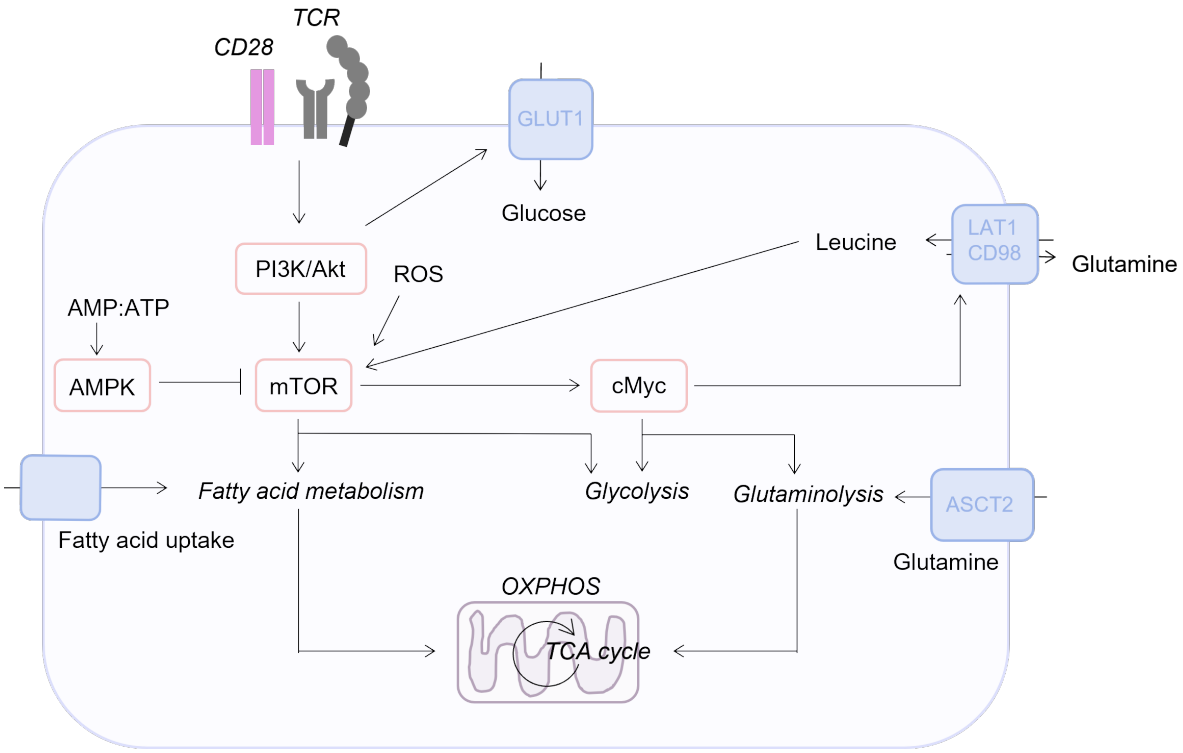

Figure 1.4 Metabolic reprogramming in CD4$^+$ T cells

Upon triggering of TCR/CD28 signalling, CD4$^+$ T cells undergo metabolic reprogramming. This is largely mediated through the PI3K/Akt pathway which drives upregulation of glucose transporter 1 (GLUT1) and glycolysis. Downstream mammalian target of rapamycin (mTOR) signalling also drives increases in glycolysis whilst activating c-Myc, a transcription factor required for glycolysis and glutamine metabolism through the tricarboxylic acid (TCA) cycle, which drives oxidative phosphorylation (OXPHOS). With activation, mTOR promotes increases in fatty acid metabolism and mitochondrial mass to support increased OXPHOS. In addition, c-Myc drives uptake of amino acids, such as leucine, through increased expression of transporters such as the LAT1/CD98 complex which acts as a glutamine antiporter. Glutamine uptake is also increased through the ASCT2 transporter to fuel OXPHOS. Both leucine and reactive oxygen species (ROS), generated by OXPHOS, have been shown to activate mTOR. Conversely, adenosine monophosphate (AMP)-activated protein kinase (AMPK) senses increasing AMP concentrations in the cell and acts to inhibit mTOR activity.

1.4.2 Metabolic profiles of CD4$^+$ T helper cell subsets

Broadly, effector CD4$^+$ Th cells, Th1, Th2 and Th17, are highly glycolytic compared to Tregs, which instead rely on an OXPHOS-dominant metabolism (Michalek *et al.*, 2011; Gerriets *et al.*, 2015). For T_{eff} cells, this is to enable sufficient biosynthesis required for production of effector molecules and proliferation. Th1 cells selectively require mTOR complex 1 (mTORC1) signalling to drive their glycolytic phenotype but are unaffected by the absence of mTORC2 (Delgoffe *et al.*, 2011). Moreover, mTORC1 was shown to promote T-bet phosphorylation, increasing its activity and subsequent IFN-γ expression in Th1 cells (Chornoguz *et al.*, 2017). In addition, aerobic glycolysis alters IFN-γ expression directly through increased glucose-derived acetyl-CoA enhancing histone acetylation and IFN-γ transcription (Peng *et al.*, 2016). Furthermore, increased activity of the glycolytic enzyme GAPDH leads to its decreased binding of IFN-γ messenger (m)RNA, thereby permitting translation (C.-H. Chang *et al.*, 2013). Furthermore, mannose, derived from glucose metabolism, was described to rescue the inhibitory effects of glucose deprivation on IFN-γ production (Zygmunt *et al.*, 2018). In comparison to Th1 cells, Th2 cells require mTORC2/protein kinase C theta (PKC-θ) signalling to drive GATA3 expression (Lee *et al.*, 2010; Delgoffe *et al.*, 2011). Although, another study also implicated a role for mTORC1-driven metabolism in Th2 differentiation (K. Yang *et al.*, 2013).

Based on their prominent role in autoimmunity, many studies have focused on controlling the balance between Th17 cells and Tregs. Like Th1 cells, Th17 cells are highly glycolytic and dependent on mTORC1 to drive this (Delgoffe *et al.*, 2011; Michalek *et al.*, 2011; Gerriets *et al.*, 2015). In contrast, Th17 cells also rely on glutamine metabolism through the TCA cycle. A pathway that was detrimental to Th1 cell differentiation (Johnson *et al.*, 2018). Additionally,

HIF1α has been shown to have a role promoting the glycolytic requirements of Th17 but not Th1 cells, alongside direct upregulation of RORγt (Dang *et al.*, 2011; Shi *et al.*, 2011). Th17 cells are additionally unique in their requirement for *de novo* fatty acid synthesis (FAS) to drive differentiation and expression of RORγt and IL-17 (Berod *et al.*, 2014; Endo *et al.*, 2015; Young *et al.*, 2017; Cluxton *et al.*, 2019). In comparison, Treg differentiation requires AMPK and FoxP3, both acting to suppress aerobic glycolysis and promote FAO-driven OXPHOS (Michalek *et al.*, 2011; Berod *et al.*, 2014; Angelin *et al.*, 2017; Howie *et al.*, 2017). Additionally, an absence of factors that drive glycolysis, such as HIF1α and mTOR, has been shown to promote Treg differentiation (Delgoffe *et al.*, 2009; Dang *et al.*, 2011; Shi *et al.*, 2011; Priyadharshini *et al.*, 2018). Other studies have shown that low-level glycolysis and mTORC1 activity are still required for Treg function, likely existing in a tightly controlled balance (Gerriets, Kishton, *et al.*, 2016; Shi *et al.*, 2019; Tanimine *et al.*, 2019). Indeed, differences in requirements for glycolysis between tTregs and iTregs have been uncovered, with highly glycolytic tTregs exhibiting increased suppressive function, whereas iTregs are inhibited by increases in glycolysis (Delgoffe *et al.*, 2009; Priyadharshini *et al.*, 2018; Tanimine *et al.*, 2019; de Kivit *et al.*, 2020). This is consistent with the improved phenotypic stability of tTregs compared to iTregs (Baron *et al.*, 2007; Floess *et al.*, 2007; Q. Chen *et al.*, 2011). Notably, the metabolism of Th17.1 cells has not been investigated. Although previously, Th1 cells undergoing plasticity towards a IFN-γ^{+}IL-10^{+} regulatory phenotype were associated with the highest expression of mTOR and metabolism in comparison to single cytokine producers, suggesting that plasticity is associated with increased metabolic demands (Kolev *et al.*, 2015).

1.5 FACTORS AFFECTING T CELL METABOLISM

Owing to their high metabolic demands, $CD4^+$ T cells are susceptible to extrinsic determinants of metabolism in the local microenvironment. For example, nutrient availability, hormones, and cytokines can all impact the survival and metabolic profile of $CD4^+$ T cells (Munford and Dimeloe, 2019; Bishop *et al.*, 2021). Limited glucose availability, for example in cancer where tumour cells are also significant consumers of glucose, permits a Treg dominant phenotype and suppresses the function of T_{eff} cells (Chang *et al.*, 2015; Ho *et al.*, 2015; Angelin *et al.*, 2017). Chronic inflammatory environments, such as the rheumatoid synovium, also often contain multiple highly metabolic cell types all competing for glucose, glutamine, and other substrates (Cejka *et al.*, 2010; Takahashi *et al.*, 2017; Abboud *et al.*, 2018; Koedderitzsch *et al.*, 2021). Another hallmark of cancer and inflammatory disease, hypoxia is a potent modulator of T cell responses. TF HIF1α is stabilised in hypoxic conditions and acts to increase glycolysis, yet in activated T cells, HIF1α also is upregulated irrespective of oxygen availability and drives an inflammatory Th17 cell response (Dang *et al.*, 2011; Shi *et al.*, 2011). As a consequence of heightened glycolytic activity, lactate builds up in local inflammatory environments (Haas *et al.*, 2015; Yang *et al.*, 2015). Lactate has been shown to impair the CXC-chemokine receptor (CXCR)3 and CCR6-mediated motility of $CD4^+$ T cells through its suppressive effects on glycolysis and enhancement of FAS (Haas *et al.*, 2015; Pucino *et al.*, 2019). Taken up by SLC5A12 on $CD4^+$ T cells, lactate can be converted to pyruvate in a reverse LDH reaction which produces NADH, this overproduction of reduced NADH causes a deficiency in NAD^+ available for glycolysis and consequential inhibition of the pathway (Pucino *et al.*, 2019; Quinn *et al.*, 2020). Furthermore, lactate is suppressive of Th1 cells, but perhaps in contradiction to its effects on metabolism is able to drive a Th17 cell phenotype by increasing FAS and pyruvate

kinase M2 (PKM2), both drivers of signal transducer and activator of transcription 3 (STAT3) which promotes RORγt and IL-17 (Haas *et al.*, 2015; Comito *et al.*, 2019; Pucino *et al.*, 2019). However, another study reported that increased lactate metabolism through the TCA cycle decreased the expression of IL-17 in Th17 cells due to increased ROS and subsequent IL-2 production which instead promoted FoxP3 expression (Lopez Krol *et al.*, 2022). Several studies have reported that Tregs metabolise lactate through the TCA cycle to improve their function in inflammatory environments (Angelin *et al.*, 2017; Watson *et al.*, 2021; Gu *et al.*, 2022). Furthermore, an overabundance of succinate taken up by $CD4^+$ and $CD8^+$ T cells has recently been implicated in the suppression of mitochondrial glucose oxidation leading to impaired effector function (Gudgeon *et al.*, 2022). Other environmental modulators of $CD4^+$ T cell metabolism include hormones such as leptin and adiponectin, and the active metabolite of vitamin D, 1,25-dihydroxyvitamin D_3 (Gerriets, Danzaki, *et al.*, 2016; Surendar *et al.*, 2019; Bishop *et al.*, 2021, 2022).

1.5.1 Effects of cytokines on T cell metabolism

Of particular interest to this project, several cytokines have been implicated in modulating $CD4^+$ T cell metabolism. As described above, through Akt signalling, IL-7 and IL-2 have important roles in driving glycolysis in quiescent and activated naïve $CD4^+$ T cells respectively (Wofford *et al.*, 2008; Jacobs *et al.*, 2010; Ray *et al.*, 2015). In studies focused on $CD8^+$ T cells, IL-15 was found to promote expression of carnitine palmitoyl transferase 1-a (CPT1a) in memory cells, an enzyme required for FAO, alongside increased mitochondrial biogenesis. Increased mitochondrial content enabled increased OXPHOS capacity which was essential for optimal memory responses (van der Windt *et al.*, 2012; Richer *et al.*, 2015). This was also

matched with an increase in antioxidants to counterbalance increased ROS production (Kaur *et al.*, 2011). Furthermore, IL-21 has been reported to have IL-15-like effects on FAO and mitochondrial capacity in $CD8^+$ T cells, implicating them both as therapeutic targets in immunotherapy (Loschinski *et al.*, 2018; Alizadeh *et al.*, 2019; Hermans *et al.*, 2020). However, studies investigating the role of IL-15 and IL-21 on $CD4^+$ T cell metabolism are lacking and require future investigation. IL-1β and IL-23 are both essential for the differentiation of Th17 cells, synergistically shown to drive sufficient, albeit reduced, metabolic reprogramming in Th17 cells in the absence of CD28 (Revu *et al.*, 2018). IL-1β acts through activation of PI3K/Akt/mTOR to drive glycolysis early in the commitment to a Th17 cell lineage, with IL-23 engaging mTOR later (Gulen *et al.*, 2010; J. Chang *et al.*, 2013; Deason *et al.*, 2018). Consistent with the role of IL-23 in maintaining but not driving Th17 cell differentiation (Stritesky *et al.*, 2008). Furthermore, IL-1β was shown to inhibit iTreg differentiation through upregulation of mTOR activity and downstream increases in HIF1α (Feldhoff *et al.*, 2017). As both IL-1β and HIF1α have been previously shown to drive Th17 cell differentiation, it may be hypothesised that the induction of HIF1α is an additional mechanism by which IL-1β induces a Th17 cell phenotype. However, in this study they were unable to detect an increase in IL-17. Of note, this study was performed on human $CD4^+$ T cells unlike the others which were performed on murine $CD4^+$ T cells. Further studies are required to fully elucidate the role of IL-1β in modulating $CD4^+$ T cell metabolism. TGF-β, a cytokine instrumental in Treg differentiation, has been shown to inhibit PI3K/Akt/mTOR-driven glycolysis in favour of FAO-driven OXPHOS (Delisle *et al.*, 2013; Priyadharshini *et al.*, 2018). TGF-β has also been reported to impair T_{eff} cell function in tumours, specifically targeting ATP-synthase (complex V), to suppress ATP-coupled respiration and resulting in decreased IFN-γ (Dimeloe *et al.*, 2019). As highlighted

here previously, TNF-α signalling via TNFR2 on Tregs is a subject with many context-dependent nuances, yet to be fully understood. Just two studies from the same group have investigated the role of TNF:TNFR2 signalling in Treg metabolism. They were able to show that TNFR2 ligation with a monoclonal antibody drives glycolysis and promotes a superior suppressive capacity of tTregs but also promotes glutamine metabolism in T_{eff} cells, when in combination with anti-CD3 stimulation (de Kivit *et al.*, 2020; Mensink *et al.*, 2022). Further studies are required to fully elucidate the role of TNF-α on $CD4^+$ T cell metabolism and function.

1.6 RHEUMATOID ARTHRITIS

RA is a systemic, chronic inflammatory disease estimated to affect 0.5-1% of the population worldwide (Yap *et al.*, 2018; Chemin *et al.*, 2019; Almutairi *et al.*, 2021). Pathogenesis is often localised to the joints where a significant immune infiltrate and highly invasive fibroblast-like synoviocytes (FLS) cause progressive erosion of the articular cartilage and bone (Yap *et al.*, 2018; Chemin *et al.*, 2019). Genome wide association studies (GWAS) have identified the specific human leukocyte antigen (HLA), in humans encoding MHCII molecules, variant *HLA-DRB1* to predispose to RA (Hill *et al.*, 2003; Scally *et al.*, 2013; Chemin *et al.*, 2016; Gerstner *et al.*, 2016). Citrullination involves the conversion of arginine to citrulline on proteins such as fibrinogen, type II collagen, and glycolytic enzyme alpha-enolase. Anti-citrullinated protein antibodies (ACPA) against these antigens are detected in around 60-80% of RA patients dependent on disease stage (Matsui *et al.*, 2006; Ioan-Facsinay *et al.*, 2008; Aggarwal *et al.*, 2009; Kurowska *et al.*, 2017). ACPA-positive RA is also associated with smoking and the *HLD-DRB1* allele (Hill *et al.*, 2003; Scally *et al.*, 2013; Chemin *et al.*, 2016; Gerstner *et al.*, 2016). Additionally characteristic of RA, although reported to be less specific

than ACPA, rheumatoid factor (RF) refers to antibodies against the Fc portion of immunoglobulin (Ig)G itself (Ioan-Facsinay *et al.*, 2008; Aggarwal *et al.*, 2009). Presence of these autoantibodies in the synovial joint then drives activation of innate cells such as macrophages to potentiate inflammation (Kurowska *et al.*, 2017).

1.6.1 $CD4^+$ T cells in the pathogenesis of RA

As highlighted earlier, reports of Treg function and abundance in RA are contradictory. Studies have suggested their increase (van Amelsfort *et al.*, 2004; Zhang *et al.*, 2022), unaltered presence (Liu *et al.*, 2005; Möttönen *et al.*, 2005), and decrease (Kawashiri *et al.*, 2011; Niu *et al.*, 2012), in peripheral blood of RA patients compared to healthy controls (HC). Of note, these studies characterise Tregs as $CD4^+CD25^+$ cells, as CD25 is also known to be a marker of activation, the specificity of this identifier may account for some of the variability in these results. Indeed, studies have begun to further characterise the phenotype of Tregs in RA and found them to be converted by the local inflammatory environment into both Th1- and Th17-like Tregs with associated pathogenic functions (Komatsu *et al.*, 2014; Wang *et al.*, 2015; Shevyrev *et al.*, 2021; Zhang *et al.*, 2022). Tregs are present in RA synovial fluid (SF) but reports on their function are again inconsistent. An impairment of suppressive function has been attributed to decreased co-inhibitory receptor expression (Flores-Borja *et al.*, 2008; Sun *et al.*, 2017). However, studies have also implicated the increased activity of T_{eff} cells causing resistance to RA Treg-mediated suppression (van Amelsfort *et al.*, 2004; Han *et al.*, 2008).

Th1 cells have been identified in the SF of RA patients, with infiltration attributed to their expression of CXCR3 and aberrant production of the CXCR3-binding chemokines, CXC-chemokine ligand (CXCL)9 and CXCL10, by FLS in RA (Ueno *et al.*, 2005; Aldridge *et al.*,

2020). Furthermore, citrulline-specific $CD4^+$ T cells in RA peripheral blood were shown to be of a predominantly Th1 cell phenotype (James *et al.*, 2014). However, overall Th1 cell percentages were unchanged (Shen *et al.*, 2009; Kim *et al.*, 2013). Mechanistically, IFN-γ drives inflammatory macrophage activation and production of CXCL10 by FLS (Aldridge *et al.*, 2020). Yet, IFN-γ has also been shown to regulate Th17 cell responses, limiting RA pathogenesis (Lee *et al.*, 2013, 2017).

Both Th17 cells and IL-17 are upregulated in RA peripheral blood and SF and are strongly correlated with disease (Raza *et al.*, 2005; Zizzo *et al.*, 2011; Wang *et al.*, 2012; Penatti *et al.*, 2017). The migration of Th17 cells to the rheumatoid synovium is mediated by their expression of CCR6 and high levels of CCL20 present in the tissue (Hirota *et al.*, 2007; Aldridge *et al.*, 2020). Furthermore, Th17.1 cells, recruited to the RA synovium via their expression of CXCR3 and CCR6, express higher amounts of cytokine than Th17 or Th1 cells and were shown to be more resistant to suppression by Tregs (Basdeo *et al.*, 2017). Recent studies have begun to correlate their presence with patient response to RA therapies (Maeda *et al.*, 2019; Millier *et al.*, 2022). However, further research is required to fully understand the roles and therapeutic potential for targeting Th17.1 cells in RA. Th17 cell-associated pathology is primarily attributed to the release of inflammatory cytokines IL-17 and TNF-α. The effects of IL-17 in RA constitute multiple mechanisms (Beringer and Miossec, 2019; P. Yang *et al.*, 2019). IL-17 stimulates osteoclastogenesis through the upregulation of receptor activator of NF-κB (RANK) ligand (RANKL) on FLS and direct stimulation of osteoclasts which promotes excessive bone resorption and destruction (Yago *et al.*, 2009; Adamopoulos *et al.*, 2010; Kim *et al.*, 2015). FLS are a potent mediators of inflammation and tissue destruction in RA (Németh *et al.*, 2022). IL-17 has been shown to drive their expression of inflammatory mediators and

hyperproliferation (van Hamburg *et al.*, 2011; Chang *et al.*, 2019). This latter effect thought to be induced by mitochondrial dysfunction causing impaired autophagy and a resistance to apoptosis (Kim *et al.*, 2018; Chang *et al.*, 2019). Additionally, IL-17 is implicated in angiogenesis and neutrophil recruitment (Pickens *et al.*, 2010; Griffin *et al.*, 2012). Of note, a recent study identified a subset of pathogenic polyfunctional $CD4^+$ T cells, able to produce multiple pro-inflammatory cytokines, present in the rheumatoid joint to precede clinical RA symptoms (Floudas *et al.*, 2022)

1.6.2 Roles of TNF-α in RA

The other major mediator of Th17 cell-driven inflammation in RA is TNF-α (Figure 1.5). TNF-α is overexpressed by RA T cells compared to HC and is abundant in both peripheral blood and SF (Tetta *et al.*, 1990; Manicourt *et al.*, 2000; Cai *et al.*, 2020; Wu *et al.*, 2021). TNF-α has been shown to work synergistically with other cytokines including IL-1β and IL-17 to exert its effects. In combination, these cytokines drive increased expression of cytokines, matrix metalloproteinases (MMPs), and chemokines from FLS, whilst promoting a hyperproliferative, migratory phenotype to augment cartilage destruction in RA pathogenesis (Goldberg *et al.*, 2008; Mu *et al.*, 2016). Mechanistically, TNF-α has been shown to signal via the PI3K and NFκB pathways to promote a pro-inflammatory and invasive phenotype in FLS (Shibuya *et al.*, 2015; Mu *et al.*, 2016; Yu *et al.*, 2018). In separate studies, both TNFR1 and TNFR2 signalling have been implicated in inducing expression of inflammatory cytokines such as IL-6 and IL-8, and chemokines such as CXCL10 (Zhang and Xiao, 2017; Suto *et al.*, 2022). Treatment of FLS with TNF-α was shown to increase both their glycolytic and mitochondrial metabolism, but alike to metabolic reprogramming in $CD4^+$ T cells, predominantly inducing a transformation towards

glycolysis through upregulation of GLUT1 and HIF1α. This metabolic shift was then shown to be linked to their increased expression of pro-inflammatory mediators (Koedderitzsch *et al.*, 2021). Comparatively, tumour necrosis factor-like ligand 1A (TL1A), a tumour necrosis factor superfamily member found to be upregulated in RA, was seen to signal through TNFR2 to drive mitochondrial dysfunction and induce overproduction of ROS. Inhibition of this pathway was able to dampen the FLS inflammatory phenotype (Al-Azab *et al.*, 2020). It has also been shown that TNF-α can stimulate FLS indirectly, through activation of $CD4^+$ T cells which then promote IL-6 and IL-8 production by FLS (Povoleri *et al.*, 2020). Indeed, as discussed above, TNF-α is thought to act as a co-stimulatory molecule on $CD4^+$ T cells. Yet, chronic exposure to the cytokine, as in RA, was seen to downregulate TCR/CD28 signalling and cytokine production (Cope *et al.*, 1994; Bryl *et al.*, 2001; Aspalter *et al.*, 2005). One study identified that a TNF-α gradient from the inflamed RA synovium was able to recruit TNFR1-expressing $CD4^+$ T cells (Rossol *et al.*, 2013). It was seen that TNF-α could promote the differentiation of pathogenic murine Th17 cells and that TNFR2 deficiency could protect against a mouse model of colitis. Any effect on RA pathogenesis was not assessed, but due to the predominance of Th17 cells in RA, a similar protective effect is feasible (Alam *et al.*, 2021). A recent study on human $CD4^+$ T cells also demonstrated that TNF-α could promote IL-17 production in Th17 cells but was suppressive of IFN-γ in Th1 cells (Pesce *et al.*, 2022). Furthermore, TNF:TNFR2 interactions on Tregs are in contradiction, reported to both enhance and suppress function (Chen *et al.*, 2013; Nie *et al.*, 2013). These studies highlight a need to better understand the role of TNF-α signalling on $CD4^+$ T cells, particularly in the context of RA. TNF-α has also been implicated in driving an inflammatory macrophage phenotype and priming them for increased osteoclastogenesis in response to RANK:RANKL signalling (Lam *et al.*, 2000; Yarilina *et al.*,

2011; Degboé *et al.*, 2019). Indeed, TNF-α is a potent driver of bone resorption in RA, inducing FLS to express RANKL and directly promoting osteoclast differentiation (Kobayashi *et al.*, 2000; Hashizume *et al.*, 2008). Lastly, TNF-α is known to cause endothelial dysfunction which then promotes immune cell recruitment and inflammation, further exacerbating disease (Rajan *et al.*, 2008; Steyers and Miller, 2014).

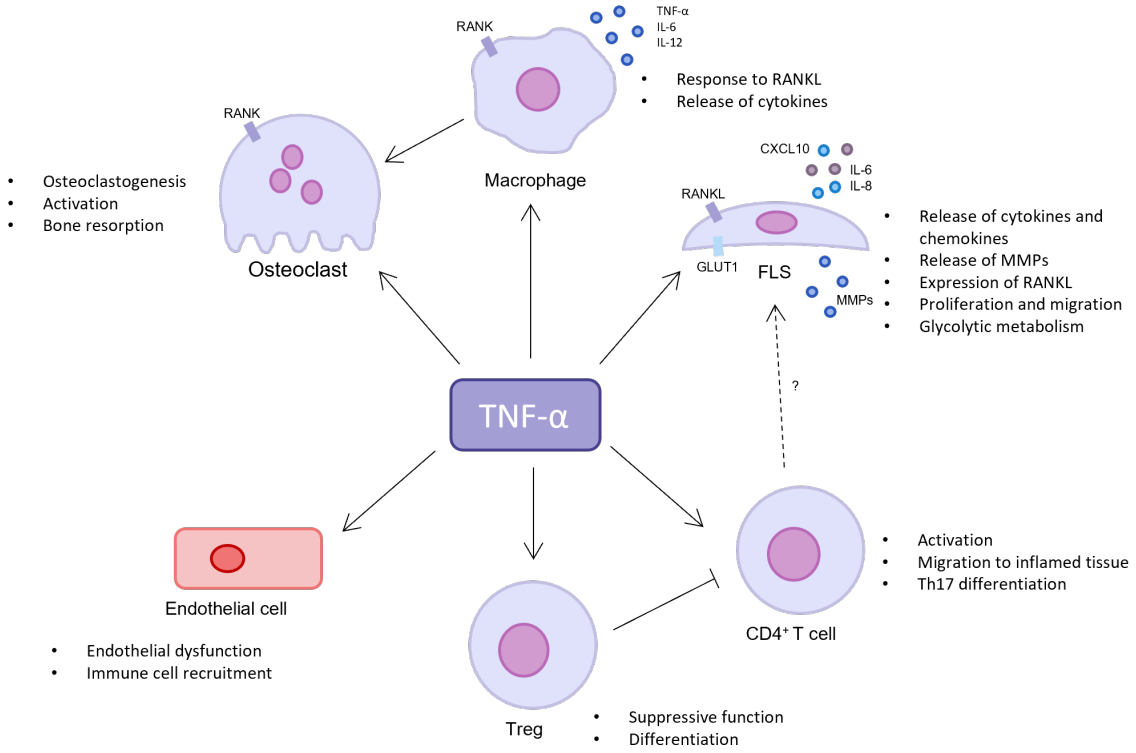

Figure 1.5 Roles of TNF-α in rheumatoid arthritis

TNF-α has a multitude of roles in rheumatoid arthritis (RA) on multiple cell types. TNF-α promotes differentiation and activation of osteoclasts, both directly and through increased expression of RANK ligand (RANKL) on fibroblast-like synoviocytes (FLS). Furthermore, TNF-α primes macrophages to respond to RANKL and promote osteoclastogenesis. TNF-α induces inflammatory cytokine production from macrophages (IL-6, IL-12, TNF-α) and FLS (IL-6, IL-8). FLS are also stimulated to release chemokines such as CXCL10 and matrix metalloproteinases (MMPs). Moreover, TNF-α drives glucose uptake via glucose transporter 1 (GLUT1) and glycolysis in FLS, as well as inducing a hyperproliferative, invasive phenotype. TNF-α drives activation, a Th17 cell phenotype, and migration of $CD4^+$ T cells which are then able to induce cytokine production in FLS. TNF-α enhances the differentiation and suppressive capacity of regulatory T cells (Tregs). Endothelial dysfunction is also induced by TNF-α in RA, promoting recruitment of immune cells to the inflamed site.

1.6.3 Dysregulated CD4$^+$ T cell metabolism in RA

As described above, lactate uptake by CD4$^+$ T cells in RA promotes FAS to drive Th17 cell differentiation (Pucino *et al.*, 2019). Moreover, naïve CD4$^+$ T cells in RA have an intrinsic defect in expression of the glycolytic enzyme PFKFB3. Instead, naïve CD4$^+$ T cells in RA demonstrate increased activity of the PPP which results in overproduction of NADPH and overconsumption of ROS (Z. Yang *et al.*, 2013). This imbalance in ROS results in defective activation of the DNA repair protein ataxia telangiectasia mutated (ATM), leading to hyperproliferation of the cell but also increased sensitivity to apoptosis and limited autophagy (Shao *et al.*, 2009; Z. Yang *et al.*, 2013; Yang *et al.*, 2016). Overexpression of ATM was then shown to increase production of meiotic recombination 11 homolog A (MRE11A) in RA CD4$^+$ T cells which promotes telomere damage and premature ageing of the cell (Shao *et al.*, 2009; Li *et al.*, 2016). Impaired ATM activation was also shown to bias naïve CD4$^+$ T cell differentiation towards inflammatory Th1 and Th17 cell phenotypes (Yang *et al.*, 2016). Comparatively, activated CD4$^+$ T cells in RA have been shown to have increased autophagy rendering them more resistant to apoptosis and aiding their persistence in disease (van Loosdregt *et al.*, 2016). RA naïve CD4$^+$ T cells were additionally shown to have a defect in N-myristoyltransferase 1 (NMT1) activity resulting in impaired activation of AMPK and reciprocal hyperactivity of mTOR (Z. Wen *et al.*, 2019). This increased mTOR activity then promoting inflammatory Th1 and Th17 cell differentiation. Furthermore, defective expression of succinyl-CoA ligase was attributed to a reversal of the TCA cycle resulting in accumulation of acetyl-CoA which was able to stabilise the microtubule cytoskeleton and promote an invasive T cell phenotype (Wu *et al.*, 2020). Most recently, the same group identified that an impairment in mitochondrial aspartate production caused dysregulated endoplasmic reticulum (ER) expansion and led to increased production of TNF-α

in RA naïve $CD4^+$ T cells compared to HC (Wu *et al.*, 2021). These studies show a significant metabolic dysregulation in RA $CD4^+$ T cells. However, little is known about the mechanisms that drive this. Further work to understand these triggers and the subsequent impact on pathogenic cell function will aid in the development of novel therapeutic targets in RA.

1.7 THERAPEUTIC TARGETS IN RHEUMATOID ARTHRTIS

Therapies for RA include non-steroidal anti-inflammatory drugs (NSAIDs), which target synthesis of inflammatory prostaglandins, and corticosteroids. However, these are non-specific suppressors of inflammation and so also elicit side effects (Crofford, 2013; Huang *et al.*, 2021). More targeted to the specific pathogenesis of RA are a category of therapies termed disease-modifying antirheumatic drugs (DMARDs). The most commonly prescribed of these, methotrexate, inhibits dihydrofolate reductase which is essential for purine and pyrimidine synthesis required in cell growth (Cutolo *et al.*, 2001). Methotrexate is also often used in combination with other DMARDs to promote a synergistic effect (Cronstein and Aune, 2020). Other examples of DMARDs include leflunomide and hydroxychloroquine which target pyrimidine synthesis and lysosome formation respectively (Fox, 1993; Fox *et al.*, 1999; Schrezenmeier and Dörner, 2020). Again, these treatments have multiple side effects and varied responses in patients, eliciting the need for more specific therapeutic targets (Mittal *et al.*, 2012; Huang *et al.*, 2021). More directed at modulating the $CD4^+$ T cell compartment in RA are therapies such as baricitinib, small molecule inhibitor of signalling molecule Janus kinase (JAK), and abatacept, an antibody against CD80/86 to limit CD28 signalling (Emery *et al.*, 2015; Harrington *et al.*, 2020; Huang *et al.*, 2021). Largely,

developments have been made targeting the action of the multiple inflammatory cytokines implicated in RA with varying degrees of success.

1.7.1 Anti-cytokine biologic therapies

Several anti-cytokine biologic therapies are currently approved for the treatment of RA, targeting IL-6 (e.g. tocilizumab), IL-1β (e.g. anakinra), and TNF-α (e.g. infliximab) (Huang *et al.*, 2021). Variations of these biologics target either the cytokine or the cytokine receptor. Yet, some patients fail to respond adequately. Anti-cytokine biologic therapies against other inflammatory mediators such as IL-17 and IFN-γ have been halted at clinical trials due to lack of clinical efficacy in RA (PDL BioPharma, Inc., 2008; Blanco *et al.*, 2017; Huang *et al.*, 2021), whilst new targets such as CXCR3 are undergoing development in animal models (Bakheet *et al.*, 2019).

Of particular interest to the current study is the treatment of RA patients with anti-TNFα. Clinically used anti-TNFα biologic therapies include etanercept, a soluble TNFR fusion protein, and adalimumab and infliximab, monoclonal anti-TNFα antibodies (Ma and Xu, 2013). These drugs are effective in improving RA outcomes due to suppression of the range of TNF-α effects shown in Figure 1.5. Focusing on $CD4^+$ T cell effects, patients on anti-TNFα therapy often present with a paradoxical increase in circulating Th1 and Th17 cells compared to untreated controls, despite an improvement in disease symptoms (Aerts *et al.*, 2010; D.-Y. Chen *et al.*, 2011; Dulic *et al.*, 2017). Some studies have reported that increases in circulating IL-17 correlate with patients not responding to treatment, whilst others have found no such association (Aerts *et al.*, 2010; D.-Y. Chen *et al.*, 2011; Sikorska *et al.*, 2018). Notably, one study identified that anti-TNFα therapy downregulated expression of CCR6 on circulating Th17 cells

in RA, likely preventing their recruitment to the inflamed synovium (Aerts *et al.*, 2010). Anti-TNFα is reported to increase the expression of IL-10 in Th1 and Th17 cells in RA in a FoxP3-independent manner (Evans *et al.*, 2014; Roberts *et al.*, 2017; Povoleri *et al.*, 2020). Alongside delayed activation and reduced ability to activate FLS, these data suggest suppressed inflammatory function of $CD4^+$ T cells in RA but this is yet to be fully elucidated (Povoleri *et al.*, 2020). Additionally, modulating this key pro-/anti-inflammatory balance may be reciprocal increases in numbers and suppressive capacity of Tregs (Dulic *et al.*, 2017). Anti-TNFα treatment has been shown to rescue the impaired function of Tregs in RA (Ehrenstein *et al.*, 2004; Valencia *et al.*, 2006; Nie *et al.*, 2013). This effect is in direct contradiction to role described for TNF:TNFR2 in supporting Treg function. However, is thought to be due to the paradoxical increased binding of anti-TNFα-treated monocytes to Tregs via increased mTNF:TNFR2 interactions (Nguyen and Ehrenstein, 2016). Many patients fail to mount an adequate response to anti-TNFα therapy and the reasons for this are unknown. Better understanding of the pathogenic mechanisms of TNF-α in RA may aid in future novel therapeutic targets and the ability to stratify patients into groups with the most effective treatment approach.

1.7.2 Targeting metabolism

Leflunomide and methotrexate, both DMARDs used for RA treatment, target the metabolic process of nucleotide synthesis. Furthermore, methotrexate has been implicated in the generation of ROS and adenosine, an inhibitor of $CD4^+$ T cell function (Cronstein and Aune, 2020). Aside from these, few developments have been made in targeting cellular metabolism for the treatment of RA, despite its central role in driving the pathogenic function of multiple

cell types (Hanlon *et al.*, 2022). Metformin, an agonist of AMPK and inhibitor of complex I of the ETC, has shown promise in early stage clinical trials (Abdallah *et al.*, 2021; Gharib *et al.*, 2021). Similarly, sirolimus, an inhibitor of mTOR, was shown to improve disease score and Treg numbers (H.-Y. Wen *et al.*, 2019). An agonist of PPARγ, a regulator of fatty acid metabolism that is decreased in RA, has also shown clinical efficacy in a pilot trial (Ormseth *et al.*, 2013; Li *et al.*, 2017). Elsewhere, modulators targeting PI3K and glutamine metabolism have been proposed as potential novel therapeutic approaches (Ueda *et al.*, 2019; Kim *et al.*, 2020; Hanlon *et al.*, 2022). Future studies should investigate the modulation of cellular metabolism as a treatment for RA, likely in combination with other immunomodulatory drugs such as anti-TNFα. Interrogating the mechanisms of TNF-α signalling, how they link to cellular metabolism, and how they then drive pathogenic $CD4^+$ T cell function in chronic inflammatory disease will be crucial to these developments.

1.8 AIMS AND HYPOTHESIS

Previous studies have highlighted the role of TNF-α in driving optimal activation of $CD4^+$ T cells. However, a role for TNF-α in modulating $CD4^+$ T cell metabolism has not been described. Therefore, this study sought to investigate the impact of TNF-α on $CD4^+$ T cell metabolism. Furthermore, as cellular metabolism is linked to cell function, the functional impacts of these metabolic alterations will be assessed. In particular, TNF-α is a major driver of inflammatory responses but its full effects on $CD4^+$ T cell function are not completely understood. This may be especially pertinent in chronic inflammatory diseases, such as RA, where TNF-α is abundant and dysregulated metabolic phenotypes of $CD4^+$ T cells are present. Further investigation into the mechanisms of action of TNF-α are required to better understand RA pathogenesis and drive the development of novel therapeutic approaches.

This study will investigate the hypothesis that T cell derived TNF-α is required for the metabolic reprogramming of $CD4^+$ T cells and that blockade of this signal will have downstream effects on T cell function.

The aims of this study are as follows.

AIM 1: Investigate a role for T cell-derived TNF-α in the metabolic reprogramming of $CD4^+$ T cells and understand the signalling pathways involved

AIM 2: Understand the functional impacts of the metabolic alterations driven by TNF-α

AIM 3: Explore the observed *in vitro* effects of T cell-derived TNF-α on $CD4^+$ T cell metabolism and function in the context of RA

CHAPTER 2: MATERIALS AND METHODS

2.1 MEDIA AND BUFFERS

The media and buffers listed here were used throughout the experiments in this study.

Table 2.1 MACS buffer

Reagents	Manufacturer (Cat#)	Final concentration
Phosphate-buffered saline (PBS)	Sigma-Aldrich (806544)	-
Foetal bovine serum – heat inactivated (FBS)	Sigma-Aldrich (F9665)	5%
Ethylenediaminetetraacetic acid (EDTA) disodium salt solution	Sigma-Aldrich (E7889)	2 mM

Table 2.2 T cell culture medium

Reagents	Manufacturer (Cat#)	Final concentration
Roswell Park Memorial Institute 1640 Medium (RPMI)	Sigma-Aldrich (R8758)	-
FBS	Sigma-Aldrich	10%
Penicillin-Streptomycin solution (P/S; 10,000 U penicillin and 10 mg/ml streptomycin)	Sigma-Aldrich (P4333)	1%
Recombinant human (rh)IL-2	PeproTech (200-02)	50 IU/ml

Table 2.3 Staining buffer

Reagents	Manufacturer	Final concentration
PBS	Sigma-Aldrich	-
FBS	Sigma-Aldrich	2%

Table 2.4 Seahorse extracellular flux medium

Reagents	Manufacturer (Cat#)	Final concentration
Seahorse extracellular flux (XF) RPMI Medium pH 7.4	Agilent (103576-100)	-
D-glucose	Sigma-Aldrich (G7021)	10 mM
Sodium pyruvate	Thermo Scientific (J61840)	1 mM
L-glutamine	Sigma-Aldrich (G8540)	2 mM
N-2-hydroxyethylpiperazine-N-2-ethane sulfonic acid (HEPES)	Gibco (15630056)	5 mM

Table 2.5 Tracing medium

Reagents	Manufacturer (Cat#)	Final concentration
Stable isotope labelling with amino acids in cell culture (SILAC) RPMI 1640 Flex Medium, no glucose, no phenol red	Gibco (A2494201)	-
FBS	Sigma-Aldrich	10%
rhIL-2	Sigma-Aldrich	50 IU/ml
L-arginine	Sigma-Aldrich (A8094)	20 mg/ml
L-lysine monohydrochloride	Sigma-Aldrich (L8662)	4 mg/ml

2.2 PERIPHERAL BLOOD SAMPLES

Fully anonymised leukocyte cones were obtained from NHS Blood and Transplant (NHSBT), Birmingham, UK. Peripheral blood samples were collected from anonymised healthy volunteers into Vacutainer K2EDTA 10 ml tubes (BD, Cat# VS367525). All volunteers signed a consent form, and all studies were approved by the University of Birmingham STEM Ethics Committee (Ref. ERN 17_1743). Collection of RA patient peripheral blood samples was arranged in collaboration with Professor Karim Raza at Sandwell and West Birmingham NHS Hospitals Trust. Blood was collected in Vacutainer Lithium Heparin 3 ml tubes (BD, Cat# VS367885) from patients with RA. Details of the patient cohort are listed in Table 2.6 and

a summary of the patient and control cohorts detailed in Table 6.1. All patients provided written informed consent and the study was approved by the West Midlands - Black Country Research Ethics committee (Ref 12/WM/0258).

Table 2.6 Details of RA patient cohort

Sample no.	Sex*	Age	Age at onset	DAS28 (ESR)*	Medication
1	F	73	39	5.63	Methotrexate, Folic acid, Amlodipine, Atorvastatin, Montelukast, Metformin, Clopidogrel, Thyroxine, Frusemide, B12 injections, Co-codamol 30/500, Cholecalciferol, Alendronate
2	F	84	77	3.95	Methotrexate, Voltrol, Prednisolone, Paracetamol, Tramadol, Mirbegron, Ibandronic Acid, InVita D3, Lansoprazole, B12 injections
3	F	80	75	5.31	Amlodipine, Indapamide, ProD3, Co-Codamol, Candesaratan, Furosemide, Bendroflumethazide, Apixaben, Alendronate
4	F	51	48	2.45	Methotrexate, Folic acid, Vitamin D, Codeine
5	F	60	51	5.00	Baricitinib, Naproxen, Amitryptyline, Omeprazole, Paracetamol
6	F	40	38	2.77	Cimzia, Prednisolone, Folic Acid, Omeprazole
7	F	31	27	4.11	Ibuprofen, Hydroxychloroquine, Prednisolone
8	F	29	21	4.06	Hydroxychloroquine, Methotrexate, Adalimumab, Folic Acid, Adcal D3, Lansoprazole, Colecalciferol, Mebeverine
9	F	51	50	4.83	Ibuprofen, Thyroxine, Fultium D3, Paracetamol
10	F	38	34	4.21	Methotrexate, Folic Acid, Omeprazole, Amitryptyline
11	F	57	42	4.79	Amlodipine, Aspirin, Atorvastatin, Bisoprolol, Losartan, Omeprazole
12	M	52	49	3.66	Methotrexate, Hydoxychloroquine, Folic Acid, Amlodipine, Paracetamol, Lansoprazole, Latanoprost
13	F	55	49	5.17	Baricitinib, Methotrexate, Folic Acid, Esomeprazole, Paracetamol, Co-codamol, HRT

14	F	57	47	0.49	Methotrexate, Hydroxychloroquine, Prednisolone, Folic Acid, Thealoz Duo, Hylonight, Beclomethason
15	F	52	49	3.44	Methotrexate, Folic acid, Metformin, Atorvastatin, Losaratan, Mometasone
16	F	58	53	5.12	Methotrexate, Folic Acid, Atorvastatin, Candesartan, Indapamide, Latanoprost, Sodium Hyaluronate eye drops, Lercanidipine, Metformin, Pregabalin, Toujeo, Co-amoxiclav
17	F	67	66	7.04	Naproxen, Omeprazole
18	F	59	41	4.72	Hydroxychloroquine, Naproxen, Co-Codamol, Amlodipine, Atorvastatin, Lansoprazole, AMT
19	M	53	49	4.32	Methotrexate, Naproxen, Folic Acid, Adcal D3, Dihydrocodeine

* F=Female; M=Male; DAS28 (ESR)=Disease Activity Score (using 28 joint counts) (erythrocyte sedimentation rate)

2.3 PBMC ISOLATION

2.3.1 Leukocyte cones and peripheral blood donors

Peripheral blood mononuclear cells (PBMCs) were isolated from whole blood using Ficoll-Paque PLUS (GE Healthcare, Cat# 17-1440-02) density gradient centrifugation. Samples were stored at room temperature (RT) and processed in a sterile environment within 24 h. Whole blood was diluted in sterile phosphate buffered saline (PBS) and layered onto Ficoll-Paque PLUS using LeucoSEP tubes (Greiner Bio-One, Cat# 10349081). Samples were centrifuged for 10 mins at 1,000 x g with the brake set to 3. After discarding the plasma layer, the PBMC cell layer was collected into a 50 ml tube and resuspended in 50 ml sterile PBS, then centrifuged at 300 x g for 10 mins with the brake back on the usual setting of 9 to remove remaining Ficoll-Paque PLUS. PBMCs were washed for a final time in 50 ml PBS and centrifuged at 300 x g for 5 mins, following centrifugation the supernatant was discarded. Isolated PBMCs

were then counted using a Fast-Read 102 disposable counting slide (Biosigma, Cat# 630-1893) and used immediately for flow cytometric staining or further cell isolation.

2.3.2 RA patient and matched healthy control peripheral blood

PBMCs from RA patients or matched HC were isolated as above with a few minor alterations. At the first dilution, sterile Roswell Park Memorial Institute 1640 Medium (RPMI) + 1% Penicillin-Streptomycin solution (P/S; 10,000 U penicillin and 10 mg/ml streptomycin) pre-warmed to 37°C was used in place of PBS at a 1:1 ratio with the blood. This was done in case the blood plasma was required for use in future cell culture experiments where presence of RPMI would aid in maintaining cell viability. After Ficoll density gradient centrifugation 4 x 1 ml aliquots of blood plasma were collected into 1 ml cryovials (Greiner Bio-One, Cat# 123280). Once PBMCs were isolated and counted, cells were resuspended in freezing medium (90% heat-inactivated foetal bovine serum (FBS) + 10% filter-sterile dimethyl sulfoxide (DMSO; Sigma-Aldrich, Cat# 472301)) at a density of 5-10 x 10^6 cells / ml and 1 ml aliquoted into each cryovial. To optimise cell viability, PBMC aliquots were slowly frozen to -80°C using a CoolCell (Corning, Cat# 432001), both PBMCs and plasma were stored at -80°C before use. For long-term storage, PBMCs were transferred on dry ice to liquid nitrogen.

2.4 MAGNETIC-ACTIVATED CELL SORTING

2.4.1 $CD4^+$ T cell isolation

For $CD4^+$ T cell magnetic-activated cell sorting (MACS) separation, PBMCs were incubated with CD4 MicroBeads (Miltenyi Biotec, Cat# 130-045-101), or CD4 MultiSort MicroBeads (Miltenyi Biotec, 130-055-101), diluted in MACS buffer (Table 2.1) for 15 mins at 4°C, 200 µl of beads were used for ~5 x 10^8 PBMCs, all reagents and dilutions used in MACS are detailed

in Table 2.7. Following incubation with the beads, PBMCs were washed with MACS buffer by centrifuging at 300 x g for 5 mins then discarding the supernatant. PBMCs were then resuspended in 1 ml of buffer ready to be run through an LS column (Miltenyi Biotec, Cat# 130-042-401) for separation. LS columns were inserted into a magnetic MidiMACS, or QuadroMACS Separator attached to a MultiStand (all Miltenyi Biotec, Cat# 130-042-302, 130-091-051, and 130-042-303 respectively) and pre-washed by running through 3 ml of MACS buffer just before use. PBMCs labelled with CD4 magnetic beads were passed through the column resulting in the attachment of only CD4 cells to the column and the run through of anything not labelled. Columns were washed 3 times further with 3 ml MACS buffer to fully clear the negative fraction. Columns were then removed from the magnet and the positive fraction (CD4-labelled cells) collected by forcing 5 ml MACS buffer through the column with a syringe plunger, purity >97% (Figure 2.1A-B). In later experiments, due to the discontinuation of the CD4 MultiSort MicroBead kit, the CD4 REAlease MicroBead kit (Miltenyi Biotec, Cat# 130-117-037) was used to positively select for $CD4^+$ T cells. PBMCs were resuspended in REAlease CD4-Biotin diluted in MACS buffer for 5 mins at RT, 100 µl of reagent was used for ~5 x 10^8 PBMCs. REAlease anti-Biotin MicroBeads were then added for an additional 5 mins at RT to bind CD4-Biotin-labelled cells to magnetic beads. Following incubation, PBMCs were immediately run through a pre-washed LS column and washed with 3 x 3 ml of MACS buffer, ensuring all liquid had run through the column before the next 3 ml was added. To collect the positive fraction, the column was removed from the magnet and 5 ml of REAlease Bead Release Reagent diluted in MACS buffer was forced through the column with a plunger. CD4-labelled cells were then incubated in REAlease Bead Release Reagent for 10 mins at RT to remove the magnetic beads. Purified $CD4^+$ cells were washed, counted with a counting

slide, and resuspended to a desired concentration in T cell medium for cell culture, or MACS buffer for further separation.

2.4.2 Isolation of naïve and memory cell subsets

For naïve $CD4^+$ T cell isolation, $CD4^+$ T cells were purified from PBMCs as described above using CD4 MultiSort MicroBeads (Table 2.7). After counting, $CD4^+$ cells were resuspended in MultiSort Release Reagent, from the CD4 MultiSort MicroBeads kit, diluted in 5 ml MACS buffer for 10 mins at 4°C, to release the magnetic CD4 MicroBeads bound to the cells. Cells were washed (300 x g for 5 mins), the supernatant was discarded, and cells were resuspended in a mix of MultiSort Stop Reagent, to stop the Release Reagent, and CD45RA MicroBeads (Miltenyi Biotec, Cat# 130-045-901) diluted in MACS buffer (100 µl total per 10^7 cells). After 15 mins of incubation at 4°C, cells were washed again, and resuspended in 1 ml MACS buffer. CD4 cells labelled with CD45RA magnetic beads were then run through a pre-washed LS column. Columns were washed with 3 ml MACS buffer 3 times more to wash through the negative fraction ($CD4^+CD45RA^-$ memory T cells) and the positive fraction ($CD4^+CD45RA^+$ naïve T cells) was again eluted by forcing 5 ml MACS buffer through the column with a syringe plunger, purity >70% (Figure 2.1A-B). Here, the negative fraction comprised of memory $CD4^+$ T cells and was retained. In later experiments, due to discontinuation of the CD4 MultiSort Kit, the CD4 REAlease MicroBead kit was used to positively select for $CD4^+$ cells and then $CD45RA^+$ cells. After incubation with Release Reagent, bead-free $CD4^+$ cells were washed and resuspended in CD45RA MicroBeads diluted in MACS buffer (100 µl total per 10^7 cells). As before, cells were incubated with the beads for 15 mins at 4°C then separated using a LS column, purity >75% (Figure 2.1A-B). Again, the negative fraction containing memory $CD4^+$ T

cells was kept. Both naïve and memory cell fractions were counted using a counting slide, then centrifuged at 300 x g for 5 mins, the supernatant was discarded, and cells were resuspended to a desired concentration in appropriate medium for cell culture.

Table 2.7 MicroBeads and reagents used in magnetic-activated cell sorting

MicroBeads and reagents	Dilution	Manufacturer
CD4 MicroBeads, human	1:5	Miltenyi Biotec
CD4 MultiSort MicroBeads, human	1:5	Miltenyi Biotec
MultiSort Release Reagent	1:50	Miltenyi Biotec
MultiSort Stop Reagent	3:10	Miltenyi Biotec
CD45RA MicroBeads, human	1:5-1:20	Miltenyi Biotec
REAlease CD4-Biotin	1:5	Miltenyi Biotec
REAlease Anti-Biotin MicroBeads	1:1	Miltenyi Biotec
REAlease Bead Release Reagent	1:50	Miltenyi Biotec

2.4.3 Analysis of cell purity

After MACS separation, a small number of cells (~200,000) from each desired fraction were removed and stained immediately for flow cytometric analysis of cell purity. Analysis was performed following the cell surface staining protocol described below in section 2.6.2. $CD4^+$ T cells were stained with anti-CD4, and naïve and memory T cell enrichments were stained with anti-CD4 and anti-CD45RA (all BioLegend, antibodies listed in Table 2.12). First, a lymphocyte gate based on forward (FSC-A) and side scatter (SSC-A) was identified, cells were then gated as single cells based on their equal forward scatter area (FSC-A) and forward scatter height (FSC-H). A dissimilarity here would indicate two cells stuck together with a low height but increased area, these cells need to be removed from future analysis as they may generate false data on co-expression. Cells were then gated as $CD4^+$ and further by expression of

CD45RA (Figure 2.1A). Purity was measured as the proportion of the desired population after excluding debris and gating on single cells (Figure 2.1B).

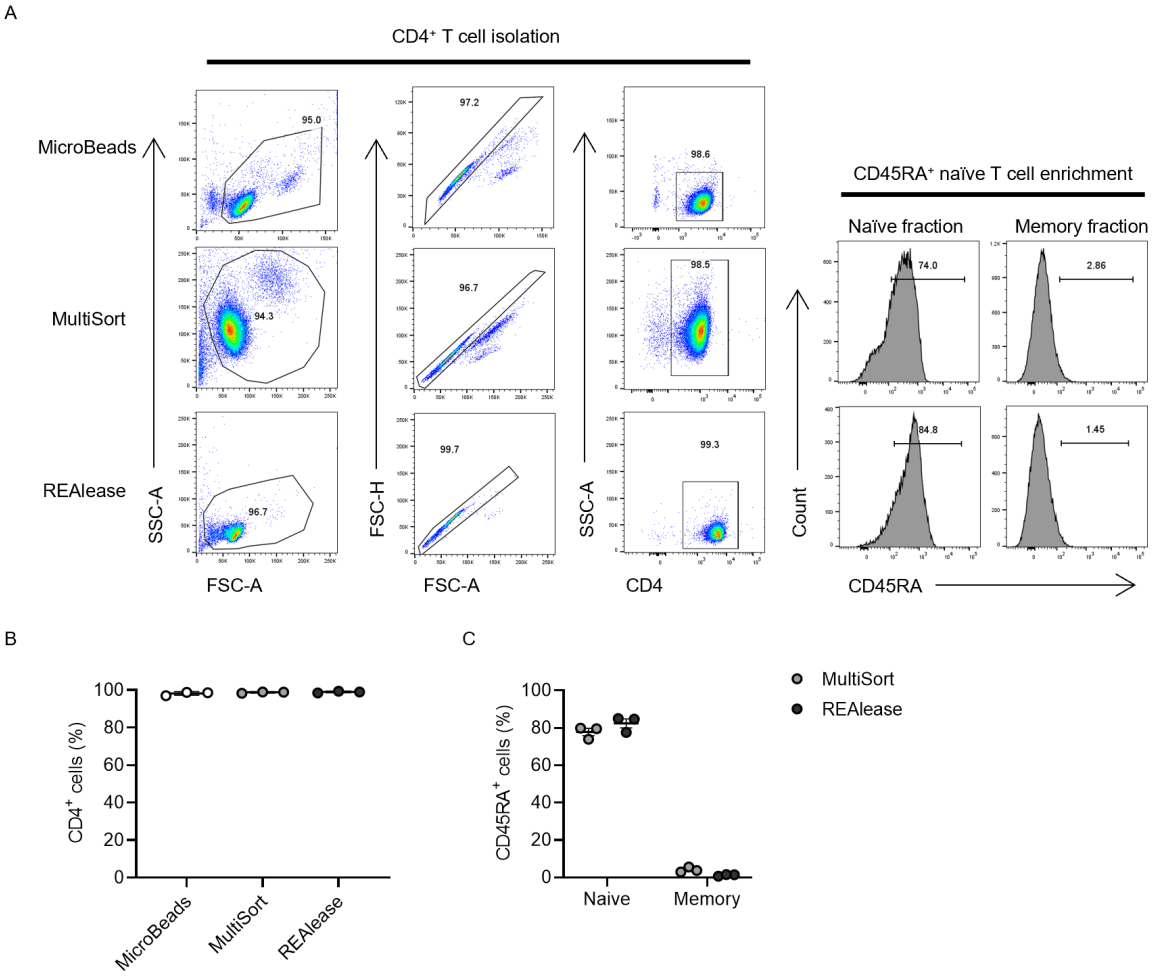

Figure 2.1 Purity of T cell isolation

(**A-C**) Cell purity of the desired populations was assessed following each method of cell separation. Forward (FSC-A) and side scatter (SSC-A) were first used to identify a lymphocyte gate. Cells were then gated by height (FSC-H) and area (FSC-A) to exclude doublets. Cells were gated on positive CD4 expression, then, for naïve CD4$^+$ T cell isolation cells were further gated as CD45RA$^+$. (**B-C**) Quantification of the percentage of (**B**) CD4$^+$ and (**C**) CD4$^+$CD45RA$^+$ cells isolated from PBMCs after CD4 T cell and naïve CD4 T cell isolation respectively (A-C, n=3 independent donors).

(B-C) Each symbol represents a different donor. Data is presented as the mean ± SD.

2.5 CELL CULTURE

2.5.1 Thawing frozen PBMCs

Frozen PBMC aliquots were removed from the -80°C freezer on dry ice and transferred to a water bath pre-warmed to 37°C. Once just thawed, PBMCs were transferred into 10 ml of pre-warmed, sterile RPMI + 1% P/S + 10% FBS (RPMI/10% FBS) and centrifuged at 300 x g for 5 mins. The supernatant was discarded, and cells were again washed in 10 ml of warmed RPMI/10% FBS. Following removal of the supernatant, PBMCs were resuspended in T cell medium (Table 2.2) at a density of 2 x 10^6 cells/ml and added to a 6 well plate. Cells were rested overnight in an incubator at 37°C before staining for flow cytometry the next day.

2.5.2 T cell activation

$CD4^+$ T cells were cultured at a density of 1 x 10^6 cells/ml in T cell culture medium, unless otherwise indicated. $CD4^+$ T cells were activated using 12 µl/ml ImmunoCult Human CD3/CD28 T Cell Activator (STEMCell, Cat# 10971), unless otherwise stated. For the studies utilising a low dose of activation, 1.2 µl/ml of T cell activator was used. In experiments using anti-CD3 stimulation alone or in combination with anti-CD28, 1 µg/ml soluble anti-CD3 and 5 µg/ml soluble anti-CD28 (both BioLegend) were added to cell culture (Table 2.8).

Table 2.8 Antibodies used in T cell activation

Antibody	Clone	Isotype	Stock conc.	Dilution	Manufacturer (Cat#)
Ultra-LEAF Purified anti-human CD3	OKT3	Mouse IgG2a, κ	1 mg/ml	1:800	BioLegend (317326)
Ultra-LEAF Purified anti-human CD28	CD28.2	Mouse IgG1, κ	1 mg/ml	1:1000	BioLegend (302934)

2.5.3 Cytokine blocking antibodies

Blocking antibodies and the relevant isotype control were added at a working concentration of 5 µg/ml immediately prior to T cell activation and remained present for the duration of cell culture (Table 2.9).

Table 2.9 Cytokine blocking, and isotype control antibodies used in cell culture

Antibody	Clone	Isotype	Stock conc.	Dilution	Manufacturer (Cat#)
Ultra-LEAF Purified anti-human IFN-γ	NIB42	Mouse IgG1, κ	1 mg/ml	1:200	BioLegend (502405)
Ultra-LEAF Purified anti-human TNF-α	MAb1	Mouse IgG1, κ	1 mg/ml	1:200	BioLegend (502806)
Ultra-LEAF Purified Mouse IgG1, κ (Isotype control)	MOPC-21	Mouse IgG1, κ	2.5 mg/ml	1:500	BioLegend (400166)

2.5.4 Inhibitors

To inhibit mTOR, rapamycin (Sigma-Aldrich, Cat# 553210) was added to cell culture immediately prior to T cell activation. Rapamycin was prepared to a stock concentration of 5 mg/ml in DMSO and used at 20 ng/ml in the well. LY294002 (Cell Signalling, Cat# 9901) was used in cell cultures to fully inhibit PI3K, LY294002 was dissolved in DMSO to a 50 mM stock and used at 50 nM. Akt inhibitor (Akti-1/2) (abcam, Cat# ab142088) was dissolved in DMSO to a stock concentration of 5 mM, concentrations in the well ranged from 0.3 - 2.5 µM, specific details for each experiment are described in figure legends. To prevent the cleavage of mTNF-α, TAPI-0 (Sigma-Aldrich, Cat # 579050), an inhibitor of TACE, was added to naïve $CD4^+$ T cell cultures at 10 µM. TAPI-0 was dissolved in DMSO to a stock concentration of 10 mM. All

inhibitors were stored in aliquots at -20°C. Control wells were treated with the relevant concentration of DMSO.

2.5.5 T cell differentiation

Purified naïve $CD4^+$ T cells were plated at a density of 1 x 10^6/ml in AIM V serum-free medium (Gibco, Cat# 12055091) with 50 IU/ml recombinant human (rh)IL-2. Cells were activated with ImmunoCult T Cell Activator, anti-CD3 and anti-CD28, or anti-CD3 alone, details for each experiment can be found in figure legends. Cells in the Th1 condition were differentiated with 20 ng/ml rhIL-12, and 2.5 μg/ml anti-IL-4. Th17 cells with 30 ng/ml rhIL-23, 30 ng/ml rhIL-6, 20 ng/ml rhIL-1β, 2 ng/ml rhTGF-β, 2.5 μg/ml anti-IL-4, and 1 μg/ml anti-IFNγ (all blocking antibodies from BioLegend, detailed in Table 2.10). Treg cells were differentiated with 5 ng/ml rhTGF-β (all cytokines from PeproTech, IL-12 Cat# 200-12H, IL-23 Cat# 200-23, IL-6 Cat# 200-06, IL-1β Cat# 200-01B, TGF-β Cat# 100-21). Cells were incubated for 3 days at 37°C. On day 3, AIM V medium pre-warmed to 37°C was added at a volume equal to that in the well and cells were incubated for a further 3 days at 37°C before analysis.

Table 2.10 Cytokine blocking antibodies used in T cell differentiation

Antibody	Clone	Isotype	Stock conc.	Dilution	Manufacturer (Cat#)
Ultra-LEAF Purified anti-human IFN-γ	NIB42	Mouse IgG1, κ	1 mg/ml	1:1000	BioLegend
Ultra-LEAF Purified anti-human IL-4	MP4-25D2	Rat IgG1, κ	1 mg/ml	1:400	BioLegend (500837)

2.6 FLOW CYTOMETRY

For flow cytometry, ~200,000 cells per condition were added to a 96-well plate. For assessment of TF and cytokine expression by intracellular staining, cells were first activated

for 4 h by the addition of Cell Activation Cocktail with Brefeldin A (BioLegend, Cat# 423303), containing phorbol 12-myristate-13-acetate (PMA) (40.5 μM), ionomycin (670 μM), and brefeldin A (2.5 mg/ml), diluted 1:500 into the well. When analysing PBMCs from RA patient and HC peripheral blood, cells were instead activated for 4 h with 12 μl/ml ImmunoCult Human CD3/CD28 T Cell Activator in combination with 10 μM brefeldin A (Invitrogen, Cat# 297140050) if analysing TF and cytokine expression, or without brefeldin A if analysing surface TNF-α or phosphorylated (p)-Akt. Brefeldin A was reconstituted in DMSO to a stock concentration of 10 mM.

2.6.1 Fluorescent mitochondrial probes

After culture, cells were resuspended in 200 μl of fluorescent mitochondrial probe cocktail diluted in pre-warmed T cell medium and incubated for 20 mins at 37°C to maintain normal metabolic function of the cells. Fixable Viability Dye eFluor 780 (eBioscience, Cat# 65-0865-14) was included in the staining cocktail at a dilution of 1:1000 to assess cell viability. If using cell surface antibodies for co-staining, these were also included in the cocktail with the fluorescent mitochondrial probes. MitoView Green (MVG; Biotium, Cat# 70054) was used to measure mitochondrial mass and MitoSpy Orange (MSO; BioLegend, Cat# 424803) was used to measure mitochondrial membrane potential. Both were reconstituted in DMSO to the stock concentration listed in Table 2.11, aliquots were stored at -20°C. As a negative control for MSO, carbonyl cyanide 4-(trifluoromethoxy) phenylhydrazone (FCCP; Cayman Chemical, Cat# 15218) was also included to uncouple the membrane potential. FCCP was dissolved in DMSO to a concentration of 100 mM then further diluted 1:10 to a stock concentration of 10 mM in PBS, aliquots were stored at -20°C. Fluorescent mitochondrial probes (Table 2.11)

and antibodies (Table 2.12) used in flow cytometry are detailed in the tables below. Immediately following incubation, 150 µl of ice-cold staining buffer was added to each well to stop further metabolic reaction in the cells. The plate was centrifuged at 300 x g for 4 mins and the supernatants were discarded. Cells were washed once more in 200 µl staining buffer and supernatants removed. Cells were resuspended and transferred to fluorescent-activated cell sorting (FACS) tubes in 200 µl of staining buffer. Samples were kept in the dark on ice and analysed within the hour.

Table 2.11 Fluorescent mitochondrial probes and relevant control treatments used in flow cytometry

Reagent	Detection channel	Stock conc.	Dilution	Manufacturer
MVG	FITC	200 µM	1:4000	Biotium
MSO	PE	1 mM	1:40000	BioLegend
FCCP	-	10 mM	1:2000	Cayman Chemical

2.6.2 Surface staining

If using Zombie NIR Fixable Viability dye (BioLegend, Cat# 423105), cells were first washed once in PBS (300 x g for 4 mins), the supernatants were discarded, then cells were resuspended in 50 µl Zombie NIR Fixable Viability dye diluted 1:2000 in PBS. Cells were Incubated for 15 mins in the dark at RT. To wash the cells following incubation, 150 µl of ice-cold staining buffer was added to each well before centrifugation at 300 x g for 4 mins. Supernatants were discarded and cells were washed once more in 200 µl staining buffer. After the supernatants were removed, cells were resuspended in 50 µl of antibody cocktail diluted in staining buffer. If using Fixable Viability Dye eFluor 780, cells were first washed twice in staining buffer, then incubated with the antibody cocktail containing Fixable Viability Dye

eFluor 780 (1:1000). After 30 mins incubation in the dark at 4°C, cells were washed as before and either transferred to FACS tubes in 200 µl staining buffer for analysis or prepared for intracellular staining.

2.6.3 Intracellular staining

After surface staining, cells were fixed and permeabilised using Foxp3 / Transcription Factor Staining Buffer Set (eBioscience, Cat# 00-5523-00). Cells in each well were resuspended in 50 µl fixative solution, made up of 1 part Fixation Concentrate and 3 parts Fixation Diluent, and incubated at 4°C for 20 mins. Permeabilisation (Perm) Buffer was diluted 1:10 in deionised (d)H_2O and 150 µl added to each well after fixation. Cells were centrifuged at 300 x g for 4 mins and the supernatants removed. Cells were washed once more with 200 µl of Perm Buffer and the supernatants discarded. To each well, 50 µl of intracellular antibody cocktail diluted in Perm Buffer was added and cells were incubated for 30-60 mins in the dark at RT. Panels including RORγt or T-bet antibodies were incubated in the dark overnight at 4°C to increase signal intensity. Cells were washed as before and, if required, resuspended here in 50 µl of secondary antibody, Donkey anti-rabbit IgG (BioLegend, Cat# 406410), diluted 1:100 in staining buffer for 20 mins in the dark at 4°C. Fluorescent and primary, unconjugated antibodies used in flow cytometry are detailed in Table 2.12 and Table 2.13 respectively. If stained with a secondary antibody, cells were washed for a final two times as before. Cells were resuspended in 200 µl staining buffer and transferred to FACS tubes for flow cytometric analysis.

2.6.4 Staining of phosphorylated proteins

Cells added to a 96 well plate straight from culture were centrifuged at 300 x g for 5 mins and the supernatants discarded. Cells were then immediately resuspended in 100 µl of pre-warmed fixative solution and incubated at 37°C for 20 mins. Following incubation, cells were centrifuged at 300 x g for 4 mins and the supernatants discarded. Cells were then washed once more with 200 µl of staining buffer and centrifuged at 300 x g for 4 mins. After the supernatants were discarded, cells were resuspended in 50 µl of primary antibody diluted in Perm Buffer and stained for 30 mins at RT. Following staining, cells were washed twice in Perm Buffer as before. Cells were then resuspended in 50 µl secondary antibody, Donkey anti-Rabbit IgG1, diluted 1:100 in staining buffer for 20 mins at RT. Primary antibodies used in intracellular flow cytometry of phosphorylated proteins (phospho-flow) are listed in Table 2.13. Samples were washed twice more and transferred to FACS tubes in 200 µl staining buffer.

2.6.5 Kynurenine assay

L-Kynurenine (Sigma-Aldrich, Cat# K8625) was reconstituted in DMSO to a stock solution of 80 mM, aliquots were stored at -80°C. An inhibitor of the kynurenine transporter, LAT1, 2-Amino-2-norbornanecarboxylic acid (BCH; Sigma-Aldrich, Cat# A7902) was dissolved in Hanks' Balanced Salt Solution (HBSS; Gibco, Cat# 24020117) to a stock concentration of 40 mM and stored at -20°C for up to one month. Kynurenine was diluted to a concentration of 800 µM in HBSS and, along with an aliquot of BCH, was added to the incubator to pre-warm to 37°C. Cells were resuspended in 100 µl pre-warmed HBSS, to each well, 50 µl of kynurenine was added to reach a concentration of 200 µM in the well, then either 50 µl of 40 mM BCH (final concentration 10 mM) was added to inhibit the transport of kynurenine, or wells were

topped up with 50 µl HBSS to reach a total volume of 200 µl. Cells were incubated for 15 mins at 37°C. Immediately following incubation, 70 µl of 4% formaldehyde (Thermo Scientific, Cat# J60401-AK) was added to each well to fix the cells. After 30 mins at RT, cells were washed twice with staining buffer and supernatants discarded. Cells were resuspended in 200 µl staining buffer and transferred to FACS tubes for analysis by flow cytometry.

2.6.6 Flow cytometric analysis

All samples were run on the BD LSRFortessa X-20 (BD Biosciences) and data collected using BD FACSDiva Software (BD Biosciences). Compensation was calculated using single stain controls for each fluorochrome, 1 µl of antibody was added to 1 drop of UltraComp eBeads (Invitrogen, Cat# 01-2222-42) for 15 mins on ice before 400 µl of staining buffer was added and FACS tubes were centrifuged at 300 x g for 5 mins. Supernatants were discarded and stained beads were resuspended in 400 µl of staining buffer ready for use. All analysis was performed using FlowJo version (v)10.8.1 (BD Biosciences), Microsoft Excel, and GraphPad Prism 9.

Table 2.12 Fluorescent antibodies used in flow cytometry

Target	Conjugate	Clone	Stock conc.	Dilution	Manufacturer (Cat#)
CD4	BV785	OKT4	80 µg/ml	1:50-100	BioLegend (317442)
CD69	APC	FN50	100 µg/ml	1:100	BioLegend (985206)
CD25	BV605	BC96	100 µg/ml	1:100	BioLegend (302610)
	AF700	M-A251	100 µg/ml	1:100	BioLegend (356118)
CCR4	BV421	L291H4	50 µg/ml	1:50-100	BioLegend (359414)
CCR6	BV605	G034E3	50 µg/ml	1:50-100	BioLegend (353420)
CXCR3	AF647	G025H7	100 µg/ml	1:50-100	BioLegend (353712)
	AF700	G025H7	100 µg/ml	1:50-100	BioLegend (353742)
CD127	APC	A019D5	200 µg/ml	1:100	BioLegend (351316)
TNFR1 (CD120a)	APC	W15099A	100 µg/ml	1:50	BioLegend (369906)
TNFR2 (CD120b)	PE/Dazzle 594	3G7A02	50 µg/ml	1:50	BioLegend (358414)
CD45RA	BV421	HI100	6 µg/ml	1:100	BioLegend (304130)
	BV650	HI100	25 µg/ml	1:100	BioLegend (304136)
CD45RO	BV711	UCHL1	35 µg/ml	1:100	BioLegend (304236)
IκBα	PE	3D6C02	25 µg/ml	1:50	BioLegend (662412)
RORγt	BV650	Q21-559	6 µg/ml	1:50	BD Biosciences (563424)
	AF647	Q21-559	50 µg/ml	1:50	BD Biosciences (563620)

T-bet	PE	4B10	200 µg/ml	1:50	BioLegend (644810)
	BV605	4B10	200 µg/ml	1:50	BioLegend (644817)
FoxP3	PE	206D	60 µg/ml	1:100	BioLegend (320108)
	AF647	206D	60 µg/ml	1:100	BioLegend (320114)
IFN-γ	FITC	B27	50 µg/ml	1:100	BioLegend (506504)
TNF-α	BV650	MAb11	100 µg/ml	1:50-100	BioLegend (502938)
IL-10	PE	JES3-9D7	25 µg/ml	1:50	BioLegend (501404)
	BV421	JES3-9D7	40 µg/ml	1:50	BioLegend (501422)
IL-17A	AF488	BL168	30 µg/ml	1:50	BioLegend (512308)
	BV711	BL168	30 µg/ml	1:50	BioLegend (512328)
Acetyl-Histone H3 (Lys27)	PE	D5E4	25 µg/ml	1:100	Cell Signalling Technology (8173)
Donkey anti-rabbit IgG	BV421	Poly4064	100 µg/ml	1:100	BioLegend (406410)

Table 2.13 Primary, unconjugated antibodies used in flow cytometry

Target	**Clone**	**Host**	**Dilution**	**Manufacturer (Cat#)**
Phospho-Akt (T308)	C31E5E	Rabbit	1:100	Cell Signalling Technology (2965)
Phospho-p70S6K (Thr421/Ser424)	Polyclonal	Rabbit	1:100	Cell Signalling Technology (9204)
c-Myc	E5Q6W	Rabbit	1:200	Cell Signalling Technology (18583)
Akt (pan)	11E7	Rabbit	1:100	Cell Signalling Technology (4685)

2.7 MEASURING CYTOKINE LEVELS IN MEDIA

2.7.1 Enzyme-linked immunosorbent assay

Supernatants were collected from cells in culture into a 96 well plate at the time point stated and stored at -20°C until analysis. Quantification of IFN-γ and TNF-α production was performed using standard human IFN-γ and TNF-α enzyme-linked immunosorbent assay (ELISA) respectively. For IFN-γ quantification, 50 µl anti-human IFN-γ capture antibody (Bio-Rad, Clone AbD00676, Cat# HCA043) diluted in PBS (0.8 µg/ml) was added to each well of a Nunc MaxiSorp 96-well plate (ThermoFisher, Cat# 44-2404-21) and incubated overnight at 4°C to coat the plate. The following day, the antibody was removed and 200 µl of blocking buffer (1% bovine serum albumin (BSA; Sigma-Aldrich, Cat# A2153) + 0.05% polysorbate 20 (Tween-20; Thermo Scientific, Cat# L15029-AP) in PBS) was added for 1 hour at RT. The plate was washed 4 times with wash buffer (0.05% Tween-20 in PBS) before 50 µl of standard or sample was added to each well for incubation either overnight at 4°C or for 2-3 h at RT. The top rhIFN-γ (Bio-Rad, Cat# PHP050) standard was made by diluting the stock solution (200 ng/ml) 1:20, subsequent standards were prepared by serial dilution in blocking buffer for 10,000 – 312.5 pg/ml IFN-γ. Supernatants were diluted appropriately in relevant cell culture medium in order for the IFN-γ concentration to sit within the standard curve. Wells were washed 4 times and 50 µl of biotinylated detection anti-IFNγ antibody (Bio-Rad, Clone 2503, Cat# HCA044P) diluted in blocking buffer (0.4 µg/ml) was added to each well for 1 hour at RT. The plate was again washed 4 times and 50 µl of ExtrAvidin-Peroxidase (Sigma-Aldrich, Cat# E2886) diluted 1:1000 in blocking buffer was added for 30 mins at RT. The plate was washed 6 times before the addition of 100 µl of TMB Substrate Reagent Set (1:1, Reagent A:Reagent B; BD Biosciences, Cat# 555214) for 5-10 mins, until the blue colour developed.

Once developed, 100 µl of 1M hydrochloric acid (HCl) was added to each well to stop the reaction.

TNF-α was quantified using TNF alpha human matched antibody pair and ELISA buffer kit (both Invitrogen, Cat# CHC1753 and CNB0011 respectively). Anti-human TNF-α capture antibody was diluted in Coating Buffer A (2 µg/ml) and 100 µl added to each well of a Nunc MaxiSorp 96-well plate. Plates were incubated overnight at 4°C to coat the wells. The next day, the antibody was removed, and the plate washed once with Wash Buffer (diluted 1:25 in dH_2O). To each well, 300 µl of Assay Buffer (diluted 1:5 in dH_2O) was added for 1 hour at RT to block the plate. Lyophilised rhTNF-α was reconstituted to a stock concentration of 10,000 pg/ml in Assay Buffer and stored in aliquots at -80°C. The top standard was prepared by diluting the stock concentration 1:10, then subsequent standards were prepared by serial dilution of TNF-α in Assay Buffer from 1,000 - 15.6 pg/ml. The plate was then washed 5 times with Wash Buffer and 100 µl of standard or sample was added to each well followed immediately by 50 µl of biotinylated TNF-α detection antibody diluted to 0.32 µg/ml in Assay Buffer. The plate was gently agitated on a Vibrax-VXR plate shaker (IKA) at ~600 rpm for 2 h at RT. The plate was washed 5 times and 100 µl of streptavidin-HRP diluted 1:625 in Assay Buffer was added for a further 30 mins on the plate shaker at RT. The plate was again washed 5 times before addition of 100 µl of Stabilised Chromogen. Once the blue colour of the assay was sufficiently developed, 100 µl of Stop Solution was added to each well. Absorbance was measured using a SpectraMax ABS Plus Microplate Reader (Molecular Devices) at 450 nm, data collected using SoftMax Pro (Molecular Devices), and analysis performed using GraphPad Prism 9.

2.7.2 LEGENDplex assay

Supernatants were harvested on day 6 of culture into a 96 well plate and stored at -20°C until analysis. Concentrations of IL-6, IL-22, IL-10, IL-17A, and IL-17F were analysed using the LEGENDplex human Th17 panel kit (7-plex) (BioLegend, Cat# 741032) according to the manufacturer's instructions. A mix of Antibody-Immobilized Beads was made by adding each individual bead reagent to the mix at a dilution of 1:13, the mix was then made up to the final volume with Assay Buffer. Supernatants were added to a 96 well V-bottom plate at a volume of 25 µl along with 25 µl of Assay Buffer and 25 µl of mixed beads. The plate was covered with a film and aluminium foil to protect it from light. The plate was then gently agitated on a plate shaker at ~800 rpm for 2 h at RT. The plate was washed once by adding 200 µl of Wash Buffer (diluted 1:20 with dH_2O) to each well and centrifuging the plate at 300 x g for 5 mins. The supernatants were discarded and 25 µl of biotinylated Detection Antibodies were added to each well before the plate was covered with a new film and foil and incubated for 1 h on the plate shaker at RT. Immediately following this, 25 µl of streptavidin (SA)-PE was added to each well, the plate covered with a new film and foil, and incubated for a further 30 mins on the plate shaker at RT. The plate was washed again, the supernatants discarded, and samples resuspended in 200 µl of staining buffer to be transferred to FACS tubes for flow cytometric analysis. Samples were acquired on the BD LSRFortessa X-20 and analysed using the LEGENDplex Data Analysis Software Suite (BioLegend).

2.8 MEASURING GENE EXPRESSION

2.8.1 Preparation of RNA

From cell culture of 4 x 10^6 cells per condition, cells were harvested into 1.5 ml tubes and centrifuged at 300 x g for 5 mins. The supernatant was discarded, and cell pellets were resuspended in 1 ml of ice-cold PBS, the cells were centrifuged again, and the supernatant removed. Immediately, the cell pellets were snap frozen on dry ice. Samples were stored at -80°C until RNA extraction was performed using the NucleoSpin RNA Mini Kit (Macherey-Nagel, Cat# 740955.50) according to manufacturer's instructions. After thawing on ice, 350 µl of RA1 buffer + 3.5 µl β-mercaptoethanol (Sigma-Aldrich, Cat# M6250) was added to each cell pellet. Samples were vortexed to disrupt the pellet and all liquid transferred to a NucleoSpin Filter tube before centrifuging at 11,000 x g for 1 min. To the filtered sample collected in the 2 ml collection tube, 350 µl of 70% ethanol was added and mixed well until clear, this lysate was then added to a NucleoSpin RNA Column and centrifuged at 11,000 x g for 30 seconds. The column was added to a new 2 ml collection tube and 350 µl of membrane desalting buffer was added. The samples were centrifuged for 1 min at 11,000 x g and the column moved to a new collection tube. To remove DNA, a DNase reaction mixture was prepared (1:10, recombinant (r)DNase:rDNase reaction buffer) and 95 µl added directly to the bottom of the column, the samples were then incubated for 15 mins at RT. After incubation, 200 µl of RAW2 buffer was added to the column and samples were centrifuged for 30 s at 11,000 x g. The column was moved to a new collection tube and 600 µl of RA3 buffer was added. Samples were centrifuged again for 30 secs and the liquid in the collection tube was discarded. A final wash of 250 µl RA3 buffer was added to the column and the tubes centrifuged at 11,000 x g for 2 mins. The columns were then transferred to a 1.5 ml collection

tube and 30 µl of RNase-free water was added directly to the bottom of the column. The tubes were centrifuged at 11,000 x g for 1 min to elute the RNA into the tube. RNA concentrations were determined using the Nanodrop 1000 (ThermoFisher). RNA samples were stored at -80°C.

2.8.2 RNA-sequencing

RNA samples were submitted to Genomics Birmingham for RNA-sequencing (RNA-seq). Each sample was checked using Qubit High Sensitivity RNA assay (Invitrogen) and an RNA ScreenTape on TapeStation (both Agilent). Sequencing libraries were prepared from 75 ng RNA using QuantSeq 3' mRNA-Seq Library Prep Kit (Lexogen) then quantified using Qubit High Sensitivity DNA assay and High Sensitivity D100 tape. Pooled libraries were sequenced using the NextSeq 500 with a NextSeq High 75 v2.5 flow cell (Illumina).

FASTQ files were downloaded from BaseSpace (Illumina) and uploaded to BlueBEAR, the high performance computing platform at the University of Birmingham, for further analysis. The command line interface of the server was accessed using MobaXterm v21.5 (Mobatek). All 4 lanes were merged to create the final FASTQ file for each sample which were then quality checked by FastQC v0.11.9 (Andrews, 2010). BBDuk v37.99 from the BBMap suite (Bushnell, 2014) was used for trimming low-quality reads, poly(A) tails, and ribosomal (r)RNA and adapter contamination. Samples were then checked again by FASTQC. Quality trimmed FASTQ files were aligned to the human GRCh83 genome with gencode v39 annotation using STAR v2.7.2b aligner (Dobin *et al.*, 2013). BAM files generated by STAR aligner were used with HTSeq-count v0.13.5 (Anders *et al.*, 2015) to generate raw read counts. The raw read counts

were then used for further analysis by DESeq2 v1.30.1 (Love *et al.*, 2014) in R v4.0.5 using RStudio v2022.07.01.554.

Data were filtered to remove genes where less than 6 samples had a normalised count of 10 or higher. Differentially expressed genes (DEGs) were identified as those with an adjusted p-value ≤ 0.05, DESeq2 uses Benjamini-Hochberg method to minimise false discovery rate (FDR). Principal component analysis (PCA) plots were made using DESeq2. Volcano plots created using the R package ggplot2 v3.3.5 (Wickham *et al.*, 2016). For individual genes, the normalised counts generated by DESeq2 are presented. Heatmap analysis was performed on the normalised count data using gplots v3.1.1 (Warnes *et al.*, 2015). For gene ontology pathway analysis, ENSEMBL IDs were converted to gene symbols using org.Hs.eg.db v3.12.0 (Carlson, 2019), then the ENTREZ IDs of the genes were found. Pathway analysis using the ENTREZ IDs was performed by clusterProfiler v3.18.1 (Yu *et al.*, 2012). Venn diagram generated using Venny v2.1 (Oliveros, 2007).

2.9 MEASURING CELLULAR METABOLISM

2.9.1 Seahorse extracellular flux assay

Oxygen consumption rate (OCR, pmol/min) and extracellular acidification rate (ECAR, mpH/min) were measured using the Seahorse XFe96 Metabolic Flux Analyzer (Agilent). Prior to use, the sensor cartridge (Agilent, Cat# 102416-100) was hydrated overnight by placing it in 200 µl of autoclaved dH_2O at RT. On the day of Seahorse assay, dH_2O was removed from the plate and 200 µl of Seahorse extracellular flux (XF) Calibrant Solution (Agilent, Cat# 102416-100) pre-warmed to 37°C was added to each well. The probes were then returned to the plate into the calibrant solution for a few hours before running the assay. In

order for the probes to take measurements accurately, the cells must be in an even layer at the bottom of the well. To adhere the cells, 30 µl of either poly-d-lysine (Gibco, Cat# A3890401) or Cell-Tak (Corning, Cat# 10317081; diluted 1:15 in sterile sodium bicarbonate ($NaHCO_3$; Sigma-Aldrich, Cat# S6014) pH 8) was added to each well of the 96-well cell culture plate (Agilent, Cat# 102416-100) for 1-2 h at RT. Before cells were added, wells were washed twice with autoclaved dH_2O and left to dry at RT. From culture, (~3 x 10^6 cells per condition) cells were harvested and washed twice in 2 ml unbuffered Seahorse XF medium pH 7.4 (Table 2.4), pre-warmed to 37°C. To wash, cells were centrifuged at 300 x g for 5 mins and the supernatants discarded. Each sample was counted using a haemocytometer and cells were added to the 96-well cell culture plate at a density of 2.5 x 10^5 cells/well in 75 µl of Seahorse XF medium. To ensure the cells were stuck in an even layer to the bottom of the well, the plate was pulsed in a centrifuge at 50 x g with acceleration 3 and no brake until full speed was reached. Each well was carefully topped up to 175 µl with Seahorse XF medium and the plate was kept incubated at 37°C in a no CO_2 incubator to prevent acidification of the unbuffered medium. Mitochondrial respiration and glycolysis were measured using the Seahorse XF Mito Stress Test (Figure 2.2A-B). Each port contained 25 µl of compound diluted in Seahorse XF medium, which was injected sequentially during the assay to generate a metabolic profile of the cells (Table 2.14). Basal respiration, ATP-coupled respiration, spare respiratory capacity (SRC), maximal (max.) respiration, basal ECAR, and max. ECAR were all calculated as demonstrated in Figure 2.2A-B.

After the assay finished running, the number of cells in each well was quantified by staining the amount of DNA present using CyQUANT Direct Cell Proliferation Assay (Invitrogen, Cat# C35011). From each well, 200 µl of medium was removed, leaving 50 µl. To this, 25 µl of

CyQUANT reagent mix was added and cells were incubated for 1 h at RT. CyQUANT reagent mix contained 1:50 background suppressor and 1:250 nucleic acid stain in unsupplemented Seahorse XF medium. Following incubation, fluorescence was read from the bottom of the well at 480 nm using a FLUOstar Omega Microplate Reader (BMG Labtech). Data collected using MARS Data Analysis software (BMG Labtech). To account for differences in number of cells plated, OCR and ECAR measurements for each well were normalised to CyQUANT values. Analysis was performed using Wave Software and BD Biosciences FlowJo v10.

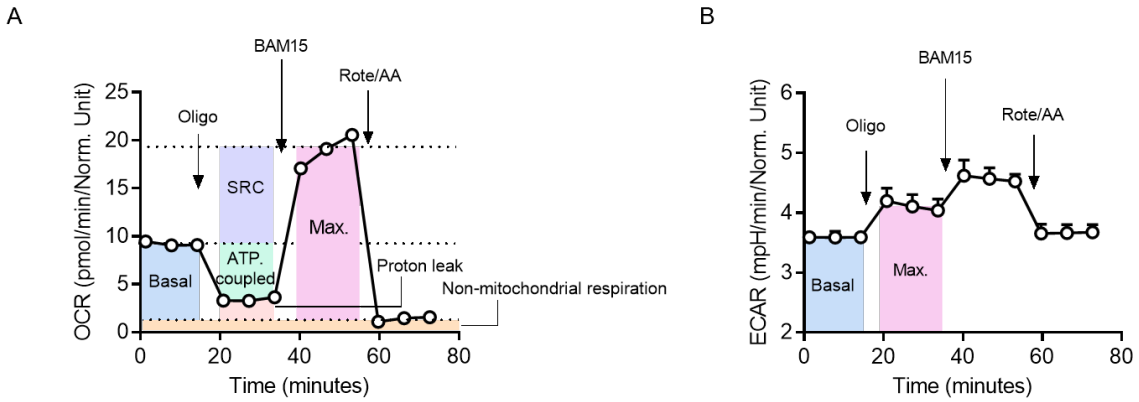

Figure 2.2 Schematic diagram of Seahorse extracellular flux assay calculations

(**A**) Seahorse plot of oxygen consumption rate (OCR) detailing the four measurements calculated as below. Arrows show time of injection of the indicated compounds: oligomycin (oligo), BAM15, and rotenone/antimycin A (rote/AA). Basal non-corrected (nc) refers to the initial 3 measurements before oligo injection. For each period after an injection the mean of all 3 measurements is taken.

(1) Basal respiration (OCR) = [OCR(basal nc)] – [OCR(rote/AA)]

(2) ATP-coupled respiration = [OCR(basal nc)] – [OCR(oligo)]

(3) Maximal (max.) respiratory capacity = [OCR(BAM15)] – [OCR(rote/AA)]

(4) Spare respiratory capacity (SRC) = [OCR(BAM15)] – [OCR(basal nc)]

(**B**) Seahorse plot as in (A) of extracellular acidification rate (ECAR) detailing the two measurements calculated as below.

(1) Basal ECAR = [ECAR(basal nc)]

(2) Max. ECAR = [ECAR(oligo)]

Table 2.14 Compounds used in extracellular flux analysis

Compound	Port	Conc. in port	Final conc.	Manufacturer (Cat#)
Oligomycin	A	8 µM	1 µM	Sigma-Aldrich (O4876)
BAM15	B	27 µM	3 µM	Sigma-Aldrich (SML1760)
Rotenone	C	20 µM	2 µM	Sigma-Aldrich (R8875)
Antimycin A	C	20 µM	2 µM	Sigma-Aldrich (A8674)

2.9.2 Stable isotope tracing

After culture of ~4 x 10^6 cells/well, cells were harvested into 15 ml tubes and centrifuged at 300 x g for 5 mins. The supernatant was discarded, and cells were resuspended in 2 ml of PBS, then centrifuged again and the supernatant discarded. The cells were finally resuspended in 3 ml tracing medium (Table 2.5) and re-plated into a 6 well plate. For glucose tracing, 10 mM U-$^{13}C_6$-glucose (CK Isotopes, Cat# CLM-1396) and 2 mM L-glutamine (Sigma Aldrich) were added to each well and cells were incubated for 4 h at 37°C. For glutamine tracing, 2 mM $^{13}C_5$-glutamine (CK Isotopes, Cat# CLM-1822-H) and 10 mM glucose (Sigma Aldrich) were added to each well before incubation for 6 h at 37°C. Following incubation, cells were harvested into tubes kept on ice and counted using a haemocytometer. Cells were centrifuged at 300 x g for 5 mins at 4°C and the supernatant removed. Cells were transferred to a 1.5 ml tube in 1 ml of ice-cold saline (0.9% sodium chloride (NaCl; J.T.Baker) in dH_2O) and washed twice more, centrifuging at 300 x g for 5 mins at 4°C. After the final supernatant was discarded the cell pellet was snap frozen on dry ice and stored at -80°C.

For extraction of metabolites, cell pellets were thawed on ice and mixed well with 500 µl ice-cold methanol (Sigma-Aldrich, Cat# 34860) to disrupt the pellet and quench metabolic activity. To this, 200 µl of pentanedioic-d_6 acid (C/D/N Isotopes Inc., Cat# D-5227) at a

concentration of 8.75 µg/ml in high-performance liquid chromatography (HPLC)-grade H_2O (Thermo Scientific, Cat# 11338217) was added to ensure 1.75 µg of pentanedioic-d_6 acid was present in each sample for use as an internal standard. Next, 500 µl of ice-cold chloroform (Sigma-Aldrich, Cat# 366927) was added to each sample with the use of Solvent Safe tips (Molecular BioProducts, Cat# 5079EB). Samples were repeatedly inverted with the use of a Tube Rotator (Fisher Scientific) for 15 mins at 4°C, then centrifuged at 12,000 x g for 15 mins at 4°C. The top layer, containing the polar metabolites, of the solution was transferred to a 1.5 ml tube and stored at -20°C. Samples were evaporated using a CentriVap Concentrator (Labconco) under vacuum and submitted to the Metabolic Tracer Analysis Core at University of Birmingham to be analysed by gas chromatography-mass spectrometry (GC-MS). Data were provided as mass isotopomer distribution (MID), and metabolite abundance normalised to the internal standard.

2.9.3 Glucose and lactate concentrations

Supernatants were harvested at 48 h and stored at -20°C before analysis. Analysis of glucose and lactate concentrations in the supernatants were performed by Dr Jonathan Barlow at the Mitochondrial Profiling Centre, University of Birmingham using Glucose-Glo (Promega, Cat# J6021) and Lactate-Glo Assays (Promega, Cat # J5021) respectively. Alternatively, glucose was measured by adding 10 µl of supernatant to a glucose test strip inserted into a Safe-Accu 2 blood glucose monitor (both Sinocare). Lactate was also measured using a Lactate Assay Kit (Sigma-Aldrich, Cat# MAK064), according to the manufacturer's instructions. A master reaction mix was made by diluting Lactate Enzyme Mix (1:25) and Lactate Probe (1:25) in Lactate Assay Buffer. Standards were added to the plate at 0, 20, 40, 60, 80, and

100 pmole/well in 50 µl of assay buffer. Samples were diluted as required to fit within the standard curve (1:50-1:200) and 50 µl was added to the appropriate well. To each well of standard and samples, 50 µl of master mix was added and the plate incubated for 30 mins at RT with gentle agitation on a plate shaker ~600 rpm. Absorbance was read at 570 nm using the SPECTROstar OMEGA plate reader and analysis performed using GraphPad Prism 9.

2.10 STATISTICAL ANALYSIS

2.10.1 Normalisation of data

Due to inter-donor and inter-assay variations, some readouts are normalised. To calculate this, the mean of all the values from each independent experiment was taken and then each value was divided against the mean to generate the normalised value (Figure 2.3A). This variation is due to natural biological variation within human data. Additionally, the flow-based fluorescent mitochondrial probes used here, MVG and MSO, vary in mean fluorescence intensity (MFI) between assays, despite consistent dilution and staining approaches (Figure 2.3B-C). Therefore, data are normalised to the experiment mean to account for this variability.

2.10.2 Analysis of significance

Data were presented as mean ± standard deviation (SD), unless non-normally distributed where the median was presented. Normal distribution of data was assessed by Shapiro–Wilk test and considered normally distributed if p-value ≥ 0.05. Non-parametric statistical tests were performed on all normalised data. Data with a normal distribution were analysed by paired or unpaired t test. Paired data with more than two-groups were analysed by repeated measures (RM) one- or two-way analysis of variance (ANOVA) with Holm-Šídák's or Šídák's multiple comparisons test respectively. Unpaired data were analysed by one- or two-way

ANOVA, with Tukey's or Šídák's multiple comparisons test respectively. Non-normally distributed data were analysed by Wilcoxon test if paired, and Mann-Whitney test if unpaired. Kruskal-Wallis with Dunn's multiple comparisons test was used to analysed non-normally distributed data with more than two groups. Correlations were assessed by Pearson's correlation coefficient. Analysis performed using GraphPad Prism 9, * $p < 0.05$, ** $p < 0.01$, *** $p < 0.001$.

A

Expt. 3	MFI	Normalised value (MFI/Average MFI)
	4889	1.162940057
	4466	1.062321598
	3396	0.807802093
	4065	0.966936251
Average MFI	4204	

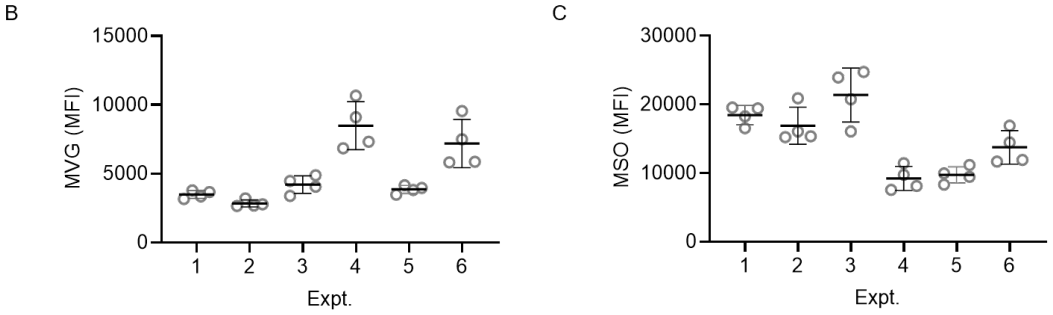

Figure 2.3 Variation in MVG and MSO mean fluorescence intensity by assay

(**A**) Example calculation for normalisation of data.

(**B-C**) Mean fluorescence intensity (MFI) of (**B**) MVG and (**C**) MSO staining of naïve $CD4^+$ T cells within assays performed on different dates in independent experiments (expt.) (B-C, n=6 independent donors).

(B-C) Each symbol represents a measurement from cells in a different treatment condition measured on the same day. Data is presented as mean ± SD.

CHAPTER 3: TNF-A DRIVES METABOLIC REPROGRAMMING IN NAÏVE CD4$^+$ T CELLS

3.1 INTRODUCTION

TNF-α is expressed in its two forms, membrane-bound and soluble, by a range of cell types, including CD4$^+$ T cells. Indeed, naïve CD4$^+$ T cells express high levels of TNF-α upon activation (Ohshima *et al.*, 1999; Priyadharshini *et al.*, 2010). Early studies identified autocrine TNF-α to act as a co-stimulatory molecule on T cells, driving increased proliferation, survival, and cytokine production upon activation (Yokota *et al.*, 1988; Tartaglia *et al.*, 1991, 1993; Aspalter *et al.*, 2003). More recently, a study has shown that the blocking of T cell-derived TNF-α with clinically used TNF-α biologic, adalimumab, also suppresses CD4$^+$ T cell activation (Povoleri *et al.*, 2020). Of note, these studies have used either bulk lymphocytes, thymocytes, or CD4$^+$ T cells; the specific effects of autocrine TNF-α signalling on naïve and memory CD4$^+$ T cells are yet undescribed. Upon activation, CD4$^+$ T cells integrate signals from the TCR, co-stimulatory molecules such as CD28, and cytokines such as IL-2 to drive metabolic reprogramming (Frauwirth *et al.*, 2002; Jacobs *et al.*, 2008; Ray *et al.*, 2015).

Activated CD4$^+$ T cells undergo a substantial shift from an OXPHOS predominant, catabolic metabolism to a highly glycolytic, anabolic metabolism. Specifically, naïve CD4$^+$ T cells, which previously relied on a low-level OXPHOS metabolism supplied by glucose-derived pyruvate, upregulate the uptake of substates from the environment. Increases in glucose uptake support conversion of glucose-derived pyruvate to lactate in aerobic glycolysis, which drives

rapid ATP production and biosynthesis of effector molecules via the PPP. Additional upregulation of mitochondrial biogenesis and uptake of glutamine and fatty acids support increased OXPHOS to maintain production of ATP, TCA cycle intermediates, and ROS (Wang *et al.*, 2011; Angela *et al.*, 2016; Jones *et al.*, 2019). Alongside the increased uptake of amino acids, such as leucine, these molecules support the signalling, metabolism, and effector function of activated $CD4^+$ T cells (Sinclair *et al.*, 2013; Previte *et al.*, 2017). Similarly relying on OXPHOS at rest, memory $CD4^+$ T cell also undergo this significant metabolic reprogramming (Maekawa *et al.*, 2015). However, having previously experienced naïve cell priming, mitochondrial and epigenetic changes result in memory cells exhibiting increased metabolic capacity and rapid engagement of effector function upon activation (Bevington *et al.*, 2016; Dimeloe *et al.*, 2016). Predominantly, CD28 signalling drives metabolic reprogramming. Yet, any role for T cell-intrinsic TNF-α signalling in the modulating $CD4^+$ T cell metabolism is relatively unknown. Studies have shown that CD28 and TNF-α have comparable but non-redundant roles in driving optimal $CD4^+$ T cell activation with full mechanisms not yet described (Aspalter *et al.*, 2003, 2007). One study had previously investigated the metabolic effects of infliximab, a clinically used anti-TNFα treatment on $CD4^+$ T cells. Measurements of a range of metabolites by liquid chromatography-mass spectrometry (LC-MS) after 24 h of *in vitro* treatment revealed subtle trends but no significant changes (Chimenti *et al.*, 2013). However, variation in the data was substantial, analysis of individual $CD4^+$ T cells subsets may improve this in future studies. Additionally, TCA cycle intermediates were not analysed here (Chimenti *et al.*, 2013). Further investigation is required to better understand the metabolic effects of TNF-α on $CD4^+$ T cells.

3.1.1 AIMS

TNF-α is known to act as a co-stimulatory molecule on T cells, driving increased cell function upon activation. Despite this, it is not described whether TNF-α has any role in the modulation of T cell metabolism. This chapter aims to identify and interrogate a role for T cell-derived TNF-α in the metabolic reprogramming of naïve and memory $CD4^+$ T cells. Using *in vitro* culture of purified naïve and memory $CD4^+$ T cells in presence of increased TNF-α, a neutralising anti-TNFα antibody, or relevant isotype control, the hypothesis that TNF-α signalling drives $CD4^+$ T cell metabolic reprogramming will be interrogated.

3.2 RESULTS

3.2.1 Intrinsic TNF-α signalling in CD4$^+$ T cells

To begin to understand the role of intrinsic TNF-α signalling in naïve and memory CD4$^+$ T cells, expression levels of the TNF receptors, TNFR1 and TNFR2, were first assessed. Purified CD4$^+$ T cells were activated with anti-CD3/28 and stained for surface expression of CD45RA, TNFR1, and TNFR2 (Figure 3.1A-C). Single cells were gated as naïve (CD45RA$^+$) or memory (CD45RA$^-$) CD4$^+$ T cells (Figure 3.1A). TNFR1 stained at comparable levels to the unstained control (US) on both naïve and memory CD4$^+$ T cells with no change in expression after 4 h of activation (Figure 3.1B). In contrast, TNFR2 was highly expressed (Figure 3.1C-D). Naïve CD4$^+$ T cells expressed a lower level of TNFR2 than memory CD4$^+$ T cells, yet the dynamics of TNFR2 expression were comparable. After 4 h of activation, TNFR2 expression on naïve cells trended towards a decrease, and in memory cells this downregulation reached significance. Yet, in both subsets at 48 h expression was significantly upregulated to a level above that at rest (Figure 3.1C-D). RNA-seq of non-activated (NA) and activated naïve CD4$^+$ T cells confirmed that TNFR1 transcripts were expressed at very low levels compared to that of TNFR2 (Figure 3.1E). In agreement with protein expression on the surface of the cell, TNFR2 transcript levels increased after 48 h of activation of naïve CD4$^+$ T cells. Next, cells were again activated for 4 h or 48 hrs and the supernatants were assessed for concentration of sTNF-α. NA cells were used as a control and did not produce detectable levels of TNF-α (Figure 3.1F). TNF-α could be detected at a similar level in both naïve and memory cell supernatants at 4 h. TNF-α concentration increased by 48 h but remained comparable between naïve and memory cell cultures. Together, these data show that TNFR2 is the primary TNF receptor expressed by CD4$^+$ T cells, and that a monoculture of naïve CD4$^+$ T cells is able to produce and respond to TNF-α.

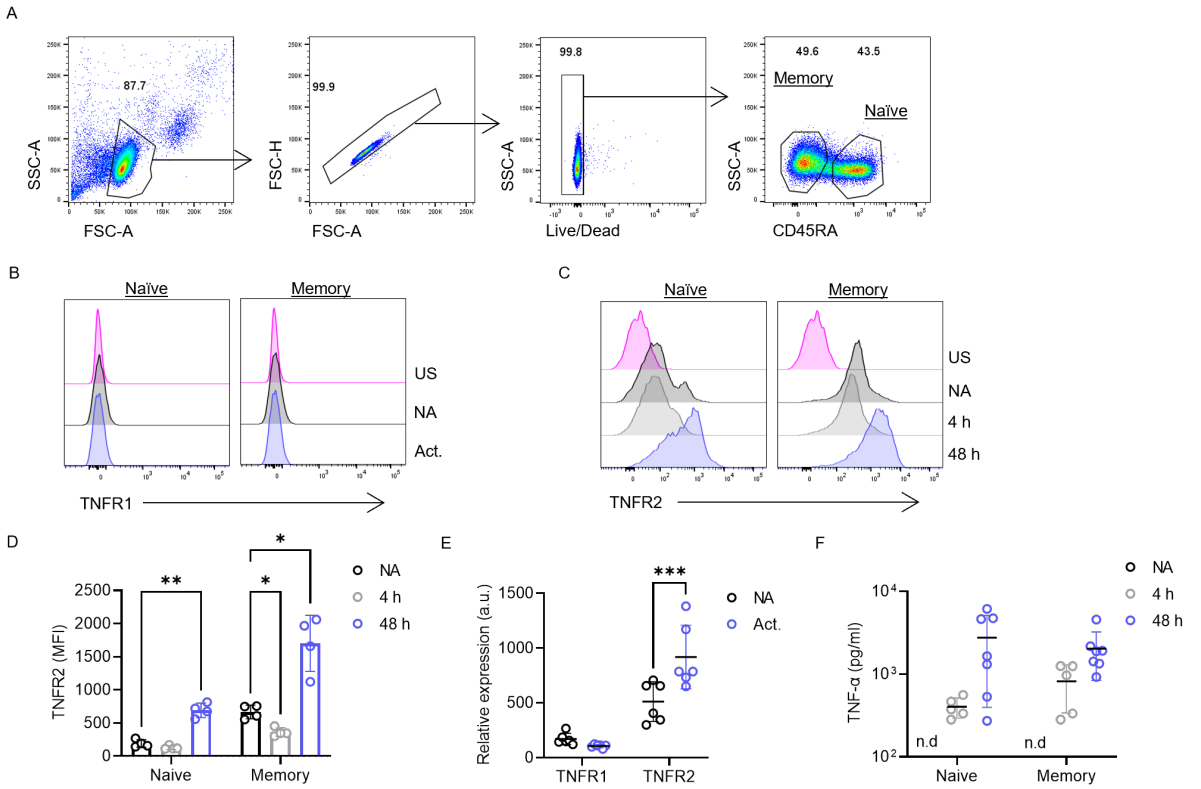

Figure 3.1 TNF receptor and TNF-α expression in CD4⁺ T cells

(**A**) Purified CD4⁺ T cells were gated as lymphocytes, then single cells; dead cells were then gated out and cells put into naïve (CD45RA⁺) or memory (CD45RA⁻) subsets (representative plot of n=6 independent donors).

(**B**) Purified CD4⁺ T cells were either non-activated (NA) or activated for 4 h with anti-CD3/28 (Act.) then analysed by flow cytometry. Cells were gated as in (A) and assessed for expression of TNFR1, US=unstained control (representative plot of n=6 independent donors).

(**C-D**) Cells were cultured as in (B) with the addition of a 48 h condition and cells gated as in (A) were assessed for expression of TNFR2, US=unstained control (representative plot of n=4 independent donors). (**D**) Mean fluorescence intensity (MFI) of TNFR2 in naïve and memory cell subsets (n=4 independent donors).

(**E**) Transcript abundance of *TNFRSF1A* (TNFR1) and *TNFRSF1B* (TNFR2) in NA and activated (Act.) purified naïve CD4⁺ T cells from RNA-seq data, a.u.=arbitrary units (n=6 independent donors).

(**F**) Concentration of TNF-α in the supernatants of purified naïve and memory CD4⁺ T cells either NA or activated for 4 h or 48 h (NA n=5, 4 h n=5, and 48 h n=7 independent donors) n.d=non-detectable.

(D-F) Each symbol represents a different donor. Data is presented as the mean ± SD. Significance was assessed by two-way ANOVA with Šídák's multiple comparisons test, * $p < 0.05$, ** $p < 0.01$, *** $p < 0.001$.

3.2.2 Blocking TNF-α suppresses activation of $CD4^+$ T cells

Having established the potential for T cell-intrinsic TNF-α signalling in $CD4^+$ T cells, the effect of blocking this signal during T cell activation was assessed. Cells were activated and treated with an anti-TNFα antibody or isotype control for 48 h then analysed by flow cytometry. Cells first gated as lymphocytes and single cells, were then gated on expression of CD45RA (naïve: $CD45RA^+CD45RO^-$) and CD45RO (memory: $CD45RA^-CD45RO^+$) (Figure 3.2A). TNFR1 signalling is associated with cell death pathways (Micheau and Tschopp, 2003); in accordance with its low expression on $CD4^+$ T cells, both naïve and memory cell populations showed no difference in cell viability (typically >90%) when treated with anti-TNFα or the isotype control (Figure 3.2A-B). Anti-TNFα treatment did suppress forward scatter of naïve $CD4^+$ T cells compared to the isotype control, this is a measurement which correlates with cell size and may be indicative of reduced blasting, an effect which in turn can often signal a lower metabolic capacity in a cell (Rathmell *et al.*, 2003; Jacobs *et al.*, 2008). No such effect was seen on memory cells (Figure 3.2A and C). As this analysis relied on the gating of naïve and memory $CD4^+$ T cells based on CD45RA and CD45RO staining, the percentage of naïve and memory cell populations after 4 and 48 hrs of activation was assessed to ensure there were not substantial changes in the proportion of these populations during time in culture (Figure 3.2D). Although a reciprocal increase in memory cells and decrease in naïve cells was seen between 4 h and 48 h, a considerable proportion of both subsets remained. It was therefore reasonable to continue with the use of this gating strategy at this time point.

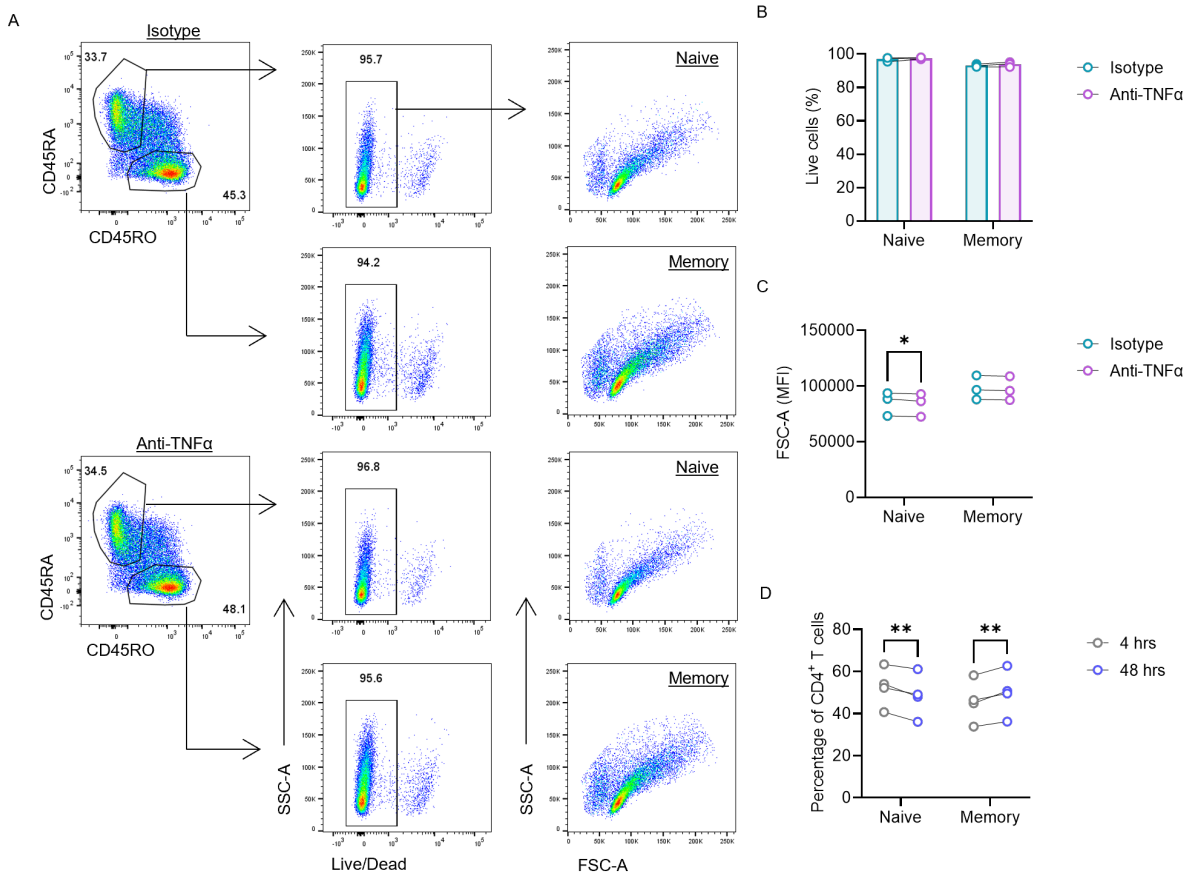

Figure 3.2 Effect of anti-TNFα on cell viability and size

(**A-C**) Purified CD4$^+$ T cells were activated and cultured for 48 h in presence of an anti-TNFα or isotype control antibody. (**A**) Cells were gated into a naïve (CD45RA$^+$CD45RO$^-$) or memory (CD45RA$^-$CD45RO$^+$) subset and assessed for viability by live/dead stain. Within these gates, cells were then assessed for the mean fluorescence intensity (MFI) of forward scatter (FSC-A) (representative plots of n=3 independent donors). (**B**) Percentage of live cells within naïve and memory cell subsets, comparing anti-TNFα treatment to the isotype control. (**C**) MFI of FSC-A as a measurement of cell size (B-C, n=3 independent donors).

(**D**) Purified CD4$^+$ T cells were activated for 4 or 48 h and assessed for the proportion of naïve and memory cells (n=4 independent donors).

(B-D) Each symbol represents a different donor with the line between denoting matched pairs. Significance was assessed by RM two-way ANOVA with Šídák's multiple comparisons test, * $p < 0.05$, ** $p < 0.01$.

Blocking T cell-derived TNF-α signalling in naïve CD4⁺ T cells suppressed the expression of T cell activation markers, CD69 and CD25 (Figure 3.3A-B). Memory cells showed a reduction in CD25 with anti-TNFα treatment but no change in CD69 (Figure 3.3C-D). These data suggest that TNF-α signalling is crucial for the full activation of CD4⁺ T cells, identifying a role in both naïve and memory cell subsets.

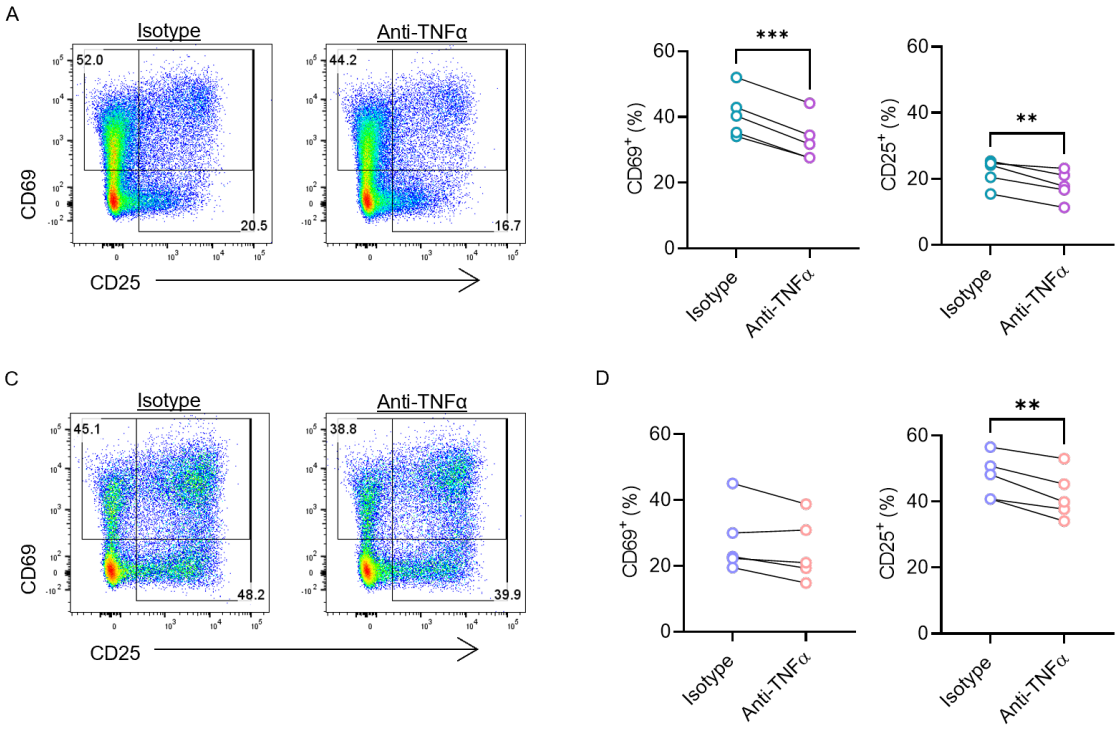

Figure 3.3 Anti-TNFα suppresses CD4⁺ T cell activation

(**A-D**) Purified CD4⁺ T cells were activated and cultured for 48 h in presence of an anti-TNFα or isotype control antibody. Cells were gated into a (**A-B**) naïve (CD45RA⁺CD45RO⁻) or (**C-D**) memory (CD45RA⁻CD45RO⁺) subset and assessed for expression of CD69 and CD25 (A and C, representative plot of n=5 independent donors; B and D, n=5 independent donors).

(B and D) Each symbol represents a different donor with the line between denoting matched pairs. Significance was assessed by paired t test, ** $p < 0.01$, *** $p < 0.001$.

3.2.3 Blocking TNF-α prevents full metabolic reprogramming of naïve CD4$^+$ T cells

Next, to further understand the effects of blocking TNF-α, the metabolic profile of the cells upon activation was assessed. For levels of mitochondrial mass, cells were stained with MVG and analysed by flow cytometry (Figure 3.4A). MVG staining was increased upon activation, however this increase was largely blunted in naïve CD4$^+$ T cells treated with anti-TNFα. MSO is a fluorescent mitochondrial probe that stains cells based on mitochondrial membrane potential, this is then paired with FCCP, a membrane potential uncoupler able to depolarise the membrane and provide a baseline level of MSO staining. The ratio of MSO staining alone to MSO in combination with FCCP (MSO:MSO+FCCP) provides a readout for mitochondrial activity. A lot of variability could be seen in the ratio of MSO:MSO+FCCP, with little difference between NA and activated cells (Figure 3.4B). It was therefore difficult to see any effect of anti-TNFα in comparison to isotype treated as no initial increase upon activation was apparent. To interrogate further the potential metabolic suppression suggested by decreased mitochondrial mass, purified naïve CD4$^+$ T cells were activated and treated for 48 h then assessed for OCR and ECAR by Seahorse XF assay (Figure 3.4C-F). Consistent with mitochondrial mass, activation increased OCR upon activation, but this was blunted in presence of anti-TNFα. Both basal and max. respiration (OCR), which is induced when cells are treated with membrane potential uncoupler BAM15, were lower in the anti-TNFα treated group. ATP-coupled respiration, calculated from the addition of ATP-synthase inhibitor, oligomycin, and spare respiratory capacity (SRC), the available increase in for cells between basal and max. OCR, were also reduced in those cells treated with anti-TNFα compared to isotype controls (Figure 3.4C-D). In addition, blocking TNF-α suppressed both basal and max. glycolytic ECAR in naïve CD4$^+$ T cells upon activation, again to a level between that of NA and

isotype control-treated cells (Figure 3.4E-F). As a control for this being a general effect of blocking cytokine signalling, cells were also treated with anti-IFNγ which had no effect on the OCR or ECAR of naïve $CD4^+$ T cells. Taken together, these data confirm that TNF-α promotes the upregulation of mitochondrial OXPHOS and glycolysis in naïve $CD4^+$ T cells upon activation.

In contrast to the effects seen with naïve cells, MVG staining of memory cells showed no effect of anti-TNFα treatment on mitochondrial mass compared to the isotype control (Figure 3.5A). Mitochondrial activity, as assessed by MSO:MSO+FCCP, was variable and again showed little increase upon activation making any differences in treatment difficult to identify (Figure 3.5B). Analysis of OCR in memory $CD4^+$ T cells demonstrated a clear upregulation with activation. However, in accordance with little effect on mitochondrial mass, anti-TNFα had no effect on basal, ATP-coupled, or max. respiration or SRC compared to the isotype (Figure 3.5C-D). Blocking TNF-α also had no impact on the glycolytic ECAR of memory $CD4^+$ T cells upon activation (Figure 3.5E-F). As on naïve cells, no metabolic effect was seen when blocking IFN-γ signalling on memory cells (Figure 3.5C-F). Overall, these data show that blocking T cell-derived TNF-α upon activation of memory $CD4^+$ T cells has little effect on metabolism.

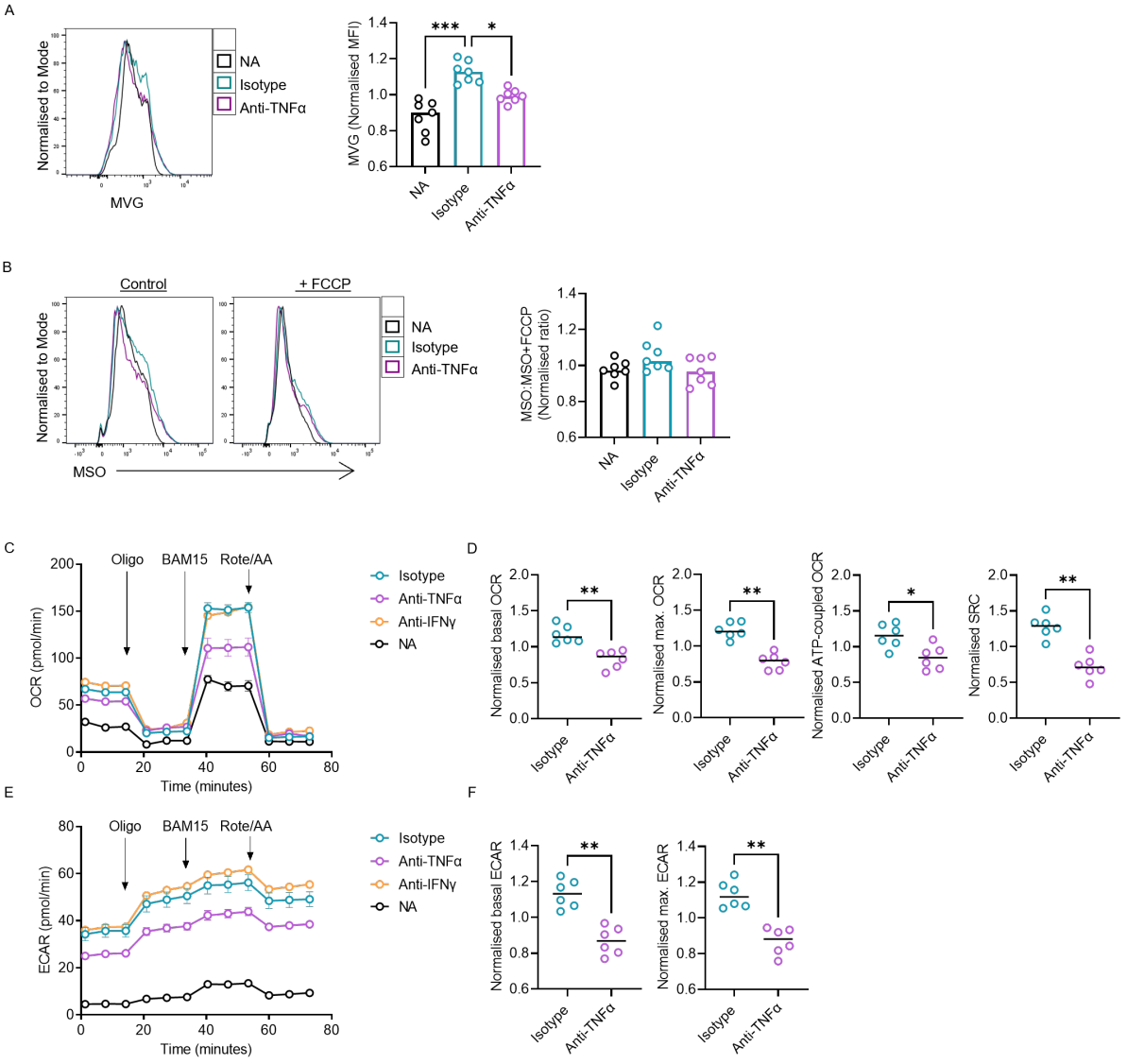
A
Normalised to Mode
MVG
NA
Isotype
Anti-TNFα
MVG (Normalised MFI)
***
*
B
Control
+ FCCP
MSO
MSO:MSO+FCCP (Normalised ratio)
C
Oligo
BAM15
Rote/AA
OCR (pmol/min)
Time (minutes)
Anti-IFNγ
D
Normalised basal OCR
Normalised max. OCR
Normalised ATP-coupled OCR
Normalised SRC
E
ECAR (pmol/min)
F
Normalised basal ECAR
Normalised max. ECAR

Figure 3.4 Blocking TNF-α signalling suppresses metabolism in naïve CD4$^+$ T cells

(**A-B**) Purified CD4$^+$ T cells were non-activated (NA) or activated and cultured for 48 h in presence of an anti-TNFα or isotype control antibody. Cells within the naïve CD4$^+$ T cell gate were assessed for the mean fluorescence intensity (MFI) of (**A**) MVG to measure mitochondrial mass, and (**B**) the ratio of MSO with and without FCCP to measure mitochondrial membrane potential (MSO:MSO+FCCP) (A-B, n=7 independent donors).

(**C-F**) Purified naïve CD4$^+$ T cells were cultured as in (A-B) with the addition of an anti-IFNγ condition. Following treatment, cells were measured for (**C-D**) oxygen consumption rate (OCR) and (**E-F**) extracellular acidification rate (ECAR) by Seahorse XF analysis. (**C and E**) Seahorse plots of (**C**) OCR and (**E**) ECAR (representative plots of NA, isotype, and anti-TNFα n=6 independent donors, and anti-IFNγ n=3 independent donors). Arrows show time of injection of the indicated compounds: oligomycin (oligo), BAM15, and rotenone/antimycin A (rote/AA). Error bars indicate technical replicates. (**D and F**) For isotype, and anti-TNFα-treated cells (**D**) basal OCR, maximal (max.) OCR, ATP-coupled OCR, and spare respiratory capacity (SRC) and (**F**) basal and max. ECAR were calculated (D and F, n=6 independent donors).

(A-B, D, and F) Data are normalised to the mean of each experiment. Each symbol represents a different donor, and the median is presented. Significance was assessed by (A-B) Kruskal Wallis with Dunn's multiple comparisons test (D and F) Mann-Whitney test, * $p < 0.05$, ** $p < 0.01$, *** $p < 0.001$.

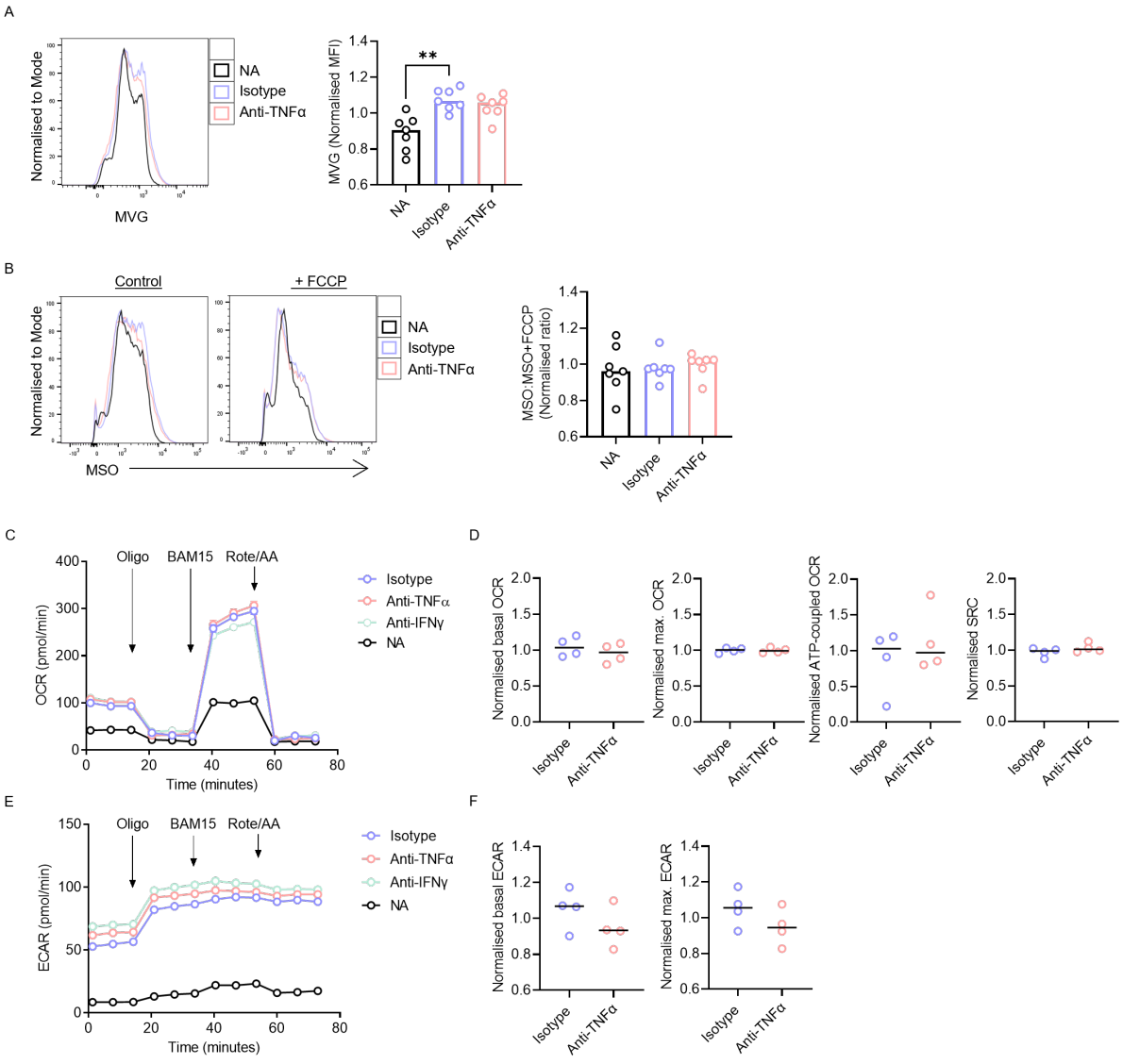
A
Normalised to Mode
MVG
NA
Isotype
Anti-TNFα
MVG (Normalised MFI)
**
B
Control
+ FCCP
MSO
MSO:MSO+FCCP (Normalised ratio)
C
Oligo
BAM15
Rote/AA
OCR (pmol/min)
Time (minutes)
Anti-IFNγ
D
Normalised basal OCR
Normalised max. OCR
Normalised ATP-coupled OCR
Normalised SRC
E
ECAR (pmol/min)
F
Normalised basal ECAR
Normalised max. ECAR

Figure 3.5 Anti-TNFα has no effect on memory CD4$^+$ T cell metabolism

(**A-B**) Purified CD4$^+$ T cells were non-activated (NA) or activated and cultured for 48 h in presence of an anti-TNFα or isotype control antibody. Cells within the memory CD4$^+$ T cell gate were assessed for the mean fluorescence intensity (MFI) of (**A**) MVG to measure mitochondrial mass, and (**B**) the ratio of MSO with and without FCCP to measure mitochondrial membrane potential (MSO:MSO+FCCP) (A-B, n=7 independent donors).

(**C-F**) Purified memory CD4$^+$ T cells were cultured as in (A-B) with the addition of an anti-IFNγ condition. Following treatment, cells were measured for (**C-D**) oxygen consumption rate (OCR) and (**E-F**) extracellular acidification rate (ECAR) by Seahorse XF analysis. (**C and E**) Seahorse plots of (**C**) OCR and (**E**) ECAR (representative plots of NA, isotype, and anti-TNFα n=4 independent donors, and anti-IFNγ n=3 independent donors). Arrows show time of injection of the indicated compounds: oligomycin (oligo), BAM15, and rotenone/antimycin A (rote/AA). Error bars indicate technical replicates. (**D and F**) For isotype, and anti-TNFα-treated cells (**D**) basal OCR, maximal (max.) OCR, ATP-coupled OCR, and spare respiratory capacity (SRC) and (**F**) basal and max. ECAR were calculated (D and F, n=4 independent donors).

(A-B, D, and F) Data are normalised to the mean of each experiment. Each symbol represents a different donor, and the median is presented. Significance was assessed by (A-B) Kruskal Wallis with Dunn's multiple comparisons test (D and F) Mann-Whitney test, * $p < 0.05$, ** $p < 0.01$, *** $p < 0.001$.

3.2.4 Understanding the different effects on naïve and memory CD4$^+$ T cells

Following these observations, the next aim was to understand why effects of blocking TNF-α were seen on naïve but not memory cells. Firstly, it is known that TNFR2 has significant roles in driving Treg responses, including increasing glycolysis (Chen *et al.*, 2013; de Kivit *et al.*, 2020). To make sure that a contamination of Tregs in the naïve or memory cell population was not accountable for the effects reported here, CD4$^+$ T cells were stained for CD45RA and FoxP3 to identify the T cell subsets and the respective proportion of FoxP3$^+$ Tregs present (Figure 3.6). Overall, the percentage of FoxP3$^+$ cells was largely <20%. In particular, the naïve cell population, in which the effects of anti-TNFα are seen, trended to have fewer FoxP3$^+$ cells than the memory cell population. These data confirm that there is not an overrepresentation of Tregs in the naïve CD4$^+$ T cell cultures and therefore effects on Tregs are unlikely to be responsible for the changes seen here in naïve CD4$^+$ T cells.

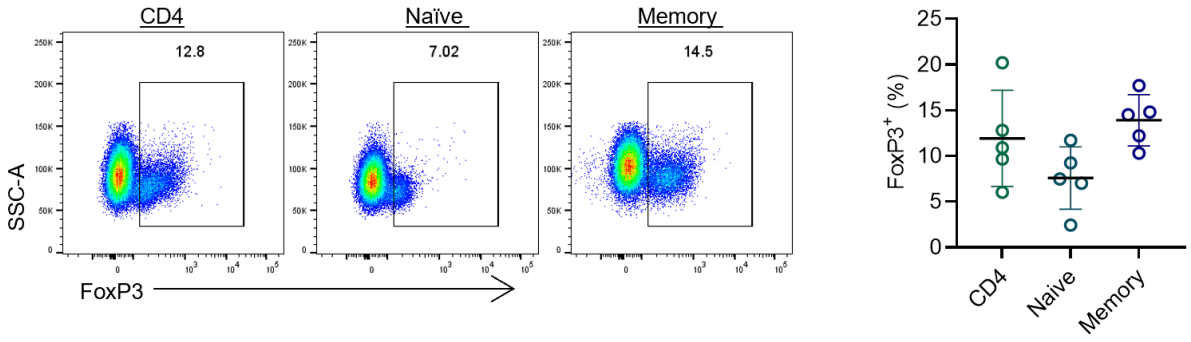

Figure 3.6 Percentage of FoxP3$^+$ Tregs in CD4$^+$ T cell subsets

Purified total, naïve, and memory CD4$^+$ T cells were assessed for the percentage of FoxP3$^+$ Tregs present (n=5 independent donors). Each symbol represents a different donor. Data is presented as the mean ± SD. Significance was assessed by one-way ANOVA with Tukey's multiple comparisons test.

As memory cells have previously undergone activation, epigenetic modifications, and metabolic adaptations, the threshold for the next TCR activation is lowered (Dimeloe *et al.*, 2016; Barski *et al.*, 2017; Bevington *et al.*, 2021). Therefore, it was hypothesised that memory $CD4^+$ T cells may be more sensitive to the *in vitro* anti-CD3/28 stimulation given. To test this, $CD4^+$ T cells were activated as before (norm. act) but also with a 10-fold lower dose of anti-CD3/28 (low act.). Cells stimulated with the lower dose were then assessed for their level of activation when treated with an anti-TNFα or isotype control antibody (Figure 3.7A-D). With the lower activation strength, naïve cells maintained the decrease in CD25 expression with anti-TNFα treatment and no changes in memory cell activation were indicated. To understand if this lower dose could reveal a metabolic effect of blocking TNF-α signalling on memory $CD4^+$ T cells, Seahorse XF assay was employed to measure OCR and ECAR (Figure 3.7E-H). Firstly looking at naïve cells, the effect of strength of stimulation on metabolic reprogramming was clear with isotype and low dose-treated cells increasing OCR and ECAR slightly over NA cells but remaining much lower than normally activated isotype-treated cells (Figure 3.7E-F). In the normal activation conditions, the suppressive effect of anti-TNFα was apparent on both mitochondrial OXPHOS and glycolysis measurements as before. A reduction was also clear between anti-TNFα and isotype-treated cells in the low activation condition with anti-TNFα treatment suppressing OCR and ECAR to a level comparable with NA cells. In memory cells, the three levels of activation also separated clearly in both OCR and ECAR measurements into NA, low act., and norm. act. (Figure 3.7G-H). As before, no consistent difference in max. OCR was seen between anti-TNFα and isotype-treated memory $CD4^+$ T cells at the normal level of activation. Although a decrease in basal OCR was seen in the representative plot shown here, this was not a consistent observation and is feasibly due to human donor variability

(Figure 3.7G and Figure 3.5C-D). No effect of blocking TNF-α was seen on OCR or ECAR measurements of memory cells at the lower activation (Figure 3.7H). In summary, under reduced activation strength anti-TNFα still had little effect on memory CD4$^+$ T cell metabolism. From this, it was resolved to continue the project focusing on the role of T cell-derived TNF-α signalling in naïve CD4$^+$ T cells only.

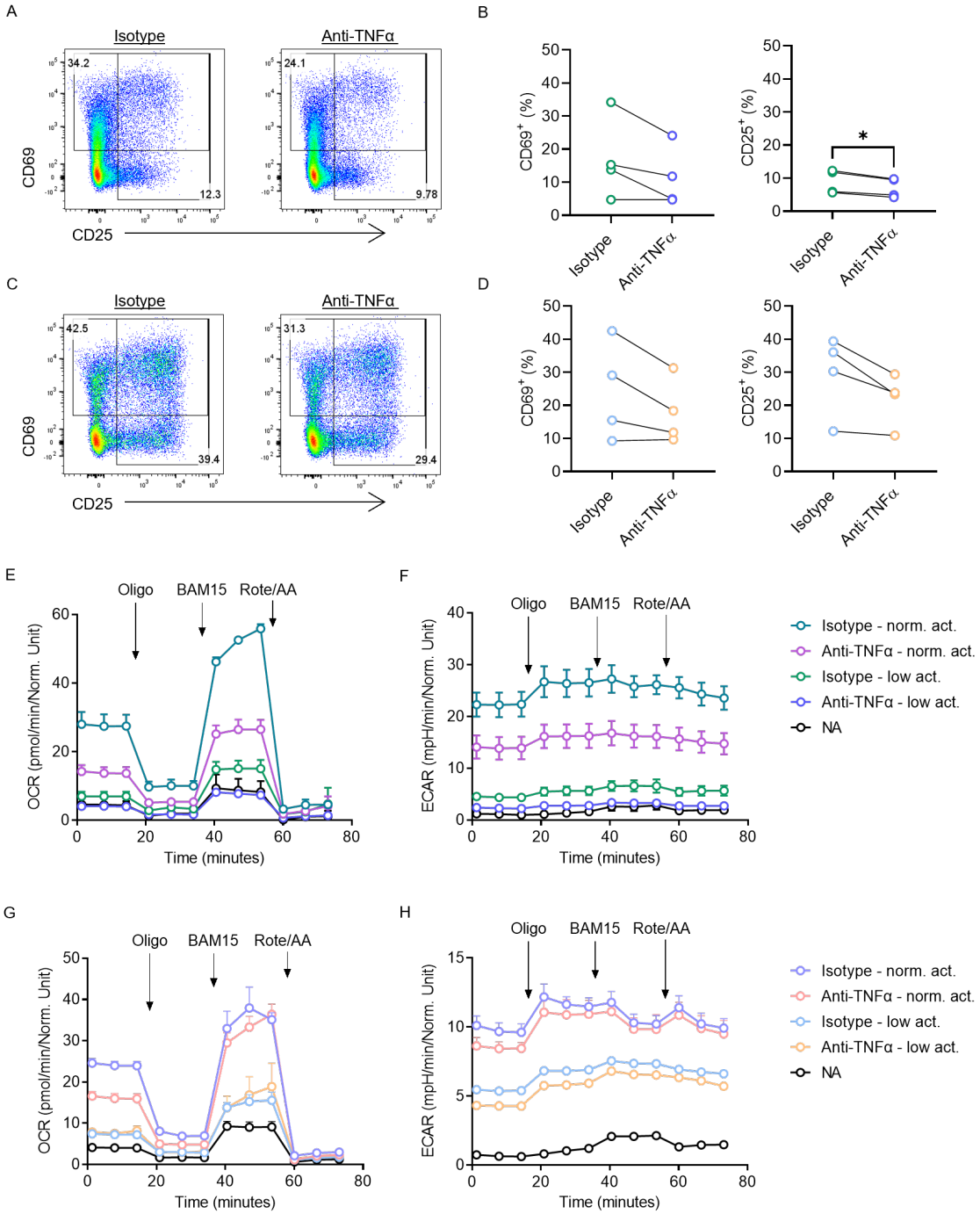

Figure 3.7 Effect of a lower dose stimulation on anti-TNFα treatment of $CD4^+$ T cells

(**A-D**) Purified $CD4^+$ T cells were activated with a 10-fold lower activation compared to previous experiments (low act.; 1.2 µl/ml T cell activator) and cultured for 48 h in presence of an anti-TNFα or isotype control antibody. Cells were gated as lymphocytes, then single cells; dead cells were then gated out and cells put into (**A-B**) naïve ($CD45RA^+$) or (**B-C**) memory ($CD45RA^-$) subsets and assessed for expression of CD69 and CD25 (A and C, representative plots of n=4 independent donors; B and D, n=4 independent donors).

(**E-H**) Purified (**E-F**) naïve and (**G-H**) memory $CD4^+$ T cells were cultured as in (A-D) with the addition of a non-activated (NA) and activated as normal condition (norm. act.; 12 µl/ml T cell activator) then assessed for (**E and G**) oxygen consumption rate (OCR) and (**F and H**) extracellular acidification rate (ECAR) by Seahorse XF assay (representative plots of n=3 independent donors). Arrows show time of injection of the indicated compounds: oligomycin (oligo), BAM15, and rotenone/antimycin A (rote/AA). Error bars indicate technical replicates.

(B and D) Each symbol represents a different donor with the line between denoting matched pairs. Significance was assessed by paired t test, * $p < 0.05$.

3.2.5 Anti-TNFα suppresses glutamine metabolism through the TCA cycle

To further investigate the metabolic perturbations caused by blocking TNF-α upon activation of naïve $CD4^+$ T cells, stable isotope tracing of $^{13}C_6$-labelled glucose was employed for naïve $CD4^+$ T cells activated in presence of an anti-TNFα or isotype control antibody (Figure 3.8). Stable isotope tracing of a substrate, here $^{13}C_6$-glucose, enables the metabolism of the substrate to be tracked based on the number of labelled carbons incorporated into downstream intermediates, i.e. citrate M+2 indicating that two carbons from the original labelled glucose molecule are present in the metabolite. Based on the incorporation of different labelling patterns, how the cell is utilising the labelled substrate through each metabolic pathway can then be inferred.

Following conversion into pyruvate (which remained unchanged with anti-TNFα treatment) the majority of glucose was incorporated into lactate. Lactate incorporation into glucose trended towards a decrease in anti-TNFα-treated cells compared to the isotype but this was not a significant effect. Additionally, some glucose-derived pyruvate was converted into alanine, yet this was again unchanged in presence of anti-TNFα. In the TCA cycle, glucose incorporation into citrate was present with most of this then being converted into glutamate via αKG. No difference between anti-TNFα and isotype-treated cells was seen. Overall, very little incorporation of labelled glucose can be seen into the TCA cycle, suggesting usage of other substrates to maintain oxidative metabolism in activated naïve $CD4^+$ T cells.

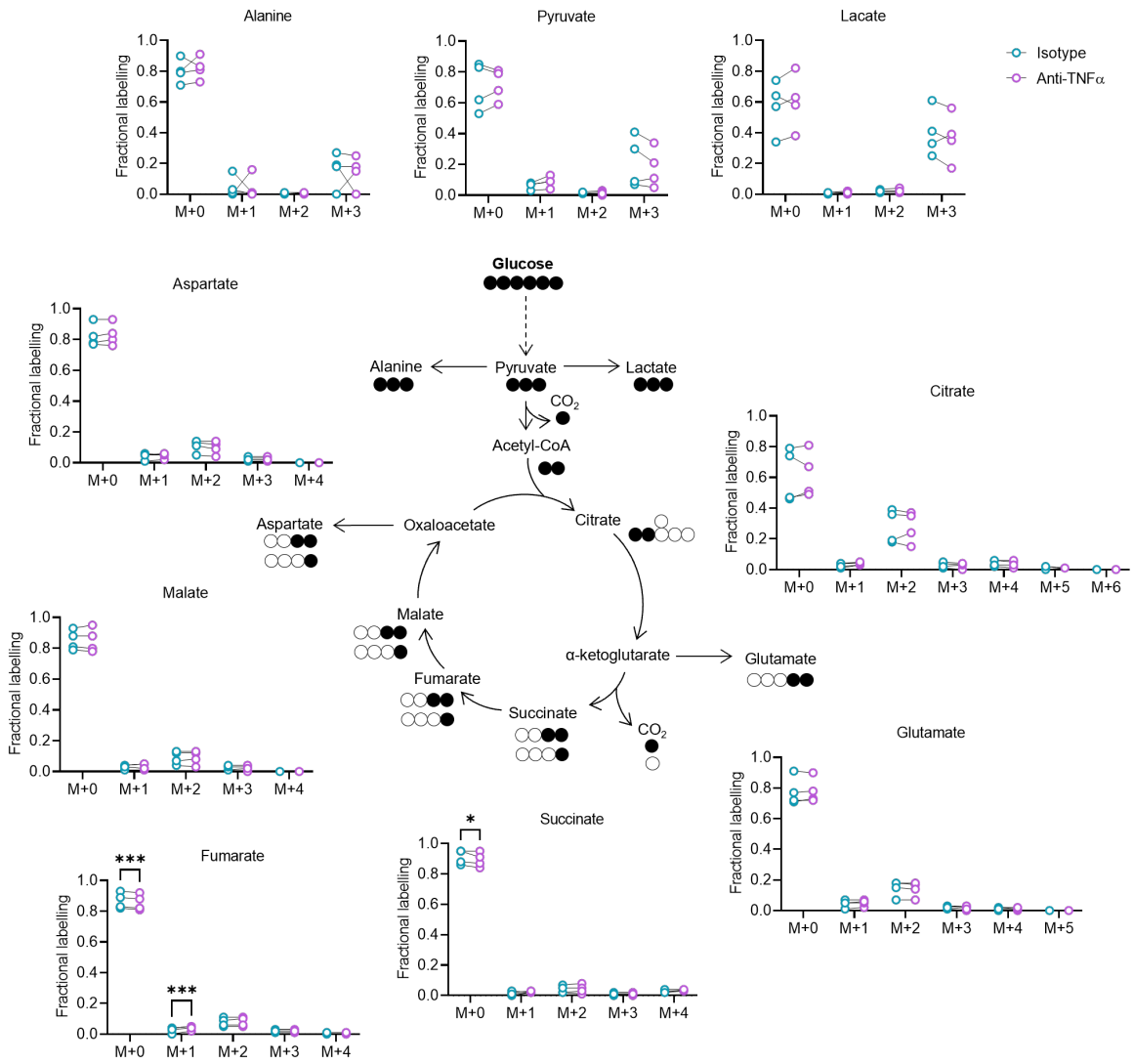

Figure 3.8 $^{13}C_6$-glucose tracing in naïve CD4$^+$ T cells treated with anti-TNFα

Purified naïve CD4$^+$ T cells were activated for 48 h with an anti-TNFα antibody or isotype control, then cultured for an additional 4 h in presence of 10 mM $^{13}C_6$-labelled glucose and assessed for mass isotopomer distribution (MID) of indicated metabolites (n=4 independent donors). Centre diagram represents the likely metabolism of fully labelled glucose into the indicated metabolites and the resulting MID (black circles indicate a labelled carbon and white circles an unlabelled carbon). Each symbol represents a different donor with the line between denoting matched pairs. Significance was assessed by RM two-way ANOVA with Šídák's multiple comparisons test ***$p < 0.001$.

Assessing the total abundance of each metabolite, a trend towards lower pyruvate and alanine could be seen in the anti-TNFα condition (Figure 3.9A). Intracellular lactate levels were comparable between the two groups. A trend towards a decrease in several TCA cycle intermediates could be seen, in particular citrate, in the anti-TNFα condition (Figure 3.9B). This observation provided further evidence to suggest that the metabolism of a different substrate through the TCA cycle was being affected by blocking TNF-α.

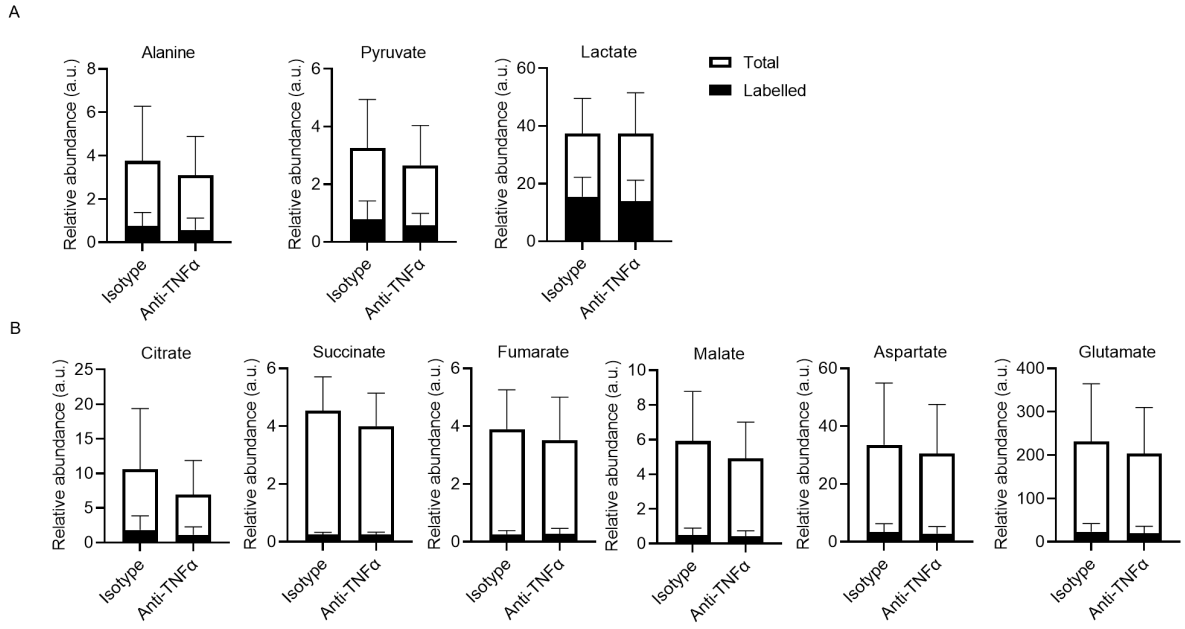

Figure 3.9 Abundance of total and labelled metabolites in $^{13}C_6$-glucose tracing of anti-TNFα-treated naïve CD4$^+$ T cells.

(**A-B**) Purified naïve CD4$^+$ T cells were activated for 48 h with an anti-TNFα antibody or isotype control, then cultured for an additional 4 h in presence of 10 mM $^{13}C_6$-labelled glucose and assessed for total and labelled abundance of (**A**) alanine, pyruvate, and lactate (**B**) indicated TCA cycle metabolites (A-B, n=4 independent donors). White bars represent total abundance and black bars represent the proportion of the total abundance that was labelled, calculated as total abundance multiplied by fraction labelled, a.u.=arbitrary units. Error bars show mean ± SD. Significance was assessed by RM two-way ANOVA with Šídák's multiple comparisons test.

To probe this hypothesis, the experiment was repeated with $^{13}C_5$-labelled glutamine, a substrate also required by T cells for activation (Wang *et al.*, 2011; Klysz *et al.*, 2015; Jones *et al.*, 2019) (Figure 3.10). As expected, there was very little incorporation of labelled $^{13}C_5$-glutamine into alanine, pyruvate, or lactate. However, compared to glucose, glutamine showed a much higher incorporation into TCA cycle metabolites, often >50% fractional labelling. Substantial incorporation of glutamine into glutamate was present at M+5, indicating direct conversion from glutamine. In addition, a detectable amount of M+3 was present, indicating the production of glutamate through another pathway, e.g. conversion from αKG. Incorporation of glutamine in both these cases was reduced with anti-TNFα treatment causing a reciprocal increase in the amount of unlabelled glutamate, M+0. Following glutamine into the TCA cycle and through oxidative decarboxylation of αKG, fractional labelling of succinate was decreased in all detectable mass isotopomers in the anti-TNFα condition. For intermediates of the TCA cycle, M+4 is the most abundant mass isotopomer and indicates the metabolism of glutamine through one pass of the TCA cycle. Additional mass isotopomers are suggestive of further metabolism of the glutamine molecule through the TCA cycle and other associated metabolic pathways. Similar to succinate, a reduction in almost all mass isotopomers of fumarate was present with anti-TNFα treatment. Labelling into M+4 was decreased with anti-TNFα treatment for malate and aspartate. Furthermore, labelling of M+3 and M+4 citrate was decreased in anti-TNFα treated cells. Taken together, these data suggest that blocking TNF-α upon activation of naïve $CD4^+$ T cells results in a decrease in glutamine metabolism, initially in its conversion to glutamate, then further through the TCA cycle.

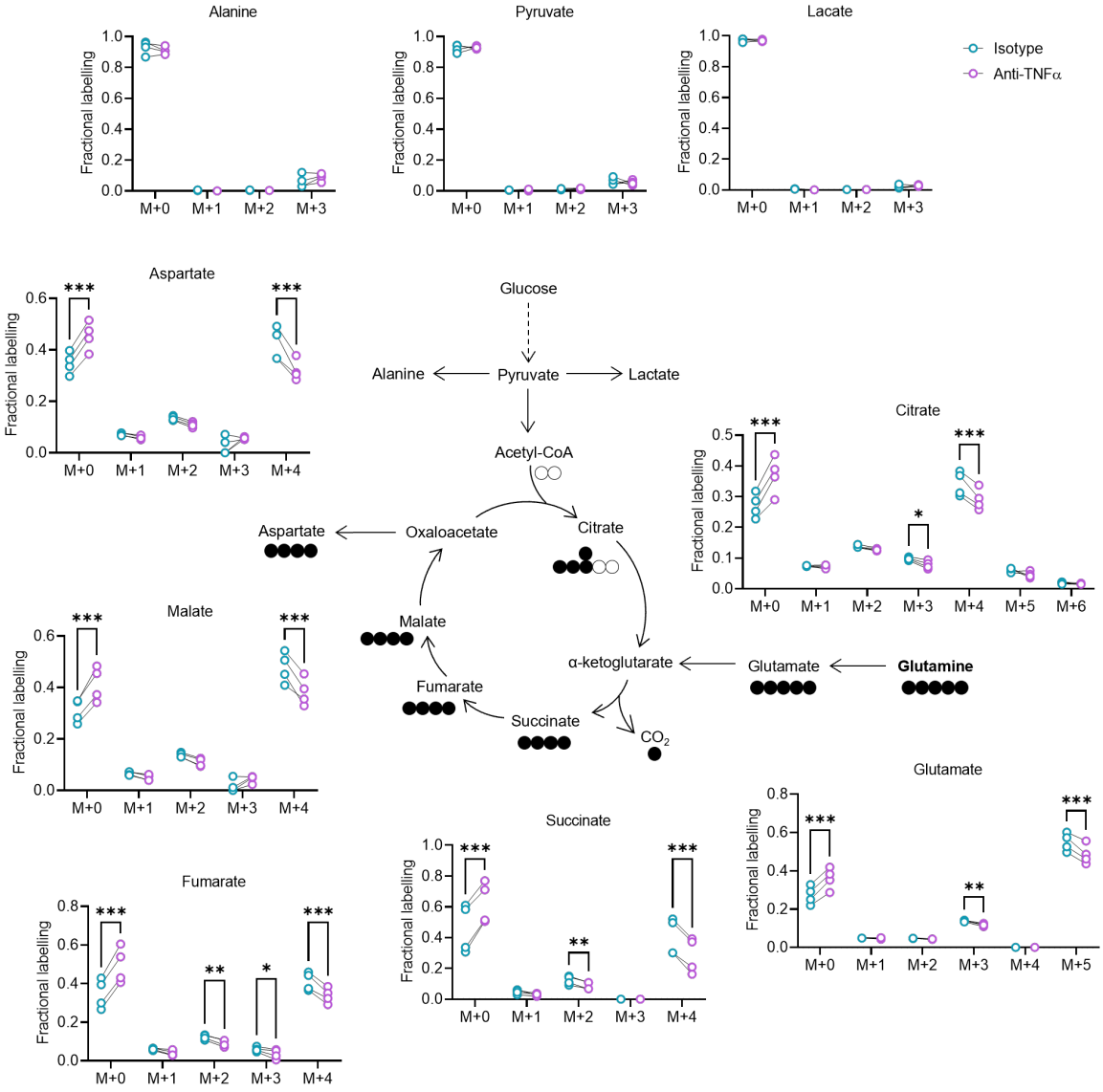

Figure 3.10 $^{13}C_5$-glutamine tracing in naïve CD4$^+$ T cells treated with anti-TNFα

Purified naïve CD4$^+$ T cells were activated for 48 h with an anti-TNFα antibody or isotype control, then cultured for an additional 6 h in presence of 2 mM $^{13}C_5$-labelled glutamine and assessed for mass isotopomer distribution (MID) of indicated metabolites by GC-MS (n=3 independent donors). Centre diagram represents the likely metabolism of fully labelled glutamine into the indicated metabolites and the resulting MID (black circles indicate a labelled carbon and white circles an unlabelled carbon). Each symbol represents a different donor with the line between denoting matched pairs. Significance was assessed by RM two-way ANOVA with Šídák's multiple comparisons test * $p < 0.05$, ** $p < 0.01$, ***$p < 0.001$.

Consistent with previous data, a reduction in the total abundance of alanine was seen with anti-TNFα treatment (Figure 3.11A). Here, a decreased total abundance of intracellular lactate was also seen in anti-TNFα-treated cells compared to isotype control-treated. Furthermore, a substantial trend towards reduced glutamine abundance in anti-TNFα-treated cells could be seen, indicating reduced uptake (Figure 3.11B). There was also lower abundance of TCA cycle intermediates in the anti-TNFα condition compared to the isotype control, although this did not reach significance for fumarate or citrate (Figure 3.11C). For glutamate, succinate, and aspartate a significant decrease was also seen in the abundance of labelled metabolite. Taken with reduced labelling of glutamine into glutamate and the TCA cycle, these data propose that anti-TNFα mediates its effects by suppressing glutamine uptake, glutamine conversion to glutamate, and metabolism through the TCA cycle, albeit little change in glucose incorporation into the TCA cycle suggests that this final mechanism may be less important. These effects likely cause the decreased activity of the ETC and associated mitochondrial oxygen consumption observed by Seahorse XF analysis.

Considering the perturbations of the TCA cycle under anti-TNFα-treatment may suggest a decreased availability of acetyl-CoA, cells were assessed for their levels of histone acetylation on histone H3 at lysine 27 (H3K27Ac), an epigenetic marker of active transcription (Creyghton *et al.*, 2010) (Figure 3.12A). A clear upregulation of H3K27 acetylation was seen upon activation of naïve $CD4^+$ T cells but there was no difference between anti-TNFα treatment and the isotype control. These data suggesting that the metabolic suppression seen here at 48 h has little epigenetic effect on the cells.

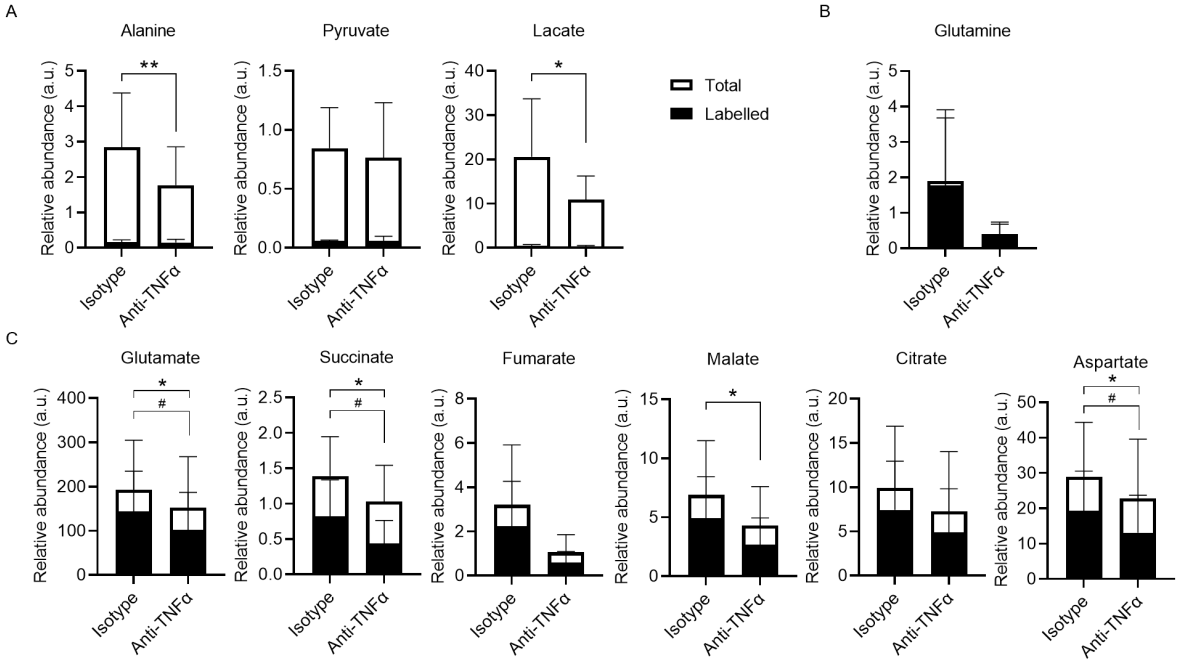

Figure 3.11 Decrease in the abundance of glutamine and TCA cycle intermediates in anti-TNFα-treated naïve cells

(**A-B**) Purified naïve $CD4^+$ T cells were activated for 48 h with an anti-TNFα antibody or isotype control, then cultured for an additional 6 h in presence of 2 mM $^{13}C_5$-labelled glutamine and assessed for total and labelled abundance of (**A**) alanine, pyruvate, and lactate (**B**) glutamine (**C**) indicated TCA cycle metabolites (A-C, n=4 independent donors). White bars represent total abundance and black bars represent the proportion of the total abundance that was labelled, calculated as total abundance multiplied by fraction labelled, a.u.=arbitrary units. Error bars show mean ± SD. Significance was assessed by RM two-way ANOVA with Šídák's multiple comparisons test, total: white bars * $p < 0.05$, ** $p < 0.01$, labelled: black bars # $p < 0.05$.

3.2.6 Anti-TNFα suppresses amino acid uptake in activated naïve CD4$^+$ T cells

Elevating the uptake of amino acids is a key process during naïve CD4$^+$ T cell activation to promote metabolic reprogramming and differentiation (Sinclair *et al.*, 2013). Therefore, the intracellular abundance of different amino acids in cells treated with an anti-TNFα or isotype control antibody was assessed by GC-MS (Figure 3.12B). Decreased leucine, phenylalanine, isoleucine, and serine levels were all observed in the anti-TNFα-treated cells. Leucine, phenylalanine, and isoleucine are taken up by the transporter LAT1. To confirm the reduced activity of this transporter, the kynurenine uptake assay was employed (Sinclair *et al.*, 2018). Kynurenine is a naturally fluorescent molecule also transported by LAT1, allowing its use as a readout for LAT1 activity and amino acid uptake capacity. BCH, an inhibitor of LAT1, was used to establish a baseline fluorescence and validate the assay. Anti-TNFα inhibited the uptake of kynurenine in naïve CD4$^+$ T cells compared to the isotype control (Figure 3.12C). These data show that blocking T cell-intrinsic TNFα signalling suppresses activity of the LAT1 transporter and uptake of multiple amino acids by activated naïve CD4$^+$ T cells.

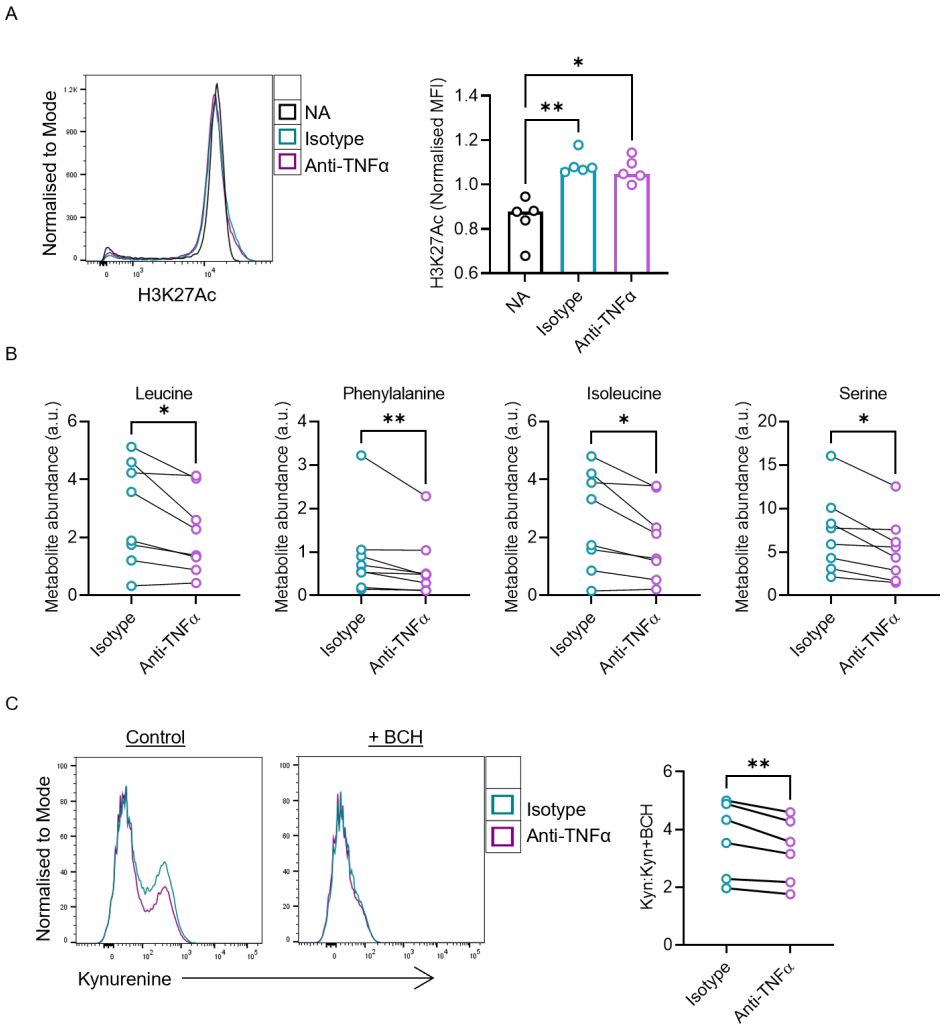

Figure 3.12 Effects of anti-TNFα on amino acid abundance in naïve CD4⁺ T cells

(**A**) Purified naïve CD4⁺ T cells were non-activated (NA), or activated for 48 h with anti-CD3/28 in the presence of an anti-TNFα antibody or isotype control and assessed for the expression of histone H3 lysine 27 acetylation (H3K27Ac) by flow cytometry (n=5 independent donors).

(**B**) Cells were cultured as in (A) without the NA condition and for an additional 4 h or 6 h in presence of 10 mM $^{13}C_6$-labelled glucose or 2 mM $^{13}C_5$-labelled glutamine respectively. Cells were then assessed for the intracellular abundance of indicated amino acids by GC-MS (n=7 independent donors).

(**C**) Cells were cultured as in (A) without the NA condition and assessed uptake of kynurenine (kyn) by flow cytometry. BCH is an inhibitor of the kyn transporter and was used to establish a baseline fluorescence. The ratio of the mean fluorescence intensity (MFI) of kyn with and without BCH was calculated (Kyn:Kyn+BCH) (n=6 independent donors).

(A-C) Each symbol represents a different donor. (A) Data were normalised to the experiment mean and the median is presented. (B-C) The line between symbols denotes matched pairs. Significance was assessed by (A) Kruskal Wallis with Dunn's multiple comparisons test (B-C) paired t test or Wilcoxon test * $p < 0.05$, ** $p < 0.01$.

3.2.7 Investigating the effects of mTNF-α and sTNF-α on naïve CD4$^+$ T cells

From the conclusion that blocking TNF-α suppresses the activation and metabolic reprogramming of naïve CD4$^+$ T cells, the next approach was to increase levels of TNF-α in the system and assess whether this could drive the opposite effect. TNF-α exists in two forms, membrane-bound and soluble, yet the distinct mechanisms of action of each are not fully understood with most studies focusing on the soluble form (Ardestani *et al.*, 2013; Su *et al.*, 2022). To start, cells were activated and cultured with or without 50 ng/ml exogenous, sTNF-α for 48 h and assessed by flow cytometry. In agreement with blocking TNF-α, no change in cell viability was seen with the addition of sTNF-α (Figure 3.13A-B). There was also no difference in cell size between the conditions (Figure 3.13A and C). STNF-α had no effect on CD69 expression but did increase CD25 levels on naïve CD4$^+$ T cells, indicating increased activation (Figure 3.13D). Next, the effect of sTNF-α on naïve CD4$^+$ T cell metabolism was assessed. MVG staining indicated no difference in mitochondrial mass between cells treated with or without sTNF-α upon activation (Figure 3.14A). Additionally, mitochondrial activity, as measured by MSO:MSO+FCCP, was unchanged with sTNF-α treatment (Figure 3.14B). As no changes could be seen with the fluorescent mitochondrial probes, the cells were next analysed by Seahorse XF assay in order to determine any subtler alterations in metabolism (Figure 3.14C-F). OCR remained broadly unaffected by the addition of sTNF-α, consistent with MVG and MSO staining (Figure 3.14C-D). However, this was accompanied by an increase in glycolytic ECAR in naïve CD4$^+$ T cells treated with sTNF-α (Figure 3.14E-F). Together, these data suggest that exogenous sTNF-α can further increase activation and aerobic glycolysis of naïve CD4$^+$ T cells but has little effect on mitochondrial oxidation.

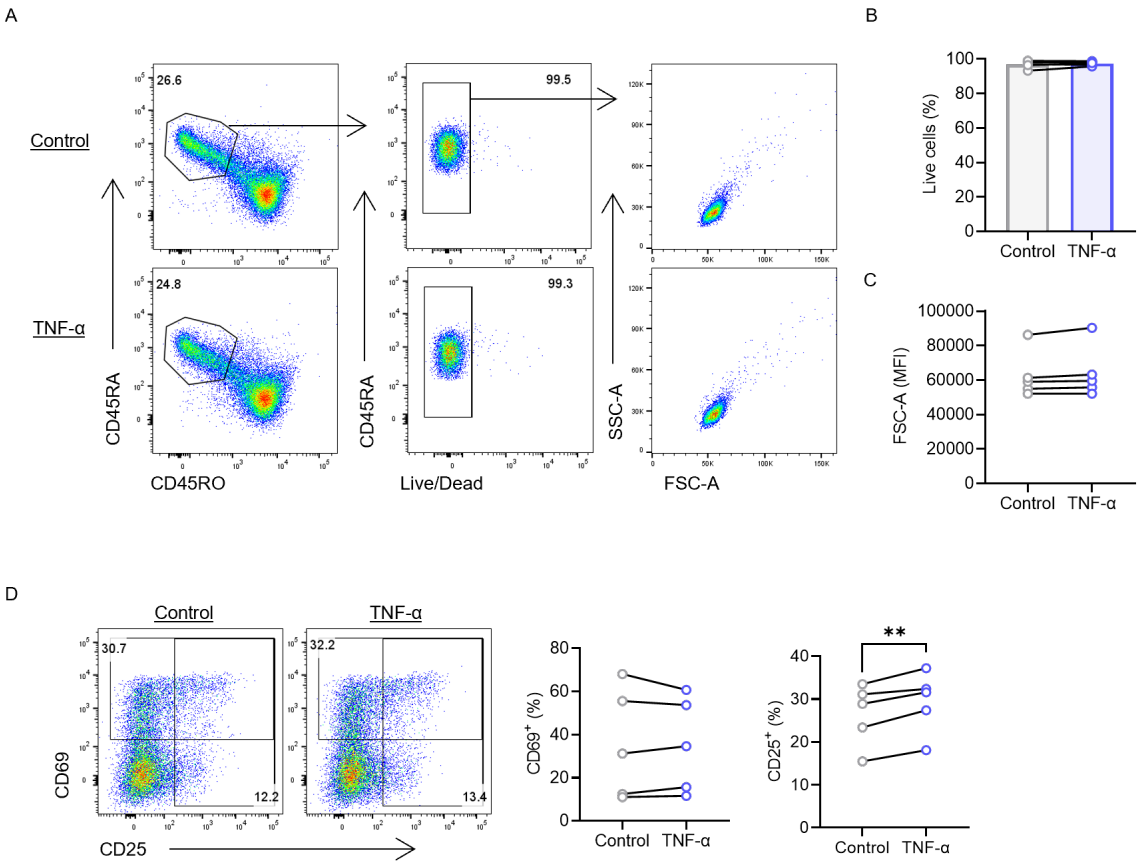

Figure 3.13 Addition of sTNF-α increases activation of naïve CD4⁺ T cells

(**A-D**) Purified CD4⁺ T cells were activated and cultured for 48 h in presence or absence of soluble TNF-α (50 ng/ml) and analysed by flow cytometry. (**A**) Cells were gated into a naïve ($CD45RA^+CD45RO^-$) subset and assessed for viability by live/dead stain. Within this gate, cells were then assessed for the mean fluorescence intensity (MFI) of forward scatter (FSC-A) (representative plots of n=5 independent donors). (**B**) Percentage of live cells within the naïve cell subset. (**C**) MFI of FSC-A as a measurement of cell size. (**D**) Percentage of $CD69^+$ and $CD25^+$ cells within the naïve cell gate (B-D, n=5 independent donors).

(B-D) Each symbol represents a different donor with the line between denoting matched pairs. Significance was assessed by paired t test, ** $p < 0.01$.

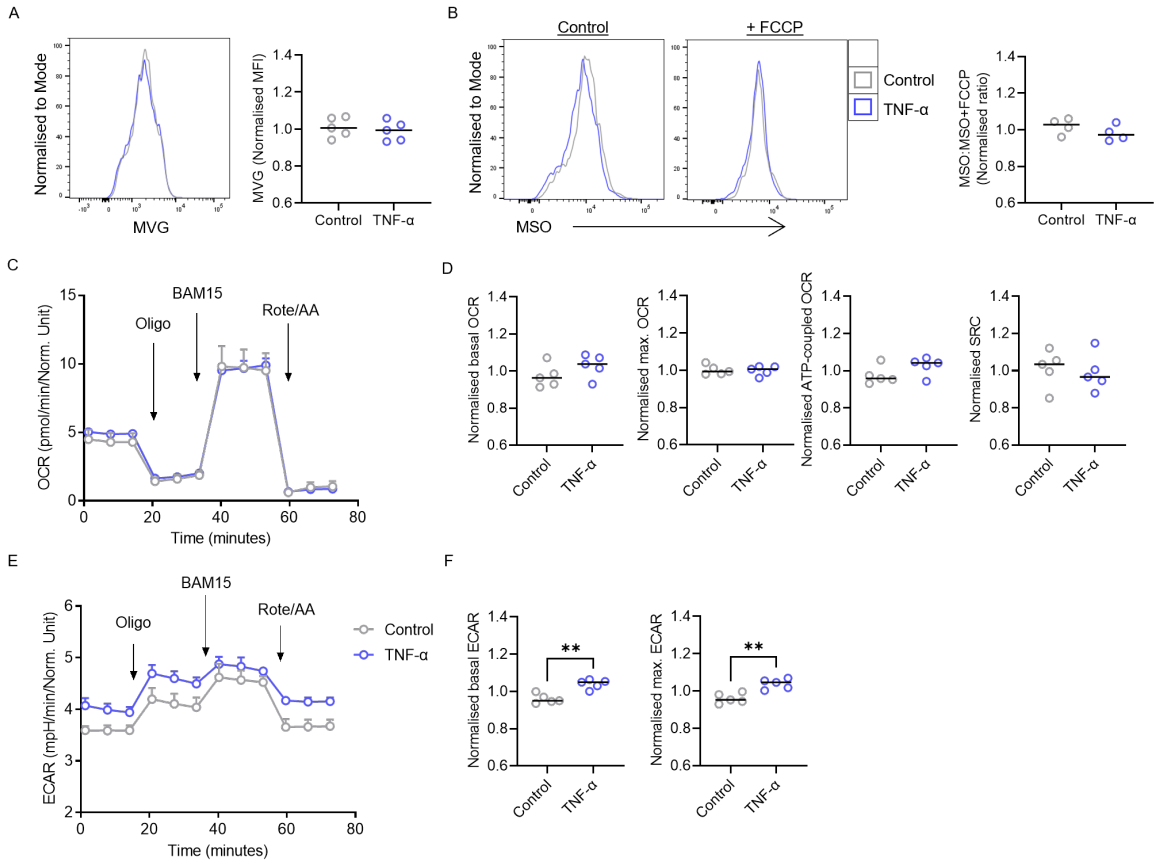

Figure 3.14 Addition of sTNF-α increases glycolysis in naïve CD4⁺ T cells

(**A-B**) Purified CD4⁺ T cells activated and cultured for 48 h in presence or absence of soluble (s)TNF-α (50 ng/ml). Cells within the naïve CD4⁺ T cell gate were assessed for the mean fluorescence intensity (MFI) of (**A**) MVG to measure mitochondrial mass (n=5 independent donors), and (**B**) the ratio of MSO with and without FCCP to measure mitochondrial membrane potential (MSO:MSO+FCCP) (n=4 independent donors).

(**C-F**) Purified naïve CD4⁺ T cells were cultured as in (A-B) and assessed for (**C-D**) oxygen consumption rate (OCR) and (**E-F**) extracellular acidification rate (ECAR) by Seahorse extracellular flux analysis. (**C and E**) Seahorse plots of (**C**) OCR and (**E**) ECAR (representative plots of n=4 independent donors). Arrows show time of injection of the indicated compounds: oligomycin (oligo), BAM15, and rotenone/antimycin A (rote/AA). Error bars indicate technical replicates. (**D and F**) For control and sTNFα-treated cells (**D**) basal OCR, maximal (max.) OCR, ATP-coupled OCR, and spare respiratory capacity (SRC) and (**F**) basal and max. ECAR were calculated (D and F, n=4 independent donors).

(A-B, D, and F) Each symbol represents a different donor, and the median is presented. Data are normalised to the mean of each experiment. Significance was assessed by Mann-Whitney test, ** $p < 0.01$.

Owing to the fact that naïve $CD4^+$ T cells produce substantial levels of TNF-α upon anti-CD3/28 stimulation (Ohshima *et al.*, 1999; Priyadharshini *et al.*, 2010) (Figure 3.1F), it was hypothesised that the system may already be saturated with near sufficient levels of TNF-α, explaining the minimal effects seen when adding additional amounts of sTNF-α into culture. CD3 alone is able to activate T cells but CD28 is required for full T cell activation and cytokine production (Kane *et al.*, 2001; Frauwirth *et al.*, 2002; Boomer and Green, 2010). Furthermore, it is reported that CD28 and TNF-α have similar roles as co-stimulatory molecules (Aspalter *et al.*, 2003; Kim and Teh, 2004). Based on this rationale, naïve $CD4^+$ T cells were activated with anti-CD3 only to investigate the role of sTNF-α in the absence of CD28 and in the presence of reduced levels of endogenous TNF-α. First, it was confirmed that anti-CD3 only stimulated cells produce significantly less sTNF-α than those activated with anti-CD3/28 (Figure 3.15A). Cells were then activated with anti-CD3 and treated with 50 ng/ml sTNF-α for 48 h. The addition of sTNF-α had no effect on cell viability but increased cell size (i.e. FSC-A) indicative of improved blasting and heightened metabolic activity (Figure 3.15B-C). STNF-α-treated cells also showed increased expression of T cell activation markers, CD69 and CD25, compared to untreated controls (Figure 3.15D). Next assessing fluorescent mitochondrial probes MVG and MSO, sTNF-α did not increase either mitochondrial mass or activity in anti-CD3 activated cells (Figure 3.15E-F). The data here suggest that exogenous sTNF-α is able to support naïve $CD4^+$ T cell activation in the absence of CD28 co-stimulation but is unable to induce the upregulation of mitochondrial metabolism.

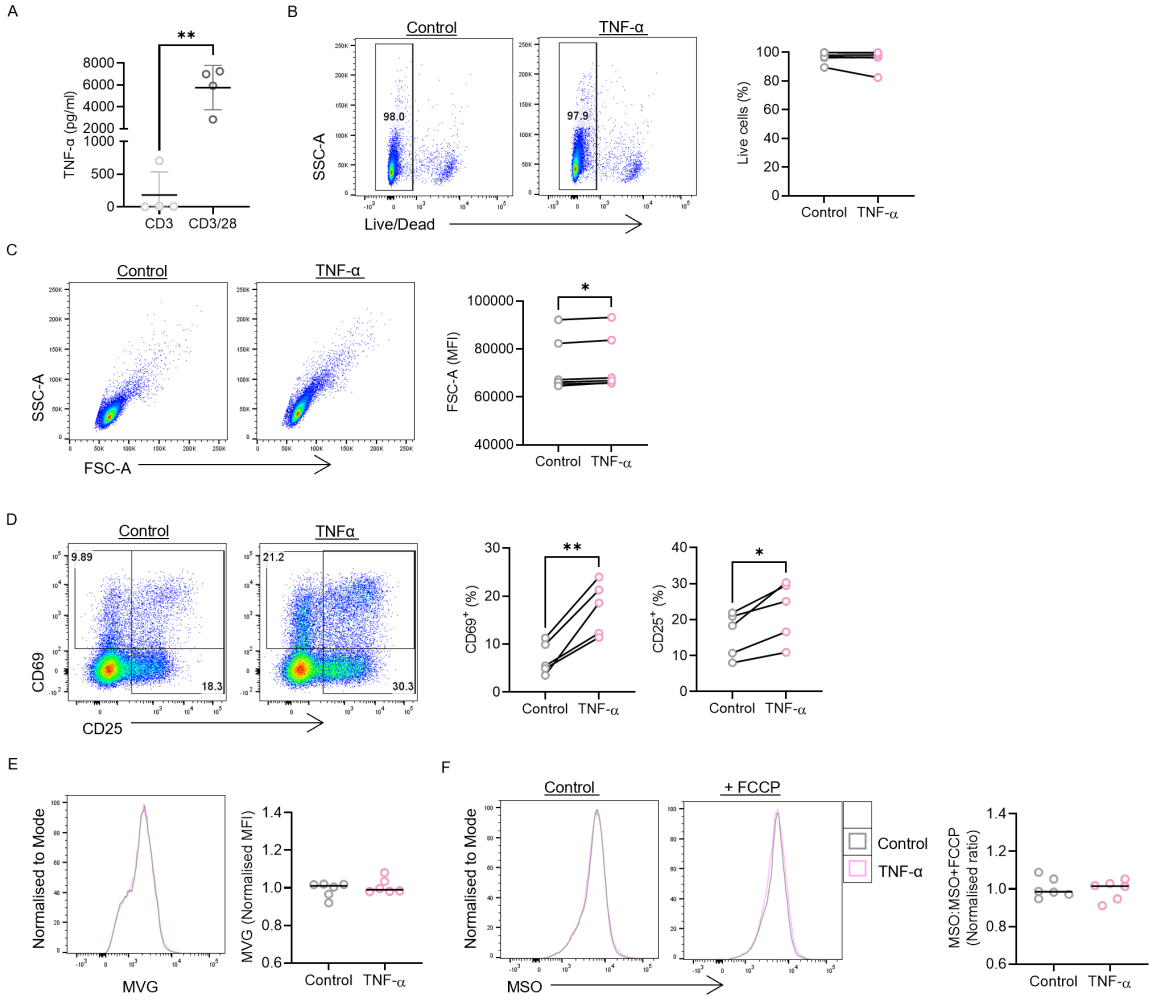

Figure 3.15 Addition of sTNF-α drives activation in anti-CD3 stimulated naïve cells

(**A**) Purified naïve CD4⁺ T cells were activated with either anti-CD3 only or anti-CD3/28 for 48 h and the supernatants analysed by ELISA for TNF-α concentration (n=4 independent donors).

(**B-F**) Purified naïve CD4⁺ T cells were activated with anti-CD3 and treated in presence or absence of soluble TNF-α (50 ng/ml) for 48 h then assessed by flow cytometry for (**B**) viability (**C**) cell size by forward scatter (FSC-A) mean fluorescence intensity (MFI) (**D**) CD69 and CD25 expression, (**E**) MFI of MVG to measure mitochondrial mass, and (**F**) ratio of MFI of MSO with and without FCCP to measure mitochondrial membrane potential (MSO:MSO+FCCP) (B-C, n=6 independent donors; D, n=5 independent donors; E-F, n=6 independent donors).

(A-F) Each symbol represents a different donor with the (A) mean ± SD (E-F) median presented. (B-D) The line between symbols denotes matched pairs. (E-F) Data were normalised to the experiment mean. Significance was assessed by (A) unpaired t test (B-C) Wilcoxon test (D) paired t test (E-F) Mann-Whitney test, * $p < 0.05$, ** $p < 0.01$.

Having investigated the effect of increasing sTNF-α in the cultures, the next approach was to increase mTNF-α. TNFR2, the predominant TNF receptor on naïve $CD4^+$ T cells (Figure 3.1B-E), has a higher affinity for mTNF-α than sTNF-α (Grell *et al.*, 1995). To increase levels of mTNF-α, cells were treated with an inhibitor of TACE, the cleavage enzyme responsible for conversion of mTNF-α to sTNF-α, TAPI-0 (Figure 3.16A). It was confirmed by ELISA that treatment with TAPI-0 at 10 μM (concentration based on a previous study (Haney *et al.*, 2011)) for 48 h profoundly decreased the concentration of sTNF-α released by activated naïve $CD4^+$ T cells (Figure 3.16B). This was matched with a substantial increase in the percentage of naïve $CD4^+$ T cells expressing surface-level TNF-α after 48 h. These data collectively certify the efficacy of TAPI-0 in increasing the ratio of mTNF-α to sTNF-α (Figure 3.16C).

A consistent but minimal decrease was seen in cell viability with TAPI-0 treatment, however percentage of live cells remained >90% which is unlikely to have any significant biological or experimental impact (Figure 3.16D). Compared to vehicle-treated controls, TAPI-0 also caused a decrease in cell size, although cells did still appear to be well blasted (Figure 3.16E). At odds with a decrease in cell size, cells treated with TAPI-0 exhibited a slight increase in CD69 expression, an early activation marker (Figure 3.16F). However, these cells also showed impaired upregulation of CD25 expression upon activation, an intermediate activation marker. To test effects of TAPI-0 on metabolic capacity, fluorescent probes of mitochondrial capacity were again utilised. In accordance with a reduced cell size, TAPI-0-treated naïve cells showed lower MVG staining than controls (Figure 3.17A). However, this was not accompanied by any change in mitochondrial activity, as measured by MSO:MSO+FCCP (Figure 3.17B). Seahorse XF analysis was then employed to better understand the effect of TAPI-0 on the metabolism of naïve $CD4^+$ T cells (Figure 3.17C-F). In agreement with a decrease in mitochondrial mass, both

basal and max. levels of OCR in TAPI-0-treated cells were reduced compared to the control (Figure 3.17C-D). However, no significant change in ATP-coupled OCR or SRC was recorded. Basal and max. levels of glycolytic ECAR were also lower in TAPI-0-treated cells than control cells (Figure 3.17E-F). Together, the Seahorse XF assay data suggest a global decrease in the metabolic capacity of TAPI-0-treated naïve $CD4^+$ T cells compared to the control, this is corroborated by a decrease in mitochondrial mass and cell size. TAPI-0 did cause a slight increase in CD69 but was suppressive of CD25. Overall, shifting the balance of mTNF-α and sTNF-α towards increased levels of mTNF-α but reduced levels of sTNF-α was inhibitory of activation and metabolism in naïve $CD4^+$ T cells.

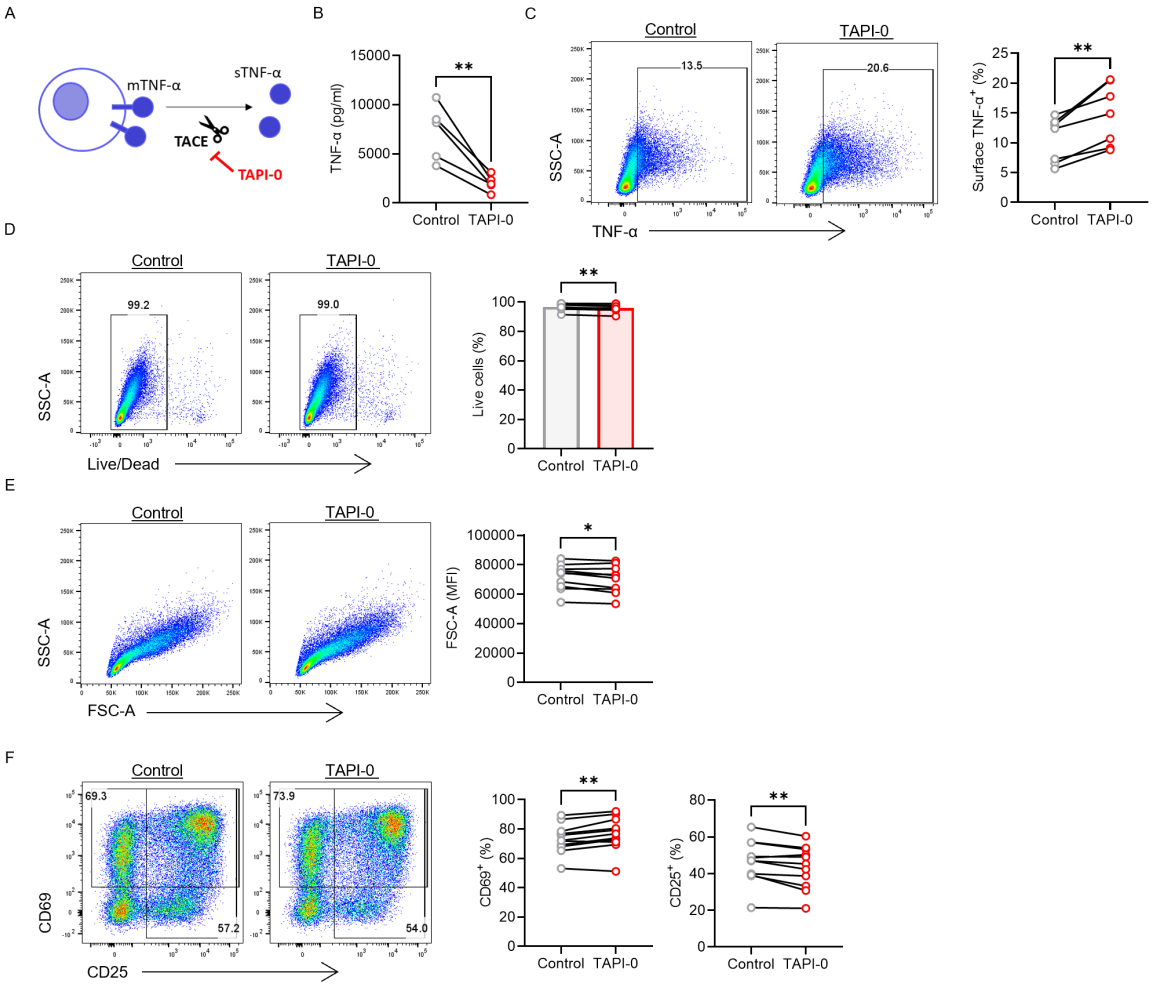

Figure 3.16 Effect of TAPI-0 on naïve CD4⁺ T cells

(**A**) Diagram detailing TNF-α release from the cell and the action of TAPI-0 on TNF-α converting enzyme (TACE).

(**B-F**) Purified naïve CD4⁺ T cells were activated in presence of TAPI-0 (10 µM) or a DMSO control for 48 h and assessed for (**B**) TNF-α concentration in the supernatant by ELISA (n=5 independent donors), and (**C**) surface expression of TNF-α (n=7 independent donors), (**D**) viability, (**E**) cell size by forward scatter (FSC-A) mean fluorescence intensity (MFI) (D-E, n=10 independent donors) and (**F**) CD69 and CD25 expression by flow cytometry (n=11 independent donors).

(B-F) Each symbol represents a different donor with the line between denoting matched pairs. Significance was assessed by paired t test, * $p < 0.05$, ** $p < 0.01$, *** $p < 0.001$.

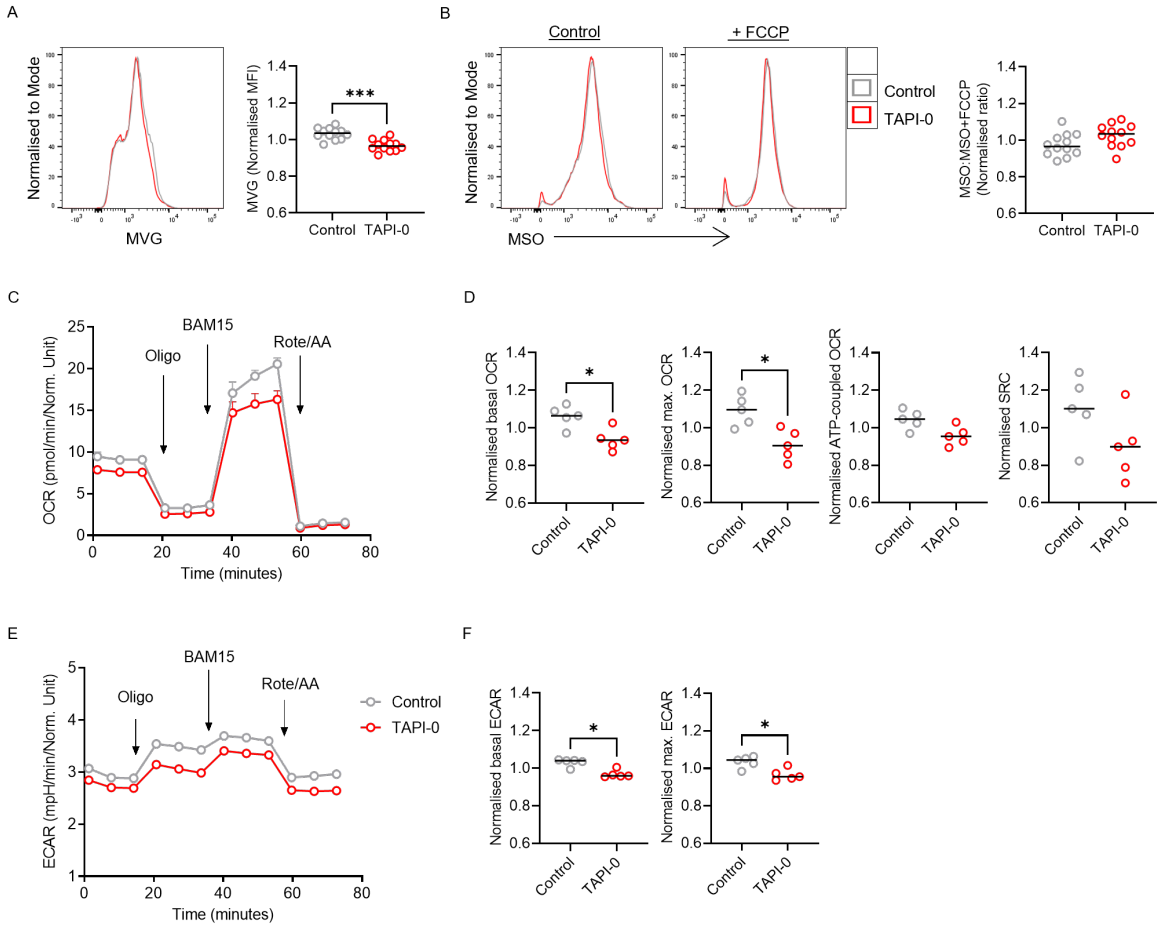

Figure 3.17 Effect of TAPI-0 on naïve T cell metabolism

(**A-F**) Purified naïve CD4$^+$ T cells were activated in presence of TAPI-0 (10 µM) or a DMSO control for 48 h and assessed for mean fluorescence intensity (MFI) of (**A**) MVG to measure mitochondrial mass and (**B**) the ratio of MSO with and without FCCP to measure mitochondrial membrane potential (MSO:MSO+FCCP) by flow cytometry (A-B, n=11 independent donors). (**C-F**) Cells were also assessed for (**C-D**) oxygen consumption rate (OCR) and (**E-F**) extracellular acidification rate (ECAR) by Seahorse XF analysis. (**C and E**) Seahorse plots of (**C**) OCR and (**E**) ECAR (representative plots of n=5 independent donors). Arrows show time of injection of the indicated compounds: oligomycin (oligo), BAM15, and rotenone/antimycin A (rote/AA). Error bars indicate technical replicates. (**D and F**) For control and TAPI-0-treated cells (**D**) basal OCR, maximal (max.) OCR, ATP-coupled OCR, and spare respiratory capacity (SRC) and (**F**) basal and max. ECAR were calculated (D and F, n=5 independent donors).

(A-B, D, and F) Each symbol represents a different donor, and the median is presented. Data are normalised to the mean of each experiment. Significance was assessed by Mann-Whitney test, * $p < 0.05$, ** $p < 0.01$, *** $p < 0.001$.

3.3 DISCUSSION

Expressed upon activation of $CD4^+$ T cells, T cell-intrinsic TNF-α has previously been reported to act as a co-stimulatory molecule, driving increased proliferation and cytokine production (Kim and Teh, 2001; Aspalter *et al.*, 2003). It was also shown that blocking T cell-derived TNF-α suppressed the activation of $CD4^+$ T cells (Povoleri *et al.*, 2020). Activation of $CD4^+$ T cells is accompanied by a significant metabolic reprogramming, mainly driven by co-stimulatory molecule CD28 (Frauwirth *et al.*, 2002; Jacobs *et al.*, 2008). Yet, any role for TNF-α in the metabolic reprogramming of $CD4^+$ T cells had not been investigated. Here, using *in vitro* culture of purified naïve and memory $CD4^+$ T cell populations activated in presence of increased TNF-α, a neutralising TNF-α antibody, or isotype control antibody, these data confirm that TNF-α is essential for full naïve and memory $CD4^+$ T cell activation. Furthermore, T cell-derived TNF-α is required for the metabolic reprogramming of naïve $CD4^+$ T cells.

3.3.1 TNFR1 and TNFR2 on $CD4^+$ T cells

Initially, expression of TNFR1 and TNFR2 was assessed. In both naïve and memory $CD4^+$ T cell populations, either resting or activated, TNFR1 could not be detected above the level of the unstained control (US). These data were corroborated by RNA-seq which showed TNFR1 transcripts in naïve $CD4^+$ T cells to be much lower than that of TNFR2 and unchanged upon activation. Similar observations of low to undetectable TNFR1 expression on $CD4^+$ T cells have been made in other studies using flow cytometry (Rossol *et al.*, 2007, 2013; Pesce *et al.*, 2022). Nevertheless, future experiments should confirm the efficacy of this antibody using a positive control of cells known to express higher levels of TNFR1, such as monocytes (Rossol *et al.*, 2007). Of note, these described studies also highlight that $CD4^+$ T cells in RA express increased

levels of TNFR1 (Rossol *et al.*, 2013; Pesce *et al.*, 2022). TNFR1 is associated with FADD and a subsequent caspase cascade to induce apoptosis (Micheau and Tschopp, 2003). In accordance with the low expression of TNFR1, data presented here also showed that blocking TNF-α had no effect on cell viability. In contrast, other studies have previously identified roles for TNF:TNFR1 signalling in co-stimulation and apoptosis of $CD4^+$ T cells (Church *et al.*, 2005; Evangelidou *et al.*, 2010; Kumar *et al.*, 2022). TNFR2 was present at the gene and protein level in all resting naïve $CD4^+$ T cells and was significantly increased upon activation after 48 h. Memory $CD4^+$ T cells expressed a higher level of TNFR2 compared to naïve cells, also upregulating expression by 48 h. Notably, in both naïve and memory cells there was a decrease in TNFR2 protein expression between rest and 4 h of activation. Reasons for this are unclear but may be due to the delay between upregulation of transcript (seen at 4 h), subsequent increases in protein translation at the ER, and trafficking to the cell membrane (Wu *et al.*, 2021). Based on the predominant expression of TNFR2 on naïve and memory $CD4^+$ T cells, it is hypothesised that T cell-derived TNF-α is signalling through TNFR2 to induce effects on metabolism. Nevertheless, future studies selectively blocking activity of TNFR1 and TNFR2 are required to confirm the specific role of each receptor in mediating the effects of TNF-α.

3.3.2 TNF-α drives full activation of naïve and memory $CD4^+$ T cells

Studies before have shown that T cell-derived TNF-α is essential for full $CD4^+$ T cell activation, through assessment of proliferation, cytokine production, and expression of T cell activation markers CD69 and CD25 (Aspalter *et al.*, 2003; Povoleri *et al.*, 2020). However, these studies have used either bulk lymphocytes or bulk $CD4^+$ T cells. Here, expression of CD45RA and CD45RO were used to gate naïve and memory cells by flow cytometry and assess their

expression of CD69 and CD25 upon activation in presence of an anti-TNFα or isotype control antibody. It was seen that blocking TNF-α impaired the upregulation of CD25 on both naïve and memory $CD4^+$ T cells but the upregulation of CD69 on only naïve cells. This effect is consistent with previous studies using bulk $CD4^+$ T cells which showed anti-TNFα to have no effect on CD69 expression but to suppress CD25 expression (Aspalter *et al.*, 2003; Povoleri *et al.*, 2020). By assessing naïve and memory cells individually, these data were able to confirm that T cell-derived TNF-α is required for full activation of both subsets. In addition, it was revealed that blocking T cell-derived TNF-α upon activation suppressed the expression of CD69 on naïve $CD4^+$ T cells. CD69 is an early activation marker induced by TCR ligation and downstream MAPK signalling, as well as HIF1α (Castellanos *et al.*, 1997; Das *et al.*, 2009; Labiano *et al.*, 2017). In comparison, CD25 is downstream of NFAT signalling induced by the TCR (Schuh *et al.*, 1998; Kim and Leonard, 2002). It is unclear why CD25 is affected but not CD69 in memory cells. Future studies may interrogate the induction of MAPK and NFAT pathways upon TCR activation of naïve and memory $CD4^+$ T cells and the effects of blocking T cell-intrinsic TNF-α on these. It is possible that naïve $CD4^+$ T cells have an increased requirement for induction of MAPK signalling, whereas memory cells, having already undergone activation, no longer require an additional TNF-α signal to promote this pathway and CD69 expression.

3.3.3 A novel role for TNF-α in the metabolic reprogramming of naïve $CD4^+$ T cells

This current study is the first to demonstrate that T cell-intrinsic TNF-α is required for the metabolic reprogramming of naïve $CD4^+$ T cells. It has been recently demonstrated that TNF:TNFR2 interactions can drive glycolysis in tTregs (de Kivit *et al.*, 2020). This study

described there to be very little effect of TNFR2 ligation on CD25 expression, proliferation, and glycolytic flux of T conventional cells (T_{CONV}) above that of anti-CD3 activation alone. This lack of effect on proliferation and CD25 expression is in contrast to other reports (Kim and Teh, 2001; Aspalter *et al.*, 2003). Additionally in contradiction, an increase in CD25 expression on anti-CD3 only activated cells in presence of exogenous sTNF-α was observed here. The largest difference between the study by de Kivit *et al*. and the results described here is the use of CD28 co-stimulation, known to be essential for increasing metabolism upon naïve $CD4^+$ T cell activation (Frauwirth *et al.*, 2002; Jacobs *et al.*, 2008). As TNF-α and CD28 have similar yet non-redundant effects on T cell activation (Aspalter *et al.*, 2003, 2007), it is possible that TNF-α requires CD28 signalling to synergistically induce metabolic reprogramming. Furthermore, de Kivit *et al*. used direct binding of TNFR2 in their experiments compared to the blocking of T cell-derived TNF-α used here. As T_{CONV} but not Tregs produce TNF-α, it is plausible that the system is already saturated with TNF-α, resulting in no additional effect of TNFR2 ligation. Indeed, this was observed in the current study as blocking TNF-α had a more profound effect on metabolic reprogramming than the addition of TNF-α. However, in their study, anti-CD3 only activation was used, which is shown here to induce much lower levels of TNF-α than anti-CD3/28 activation. The use of direct TNFR2 ligation in place of TNF-α additionally highlights the possibility for a TNFR1-dependent role which may be investigated in future studies. Similar to naïve $CD4^+$ T cells described here, T_{CONV} cells in their study were identified as $CD4^+CD25^{low}CD127^{high}CD45RA^+GPA33^{intermediate}$. Of note, de Kivit *et al*. excluded $CD25^{high}CD127^{low}$ Tregs from the analysis of T_{CONV} cells which was not done here. However, it is unlikely that any effects on Tregs are contributing to the results seen in the current study as

Tregs only made up 7.5% of the naïve $CD4^+$ T cell compartment, compared to 14.5% of memory cells where no change in metabolic reprogramming was observed.

More recently the same research group performed very similar experiments, this time analysing glutamine metabolism (Mensink *et al.*, 2022). In the data presented here, the blocking of T cell-intrinsic TNF-α under anti-CD3/28 stimulation was shown to suppress glutaminolysis and metabolism through the TCA cycle. In agreement with this, Mensink *et al*. showed that anti-CD3/TNFR2 stimulation induced higher levels of glutamine metabolism compared to anti-CD3/28. These data suggesting TNF:TNFR2 signalling to be essential for driving glutaminolysis to fuel OXPHOS in the metabolic reprogramming of naïve $CD4^+$ T cells. In the current study, it was seen that cells in the anti-TNFα treatment group trended towards a lower intracellular abundance of glutamine, suggestive of decreased uptake. In addition, unaltered incorporation of ^{13}C-glucose through the TCA cycle may suggest that the defect was not primarily within TCA cycle metabolism but before. However, these data were limited by low proportions of ^{13}C-labelled carbons present in the TCA cycle intermediates. Future studies assessing activity of the glutamine transporters and glutaminolysis enzymes may confirm the specific mechanisms by which TNF-α promotes glutamine-driven OXPHOS.

3.3.4 Comparing requirements of naïve and memory $CD4^+$ T cells

In comparison to naïve $CD4^+$ T cells, no effect of blocking T cell-derived TNF-α could be seen on the metabolic reprogramming of memory $CD4^+$ T cells. As memory $CD4^+$ T cells expressed higher levels of TNFR2 than naïve cells, it was clear that the defect was not in the capacity of the cells to respond to TNF-α. Memory $CD4^+$ T cells are primed for rapid activation upon restimulation, having undergone the epigenetic and transcriptional changes associated with

T cell activation previously (Bevington *et al.*, 2016; Barski *et al.*, 2017). Relevant to metabolic reprogramming, memory cells have increased mitochondrial content, expression of the ETC, and expression of glycolytic enzymes, each driving increased metabolic capacity (Dimeloe *et al.*, 2016; Jones *et al.*, 2019). In order to understand if the difference was due to overstimulation by the anti-CD3/28 dose given, experiments were repeated with a 10-fold lower concentration of anti-CD3/28. Suppressive effects of anti-TNFα were still present in the naïve cell subset but were again not present on memory cells. One study has shown that naïve cells increase their metabolism to a greater extent than memory cells upon activation (Jones *et al.*, 2019). Perhaps reflecting an increased need in naïve cells for pathways driving metabolic reprogramming. It is possible that there is still a role for TNF-α in modulating the metabolic reprogramming of memory $CD4^+$ T cells under different conditions. For example, the provision of MHCII molecules and CD80/86 by an APC to bind the TCR and CD28 respectively, instead of artificial ligation by antibody, may elicit varying degrees of activation and reveal a requirement for the additional TNF-α co-stimulatory signal. Moreover, it has been suggested that memory cells have an increased dependence on CD28 for proliferation and effector function compared to naïve cells (Glinos *et al.*, 2020). Future studies may investigate the role of TNF-α signalling on memory $CD4^+$ T cell metabolic reprogramming in absence of CD28 stimulation.

3.3.5 Comparing soluble and membrane-bound TNF-α

TNF-α exists in two biologically active forms, first mTNF-α from which it is then cleaved by TACE to become sTNF-α. Data presented here showed a small effect of exogenous sTNF-α on increasing glycolysis compared to a more significant decrease in glycolysis and OXPHOS when blocking T cell-derived TNF-α. Firstly, with naïve cells producing TNF-α upon activation, it was

hypothesised that the system was already near saturation. Indeed, when naïve cells were activated with anti-CD3 only and so produced much less endogenous TNF-α, exogenous sTNF-α was able to increase expression of CD69 and CD25 to a greater extent. Yet, perhaps due to a lack of CD28 stimulation, little change in metabolism was seen. Next, as it is known that TNFR2 has a higher affinity for mTNF-α than sTNF-α, which had been added previously, a selective upregulation of mTNF-α was tested (Grell *et al.*, 1995; Fischer *et al.*, 2017; Su *et al.*, 2022). To do this, cells were treated with TAPI-0, an inhibitor of TACE used previously by one study to increase levels of mTNF-α on $CD4^+$ T cells (Haney *et al.*, 2011). The membrane-bound form of TNF-α is not routinely measured by flow cytometry, papers instead focusing on intracellular levels by flow cytometry and concentrations released into the culture medium by ELISA (Wu *et al.*, 2021), but has been described in a few studies (Rossol *et al.*, 2007; Haney *et al.*, 2011; Ripoll *et al.*, 2018). Using surface staining of TNF-α it was confirmed that naïve $CD4^+$ T cells activated in a monoculture for 48 h expressed mTNF-α, with staining appearing consistent with previous studies (Haney *et al.*, 2011; Ripoll *et al.*, 2018). Levels of mTNF-α could also be significantly increased by the addition of TAPI-0. This increase was accompanied by a substantial loss in the amount of TNF-α released into the culture medium. In contrast to the expected increase in activation and metabolism with a higher amount of mTNF-α present to bind TNFR2, CD25 expression, glycolysis, and OXPHOS were decreased. As an exception, CD69 expression was increased. Reasons for this are unclear, but along with a lack of change in memory cells, adds evidence to the suggest that CD69 expression is uniquely controlled by TNF-α in naïve $CD4^+$ T cells. These data would suggest that mTNF-α is redundant for the action of TNF-α on naïve cells, effects instead being driven by sTNF-α which is reduced by TAPI-0. However, this would contradict the hypothesised signalling through TNFR2 which is known to

preferentially bind mTNF-α. Unfortunately, TACE is not specific to TNF-α cleavage and has a range of other targets including the IL-6 receptor, CD62L, co-stimulatory molecule CD40, and co-inhibitory molecule LAG-3 (Saad *et al.*, 2019). Effects on one or multiple of these molecules may have confounded the results seen here. Future studies may approach a selective increase in mTNF-α differently to ensure there are no off-target effects. Mice overexpressing mTNF-α have been developed and utilised previously in studies aiming to delineate the effects of sTNF-α and mTNF-α (Alexopoulou *et al.*, 2006; Kaaij *et al.*, 2020). In these mice, TNF-α is mutated at the cleavage site to prevent conversion to sTNF-α. Culture of naïve $CD4^+$ T cells from these mice may elucidate the relative contribution of mTNF-α and sTNF-α in driving the observed metabolic effects of TNF-α on activating naïve $CD4^+$ T cells.

3.3.6 Conclusion

Overall, data in this chapter have demonstrated a novel role for T cell-derived TNF-α in the full activation and metabolic reprogramming of naïve $CD4^+$ T cells. TNF-α promotes aerobic glycolysis, amino acid uptake, and glutamine-fuelled OXPHOS in presence of TCR and CD28-driven activation. Despite a role in driving the full activation of memory $CD4^+$ T cells, T cell-intrinsic TNF-α is redundant for their metabolic reprogramming. The next chapters will describe the work carried out to interrogate the signalling pathways downstream of TNF-α in naïve $CD4^+$ T cells able to drive these effects and aim to understand the functional impacts of TNF-α-driven metabolism.

CHAPTER 4: TRANSCRIPTIONAL AND SIGNALLING EFFECTS OF BLOCKING TNF-A

4.1 INTRODUCTION

Data in the previous chapter have highlighted a role for T cell-intrinsic TNF-α in the activation and metabolic reprogramming of naïve $CD4^+$ T cells. These effects were observed through protein staining and metabolic assays. Yet, activation of $CD4^+$ T cells is also tightly controlled by significant changes to the transcriptional landscape (Cano-Gamez *et al.*, 2020). This includes upregulation of key TFs such as c-Myc and PPARγ, and of key metabolic genes. Currently, the full effect of T cell-intrinsic TNF-α signalling on the activated naïve $CD4^+$ T cell transcriptome is unknown. However, previous studies have begun to investigate the transcriptional effects of several anti-TNFα biologics on $CD4^+$ T cells (Takeshita *et al.*, 2019; Ho *et al.*, 2021). One study identified adalimumab treatment of bulk $CD4^+$ T cells to decrease transcripts of effector cytokines including IL-17A and IL-2, yet no metabolic genes were identified (Ho *et al.*, 2021). In another study evaluating the transcriptional effects on RA peripheral $CD4^+$ T cells of patients treated with infliximab or no treatment, pathways of OXPHOS and MYC targets were found to be downregulated in the naïve $CD4^+$ T cell compartment of RA patients treated with infliximab (Takeshita *et al.*, 2019).

In addition, the signalling pathways driving these effects downstream of TNF-α ligation are not fully elucidated. The most reported pathway downstream of the TNF receptors is NFκB (Wajant and Siegmund, 2019). Previous studies investigating the co-stimulatory action of

TNF-α identified NFκB signalling to be essential for mediating the effects of TNFR2 ligation (Aspalter *et al.*, 2003; Banerjee *et al.*, 2005). The NFκB pathway is known to induce inflammation and proliferation but has not previously been implicated in driving metabolism of T cells. Of particular interest due to its known role in driving T cell metabolic reprogramming, some studies have also shown evidence to implicate the activity of PI3K/Akt in TNF-α-mediated co-stimulation of T cells (Aspalter *et al.*, 2003; Kim and Teh, 2004). The PI3K/Akt pathway and associated mTOR activity is induced primarily by CD28 co-stimulation but also modulated by IL-2 and TCR signalling. This pathway is essential for naïve $CD4^+$ T cell metabolic reprogramming, increasing glycolysis, glutamine metabolism, and OXPHOS (Frauwirth *et al.*, 2002; Jacobs *et al.*, 2008; Ray *et al.*, 2015). It is presently unclear which pathways downstream of TNF-α drive its effects on the activation and metabolic reprogramming of naïve $CD4^+$ T cells.

4.1.1 AIMS

Having established a role for TNF-α signalling in the metabolic reprogramming of naïve $CD4^+$ T cells upon activation, it was next sought to employ RNA-seq to investigate the effects of blocking T cell-intrinsic TNF-α signalling on the global transcriptional landscape changes induced upon activation. Additionally, this chapter will aim to understand which signalling pathways act downstream of TNF:TNFR ligation to drive the TNF-α-mediated effects on activation and metabolism, utilising phospho-flow to assess pathway activity.

4.2 RESULTS

4.2.1 RNA-sequencing reveals a failure of activated naïve CD4$^+$ T cells to upregulate key metabolic genes under TNF-α blockade

In order to better understand the impact of blocking TNF-α signalling on the global activation-induced transcriptome, RNA-seq was performed on naïve CD4$^+$ T cells, either NA or activated in presence of an anti-TNFα or isotype control antibody for 48 h (Figure 4.1A-E). PCA plots identified that samples clustered mainly into activated and NA (Figure 4.1A). Comparing only anti-TNFα and isotype conditions, samples did not cluster, but a separation based on treatment could be seen (Figure 4.1B). Further PCA showed that samples from the same donor also remained close together in variance (Figure 4.1C). These data confirm that the cells in the anti-TNFα and isotype conditions are well activated compared to the NA condition and no samples required removal as outliers. DEG analysis was first applied to isotype control-treated (activated) vs. NA samples to validate the process. Genes were considered differentially expressed if the adjusted p-value was ≤ 0.05. A volcano plot represents the large number of DEGs (in blue) present between activated and NA naïve CD4$^+$ T cells (Figure 4.1D). Overall, 6523 DEGs were found with 3377 upregulated and 3146 downregulated in activated cells compared to NA cells. Notable upregulated genes related to metabolic reprogramming highlighted on the volcano plot include the glycolytic enzyme *Gapdh*; *Slc2a1,* encoding the glucose transporter GLUT1; *Slc7a5*, encoding amino acid transporter LAT1; and *MYC*, a key TF promoting glycolysis and glutamine metabolism in T cells. Next, despite not clustering together, DEG analysis revealed that samples treated with anti-TNFα were transcriptionally distinct to their isotype control-treated counterparts. Comparing anti-TNFα treatment with the isotype control, 285 DEGs were identified, 191 of these upregulated and 95

downregulated (Figure 4.1E). The most highly upregulated of these included *Mx2*, *Ifi44l*, and *Gbp2*, genes primarily associated with antiviral activity (Figure 4.2A). Indeed, performing gene ontology pathway analysis on the upregulated genes in anti-TNFα vs. isotype control-treated cells identified pathways such as response to virus, regulation of viral process, and type I interferon (IFN) signalling (Figure 4.2B). Transcripts for *CD38,* an NAD consuming enzyme, were also higher in anti-TNFα-treated cells (Figure 4.2A). Of note, *Il7r* was upregulated on anti-TNFα cells compared to the control, IL-7R is downregulated following T cell activation, again indicating that blocking TNF-α signalling impairs activation of naïve $CD4^+$ T cells.

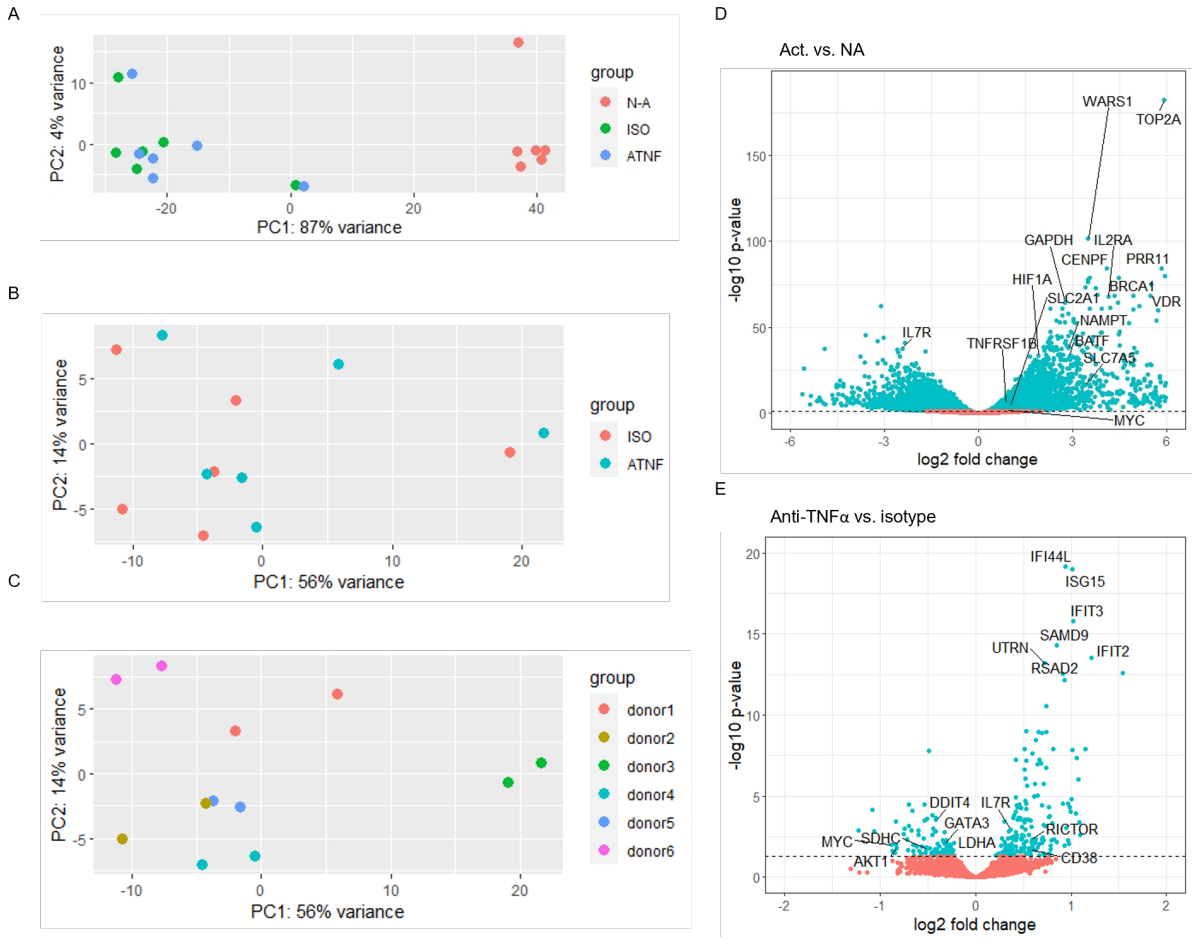

Figure 4.1 RNA-sequencing of naïve CD4⁺ T cells

(**A-E**) Purified naïve CD4⁺ T cells were either not activated (NA) or activated and cultured in presence of an anti-TNFα or isotype control antibody for 48 h and assessed by RNA-seq. (**A-C**) Principal component analysis (PCA) plot of samples from the (**A**) NA, isotype, and anti-TNFα conditions coloured by treatment and (**B-C**) isotype and anti-TNFα conditions coloured by (**B**) treatment and (**C**) donor. (**D-E**) Volcano plots showing differentially expressed genes (DEGs) in (**D**) Act. (isotype control-treated) vs. NA (**E**) anti-TNFα vs. isotype (A-E, n=6 independent donors).

(A-C) Each symbol represents an individual donor. (D-E) Each dot represents a gene, blue dots represent DEGs if adjusted p-value ≤ 0.05. Red dots represent those genes below the threshold.

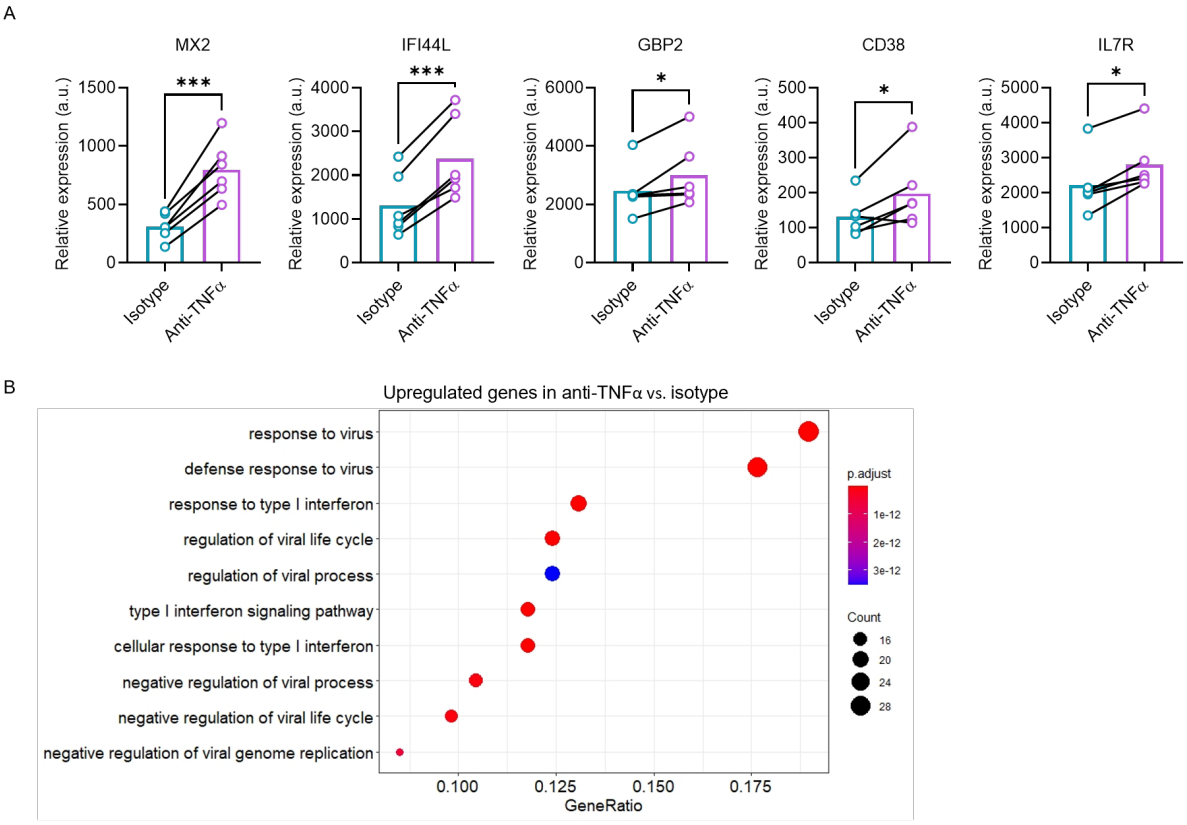

Figure 4.2 Viral and type I interferon responses, alongside CD38 and IL-7R, are upregulated by anti-TNFα

(**A-B**) Purified naïve CD4⁺ T cells were activated and cultured in presence of an anti-TNFα or isotype control antibody for 48 h and assessed by RNA-seq. (**A**) Normalised transcript abundance of selected upregulated DEGs in the anti-TNFα condition compared to isotype control, a.u.=arbitrary units (**B**) Gene ontology biological pathways analysis of all upregulated DEGs in anti-TNFα-treated cells compared to the isotype control. The top 10 pathways are shown based on GeneRatio, which denotes the proportion of DEGs in a given gene ontology term (A-B, n=6 independent donors).

(A) Each symbol represents an individual donor with lines between denoting matched pairs. Significance assessed by paired t test or Wilcoxon test, * $p < 0.05$, ** $p < 0.01$, *** $p < 0.001$.

As the data so far have pointed towards a defect in the upregulation of metabolism when blocking TNF-α signalling, downregulated DEGs in the anti-TNFα condition compared to isotype control -treated cells were of particular interest to this current study. Of these, several key metabolic DEGs were seen including *Ldha*, the enzyme able to convert pyruvate to lactate or lactate to pyruvate in glycolysis; *Sdhc*, a subunit of TCA cycle enzyme SDH; *Gata3*, a key TF for Th2 cell differentiation also recently implicated in mitochondrial fitness (Callender *et al.*, 2021); and metabolic TF *MYC* (Figure 4.1E and Figure 4.3A). Additionally, a reduction in c-Myc at the protein level was detected by flow cytometry in cells treated with an anti-TNFα antibody compared to an isotype control (Figure 4.3B). Top hits in gene ontology biological pathway analysis of these downregulated genes included ATP metabolic process, oxidative phosphorylation, and respiratory electron transport chain, again confirming a profound effect of anti-TNFα on naïve $CD4^+$ T cell metabolism (Figure 4.3C).

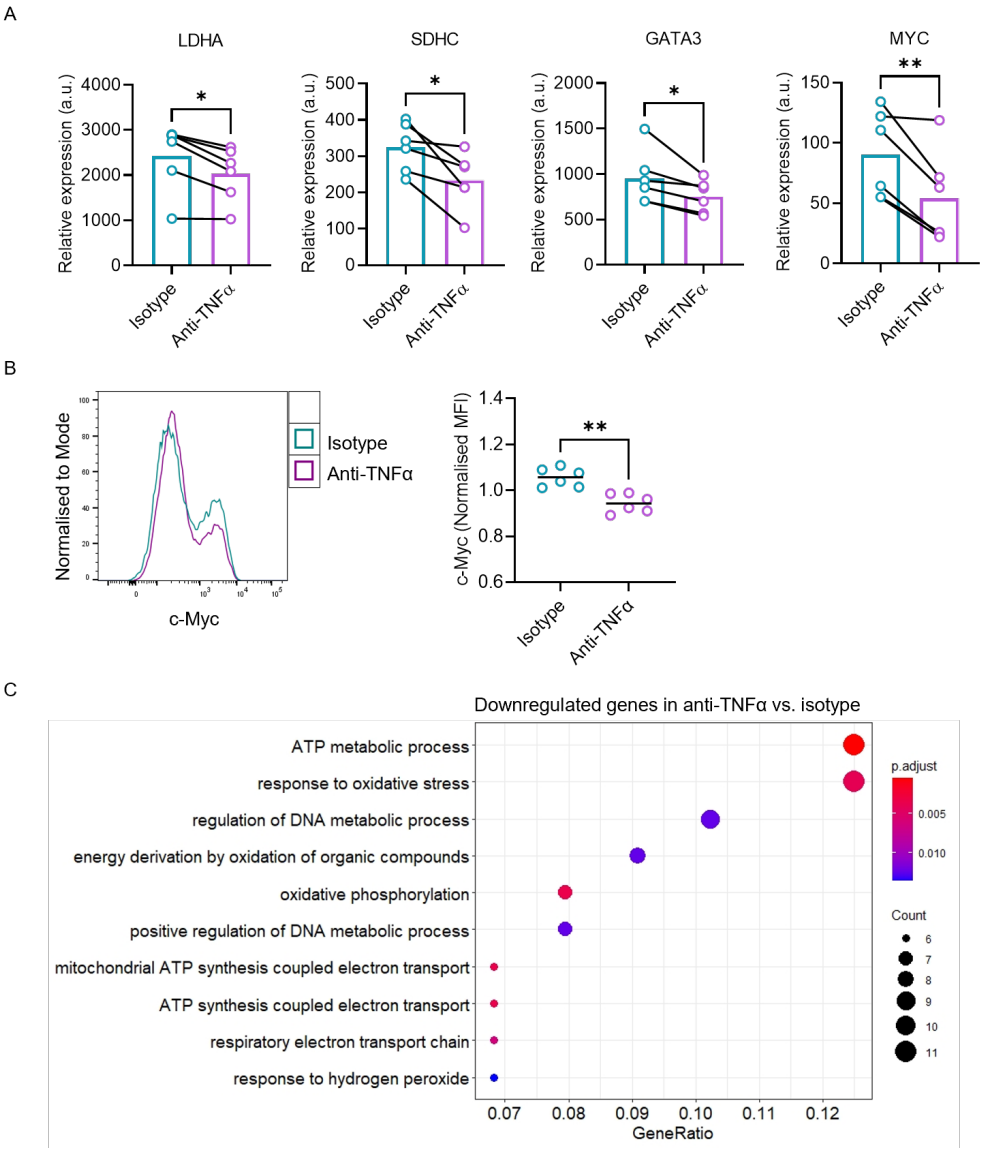

Figure 4.3 Key metabolic genes downregulated by anti-TNFα

(**A**) Purified naïve CD4⁺ T cells were activated and cultured in presence of an anti-TNFα or isotype control antibody for 48 h and assessed by RNA-seq. Normalised transcript abundance of selected downregulated DEGs in the anti-TNFα condition compared to isotype control, a.u.=arbitrary units.

(**B**) Cells were treated as in (A) and assessed for expression of c-Myc by flow cytometry, MFI=mean fluorescence intensity (n=6 independent donors).

(**C**) Downregulated DEGs as in (A) were assessed by gene ontology biological pathway analysis. The top 10 pathways are shown based on GeneRatio, which denotes the proportion of DEGs in a given gene ontology term (n=6 independent donors).

(A-B) Each symbol represents an individual donor. (A) Lines between symbols denote matched pairs (B) data normalised to the mean MFI of the experiment and presented as the median. Significance assessed by (A) paired t test or Wilcoxon test (B) Mann-Whitney test, * $p < 0.05$, ** $p < 0.01$, *** $p < 0.001$.

To further interrogate the observed failure of anti-TNFα-treated cells to fully upregulate metabolism at the transcriptional level, DEG lists were compared for isotype-treated vs. NA cells and anti-TNFα-treated vs. NA (Figure 4.4A). The intention here was to identify genes only upregulated upon activation in isotype control-treated cells, and not in anti-TNFα-treated cells. The majority of DEGs (5493 genes) in these lists overlapped, but certain genes were uniquely present in each list, 1030 and 467 respectively. As interest was focused on those genes which were failing to increase upon activation in anti-TNFα-treated cells, upregulated genes only present in isotype vs. NA were identified and analysed by gene ontology pathway analysis (Figure 4.4B). These genes only induced in isotype-treated and not anti-TNFα-treated cells upon activation were strongly associated with metabolic pathways, the top 8 pathways identified including electron transport chain, oxidative phosphorylation, and aerobic respiration. Abundance of transcripts identified as differentially expressed in the oxidative phosphorylation pathway are displayed in a heatmap (Figure 4.4C). A clear increase in gene transcripts could be seen upon activation from NA to isotype control-treated. Although still appearing slightly increased compared to NA, cells in the anti-TNFα condition failed to upregulate these metabolic genes to the level of the isotype control. Altogether, these data support the finding that blocking TNF-α suppresses metabolic reprogramming at a transcriptional level, with anti-TNFα-treated cells showing impaired upregulation of multiple genes in key metabolic pathways.

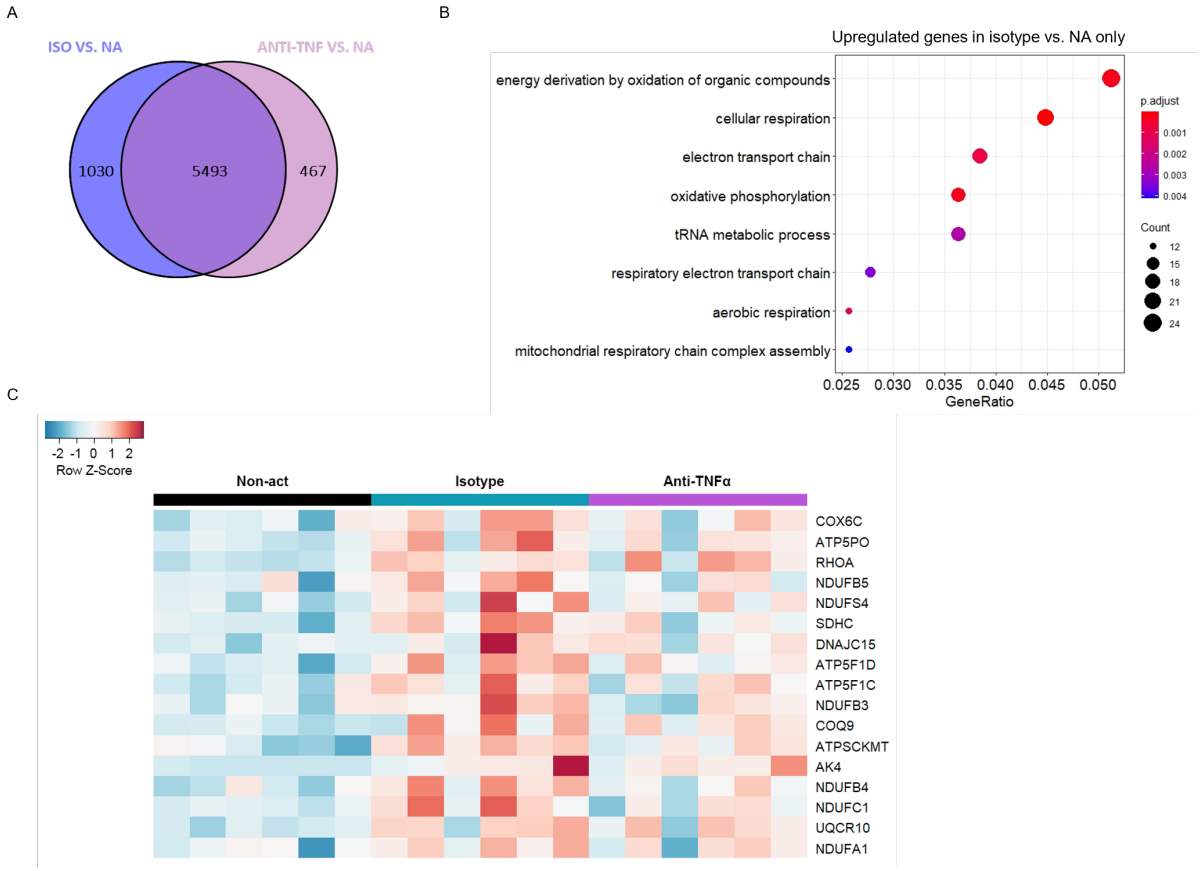

Figure 4.4 Anti-TNFα-treated cells fail to upregulate multiple genes in key metabolic pathways

(**A-C**) Purified naïve CD4$^+$ T cells were either not activated (NA) or activated and cultured in presence of an anti-TNFα or isotype control antibody for 48 h and assessed by RNA-seq. (**A**) Venn diagram comparing DEG lists of isotype-treated cells vs. NA and anti-TNFα-treated cells vs. NA. (**B**) Upregulated DEGs only present in the isotype vs. NA list were assessed by gene ontology biological processes pathway analysis. Top 8 pathways identified are shown based on GeneRatio, which denotes the proportion of DEGs in a given gene ontology term. (**C**) Relative transcript abundance of DEGs identified to be only upregulated in isotype vs. NA and part of the oxidative phosphorylation pathway are represented in a heatmap comparing relative transcript abundance of genes in NA, isotype, and anti-TNFα conditions, each column represents an individual donor (A-C, n=6 independent donors).

4.2.2 Effects of TNF-α on naïve CD4$^+$ T cells are not driven through NFκB

Next, the signalling pathways through which TNF-α may promote metabolic reprogramming of naïve CD4$^+$ T cells upon activation were interrogated. As the most widely reported downstream pathway of TNF-α (Aspalter *et al.*, 2003; Banerjee *et al.*, 2005), NFκB pathway activity was first assessed (Figure 4.5A). IκBα is a suppressor protein bound to NFκB until induction of the pathway drives IκB kinase (IKK) to phosphorylate IκBα and target it for degradation (Shi and Sun, 2018). Therefore, measuring IκBα levels in a cell provides a readout for NFκB pathway activity. At 4 h post-activation, this degradation of IκBα could be seen with lower protein abundance detected in activated cells, both isotype and anti-TNFα-treated, compared to NA. No difference in IκBα expression was seen between cells treated with an anti-TNFα or isotype control antibody (Figure 4.5B). At 24 h post-activation, all conditions exhibited the same level of IκBα expression (Figure 4.5C). Taken together, the data here suggest that TCR/CD28 engagement is sufficient to drive the transient activation of the NFκB pathway in naïve CD4$^+$ T cells, even in the absence of T cell-intrinsic TNF-α signalling.

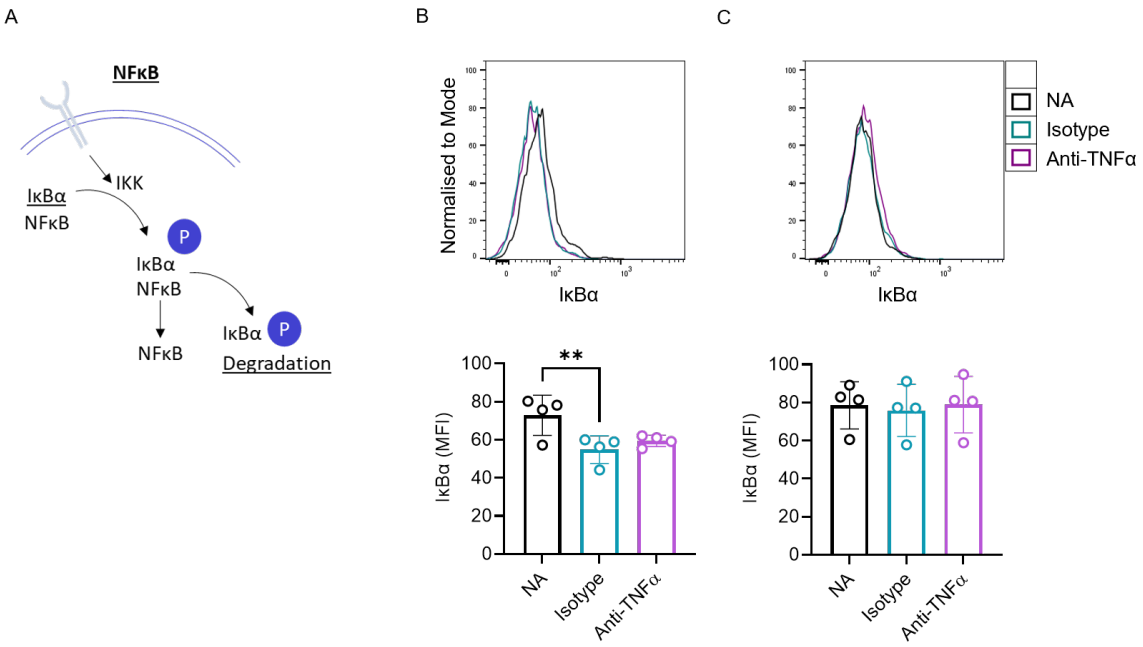

Figure 4.5 NFκB is not driven by TNF-α in naïve CD4⁺ T cell activation

(**A**) Schematic to represent NFκB signalling and the role of IκBα.

(**B-C**) Purified CD4⁺ T cells were either not activated (NA) or activated and cultured in presence of an anti-TNFα or isotype control antibody for (**B**) 4 h or (**C**) 24 h and cells in the naïve cell gate (CD45RA⁺) assessed for expression of IκBα by flow cytometry, MFI=mean fluorescence intensity (B-C, n=4 independent donors).

(B-C) Each symbol represents an individual donor, data presented as mean ± SD. Significance assessed by RM one-way ANOVA with Holm-Šídák's multiple comparisons test, ** $p < 0.01$.

4.2.3 TNF-α drives PI3K/Akt/mTOR signalling in naïve CD4$^+$ T cells

The PI3K/Akt pathway is crucial for regulation of metabolism in T cells (Shyer *et al.*, 2020), therefore, to assess activity of this pathway cells were stained for levels of p-Akt by phospho-flow (Figure 4.6A-B). Phosphorylation of the threonine 308 (T308) residue was measured as the specific residue phosphorylated by PI3K (mTORC2 is also able to phosphorylate Akt at a different position (Bozulic and Hemmings, 2009)). To understand the dynamics of the pathway, p-Akt was measured after 24 and 48 h of activation under treatment conditions. At 24 h, naïve CD4$^+$ T cells treated with anti-TNFα upon activation had reduced p-Akt levels compared to isotype control-treated cells (Figure 4.6B). LY294002 is a potent inhibitor of PI3K and used here as a control treatment. Consistently, at 48 h a similar level of impaired Akt phosphorylation was seen in anti-TNFα-treated cells (Figure 4.6C). Levels of p-Akt with anti-TNFα treatment were still slightly increased compared to LY294002-treated cells suggesting this was not a full inhibition of PI3K activity but a reduction (Figure 4.6B-C). Total levels of Akt were also assessed to ensure this effect was due to a decrease in PI3K activity and not overall suppression of Akt protein levels (Figure 4.6E). In agreement with *Akt1* being identified as a DEG in the RNA-seq analysis (Figure 4.1E), a slight decrease in total Akt expression was observed with anti-TNFα treatment. Nevertheless, the difference in p-Akt levels between isotype and anti-TNFα was greater than the difference in total Akt (Figure 4.6E-F). So, although a decline in total protein may partially contribute to the decrease in p-Akt seen, there was also an impairment in PI3K/Akt pathway activity driven by anti-TNFα.

Further downstream, Akt drives mTOR activity which modulates cellular metabolism and differentiation (Frauwirth *et al.*, 2002; Delgoffe *et al.*, 2011; Shyer *et al.*, 2020). To measure this pathway, cells were stained by phospho-flow for levels of p-S6 kinase (S6K), an enzyme phosphorylated by mTOR (Figure 4.6A). The inhibitor of mTOR, rapamycin, was used as a control treatment. At 24 h and 48 h, phosphorylation of S6K was lower in anti-TNFα-treated cells compared to isotype control-treated, although not to a level comparable to rapamycin treatment. The effect of anti-TNFα was, in this case, greatest at 48h, reflecting the position of mTOR and S6K further down in this signalling cascade than Akt (Figure 4.6F-G). In combination, these data show that blocking T cell-intrinsic TNF-α signalling supresses activity of the PI3K/Akt/mTOR pathway upon naïve $CD4^+$ T cell activation.

To assess the effect of increased sTNF-α or mTNF-α on the PI3K/Akt pathway, cells were treated with 50 ng/ml sTNF-α or TAPI-0 respectively, along with relevant controls (Figure 4.7A-D). The soluble form of TNF-α had no effect on p-Akt levels in naïve $CD4^+$ T cells but did increase levels of p-S6K upon activation compared to the control (Figure 4.7A-B). TAPI-0, which causes an increase in mTNF-α, had no effect on either p-Akt or p-S6K levels compared to the control (Figure 4.7C-D). These data show little effect of increasing levels of sTNF-α or mTNF-α on the PI3K/Akt signalling pathway in naïve $CD4^+$ T cells.

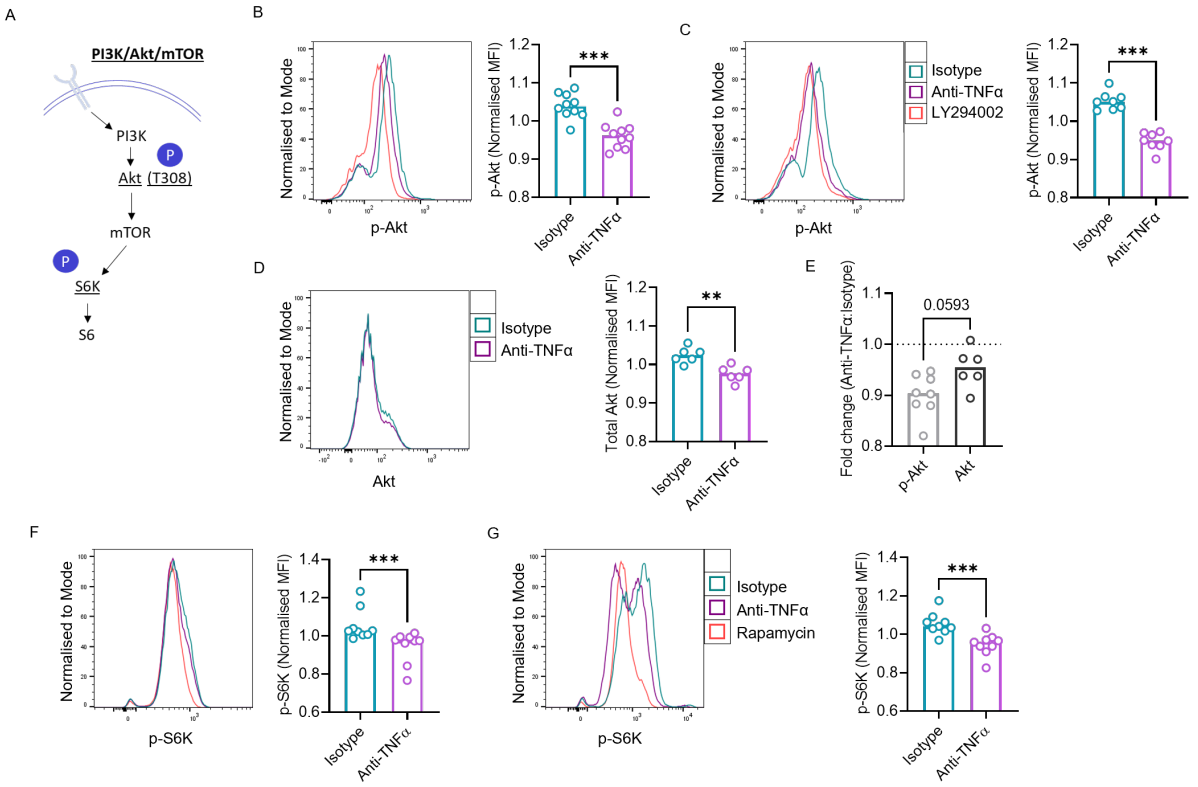

Figure 4.6 Blockade of TNF-α suppresses PI3K/Akt/mTOR signalling in naïve CD4⁺ T cells

(**A**) Schematic diagram showing the PI3K/Akt/mTOR pathway and indicating the role of phosphorylated (p)-Akt and p-S6K.

(**B-G**) Purified CD4⁺ T cells were activated and cultured in presence of an anti-TNFα or isotype control antibody for (**B and F**) 24 h or (**C-E and G**) 48 h. An additional condition of cells treated with (**B-C**) LY294002 or (**F-G**) rapamycin was included to inhibit PI3K and mTOR signalling respectively, as a control. Cells in the naïve cell gate (CD45RA⁺) were assessed for expression of (**B-C**) p-Akt (**D**) Akt or (**F-G**) p-S6K by flow cytometry, MFI=mean fluorescence intensity. (**E**) Fold change of p-Akt and total Akt MFI between isotype and anti-TNFα conditions (B, n=10 independent donors; C, n=8 independent donors; D, n=6 independent donors; F-G, n=9 independent donors; B-C, LY294002 representative plot of n=3 independent donors; F-G rapamycin representative plot of n=3 independent donors).

(B-G) Each symbol represents an individual donor and data presented as the median. (B-D and F-G) Data normalised to the mean of the experiment. Significance assessed by Mann-Whitney test, ** $p < 0.01$, *** $p < 0.001$.

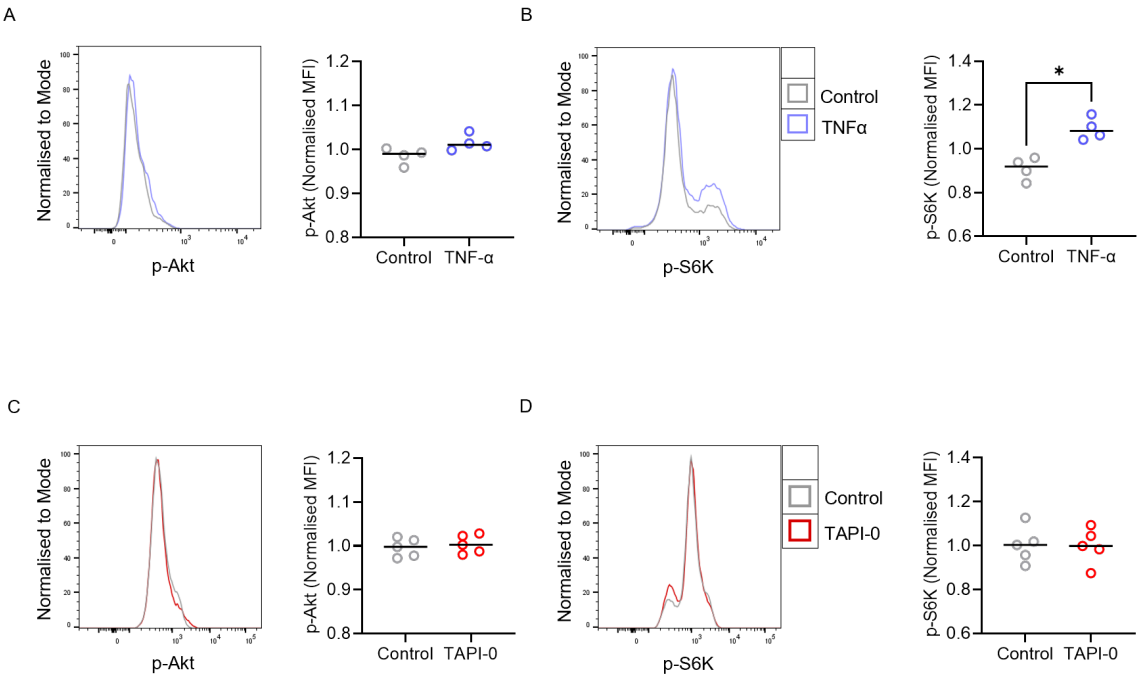

Figure 4.7 Increasing soluble and membrane-bound TNF-α has little effect on PI3K/Akt signalling in activated naïve CD4⁺ T cells

(**A-D**) Purified naïve CD4⁺ T cells were activated and cultured in presence of (**A-B**) exogenous, soluble TNF-α (50 ng/ml) (**C-D**) TAPI-0 (10 µM) or a relevant control for 48 h and assessed for expression of (**A and C**) p-Akt (**B and D**) p-S6K by flow cytometry, MFI=mean fluorescence intensity (A-D, n=5 independent donors).

(A-D) Each symbol represents an individual donor, data normalised to the mean of the experiment and presented as the median. Significance assessed by Mann-Whitney test, * $p < 0.05$.

4.2.4 TNF-α induces metabolic reprogramming through PI3K/Akt

Thus far, the data have shown that blocking TNF-α suppresses both the metabolic capacity of naïve $CD4^+$ T cells and signalling through the PI3K/Akt pathway. As PI3K/Akt is a known regulator of T cell metabolism, it is likely that through its inhibition, anti-TNFα is suppressing metabolic reprogramming. To directly confirm this, anti-TNFα and isotype control-treated cells were additionally cultured with an Akt inhibitor (Akti) or relevant DMSO control. Firstly, the Akti was titrated to find the appropriate dose, the aim was to mimic the inhibitory effects of anti-TNFα and not completely ablate the cell of Akt activity. The range of Akti doses tested (0.3-2.5 μM) was based on a previous study using human $CD4^+$ T cells (Revu *et al.*, 2018) (Figure 4.8A-G). After culture, cells were stained and analysed by flow cytometry. None of the doses used had any effect on cell viability confirming them as non-toxic (Figure 4.8A and C). A dose-dependent decline in both CD69 and CD25 expression highlighted the role of Akt in T cell activation (Figure 4.8B and D-E). A dose-dependent inhibition of p-Akt levels could be seen, along with a steady decrease in p-S6K, confirming both the efficacy of the Akti and the dependence of S6K phosphorylation on upstream PI3K/Akt function (Figure 4.8F-G). From these data, the lowest dose of 0.3 μM, was chosen for the following experiments, as this concentration was effective at decreasing all appropriate parameters and was most comparable to the degree of inhibition seen with anti-TNFα-mediated suppression.

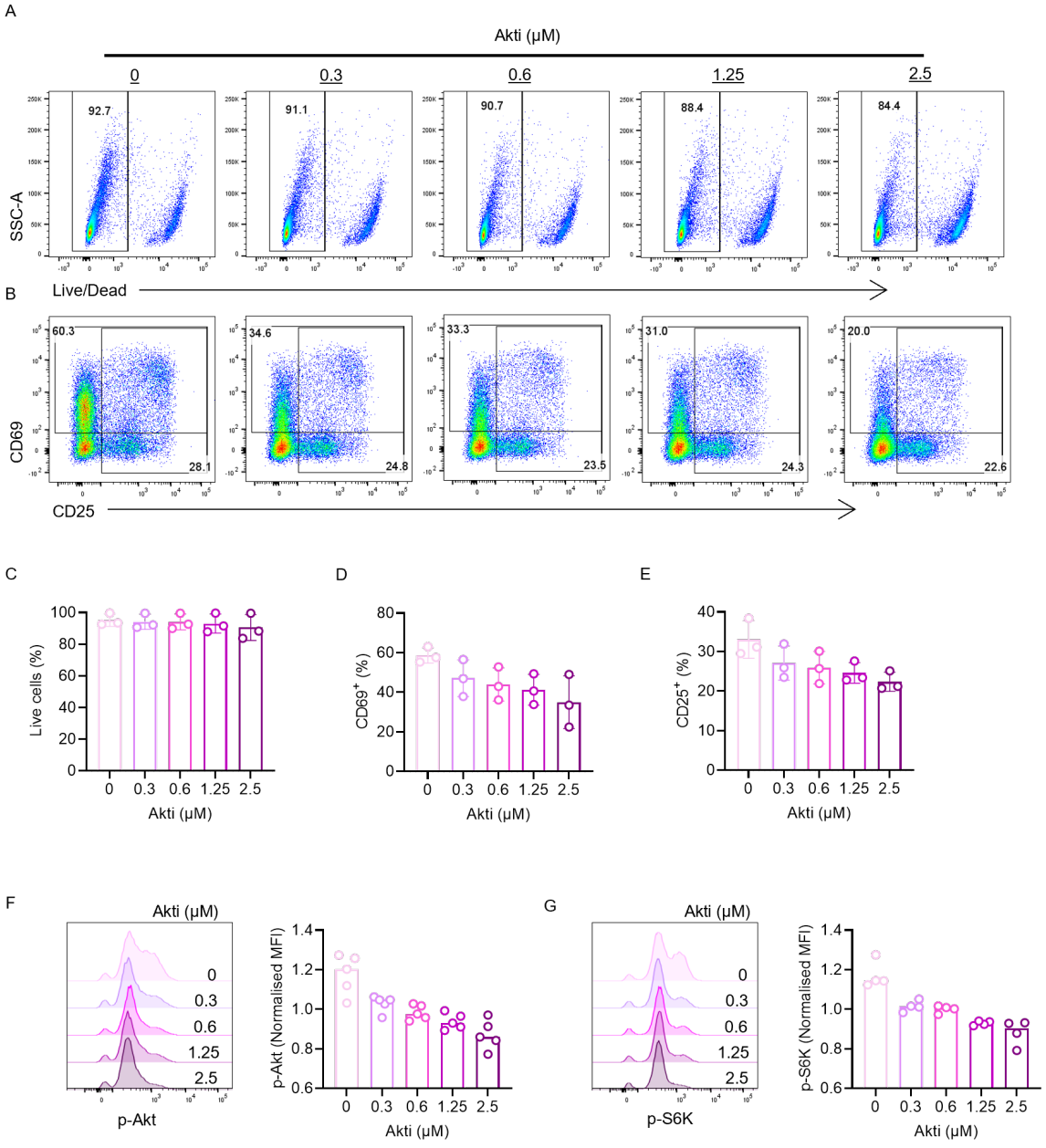

Figure 4.8 Dose-dependent effects of the Akt inhibitor

(**A-G**) Purified naïve CD4⁺ T cells were activated and cultured in presence of increasing indicated doses of Akt inhibitor (Akti; 0.3-2.5 μM) for 48 h and assessed for (**A and C**) cell viability and the expression of (**B and D-E**) CD25 and CD69 and abundance of (**F**) phosphorylated (p)-Akt and (**G**) p-S6K.

(C-G) Each symbol represents an individual donor. (C-E) Data presented as mean ± SD. (F-G) Data normalised to the mean of the experiment and presented as the median.

Substantial variability among donors meant a significant decrease in CD69 with anti-TNFα-treatment was not replicated here, however a clear trend was still apparent (Figure 4.9A-B). Indeed, this decrease could be seen in both the control and Akti conditions. The same was true of CD25 expression, with the suppressive effect of anti-TNFα present in both control and Akti-treated cells. These data suggest that blocking TNF-α is able to suppress $CD4^+$ T cell activation independently of Akt. As observed previously, anti-TNFα treatment suppressed an increase in mitochondrial mass in naïve $CD4^+$ T cells upon activation. However, this suppressive effect was completely blunted in presence of the Akti (Figure 4.10A). Notably, the Akti was able to decrease mitochondrial mass slightly further than anti-TNFα, suggesting this concentration of the Akti was inhibiting Akt to a slightly greater extent than blocking T cell-derived TNF-α. As before, no difference could be seen in mitochondrial activity between anti-TNFα-treated and isotype control-treated cells, there was also no difference within the Akti condition. Although, compared to the control the Akti did cause a reduction in MSO:MSO+FCCP (Figure 4.10B). As a readout for glycolytic activity, concentrations of glucose and lactate in the cell culture supernatants were measured after 48 h (Figure 4.10C-D). In accordance with decreased glycolysis as measured by Seahorse XF assay, anti-TNFα-treated cells had consumed less glucose from the medium during 48 h of culture than the isotype control-treated cells, resulting in a higher concentration of glucose in the supernatant (Figure 4.10C). Comparatively, no difference in glucose concentration was seen between anti-TNFα and the isotype control with the addition of the Akti. A similar trend was seen with lactate, less lactate in the supernatant after 48 h suggesting a lower rate of aerobic glycolysis, but this did not reach significance (Figure 4.10D). Altogether, these data give evidence to

suggest that TNF-α-mediated changes in mitochondrial mass and glycolysis are driven through induction of the PI3K/Akt pathway.

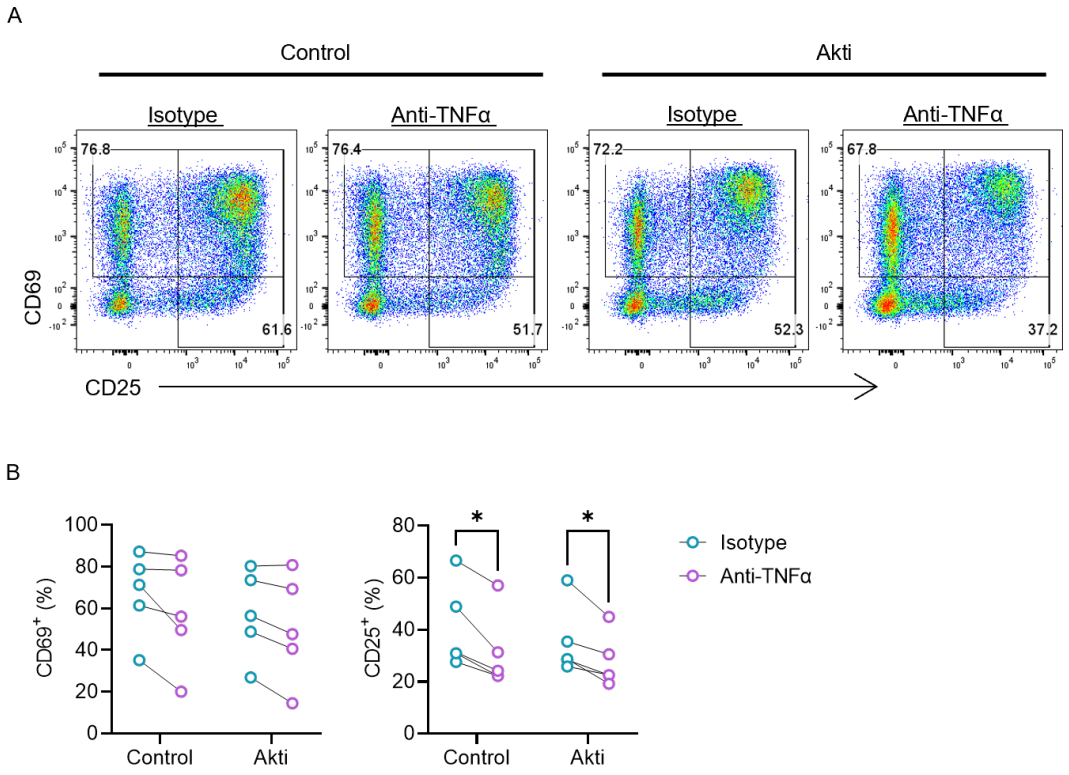

Figure 4.9 Anti-TNFα suppresses CD69 and CD25 expression independently of Akt

(**A-B**) Purified naïve $CD4^+$ T cells were activated and cultured in presence an anti-TNFα or isotype control antibody and with an Akt inhibitor (Akti; 0.3 µM) or DMSO control for 48 h and assessed for expression of CD69 and CD25 (A-B, n=5 independent donors).

(B) Each symbol represents an individual donor with the line between denoting matched pairs. Significance assessed by RM two-way ANOVA with Šídák's multiple comparisons test, * $p < 0.05$.

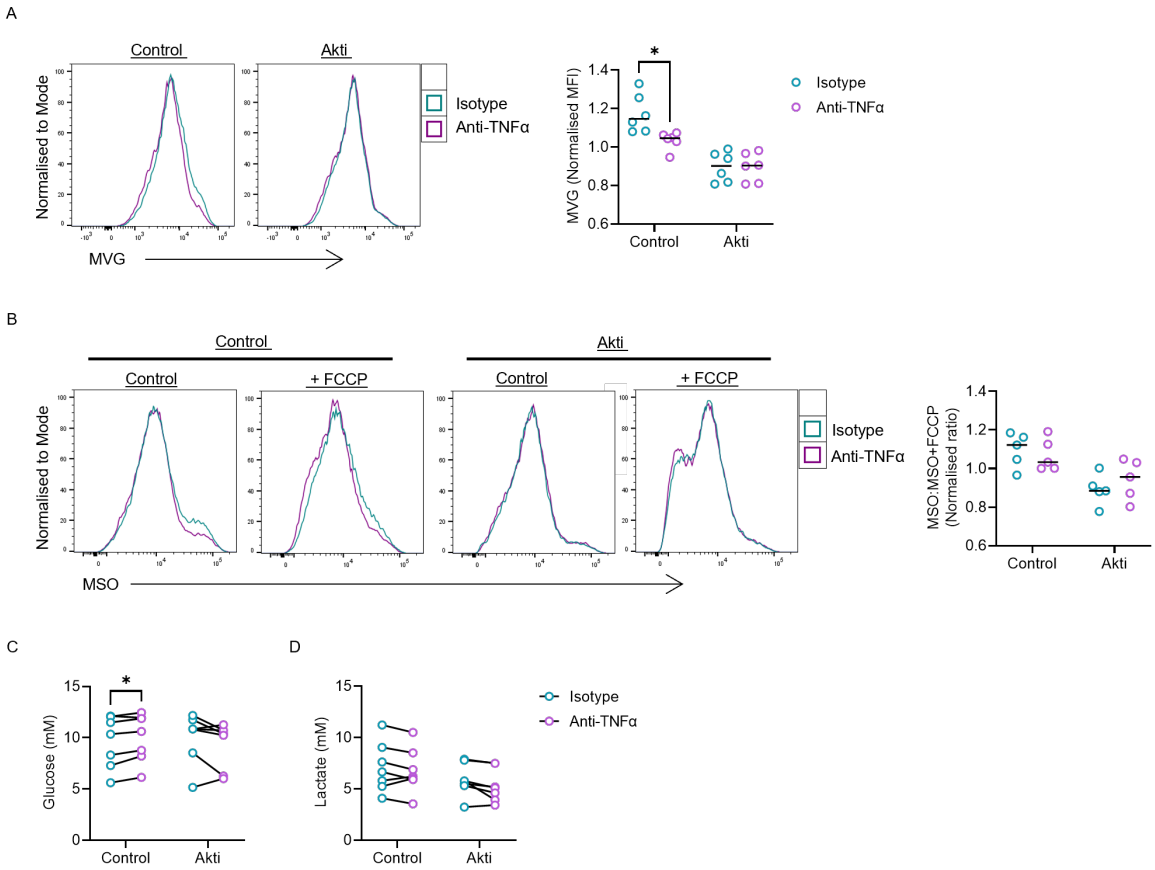

Figure 4.10 Anti-TNFα inhibits metabolism via suppression of PI3K/Akt

(**A-D**) Purified naïve CD4⁺ T cells were activated and cultured in presence an anti-TNFα or isotype control antibody and with an Akt inhibitor (Akti; 0.3 µM) or DMSO control for 48 h and assessed for mean fluorescence intensity (MFI) of (**A**) MVG to measure mitochondrial mass and (**B**) the ratio of MSO with and without FCCP to measure mitochondrial membrane potential by flow cytometry (MSO:MSO+FCCP) (A, n=6 independent donors; B, n=5 independent donors). (**C-D**) Cell culture supernatants were assessed for the concentration of (**C**) glucose and (**D**) lactate after 48 h (C-D, n=7 independent donors).

(A-D) Each symbol represents an individual donor. (A-B) Data normalised to the experiment mean and the median is presented. (C-D) The line between symbols denotes matched pairs. Significance assessed by (A-B) two-way ANOVA with Šídák's multiple comparisons test (C-D) RM two-way ANOVA with Šídák's multiple comparisons test, * p <0.05.

To confirm the role of Akt in driving mTOR activity in naïve $CD4^+$ T cells, cells were analysed by flow cytometry for phosphorylation of S6K (Figure 4.11A). In accordance with previous data, anti-TNFα-treated cells had lower levels of S6K phosphorylation than isotype controls. However, when Akt was inhibited, anti-TNFα had no effect on p-S6K levels compared to the isotype. In fact, anti-TNFα decreased p-S6K to a level comparable with the Akti. Kynurenine uptake, which was decreased by anti-TNFα treatment, also showed no change in presence of the Akti (Figure 4.11B). By comparison, the anti-TNFα-driven decrease in c-Myc expression was still present when cells were also treated with the Akti, although to a slightly lesser extent (Figure 4.11C). Taken together, these data confirm that blocking T-cell derived TNF-α upon naïve $CD4^+$ T cell activation suppresses PI3K/Akt signalling and downstream mTOR activity which results in the suppression of metabolic reprogramming. Anti-TNFα inhibits the upregulation of glucose uptake, amino acid uptake, glycolysis, mitochondrial mass, OXPHOS, and metabolism of glutamine through the TCA cycle. Anti-TNFα was also able to suppress naïve $CD4^+$ T cell expression of activation markers CD69 and CD25, and TF c-Myc in an additional manner, independent of Akt (Figure 4.12).

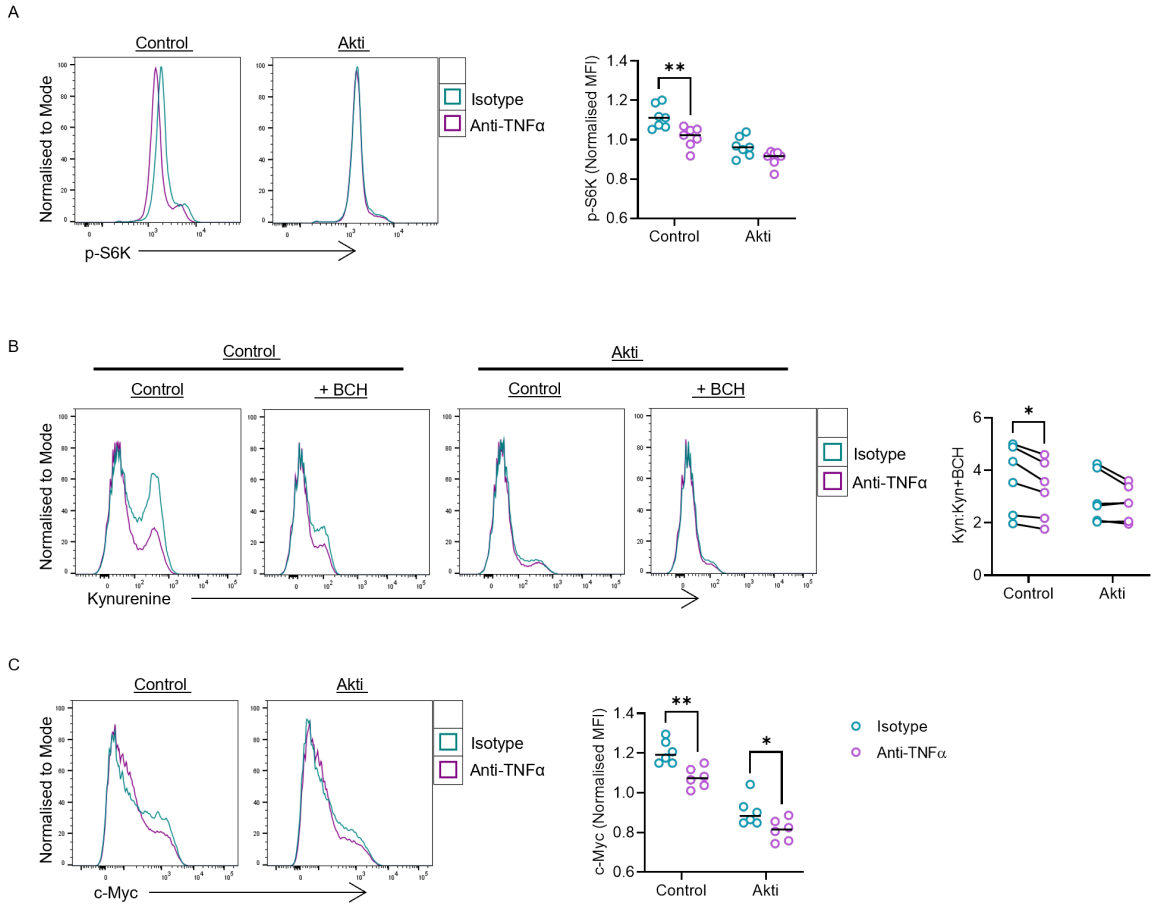

Figure 4.11 Anti-TNFα suppresses mTOR activity and kynurenine uptake via Akt

(**A-C**) Purified naïve CD4⁺ T cells were activated and cultured in presence an anti-TNFα or isotype control antibody and with an Akt inhibitor (Akti; 0.3 µM) or DMSO control for 48 h and assessed for mean fluorescence intensity (MFI) of (**A**) phosphorylated (p)-Akt (n=7 independent donors) (**B**) ratio of kynurenine (kyn) uptake with and without BCH, an inhibitor of the kyn transporter (Kyn:Kyn+BCH) (**C**) c-Myc by flow cytometry (B-C, n=6 independent donors).

(A-C) Each symbol represents an individual donor. Data normalised to the experiment mean and the median is presented. Significance assessed by (A and C) two-way ANOVA with Šídák's multiple comparisons test (B) RM two-way ANOVA with Šídák's multiple comparisons test, * p <0.05, ** p <0.01.

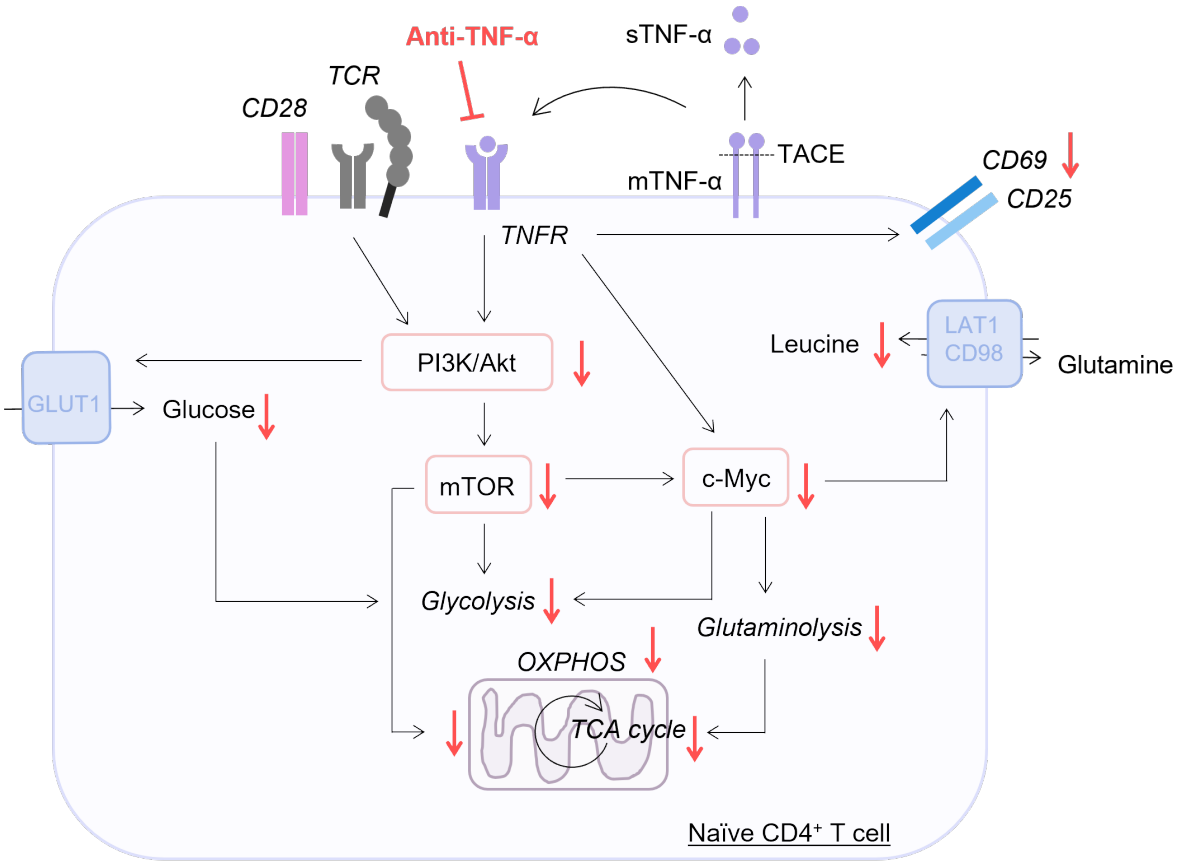

Figure 4.12 Summary diagram of TNF-α-driven metabolic reprogramming

Schematic diagram to represent the role of TNF-α in driving the activation and metabolic reprogramming of naïve $CD4^+$ T cells. TNF-α exists first membrane-bound (mTNF-α) and is then cleaved by TNF-α converting enzyme (TACE) to its soluble (sTNF-α) form. TNF-α acts on $CD4^+$ T cells through the TNFRs. Observed effects of blocking TNF-α are shown by red arrows. TNF-α drives expression of activation markers CD69 and CD25 on naïve $CD4^+$ T cells. The metabolic effects of TNF-α, including increased glucose uptake, amino acid uptake, glycolysis, mitochondrial mass, glutamine metabolism, and OXPHOS are mediated through PI3K/Akt/mTOR signalling. TNF-α also drives c-Myc upregulation through mechanisms dependent and independent of PI3K/Akt/mTOR.

4.3 DISCUSSION

The effects of blocking TNF-α on the activation-induced transcriptome of naïve $CD4^+$ T cells are yet to be described but could aid in understanding the mechanisms by which TNF-α drives activation and metabolism. Using RNA-seq, it was shown that anti-TNFα-treated naïve $CD4^+$ T cells fail to upregulate multiple key metabolic genes upon activation compared to isotope control-treated cells. Furthermore, TNF-α-mediated effects on T cells have been most commonly attributed to activation of the NFκB pathway (Kim and Teh, 2001; Aspalter *et al.*, 2003; Banerjee *et al.*, 2005). However, studies have also shown evidence for interactions with PI3K/Akt (Kim and Teh, 2001; Aspalter *et al.*, 2003). Here, it is demonstrated that T cell-derived TNF-α is not required for activation of the NFκB pathway upon naïve $CD4^+$ T cell activation but is essential for PI3K/Akt signalling and through induction of this pathway, TNF-α drives its metabolic effects.

4.3.1 RNA-sequencing suggests TNF-α upregulates metabolic genes

RNA-seq was performed on naïve $CD4^+$ T cells activated with anti-CD3/28 in presence of an anti-TNFα or isotype control antibody for 48 h. Comparisons between anti-TNFα and isotype control treatment revealed several genes upregulated by the blockade of TNF-α signalling. Pathway analysis of these genes primarily identified control of virus and type I IFN response pathways. This increase in type I IFN responses by anti-TNFα has been observed previously in psoriasis patients, attributed to effects on DCs (Conrad *et al.*, 2018). Additionally, in a study assessing the effect of adalimumab on the activated $CD4^+$ T cell transcriptome, IFN signalling was the most significantly upregulated pathway (Ho *et al.*, 2021). Investigating this effect was beyond the scope of the current study. However, further work on this potentially antiviral role

of anti-TNFα may aid understanding the risk factors and comorbidities for RA patients on TNF-α blockade therapy (Domm *et al.*, 2008; Kim and Solomon, 2010).

Relevant to the current study, pathway analysis of the genes downregulated by anti-TNFα treatment compared to the isotype control revealed multiple metabolic pathways including OXPHOS and the ETC. Comparison of the DEG lists from isotype control-treated vs. NA and anti-TNFα-treated vs. NA also revealed similar pathways enriched for downregulated genes, such as OXPHOS, the ETC, and cellular respiration. These data suggest impairment in the transcriptional upregulation of genes involved in these key metabolic pathways as one mechanism by which anti-TNFα suppresses both glycolysis and OXPHOS. Included were genes such as *Ldha* and *Sdhc*, components of aerobic glycolysis and the TCA cycle respectively. These data are consistent with a previous study assessing the transcriptome of different peripheral $CD4^+$ T cell subsets from RA patients on infliximab therapy or no treatment (Takeshita *et al.*, 2019). In contrast to the experiments described here, cells in the study by Takeshita *et al*. were analysed directly *ex vivo* and were not stimulated. Therefore effects on metabolic reprogramming may not have been detected. Nonetheless, in patients treated with infliximab, peripheral naïve $CD4^+$ T cells were enriched for downregulated genes associated with OXPHOS. Also consistent with the data here, T_{EM} cells were not associated with differences in metabolic pathways under anti-TNFα treatment. In the study by Ho *et al*. mentioned previously, RNA-seq of adalimumab-treated $CD4^+$ T cells revealed increases in IFN signalling similar to the results described here. However, downregulated genes in this study were largely effector molecules such as IL-17A, IL-2, and IFN-γ (Ho *et al.*, 2021). This discrepancy may be due to presence of naïve and memory cells in the sample, with functional suppression of memory cells by anti-TNFα dominating any effects on naïve cells. Indeed, *Gata3* transcription

in this study was seen to be unchanged by adalimumab. This contrasts with the decrease in *Gata3* seen here in naïve $CD4^+$ T cells activated in presence of anti-TNFα. GATA3 has recently been shown to have a role in inducing mitochondrial biogenesis and OXPHOS in $CD4^+$ T cells under conditions of DNA damage induced by ROS (Callender *et al.*, 2021). It is possible that lower levels of OXPHOS in anti-TNFα-treated naïve $CD4^+$ T cells results in reduced ROS production and impaired induction of GATA3. Additionally, anti-TNFα-driven suppression of GATA3 upregulation may suppress mitochondrial biogenesis and OXPHOS in these cells.

Also identified to be downregulated by anti-TNFα in RNA-seq was TF c-Myc. This was then confirmed at the protein level by flow cytometry. C-Myc is a crucial regulator of glucose and glutamine metabolism in $CD4^+$ T cells, required for proliferation and effector function (Wang *et al.*, 2011). The deficiencies seen here in glucose uptake, glycolysis, amino acid uptake, and glutaminolysis are all consistent with reduced activity of c-Myc (Wang *et al.*, 2011; Marchingo *et al.*, 2020). Use of the Myc inhibitor OMO-103 may be used in similar experiments to those performed here with the Akti, to confirm the role of c-Myc in driving TNF-α responses (Garralda *et al.*, 2022). Additionally, future studies on naïve $CD4^+$ T cells overexpressing c-Myc, for example by vector insertion (Preston *et al.*, 2015), and treated with anti-TNFα could investigate whether re-establishing c-Myc activity is able to rescue the metabolic suppression driven by anti-TNFα. It has been observed in $CD8^+$ T cells that c-Myc is rapidly degraded, so requires a high rate of protein synthesis to increase its expression (Preston *et al.*, 2015). High levels of protein synthesis require energy and amino acid uptake, both seen to be suppressed by anti-TNFα treatment of naïve $CD4^+$ T cells upon activation. It is possible that this metabolically suppressed state of the cells induced by anti-TNFα is contributing to the impairment in c-Myc upregulation. Of note, this study by Preston *et al*. also identified IL-2 to

control c-Myc expression in $CD8^+$ T cells through increasing amino acid uptake and protein synthesis. IL-2 is also known to drive glycolysis through PI3K/Akt signalling (Ray *et al.*, 2015). Additionally, impaired IL-2 production by $CD4^+$ T cells in presence of anti-TNFα has been reported (Ho *et al.*, 2021), although another study showed no effect of TNF-α on IL-2 production (Aspalter *et al.*, 2003). Here, exogenous IL-2 was added consistently to the cell cultures and so is unlikely to be contributing to the observed effects on either c-Myc or metabolism.

4.3.2 PI3K/Akt-driven TNF-α effects on metabolism

It is reported in multiple studies that NFκB signalling is induced downstream of TNF-α in T cells (Kim and Teh, 2001; Aspalter *et al.*, 2003; Banerjee *et al.*, 2005). Here, the activity of the NFκB pathway was assessed by flow cytometric analysis of IκBα protein levels. IκBα is an inhibitor of NFκB which is targeted for degradation upon activation of the pathway (Liu *et al.*, 2016). In accordance with this, a decrease in IκBα was observed after 4 h of activation in naïve $CD4^+$ T cells. By 24 h, levels of IκBα were comparable in NA and activated cells, suggesting that the induction of the NFκB pathway in naïve $CD4^+$ T cell activation occurs early and transiently. This is consistent with another study in Jurkat cells (a $CD4^+$ T cell line) which showed decreases in IκBα at around 30 mins to have increased again by 60 mins (Liu *et al.*, 2016). Additional time points of 5 mins and 1 h were also tested but not shown here as no difference in IκBα levels were seen between NA and activated cells. In the current study, anti-TNFα was unable to affect levels of IκBα, indicating that TCR/CD28 stimulation alone is sufficient to drive the NFκB pathway upon activation of naïve $CD4^+$ T cells. Validation of this result may be performed by analysis of phosphorylation levels of other proteins in the NFκB pathway, such as p65 (Liu *et*

al., 2016), or of complexes formed in the pathway by co-immunoprecipitation (Banerjee *et al.*, 2005). These experiments do not rule out a role for TNF-α-driven NFκB signalling in naïve $CD4^+$ T cell activation. However, along with little reported association between NFκB and T cell metabolism in the literature, these data were sufficient for the following investigations to be focused on a different pathway.

Here, by flow cytometry of p-Akt and p-S6K, it was demonstrated that activity of the PI3K/Akt/mTOR pathway was suppressed by anti-TNFα. These data are in agreement with a previous study which showed blockade of PI3k/Akt to partially inhibit the action of TNFR2 co-stimulation (Aspalter *et al.*, 2003). Additionally, a recent study showed TNF:TNFR2 ligation in tTregs to drive PI3K/Akt signalling and subsequent increases in glycolytic metabolism (de Kivit *et al.*, 2020). A following study by this group identified TNFR2 binding in naïve $CD4^+$ T cells to drive glutaminolysis, yet the relevant signalling pathway was not investigated (Mensink *et al.*, 2022). This TNF-α-driven PI3K/Akt metabolic axis has also been reported in other cell types such as FLS (Koedderitzsch *et al.*, 2021). In the current study, culture of cells in presence of an Akti and anti-TNFα demonstrated that anti-TNFα suppresses metabolic reprogramming in naïve $CD4^+$ T cells through the inhibition of PI3K/Akt signalling. This effect was shown by MVG staining as a readout for mitochondrial mass and levels of glucose remaining in the cell culture medium as a readout for glucose uptake. Further work could confirm this effect with Seahorse XF analysis, which is more sensitive to changes in glycolysis and OXPHOS. Stable isotope tracing of $^{13}C_5$-glutamine should also be performed to understand if the effect of TNF-α on mitochondrial oxidation of glutamine is also dependent on Akt signalling. It was seen here that inhibition of c-Myc, the major TF controlling glutamine metabolism in T cells, was only partially blunted by the Akti, suggesting the use of other

mechanisms by anti-TNFα to control its expression. Reported in several cancer studies, TNF-α has previously been shown to induce c-Myc through mechanisms such as NFκB signalling and expression of TF pituitary tumour transforming gene 1 (PTTG1) (Zhong *et al.*, 2018; Lin *et al.*, 2019). Further studies should identify the additional mechanisms of c-Myc induction by TNF-α in naïve $CD4^+$ T cells, initially investigating potential involvement of the NFκB pathway. C-Myc inhibition by anti-TNFα was at least partially blunted by the Akti, likely due to the suppression of PI3K/Akt-driven mTOR signalling by anti-TNFα which is known to promote c-Myc expression. Of note, no transcriptional change in HIF1α was detected by RNA-seq, another TF reported to be induced by mTOR (Wang *et al.*, 2011).

Inhibition of mTOR signalling by anti-TNFα was found to be Akt-dependent, suggesting a direct induction of mTOR activity by Akt. However, mTOR is also known to be dependent on leucine uptake via LAT1, expression of which is controlled by c-Myc (Sinclair *et al.*, 2013; Marchingo *et al.*, 2020). It was shown here that anti-TNFα suppresses activity of the LAT1 transporter in an Akt-dependent manner, it is likely that reduced availability of leucine is also contributing to the suppression of mTOR activity. The mechanism by which TNF-α promotes LAT1 is not elucidated but may be attributed to induction of c-Myc. Additionally, LAT1 is an antiporter of glutamine, which trended towards lower abundance in anti-TNFα-treated cells compared to isotype control-treated cells. Reduced uptake of glutamine induced by anti-TNFα may also regulate LAT1 activity. Furthermore, mTOR is stabilised by ROS, although not measured here, ROS are produced during OXPHOS (Sena *et al.*, 2013; Scharping *et al.*, 2021). It is likely that with a reduced level of OXPHOS, less ROS are present in anti-TNFα-treated cells compared to isotype controls. In the current study, it was shown that exogenous sTNF-α was able to increase p-S6K levels, indicating increased mTOR activity, but did not induce any change in

p-Akt. It is possible that one or several of these mechanisms of mTOR induction were promoted by sTNF-α and contributed to increased p-S6K. Collectively, these studies suggest that TNF-α promotes mTOR activity through multiple mechanisms, future work should confirm this effect and elucidate the contribution of each process to TNF-α-driven metabolic reprogramming.

Suppressive effects of anti-TNFα on $CD4^+$ T cell activation, assessed by expression of CD69 and CD25, were here shown to be Akt-independent. These data are consistent with the known role of TCR-driven MAPK and NFAT pathway induction promoting CD69 and CD25 expression respectively (Castellanos *et al.*, 1997; Schuh *et al.*, 1998; Kim and Leonard, 2002; Das *et al.*, 2009). The effect of TNF-α on TCR signalling was not addressed in the current study. It has been shown previously that chronic TNF-α stimulation of $CD4^+$ T cells downregulates TCR signalling (Cope *et al.*, 1994; Bryl *et al.*, 2001; Aspalter *et al.*, 2005), yet the role of T cell-derived TNF-α on TCR signalling upon naïve $CD4^+$ T cell activation is not described. Future work on naïve $CD4^+$ T cells activated in presence of an anti-TNFα or isotype control antibody, may assess TCR signalling by flow cytometry of phosphorylated proteins in the pathway such as Zap70 and LCK. Additional analysis of extracellular signal-related kinase (ERK) phosphorylation in the MAPK pathway and NFAT nuclear localisation could work towards understanding the effects of T cell-derived TNF-α on TCR signalling pathways and activation.

4.3.3 foConclusion

Overall, this chapter has shown that blockade of T cell-derived TNF-α prevents activated naïve $CD4^+$ T cells from fully upregulating a range of key metabolic genes. Furthermore, it was shown that TNF-α promotes the metabolic reprogramming of naïve $CD4^+$ T cells through induction of

the PI3K/Akt/mTOR pathway. In comparison, expression of CD69, CD25, and c-Myc are regulated by Akt-independent mechanisms. Work presented in the next chapter will interrogate the functional effects of the TNF-α/PI3K/Akt metabolic axis on naïve $CD4^+$ T cells.

CHAPTER 5: FUNCTIONAL IMPACT OF TNF-A BLOCKADE ON CD4$^+$ T CELLS

5.1 INTRODUCTION

Cellular metabolism is tightly linked to a cell's functional capacity. As data in the previous chapters have identified a TNF-α-driven PI3K/Akt metabolic axis in the activation of naïve CD4$^+$ T cells, the next approach was to investigate the functional impacts of this. TNF-α is known to increase proliferation and cytokine production in T cells upon activation, identified as part of its role in co-stimulation (Aspalter *et al.*, 2003, 2007). A study investigating the transcriptional effects of adalimumab on CD4$^+$ T cells showed decreases in IL-17A, IL-17F, and IFN-γ but no change in TFs (Ho *et al.*, 2021). Furthermore, another study on the effects of infliximab on CD4$^+$ T cells from patients with Behçet's disease, a disease causing inflammation of the blood vessels, showed blocking TNF-α to suppress Th17 cell differentiation, seen by reduced IL-17 expression but also reductions in RORγt (Sugita *et al.*, 2012). A recent study on purified Th1 and Th17 cells from peripheral blood showed that TNF-α could promote IL-17 production but was inhibitory of IFN-γ (Pesce *et al.*, 2022). In comparison, TNF-α was shown to be essential for the proliferation and inflammatory Th1 cell phenotype of CD4$^+$ T cells in a mouse model of colitis (Chen *et al.*, 2016). This study however, did not look at T-bet expression, only IFN-γ. An additional study looking at the role of TNFR2 in mouse models of colitis and MS, found that TNFR2 signalling drove the expansion of inflammatory Th1 and Th17 cells, increasing both TF and cytokine production, and again showing that TNFR2 deficiency was protective in these disease models (Alam *et al.*, 2021). This work also highlighted a requirement for TNFR2 in Treg

differentiation, an effect that has been considered by previous studies. It remains unclear whether TNFR2 is able to promote or suppress Treg function, with studies showing it to both enhance and inhibit FoxP3 expression (Zhang *et al.*, 2013; Tseng *et al.*, 2019). Of note, tTregs exhibit a more stable FoxP3 phenotype; TNF:TNFR2 binding in this subset has been shown to promote glycolysis and an increased suppressive capacity (Baron *et al.*, 2007; Q. Chen *et al.*, 2011; de Kivit *et al.*, 2020). In comparison, iTregs differentiated from naïve $CD4^+$ T cells, are less phenotypically stable and more prone to plasticity (Komatsu *et al.*, 2014; Wang *et al.*, 2015). The blockade of TNF-α has also been shown to induce the production of anti-inflammatory IL-10 by $CD4^+$ T cells independently of FoxP3 expression (Evans *et al.*, 2014; Roberts *et al.*, 2017; Povoleri *et al.*, 2020).

Previous studies have implicated dysregulated metabolism as a driver of the pathogenic function of inflammatory T cell subsets. Lactate build-up in the local microenvironment promotes Th17 cell differentiation through FAS (Pucino *et al.*, 2019). An intrinsic glycolysis defect in naïve $CD4^+$ T cells in RA promotes ROS overproduction, leading to a Th1 and Th17 cell differentiation bias (Yang *et al.*, 2016). Also demonstrated in RA naïve $CD4^+$ T cells, impairments in succinyl-CoA ligase and mitochondrial aspartate production drive an invasive phenotype and overproduction of TNF-α respectively (Wu *et al.*, 2020, 2021). Furthermore, it is known that increased inflammatory function is often coupled with higher metabolic demands (Peng *et al.*, 2016; Cluxton *et al.*, 2019). Indeed, Th1 and Th17 cells are known to be more reliant on glycolysis than Tregs (Delgoffe *et al.*, 2009; Michalek *et al.*, 2011; Gerriets *et al.*, 2015),

IL-12 is a known inducer of a Th1 cell phenotype with IFN-γ able to enhance differentiation (Hsieh *et al.*, 1993; Smeltz *et al.*, 2002). For Th17 cells, IL-1β, IL-6, IL-23, and TGF-β are all

implicated in promoting differentiation (Manel *et al.*, 2008; Volpe *et al.*, 2008; Revu *et al.*, 2018). Inflammatory cytokines, IL-17, IFN-γ, and TNF-α, produced by these cell types then promote immune cell migration, pro-inflammatory phenotypes in neighbouring cells, and further release of inflammatory mediators to exacerbate disease. The differentiation of naïve $CD4^+$ T cells into a Th1 and Th17 cell phenotype is a crucial process in the pathogenesis of inflammatory disease, yet the role of TNF-α in the induction of these subsets is not completely understood and effects are inconsistently reported. Moreover, the mechanisms by which TNF-α drives inflammatory $CD4^+$ T cell differentiation are not known, particularly in relation to the TNF-α-driven metabolic effects described here. Better insight into these effects which promote pathogenic cell function will aid in the understanding and use of anti-TNFα therapy in inflammatory disease.

5.1.1 AIMS

With previous analyses focusing on naïve $CD4^+$ T cells, this chapter will assess their ability to differentiate *in vitro* into inflammatory Th1 and Th17 cell subsets and iTregs in presence of an anti-TNFα or isotype control antibody. First, a differentiation protocol will be developed for human Th1, Th17, and Treg cells. Next, the effects of anti-TNFα on $CD4^+$ T cell differentiation will be assessed by flow cytometry and ELISA. Further experiments again utilising the Akti, will then assess whether the effects of blocking TNF-α on $CD4^+$ T cell differentiation are Akt-dependent. These experiments will test the hypothesis that the suppressive metabolic effects of anti-TNFα on naïve $CD4^+$ T cells will cause an impairment in the differentiation of Th1 and Th17 cells.

5.2 RESULTS

5.2.1 CD28 stimulation suppresses *in vitro* differentiation of human Th17 cells

To interrogate a role for TNF-α in the differentiation of naïve $CD4^+$ T cells into effector subsets, naïve cells, treated with an anti-TNFα or isotype control antibody, were polarised into Th1, Th17, and Treg cells. A Th0 condition with no additional cytokines or blocking antibodies was used as a control (Figure 5.1A-E). Naïve $CD4^+$ T cells were activated and cultured for 6 days under polarising conditions and assessed by flow cytometry on days 3 and 6. By day 3, around 50% of cells polarised towards a Th1 cell phenotype expressed IFN-γ, with cells in all other conditions remaining at around 12% IFN-γ^+ (Figure 5.1A). At day 6, the percentage of IFN-γ^+ cells in the Th1 condition had increased slightly to 58.6% with cells under Th0, Th17, and Treg cell differentiation remaining between 6-11% IFN-γ^+. In agreement with this, Th1 cells exhibited the highest expression of the Th1 cell hallmark TF T-bet on both days 3 and 6 (Figure 5.1B). For Th17 cell differentiation, although the highest percentage of IL-$17A^+$ cells was present in the Th17 condition, this was only around 3% on day 3 with other conditions at around 2% IL-$17A^+$ cells. IL-17A expression then globally dropped by day 6 with positive cells in the Th17 condition reduced to 1.5% (Figure 5.1C). Appropriately, Th17 cells did have higher RORγt expression than Th1 and Th0 cells on day 3 (Figure 5.1D). However, by day 6, this difference was reduced and levels of RORγt were comparable between Tregs and Th17 cells. Tregs were well differentiated by day 6 with over 50% of cells expressing FoxP3, more than 30% higher than other conditions (Figure 5.1E). From these data, day 6 was chosen as a suitable time point for differentiation of human naïve $CD4^+$ T cells into effector subsets. Both Th1 and Treg cells were well differentiated under these conditions. However, Th17 cells were unable to produce much IL-17A and did not have a distinctly high expression of RORγt.

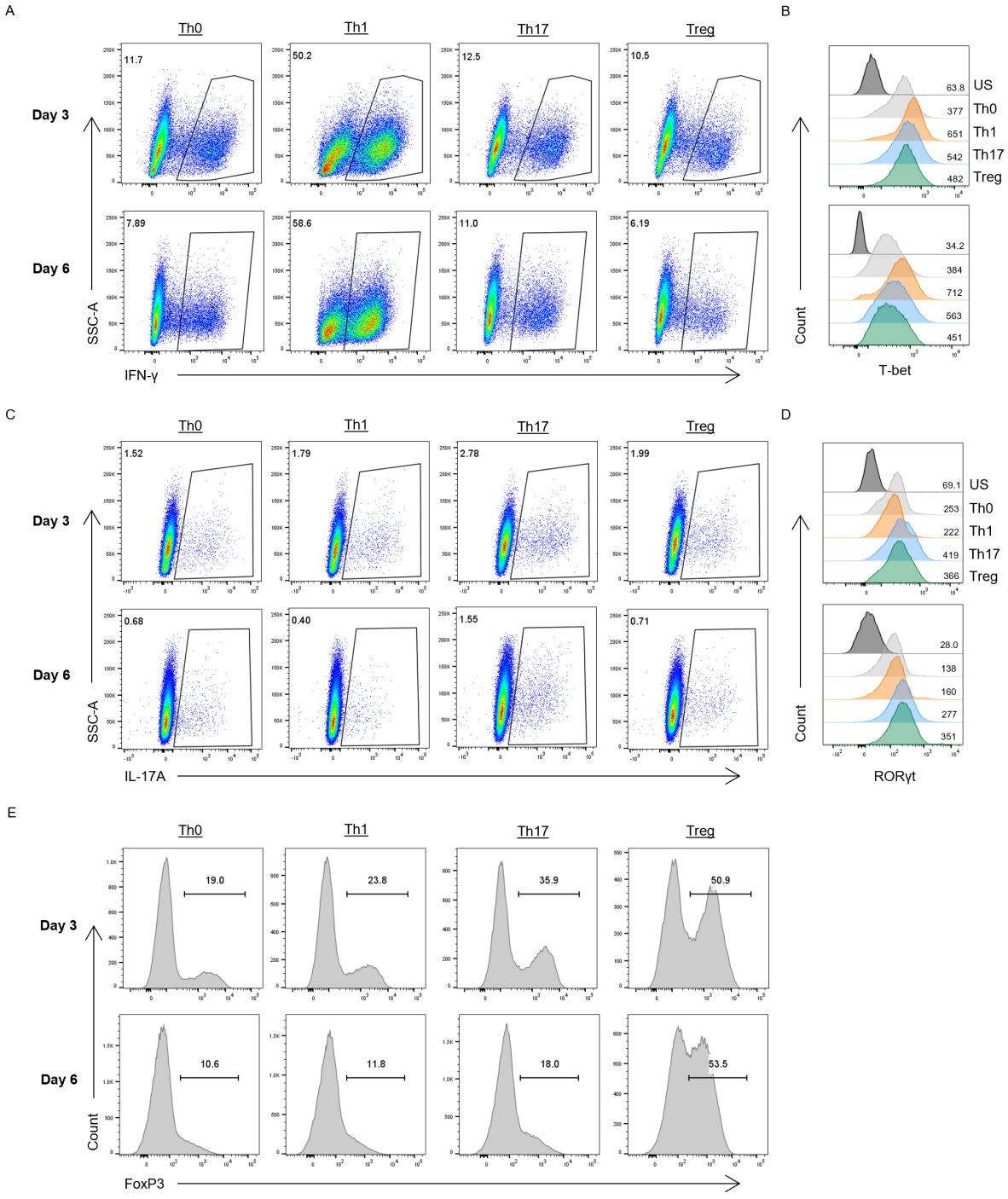

Figure 5.1 Differentiation of CD4⁺ T cell subsets

(**A-E**) Purified naïve CD4⁺ T cells were activated with anti-CD3/28 and differentiated into Th0, Th1, Th17, or Treg cells over 6 days, then assessed on days 3 and 6 for the expression of (**A**) IFN-γ (**B**) T-bet (**C**) IL-17A (**D**) RORγt (**E**) FoxP3 by flow cytometry (A-E, representative plots of n=3 independent donors).

(B and D) Numbers on the plot denote mean fluorescence intensity, US=unstained control.

One study has previously identified that CD28 signalling is suppressive of human Th17 cell differentiation through an Akt-dependent mechanism (Revu *et al.*, 2018). These findings are consistent with the poor expression of IL-17A seen here, as cells in the Th17 condition were activated with anti-CD3/28. To explore the effect of CD28 in our experiment, naïve $CD4^+$ T cells were cultured as before for 6 days but activated with anti-CD3 only (Figure 5.2A-E). Th1 cells remained well differentiated with the highest amount of IFN-γ and T-bet compared to the other conditions (Figure 5.2A-B). Overall, the levels of both IFN-γ and T-bet were slightly lower in Th1 cells with anti-CD3 only stimulation compared to anti-CD3/CD28 (Figure 5.1A-B and Figure 5.2A-B and F). In comparison, IL-$17A^+$ Th17 cells reached over 8% compared to 1.5% when activated with anti-CD28 (Figure 5.2C and G). IL-17A was also increased in Th0, Th1, and Treg conditions compared to their anti-CD28-stimulated counterparts but remained around 5% lower than in Th17 cells. RORγt expression was also clearly highest and well expressed in Th17 cells under anti-CD3-only stimulation (Figure 5.2D). $FoxP3^+$ cells were only able to reach just over 22% in the Treg condition, compared to 53.5% when activated with anti-CD28, suggesting that CD28 signalling is important for FoxP3 induction in Treg differentiation (Figure 5.2E and H). Taken together, the optimisation of these differentiation conditions shows that CD28 signalling is suppressive of human Th17 cell development but promotes Th1 cell and Treg differentiation. Polarisation of naïve $CD4^+$ T cells under these conditions for 6 days is sufficient for the *in vitro* generation of a Th1, Th17, or Treg cell population.

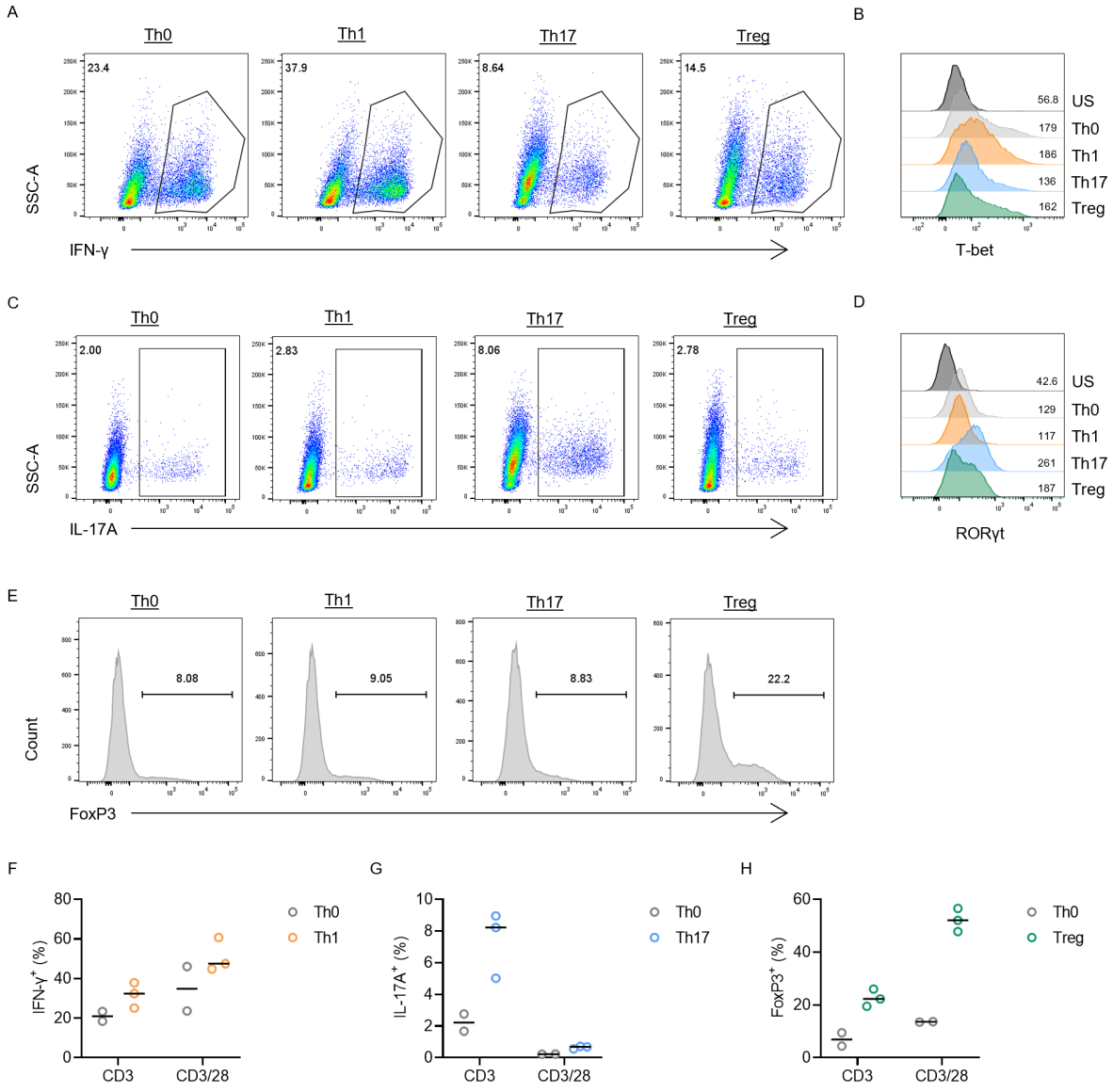

Figure 5.2 Polarisation of T cell subsets under CD3-only stimulation improves Th17 cell differentiation

(**A-E**) Purified naïve CD4⁺ T cells were activated with anti-CD3 only and differentiated into Th0, Th1, Th17, or Treg cells over 6 days then assessed on day 6 for the expression of (**A**) IFN-γ (**B**) T-bet (**C**) IL-17A (**D**) RORγt (**E**) FoxP3 by flow cytometry (A-E, representative plots of: Th0 n=2 independent donors; Th1, Th17 and Treg n=3 independent donors).

(**F-H**) Comparison of percentage of cells positive for (**F**) IFN-γ in Th1 cells (**G**) IL-17A in Th17 cells (**H**) FoxP3 in Tregs under anti-CD3 only or anti-CD3/CD28 stimulation as indicated, Th0 control included for reference (F-H, Th0 n=2 independent donors; Th1, Th17 and Treg n=3 independent donors).

(B and D) Numbers on the plot denote mean fluorescence intensity, US=unstained control. (F-H) Each symbol represents an individual donor, data presented as the median.

5.2.2 Blocking TNF-α has little effect on Treg development

Under both anti-CD3 and anti-CD3/28 activation the effect of blocking TNF-α signalling was assessed on the generation of iTregs from a naïve $CD4^+$ T cell population (Figure 5.3A-F). Consistent with earlier observations during short-term cultures, anti-TNFα had no effect on the viability of the cells, even after 6 days in culture (Figure 5.3A-C). Additionally, anti-CD3 only stimulation maintained a similar level of cell viability compared to anti-CD3/28. As seen before, the levels of FoxP3 induction in the anti-CD3 only condition were considerably less than when anti-CD28 was also present (Figure 5.3D-F). However, in this condition, anti-TNFα was able to further inhibit FoxP3 expression. This suppressive effect could not be seen in the anti-CD3/28 stimulated cells, suggesting that CD28 co-stimulation is sufficient to drive FoxP3 upregulation during iTreg differentiation from naïve $CD4^+$ T cells *in vitro*, but in its absence T cell-derived TNF-α also contributes to $FoxP3^+$ iTreg development.

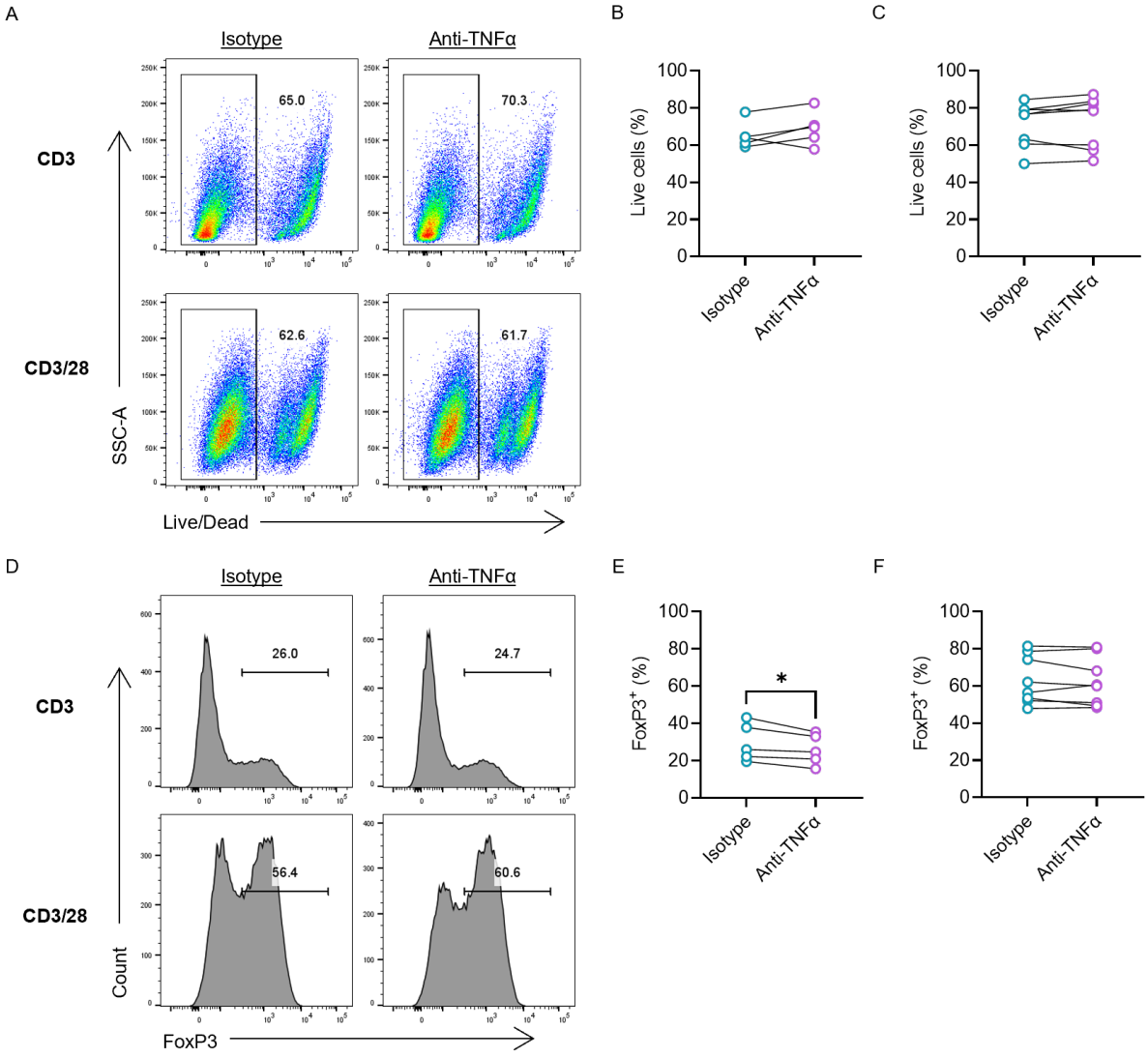

Figure 5.3 Anti-TNFα has little effect on Treg differentiation

(**A-F**) Purified naïve CD4⁺ T cells were activated with either (**A-B and E**) anti-CD3 only or (**A, C and F**) anti-CD3/28 and differentiated into Tregs in presence of an anti-TNFα or isotype control antibody over 6 days then assessed on day 6 for (**A-C**) cell viability (**D-F**) the expression of FoxP3 by flow cytometry (A and D, representative plots of: anti-CD3 n=5 independent donors; anti-CD3/28 n=8 independent donors; B and E, n=5 independent donors; C and F, n=8 independent donors).

(B-C and E-F) Each symbol represents an individual donor with the line between denoting matched pairs. Significance assessed by paired t test, * $p < 0.05$.

5.2.3 TNF-α has redundant roles with CD28 in Th1 cell differentiation

Next, development towards a Th1 cell phenotype was assessed. Under anti-CD3 activation, the percentage of IFN-γ$^+$ cells decreased in presence of anti-TNFα compared to the isotype control antibody (Figure 5.4A). This was matched with a reduction in IFN-γ release over 6 days of culture with anti-TNFα treatment, as measured in the supernatant by ELISA (Figure 5.4B). Expression of T-bet was also decreased when blocking TNF-α signalling during differentiation (Figure 5.4C). Detection of IL-10 by flow cytometry was limited with only up to 3% of cells positive for IL-10 expression (Figure 5.4D). Nonetheless, a consistent increase in IL-10$^+$ cells was seen with anti-TNFα treatment. In order to better measure IL-10 expression by these cells, concentration of IL-10 in the supernatant was assessed by multiplex cytokine assay (Figure 5.4E). These data confirmed that detectable levels of IL-10 were being released by Th1 cells in culture, despite the low percentage of IL-10$^+$ cells present in flow cytometric analysis. However, the inductive effect of anti-TNFα on IL-10 appeared more variable here, with no overall clear increase. Having seen a potential increase in IL-10 expression, FoxP3 levels were also assessed to interrogate for changes towards a FoxP3-expressing Treg phenotype (Figure 5.4F). Anti-TNFα induced no change in the percentage of FoxP3$^+$ cells in the Th1 condition. Altogether, these data suggest that in the absence of CD28 co-stimulation T cell-derived TNF-α signalling is required for the development of a Th1 cell phenotype. Blocking TNF-α was also able to induce IL-10 production without an effect on FoxP3.

In contrast, anti-TNFα had no effect on IFN-γ expression in Th1 cells when activated with anti-CD3/CD28 (Figure 5.5A-B). T-bet expression also remained unaffected by the blocking of TNF-α during Th1 cell differentiation (Figure 5.5C). Compared to expression in the anti-CD3 only conditions of up to 3%, IL-10 was barely detectable by flow cytometry when cells were

also activated with anti-CD28 (Figure 5.5D). Added to this, the concentration of IL-10 detected in the supernatants was around 10-fold lower in Th1 cells activated with anti-CD3/28 than anti-CD3 alone (Figure 5.5E). Despite the low levels, a trend towards an increase in IL-10 release by anti-TNFα-treated Th1 cells was still present. Again, this was not accompanied by a change in FoxP3 expression (Figure 5.5F). Taken together, these data suggest that CD28 co-stimulation is required for optimal Th1 cell differentiation and is able to suppress IL-10 expression. However, in the absence of this signal, T cell-intrinsic TNF-α drives IFN-γ and T-bet expression and suppresses IL-10 release.

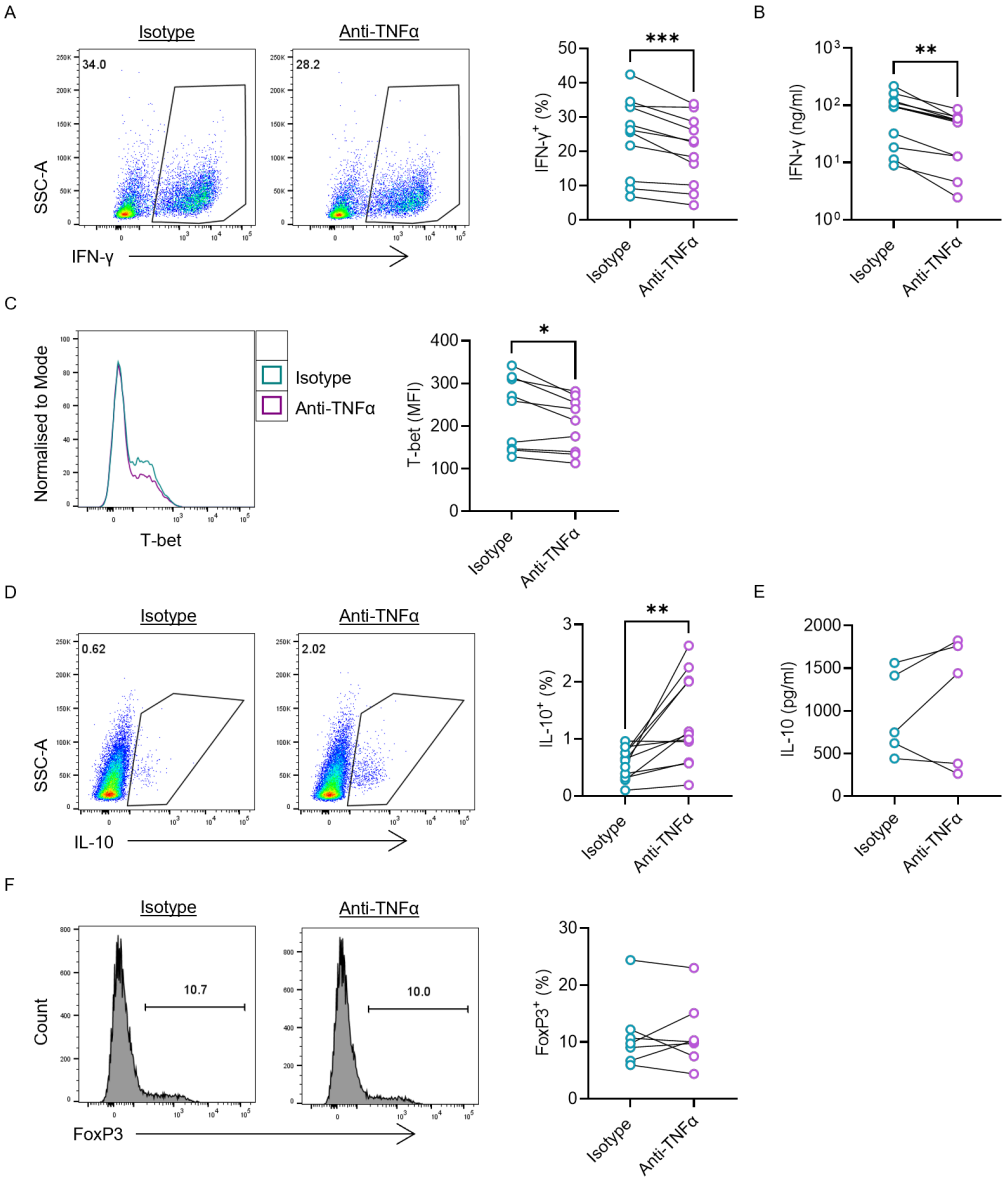

Figure 5.4 Anti-TNFα suppresses Th1 cell differentiation under anti-CD3-only activation

(**A-F**) Purified naïve CD4$^+$ T cells were activated with anti-CD3 only and differentiated into Th1 cells in presence of an anti-TNFα or isotype control antibody over 6 days then assessed on day 6 for the expression of (**A**) IFN-γ$^+$ cells by flow cytometry (n=11 independent donors) (**B**) IFN-γ concentration in the supernatant by ELISA (n=11 independent donors) (**C**) T-bet expression by flow cytometry, MFI=mean fluorescence intensity (n=9 independent donors) (**D**) IL-10$^+$ cells by flow cytometry (n=11 independent donors) (**E**) IL-10 concentration in the supernatant by multiplex cytokine analysis (n=5 independent donors) (**F**) FoxP3$^+$ cells by flow cytometry (n=7 independent donors).

(A-F) Each symbol represents an individual donor with the line between denoting matched pairs. Significance assessed by (A-E) paired t test (F) Wilcoxon test, * $p < 0.05$, ** $p < 0.01$, *** $p < 0.001$.

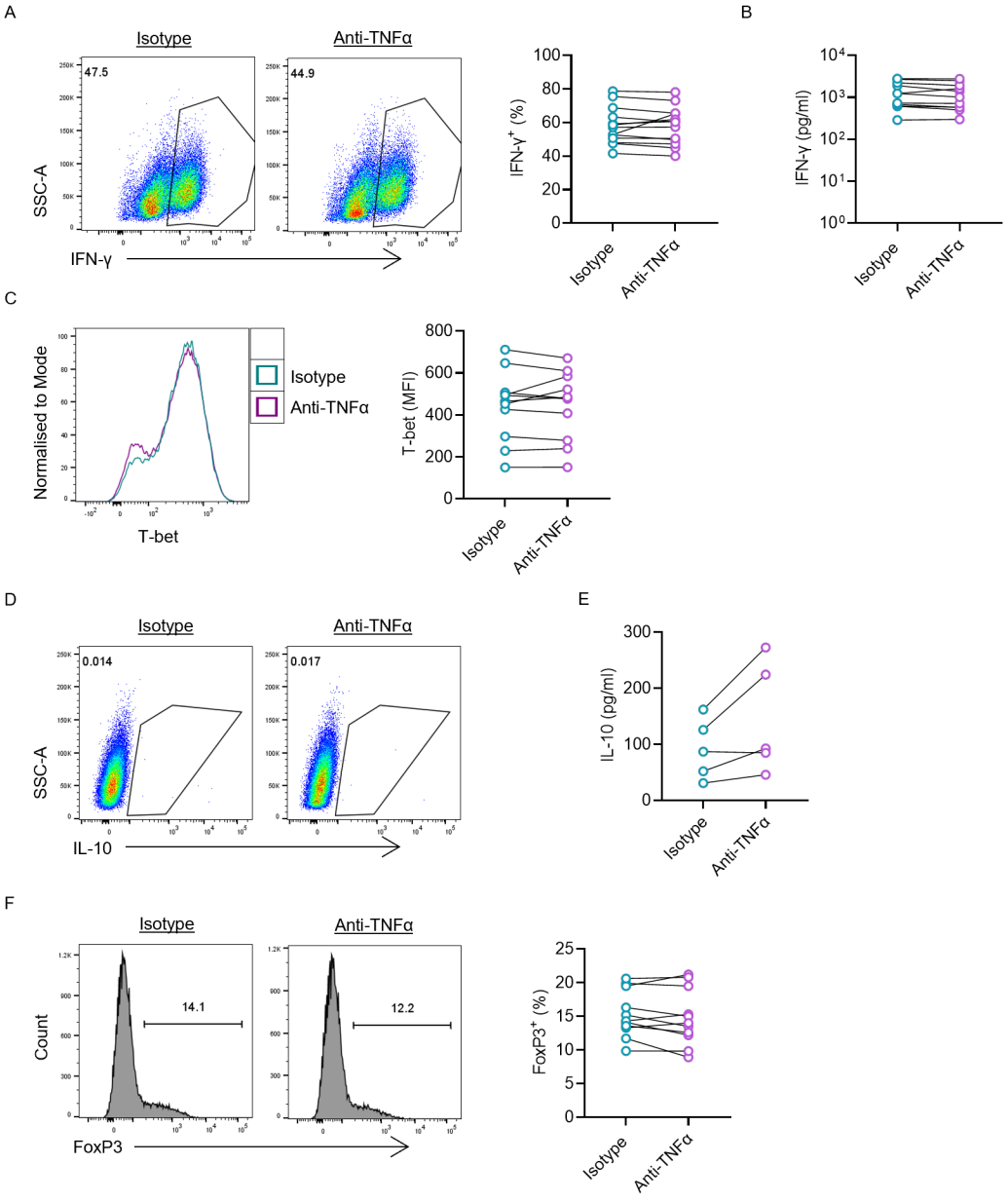

Figure 5.5 TNF-α blockade has little effect on Th1 cell polarisation under anti-CD3/CD28 stimulation

(**A-F**) Purified naïve CD4$^+$ T cells were activated with anti-CD3/28 and differentiated into Th1 cells in presence of an anti-TNFα or isotype control antibody over 6 days then assessed on day 6 for the expression of (**A**) IFN-γ$^+$ cells by flow cytometry (n=13 independent donors) (**B**) IFN-γ concentration in the supernatant by ELISA (n=11 independent donors) (**C**) T-bet expression by flow cytometry, MFI=mean fluorescence intensity (n=11 independent donors) (**D**) IL-10$^+$ cells by flow cytometry (representative plots of n=11 independent donors) (**E**) IL-10 concentration in the supernatant by multiplex cytokine analysis (n=5 independent donors) (**F**) FoxP3$^+$ cells by flow cytometry (n=11 independent donors).

(A-C and E-F) Each symbol represents an individual donor with the line between denoting matched pairs. Significance assessed by paired t test, * $p < 0.05$, ** $p < 0.01$, *** $p < 0.001$.

5.2.4 TNF-α is required for full differentiation of Th17 cells

Initially looking at the anti-CD3 only condition, where the best Th17 cell differentiation was present, anti-TNFα had no effect on the percentage of IL-17A expressing cells (Figure 5.6A). This was further confirmed by multiplex cytokine analysis which showed no effect of anti-TNFα on IL-17A or IL-17F production compared to the isotype control (Figure 5.6B-C). A decrease was observed in IL-22 expression but was not seen in IL-6 (Figure 5.6D-E). Blocking TNF-α signalling during Th17 cell differentiation was also able to suppress the expression of RORγt (Figure 5.6F). In similar fashion to Th1 cells, even though a low percentage of IL-10^{+} cells were measured, there was a consistent increase with anti-TNFα treatment (Figure 5.6G). No significant change in IL-10 concentration was evident from analysis of the supernatants, yet a trend towards increased IL-10 in the anti-TNFα condition could be seen (Figure 5.6H). Again, there was no change in FoxP3 expression with anti-TNFα treatment (Figure 5.6I). Together, these data show that T cell-derived TNF-α is required for the upregulation of RORγt and IL-22 in Th17 cell differentiation but not for IL-17.

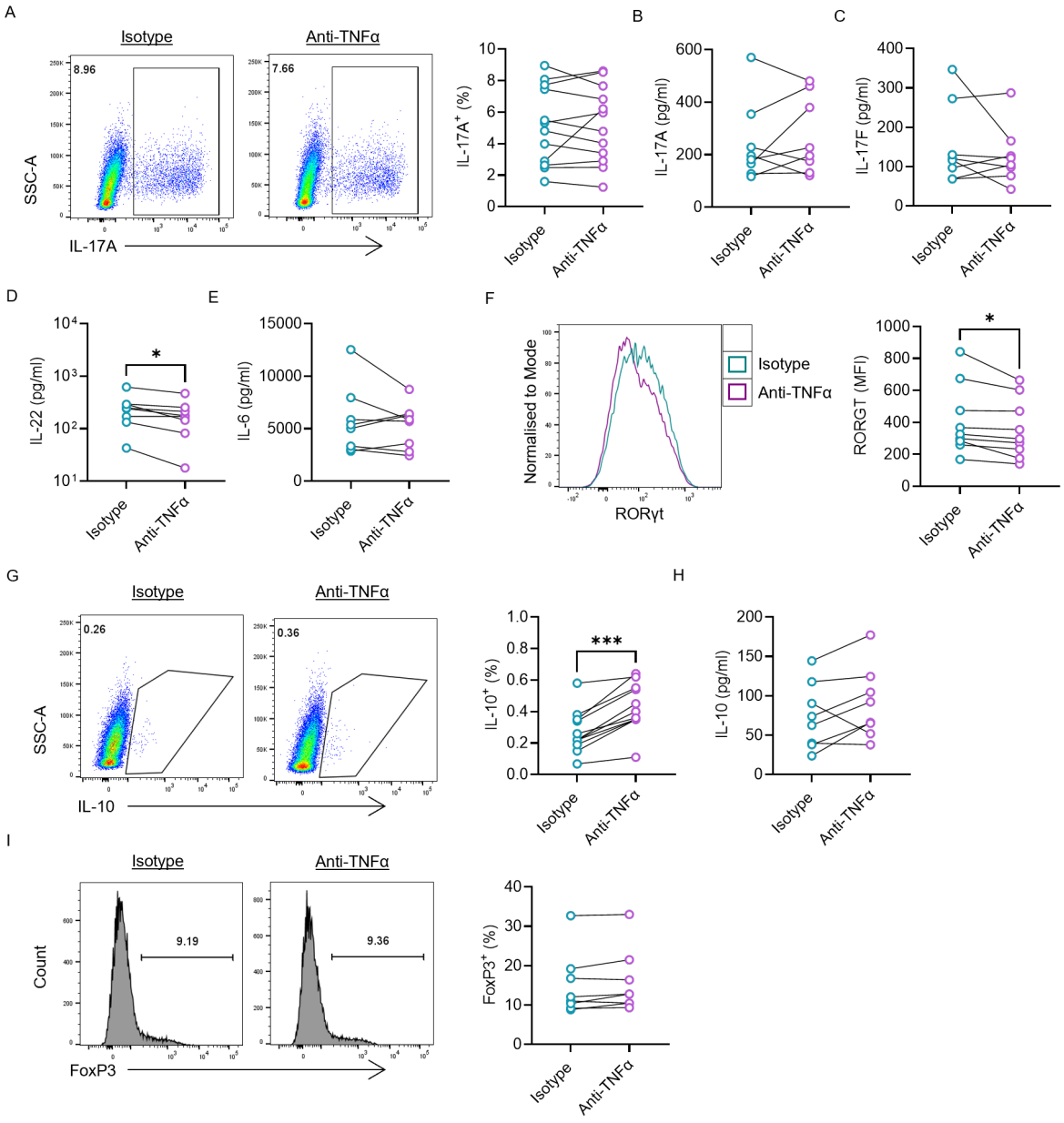

Figure 5.6 Blocking TNF-α impairs Th17 cell differentiation under anti-CD3 stimulation

(**A-F**) Purified naïve CD4$^+$ T cells were activated with anti-CD3 only and differentiated into Th17 cells in presence of an anti-TNFα or isotype control antibody over 6 days then assessed on day 6 for the expression of (**A**) IL-17A$^+$ cells by flow cytometry (n=12 independent donors) (**B**) IL-17A (**C**) IL-17F (**D**) IL-22 (**E**) IL-6 concentration in the supernatant by multiplex cytokine analysis (B-E, n=8 independent donors) (**F**) RORγt expression by flow cytometry, MFI=mean fluorescence intensity (n=9 independent donors) (**G**) IL-10$^+$ cells by flow cytometry (n=11 independent donors) (**H**) IL-10 concentration in the supernatant by multiplex cytokine analysis (n=8 independent donors) (**I**) FoxP3$^+$ cells by flow cytometry (n=8 independent donors).

(A-I) Each symbol represents an individual donor with the line between denoting matched pairs. Significance assessed by (A and D-H) paired t test (B-C and I) Wilcoxon test, * $p < 0.05$, *** $p < 0.001$.

Furthering this investigation with the polarisation of naïve $CD4^+$ T cells into a Th17 cell phenotype in presence of CD28 co-stimulation, again no change in IL-17A or IL-17F was measured (Figure 5.7A-C). Of note, despite the low percentage of IL-$17A^+$ cells compared to those in the anti-CD3 only condition (Figure 5.6A), the concentration of IL-17A and IL-17F in the supernatant of the anti-CD3/28 activated Th17 cells was substantially higher (Figure 5.6B-C and Figure 5.7B-C). Although a trend could be observed, the decrease in IL-22 driven by blocking TNFα did not reach significance under anti-CD3/CD28 activation (Figure 5.7D). As before, no change in IL-6 with anti-TNFα treatment was recorded (Figure 5.7E). Yet, a consistent decrease in RORγt expression was apparent in the anti-TNFα condition compared to the isotype control (Figure 5.7F). In agreement with the Th1 cell data, IL-10^+ cells were not detectable by flow cytometry in the anti-CD3/28 conditions (Figure 5.7G). However, analysis of IL-10 concentration in the supernatant showed that anti-TNFα promoted IL-10 production in Th17 cells under anti-CD3/28 activation, albeit at a relatively low concentration (Figure 5.7H). Consistent with other data, this was not accompanied by a change in FoxP3 (Figure 5.7I). As a whole, the data here suggest that optimal *in vitro* Th17 cell differentiation requires T cell-derived TNF-α signalling, with the exception of IL-17 expression. Additionally, although limited by measurement techniques, blocking TNF-α does appear to increase levels of IL-10 expression in Th1 and Th17 cells.

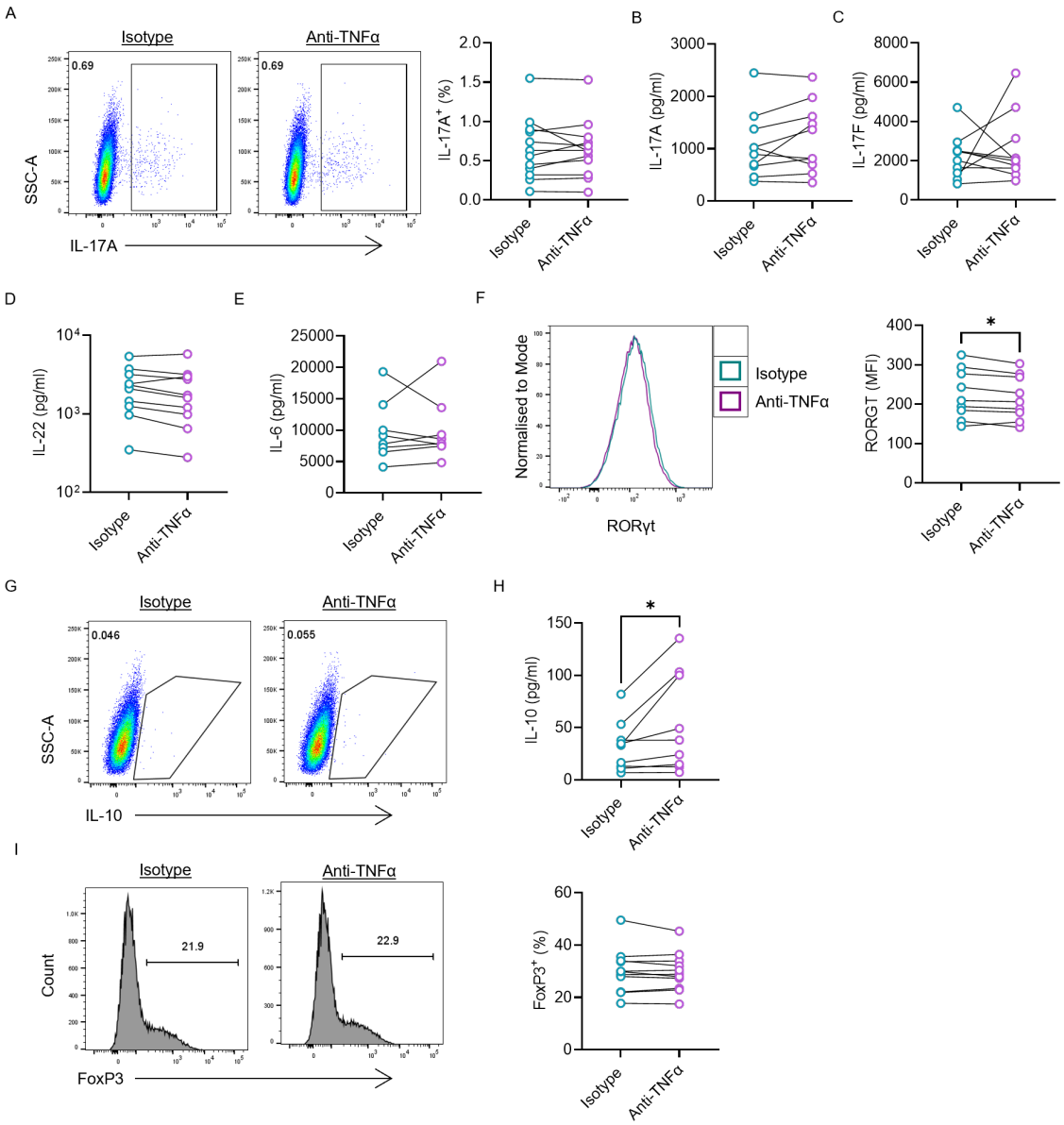

Figure 5.7 Anti-TNFα limits full Th17 cell differentiation under anti-CD3/28 stimulation

(**A-F**) Purified naïve CD4$^+$ T cells were activated with anti-CD3/28 and differentiated into Th17 cells in presence of an anti-TNFα or isotype control antibody over 6 days then assessed on day 6 for (**A**) IL-17A$^+$ cells by flow cytometry (n=12 independent donors) (**B**) IL-17A (**C**) IL-17F (**D**) IL-22 (**E**) IL-6 concentration in the supernatant by multiplex cytokine analysis (B-E, n=10 independent donors) (**F**) RORγt expression by flow cytometry, MFI=mean fluorescence intensity (n=9 independent donors) (**G**) IL-10$^+$ cells by flow cytometry (representative plots of n=11 independent donors) (**H**) IL-10 concentration in the supernatant by multiplex cytokine analysis (n=9 independent donors) (**I**) FoxP3$^+$ cells by flow cytometry (n=11 independent donors).

(A-F and H-I) Each symbol represents an individual donor with the line between denoting matched pairs. Significance assessed by (A-B, D, and F-I) paired t test (C and E) Wilcoxon test, * $p < 0.05$.

5.2.5 Akt-dependent effects of anti-TNFα on $CD4^+$ T cell differentiation

Next, it was investigated whether these functional effects of blocking TNF-α were also mediated through the suppression of PI3K/Akt signalling. To do this, naïve $CD4^+$ T cells were cultured as before under Th1 and Th17 cell polarising conditions with an anti-TNFα or isotype control antibody, this time also with the addition of the Akti or vehicle control. Cells were activated with anti-CD3 only, as this was where the largest effects of anti-TNFα had been observed previously. As evident in earlier data, analysis of IFN-γ production by flow cytometry and ELISA showed a trend towards a decrease in IFN-γ with anti-TNFα treatment of Th1 cells (Figure 5.8A-B). However, particularly for the concentration of IFN-γ released, this suppressive effect was blunted in presence of the Akti, suggesting some Akt-dependence. Indeed, the Akti was suppressive of IFN-γ production in comparison to the control (Figure 5.8A-B). Contrastingly, the inhibitory effect of anti-TNFα on T-bet expression was greater with the added presence of the Akti (Figure 5.8C). These data suggesting that the anti-TNFα effect on T-bet regulation is mediated through an Akt-independent mechanism. In contrast to the other functional effects of TNF-α blockade during Th1 cell differentiation, IL-10 was increased. Here, Akt inhibition alone suppressed IL-10 expression, and correspondingly the increase in IL-10 driven by anti-TNFα was reduced (Figure 5.8D-E).

These findings give some evidence to the involvement of the PI3K/Akt pathway in mediating the functional effects of anti-TNFα on Th1 cell cytokine production following differentiation. However, this is not a complete abrogation of the effect, so it is likely that other mechanisms also play a role. Additionally, a synergistic effect of anti-TNFα and the Akti could be seen on the suppression of T-bet, indicating two unique systems of inhibition.

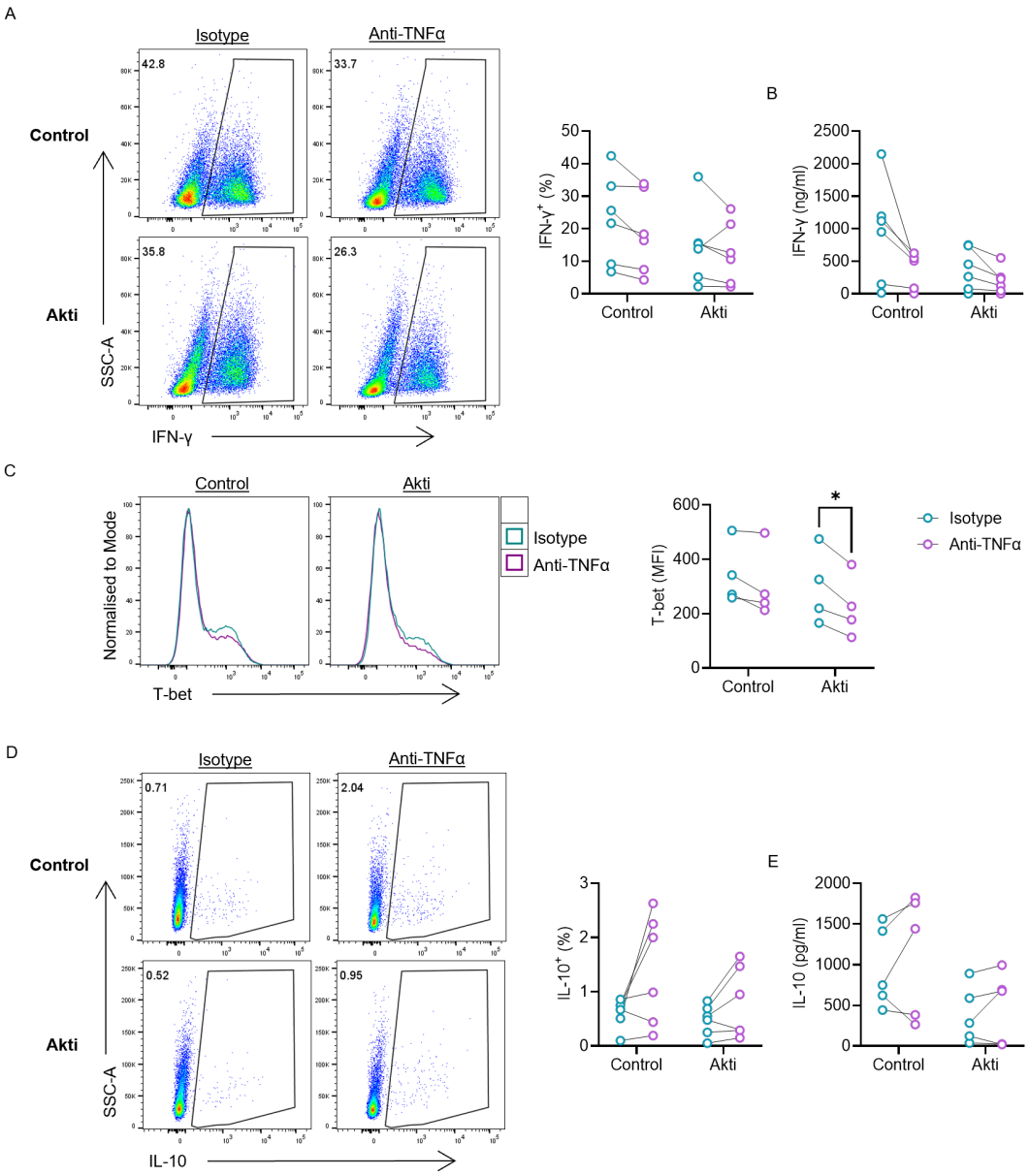

Figure 5.8 Effects of anti-TNFα on Th1 cells are partially Akt-dependent

(**A-E**) Purified naïve CD4$^+$ T cells were activated with anti-CD3 only and differentiated into Th1 cells in presence of an anti-TNFα or isotype control antibody and an Akt inhibitor (Akti) or DMSO control. Following 6 days of culture, cells were then assessed for the expression of (**A**) IFN-γ$^+$ cells by flow cytometry (n=6 independent donors) (**B**) IFN-γ concentration in the supernatant by ELISA (n=6 independent donors) (**C**) T-bet expression by flow cytometry, MFI=mean fluorescence intensity (n=4 independent donors) (**D**) IL-10$^+$ cells by flow cytometry (n=6 independent donors) (**E**) IL-10 concentration in the supernatant by multiplex cytokine analysis (n=5 independent donors).

(A-E) Each symbol represents an individual donor with the line between denoting matched pairs. Significance assessed by RM two-way ANOVA with Šídák's multiple comparisons test, * $p < 0.05$.

Analysis of Th17 cell differentiation under these conditions again confirmed that anti-TNFα had no effect on IL-17A or IL-17F expression (Figure 5.9A-C). On the contrary, the Akti was suppressive of both IL-17A and IL-17F when compared to the control. Consistent with previous experiments, IL-22 trended towards a decrease with anti-TNFα treatment. This decrease was not completely abrogated by the Akti, but partially blunted (Figure 5.9D). IL-6, as before, showed no clear change with anti-TNFα treatment and was also unaffected by the addition of the Akti (Figure 5.9E). Similar to the observed effects on Th1 cell expression of T-bet, RORγt was equally reduced by anti-TNFα in both Akti and control conditions (Figure 5.9F). Under Th17 cell differentiation conditions, the increase in IL-10 seen in the anti-TNFα-treated group was not affected by presence of the Akti. Indeed, the Akti had no effect on the expression of IL-10 in Th17 cells (Figure 5.9G-H). Of note, the levels of IL-10 production by Th17 cells were again around 10-fold less than that of Th1 cells. Overall, these data indicate that suppression of IL-22 expression by anti-TNFα in Th17 cells may be Akt-dependent, whereas effects on RORγt and IL-10 are Akt-independent.

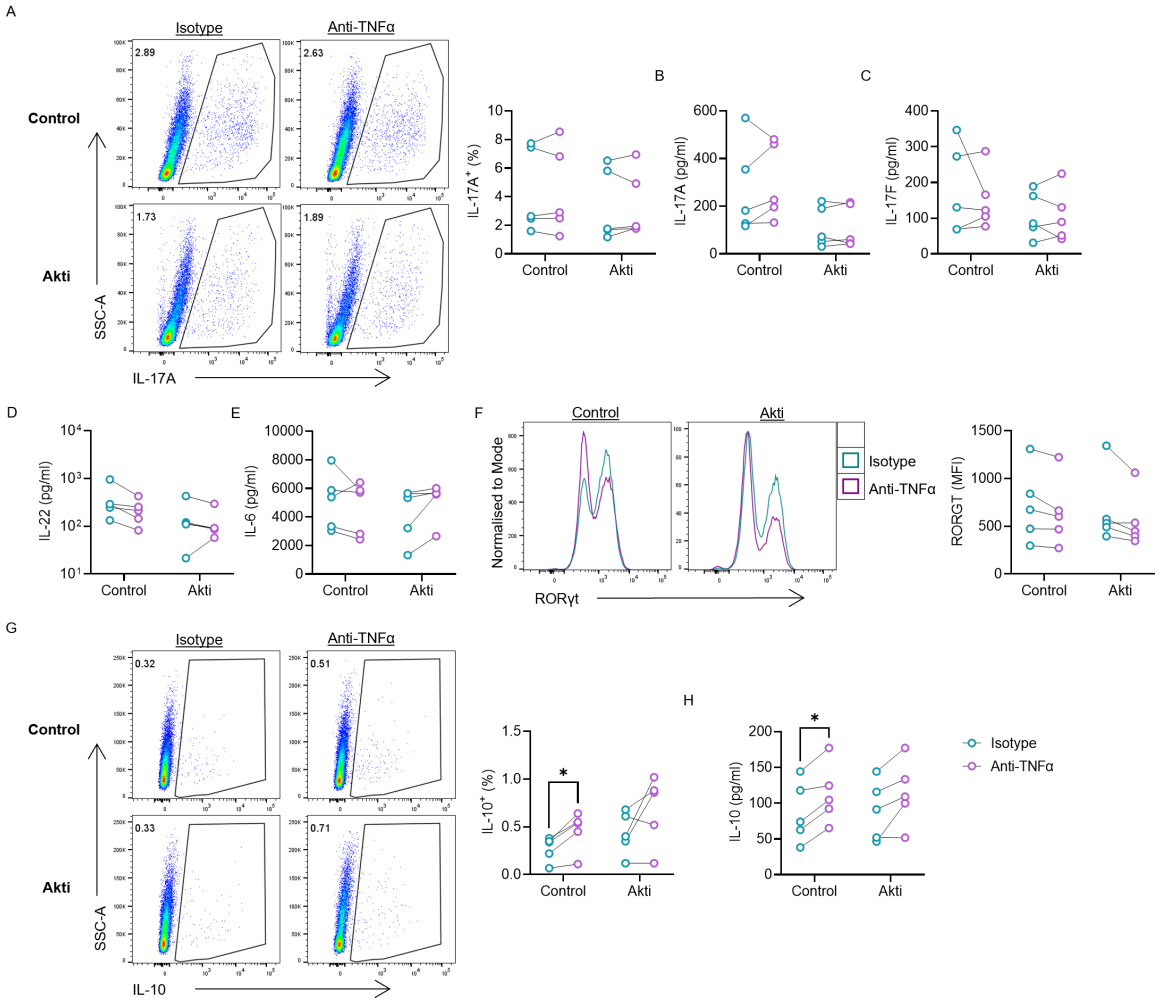

Figure 5.9 Effects of anti-TNFα on Th17 cell differentiation have little Akt-dependence

(**A-H**) Purified naïve CD4⁺ T cells were activated with anti-CD3 only and differentiated into Th1 cells in presence of an anti-TNFα or isotype control antibody and an Akt inhibitor (Akti) or DMSO control. Following 6 days of culture, cells were then assessed for the expression of (**A**) IL-17A⁺ cells by flow cytometry (**B**) IL-17A (**C**) IL-17F (**D**) IL-22 (**E**) IL-6 concentration in the supernatant by multiplex cytokine analysis (**F**) RORγt expression by flow cytometry, MFI=mean fluorescence intensity (**G**) IL-10⁺ cells by flow cytometry (**H**) IL-10 concentration in the supernatant by multiplex cytokine analysis (A-H, n=5 independent donors).

(A-H) Each symbol represents an individual donor with the line between denoting matched pairs. Significance assessed by RM two-way ANOVA with Šídák's multiple comparisons test, * $p < 0.05$.

5.2.6 Th1 and Th17 cells differentiated with anti-TNFα exhibit reduced glycolysis

Having established the effects of anti-TNFα on $CD4^+$ Th cell differentiation, the next aim was to interrogate the whether the metabolic perturbations induced by anti-TNFα extended to 6 days of *in vitro* differentiation culture and accompanied these changes. After 6 days of culture, supernatants were collected from Th1 and Th17 cells in the anti-CD3 only conditions and analysed for concentration of glucose and lactate (Figure 5.10A-B). Differentiated Th1 cells did not show any clear change in the amount of glucose in the supernatant (Figure 5.10A). However, this was coupled with a decrease in the amount of lactate produced by anti-TNFα-treated cells, indicative of reduced aerobic glycolysis. Furthermore, Th17 cells exhibited both a higher concentration of glucose, suggesting reduced glucose consumption, and a lower concentration of lactate present when cultured in presence of the TNF-α neutralising antibody (Figure 5.10A-B). These data suggest that the blockade of T cell-derived TNF-α during Th1 and Th17 cell differentiation induces a suppressed glycolytic phenotype.

As short-term metabolic effects were seen to be dependent on PI3K/Akt signalling, supernatants from the control and Akti conditions were also analysed for glucose concentration (Figure 5.10C-D). In this case, no clear effect of the Akti was seen, particularly in the Th17 condition where a significant increase in glucose concentration was present with anti-TNFα treatment. Notably, the Akti alone had little impact on glucose uptake compared to the control. Taken together, these data suggest that during longer-term culture anti-TNFα may involve mechanisms other than the PI3K/Akt pathway to suppress metabolic activity in $CD4^+$ T cells.

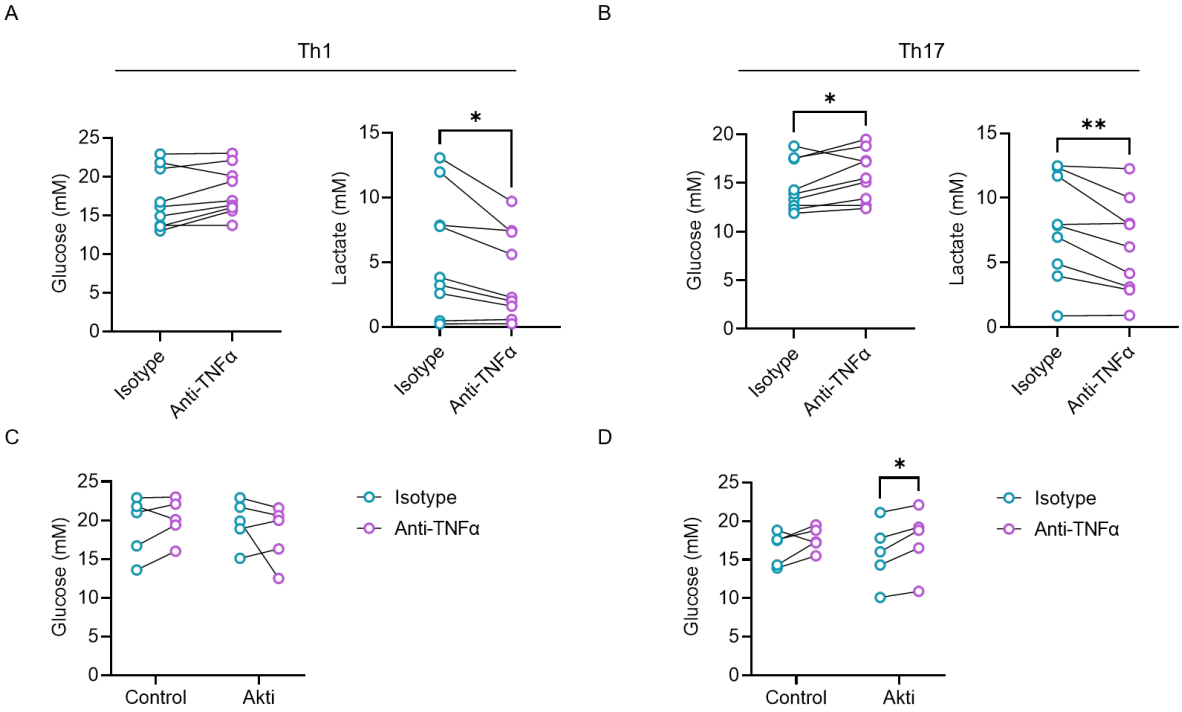

Figure 5.10 T cells differentiated with anti-TNFα have reduced metabolic capacity

(**A-B**) Purified naïve CD4⁺ T cells were activated with anti-CD3 only and differentiated into (**A**) Th1 cells (**B**) Th17 cells in presence of an anti-TNFα or isotype control antibody for 6 days and the cell culture supernatants then assessed for concentration of glucose and lactate (A-B, n=9 independent donors).

(**C-D**) Cells were cultured as in (A-B) (**C**) Th1 cells and (**D**) Th17 cells with the addition of an Akt inhibitor (Akti) or DMSO control and the cell culture supernatants assessed for concentration of glucose (C-D, n=5 independent donors).

(A-D) Each symbol represents an individual donor with the line between denoting matched pairs. Significance assessed by (A-B) paired t test (C-D) RM two-way ANOVA with Šídák's multiple comparisons test, * $p < 0.05$, ** $p < 0.01$.

5.3 DISCUSSION

Having established that T cell-intrinsic TNF-α is essential for naïve $CD4^+$ T cell metabolic reprogramming through induction of PI3K/Akt/mTOR activity. This chapter aimed to understand the functional effects of TNF-α blockade on activated naïve $CD4^+$ T cells. Previous studies have implicated TNF-α in the differentiation of Th1 and Th17 cells (Sugita *et al.*, 2012; Chen *et al.*, 2016; Alam *et al.*, 2021; Ho *et al.*, 2021; Pesce *et al.*, 2022). However, results are inconsistent. Here, using *in vitro* differentiation of naïve $CD4^+$ T cells into Th1 and Th17 cells in presence of an anti-TNFα or isotype control antibody, it was shown that blocking T cell-derived TNF-α suppressed the differentiation of Th1 and Th17 cells, yet had little effect on Tregs. Anti-TNFα also induced production of IL-10 in Th1 and Th17 cells. Effects on IFN-γ and IL-10 production in Th1 cells and IL-22 production in Th17 cells were shown to be partially Akt-dependent. This impaired differentiation driven by anti-TNFα was accompanied by a reduction in aerobic glycolysis in both Th1 and Th17 cells.

5.3.1 Differentiation of human $CD4^+$ T cell subsets *in vitro*

The first aim of this chapter was to develop a protocol for the differentiation of human naïve $CD4^+$ T cells into Th1, Th17, and Treg cells. It has been shown previously that murine and human Th17 cells require different conditions for differentiation, with the factors essential for Th17 cell generation from human naïve $CD4^+$ T cells less clear (de Jong *et al.*, 2010). Due to this, other studies have each approached *in vitro* differentiation using different concentrations and combinations of polarising cytokines, neutralising antibodies, and methods of activation. Additionally, the type of medium used, and time taken to culture the cells varies (Manel *et al.*, 2008; Volpe *et al.*, 2008; de Jong *et al.*, 2010; Revu *et al.*, 2018). Overall, IL-23, IL-6, IL-1β, and

TGF-β are all implicated in driving a Th17 cell phenotype with anti-IFNγ and anti-IL-4 aiding by suppressing the generation of Th1 and Th2 cell subsets respectively. Following optimisation of the protocols, naïve $CD4^+$ T cells were differentiated into Th1, Th17, and Treg cells over 6 days. It was resolved to use serum-free AIM V medium to prevent the addition of any exogenous cytokines, in particular TGF-β (Manel *et al.*, 2008; Volpe *et al.*, 2008). Cells were activated with anti-CD3/28 on day 0 and not stimulated again but topped up with medium on day 3 to replace nutrients and rebalance the pH, all cytokines and blocking antibodies were added on day 0. This method of differentiation was sufficient for Th1 cells and Tregs, however Th17 cells produced very little IL-17A and comparable levels of RORγt to Tregs. This finding is consistent with another study which showed CD28 ligation to inhibit human Th17 cell differentiation, in particular IL-17A production. Of note, this was reported to not be true of murine Th17 cell differentiation (Revu *et al.*, 2018). Repeating the differentiation with anti-CD3 only stimulation resulted in a higher percentage of IL-$17A^+$ Th17 cells and a more distinct RORγt expression. In contrast, increased concentrations of IL-17A and IL-17F were measured in the supernatants of Th17 cells in the anti-CD3/28 condition, compared to the anti-CD3 condition with the higher percentage of IL-$17A^+$ cells. Reasons for this are unclear but may suggest that although fewer cells express IL-17 under anti-CD3/28 stimulation, those that do release significant amounts of cytokine. For Th1 and Treg cells, differentiation was reduced compared to anti-CD3/28 stimulation but still present.

5.3.2 Little requirement for T cell-intrinsic TNF-α in Treg differentiation

In comparison to other studies reporting TNF-α to improve $FoxP3^+$ Treg differentiation (Chen *et al.*, 2016; Zaragoza *et al.*, 2016; S. Yang *et al.*, 2019), and contradictory studies

reporting anti-TNFα to improve Treg differentiation (Valencia *et al.*, 2006; Zanin-Zhorov *et al.*, 2010; Nie *et al.*, 2013; Zhang *et al.*, 2013), data here showed anti-TNFα to have no effect on the generation of iTregs when naïve $CD4^+$ T cells were activated with anti-CD3/28. This is however, in agreement with another study which showed TNF-α to have no effect on *Foxp3* transcription in human Tregs when activated with anti-CD3/28. This study did later demonstrate TNF-α to improve suppressive function of Tregs by increased expression of co-stimulatory receptors OX40 and 4-1BB (Nagar *et al.*, 2010). Function of anti-TNFα-treated Tregs was not assessed in the current study but may be investigated in future work to better understand the role of T cell-derived TNF-α on Tregs. When activated with anti-CD3 alone anti-TNFα was able to suppress FoxP3 expression compared to the isotype control, yet the percentage of $FoxP3^+$ cells was already lower in the isotype control condition when compared to anti-CD3/28 stimulation. These data are in accordance with the well appreciated role for CD28 in promoting $FoxP3^+$ Treg generation (Salomon *et al.*, 2000; Tai *et al.*, 2005; Guo *et al.*, 2008) but also highlight a role for T cell-intrinsic TNF-α in driving Treg differentiation in the absence of anti-CD28. Tregs are known to rely predominantly on an OXPHOS metabolism and are comparatively less glycolytic than Th1 and Th17 cells (Michalek *et al.*, 2011; Angelin *et al.*, 2017; Howie *et al.*, 2017). Consistent with this observation, the metabolic suppression driven by anti-TNFα did not affect Treg differentiation but also did not promote it. Recently, a heightened glycolytic phenotype driven by TNF:TNFR2 in tTregs has been shown to improve FoxP3 expression and function (de Kivit *et al.*, 2020). Data presented here confirm that T cell-derived TNF-α and accompanying metabolic reprogramming is not required for the differentiation of iTregs. However, several of these previous studies were performed with direct TNFR2 binding (Valencia *et al.*, 2006; Chen *et al.*, 2016; S. Yang *et al.*, 2019; de Kivit *et*

al., 2020), as Tregs produce less endogenous TNF-α than T_{eff} cells it is possible that the Treg culture system did not have sufficient levels of TNF-α present to drive effects above that of CD28. Further characterisation of the Treg response to TNF-α was beyond the scope of the current study. Future studies are required to fully elucidate the role of TNF-α on Treg metabolism and the consequences for fate and function.

5.3.3 Requirement for T cell derived TNF-α in Th1 and Th17 cell differentiation

Consistent with murine studies suggesting that TNF-α drives Th1 cell differentiation (Chen *et al.*, 2016; Alam *et al.*, 2021), anti-TNFα was seen here to suppress IFN-γ production and T-bet expression in Th1 cells activated with anti-CD3 only. However, when stimulated with anti-CD3/28, the suppressive effects of anti-TNFα were abrogated. This effect is consistent with a recent study which shows IFN-γ expression in human Th1 cells to be unaffected by infliximab treatment, those cells also stimulated with anti-CD28 (Pesce *et al.*, 2022). As CD28 and TNF-α both drive PI3K/Akt and metabolism and have similar roles in co-stimulation, this effect of CD28 is likely reflective of redundancy between the two signals in driving Th1 cell differentiation.

Anti-TNFα was able to suppress RORγt expression in Th17 cells but had no effect on IL-17A. This observation is in contrast to other studies on $CD4^+$ T cells which have shown TNF-α to promote IL-17 and clinical anti-TNFα biologics to inhibit IL-17 (Sugita *et al.*, 2012; Ho *et al.*, 2021; Pesce *et al.*, 2022). Reasons for this discrepancy are unclear. Several studies assessed effects on bulk $CD4^+$ T cells or Th1 and Th17 cell subsets directly *ex vivo*, as opposed to during *in vitro* differentiation. It is possible that TNF-α is only required for IL-17 production once a cell is fully differentiated (Ho *et al.*, 2021; Pesce *et al.*, 2022). Indeed, a study has shown

previously that CD28 co-stimulation was suppressive of naïve $CD4^+$ T cell differentiation into Th17 cells but not did not affect established Th17 cells, highlighting their unique requirements for regulation (Revu *et al.*, 2018). However, another study using *in vitro* human Th17 cell differentiation in presence of infliximab also showed decreases in IL-17 (Sugita *et al.*, 2012). This study by Sugita *et al.* started with purified bulk $CD4^+$ T cells, in comparison with the naïve $CD4^+$ T cell population used in the current study, therefore contamination of Th17 cells already present may account for some of the differences in results. Although, the reduction in RORγt in anti-TNFα-treated Th17 cells seen here was consistent with results from the study by Sugita *et al.*. Further experiments are required to better understand the different effects of T cell-intrinsic TNF-α on Th17 cell differentiation and on maintenance of Th17 cell function.

In previous studies and data shown here, CD28 signalling is inhibitory for Th17 cell differentiation, yet required for optimal Th1 cell differentiation (Linterman *et al.*, 2014; Revu *et al.*, 2018). In the latter study it was demonstrated that CD28 induction of Akt suppressed IL-17, with an Akti reversing the effect. It could therefore be hypothesised, that through anti-TNFα-driven suppression of Akt seen here, IL-17 production would increase. Instead, IL-17 remained unchanged in these cultures. Furthermore, the addition of an Akti to the anti-CD3 only stimulated Th17 cell differentiation cultures actually suppressed IL-17. This agrees with the study by Revu *et al.* and likely reflects a balance of Akt signalling required by the cells. The mechanism of IL-17 suppression by Akt remains unclear and further studies are required to understand this. Although also observing a suppressive effect of anti-CD28 on the Th17 cell transcriptome, the Akt-dependence of this effect was not tested (Revu *et al.*, 2018). In the current study, it was seen that anti-TNFα-mediated suppression of RORγt was Akt-independent, suggesting the existence of a different mechanism by which TNF-α can

promote development of a Th17 cell phenotype. Expression of IL-22 by Th17 cells was shown here to be inhibited by anti-TNFα with this effect blunted in the presence of the Akti and also under anti-CD3/28 stimulation. These data suggest IL-22 to be suppressed by anti-TNFα through Akt inhibition with anti-CD28 able to rescue some of this effect.

Due to the observed redundancy between TNF-α and CD28 in Th1 cell differentiation, Akti experiments were performed using anti-CD3 only stimulation, where effects of anti-TNFα were present. Although better able to dissect the role of T cell-derived TNF-α, the conditions of these experiments were manipulated for *in vitro* culture and limited by lack of physiological relevance as they exclude the influence of multiple other local factors, cytokines, and cell types. However, their use was necessary here to elucidate the role of T cell-derived TNF-α in naïve $CD4^+$ T cell metabolism and function. As with IL-22 in Th17 cells, it was seen that the suppression of IFN-γ by anti-TNFα was Akt-dependent. It is already known that Akt-driven glycolysis promotes IFN-γ expression by several posttranscriptional mechanisms (C.-H. Chang *et al.*, 2013; Peng *et al.*, 2016), and was confirmed here that anti-TNFα-treated naïve $CD4^+$ T cells not only have a suppressed metabolism upon activation but resulting Th1 cells also exhibit suppressed glycolysis compared to isotype control-treated cells. Future experiments, for example restoring glycolysis in anti-TNFα-treated Th1 cells, would confirm this mechanism of TNF-α-driven IFN-γ expression. Consistent with RORγt data in Th17 cells, T-bet was synergistically suppressed by anti-TNFα and the Akti, again suggesting an Akt-independent mechanism. This suppressive effect on TFs is in contrast to a study assessing the effect of adalimumab on the transcriptome of $CD4^+$ T cells where no change in RORγt or T-bet was seen (Ho *et al.*, 2021). It is possible that this effect of anti-TNFα is restricted to differentiation of Th1 and Th17 cells and does not apply to memory cells.

In both Th1 and Th17 cells, anti-TNFα induced expression of IL-10 without any effect on FoxP3. Percentage of IL-10$^+$ cells and concentration of IL-10 in the supernatants was low, reducing further under anti-CD28 stimulation. This was a limitation in assessing IL-10 in the experiments presented here but was comparable with expression levels seen in previous studies (Evans *et al.*, 2014; Povoleri *et al.*, 2020). Indeed, the data shown here were also in agreement with those studies which report a FoxP3-independent increase in IL-10 production by Th cell subsets under TNF-α inhibition (Evans *et al.*, 2014; Roberts *et al.*, 2017; Povoleri *et al.*, 2020). The mechanism for this is unclear, although linked in one study with TF Aiolos (Evans *et al.*, 2014). For Th1 cells, addition of the Akti suppressed the increase in IL-10 driven by anti-TNFα, suggesting the increase to be under Akt control. In keeping with this, it has been shown that Th1 cells single positive for IFN-γ can adopt expression of IL-10 to become co-expressers and following this, become IL-10 single producers. This double positive population was shown to have a higher metabolism and mTOR activity compared to single producers (Kolev *et al.*, 2015). It is possible that Akt is required for this metabolic upregulation and acquisition of IL-10 production. Furthermore, IL-10 expression in Th1 cells has previously been shown to be regulated by cholesterol biosynthesis (Perucha *et al.*, 2019). In the current study IL-10 and IFN-γ were not co-stained and so double positive cells could not be assessed. Several other mechanisms have been implicated in driving IL-10 in Th1 cells including MAPK signalling and TF c-Maf (Saraiva *et al.*, 2009; Neumann *et al.*, 2014; Perucha *et al.*, 2019). These studies highlighting IL-10 to be under complex regulation. Further work should aim to understand the mechanism of anti-TNFα induction of IL-10 and the role of TNF-α-driven effects on Akt and metabolism in this process. In contrast, anti-TNFα-driven IL-10 expression in Th17 cells was unaffected by the Akti suggesting a different mechanism of regulation to Th1 cells.

Differentiation of Th17.1 cells was not assessed here but is also likely influenced by T cell-intrinsic TNF-α signalling owing to their similarity to Th1/Th17 cells. Indeed, a previous study found TNFR2 deficiency to significantly reduce the presence of T-bet^{+}RORγt^{+} CD4^{+} T cells in a mouse model of colitis (Alam *et al.*, 2021). Th2 cells were also not assessed due to their limited role in chronic inflammatory disease pathogenesis. However, RNA-seq analysis in Chapter 4 did show the upregulation of Th2 cell master TF GATA3 to be suppressed by the blockade of T cell-derived TNF-α upon activation of naïve CD4^{+} T cells. Future investigation of Th2 cell differentiation under the conditions described here may elucidate a role for T cell-intrinsic TNF-α in this process.

5.3.4 Metabolic capacity of Th1 and Th17 cells induced in presence of anti-TNFα

After 6 days of differentiation with an anti-TNFα or isotype control antibody, it was found that those cells in the anti-TNFα condition had reduced uptake of glucose and production of lactate, indicating a reduced glycolytic capacity. These data suggest that the metabolic suppression induced by anti-TNFα upon naïve CD4^{+} T cell activation is maintained throughout differentiation into Th1 and Th17 cells, suppressing development of a Th1 and Th17 cell phenotype whilst also resulting in cells with a reduced metabolic capacity. Furthermore, these data support the hypothesis that full metabolic reprogramming driven by T cell-derived TNF-α is required for differentiation of inflammatory Th cell subsets. However, further studies are required to confirm this. Assessment of *in vitro* differentiated Th1 and Th17 cell metabolism by Seahorse XF analysis would generate a more detailed report of the effect of anti-TNFα on OXPHOS and glycolysis. However, this would require a substantial number of polarised cells. Additionally, the metabolic effects of anti-TNFα are yet to be directly linked to effects on

differentiation. It was found that anti-TNFα was able to further suppress glucose consumption of Th17 cells in the presence of the Akti, suggesting an Akt-independent mechanism. Of note, this effect was less clear in Th1 cells, again highlighting differences in TNF-α regulation of the two subsets. Further experiments interrogating the metabolism of cells under these conditions may elucidate the contribution of T cell-derived TNF-α in promoting the metabolic profile required for Th1 and Th17 cell differentiation. For example, FAS is known to be required for Th17 cells but was not assessed here (Berod *et al.*, 2014). In addition, restoration of metabolic regulators such as c-Myc, previously shown to be suppressed by anti-TNFα, could link metabolic effects to functional effects.

5.3.5 Conclusion

Overall, this chapter has established an *in vitro* differentiation protocol for human Th1, Th17, and Treg cells, and highlighted the suppressive effects of anti-CD28 on Th17 cell generation. Furthermore, data presented here have demonstrated a role for T cell-derived TNF-α in the differentiation of Th1 and Th17 cells, although effects on Th1 cells are abrogated by the addition of CD28 stimulation, likely due to redundancy between the two signals. These suppressive effects on cytokine expression are partially Akt-dependent, whereas TF expression is inhibited by an Akt-independent mechanism. This impaired differentiation under TNF-α blockade is also matched with a suppressed metabolic phenotype compared to isotype control-treated cells. Data here also back up previous reports of TNF-α inhibition driving IL-10 expression in Th1 and Th17 cells. Future studies are required to fully understand the role of T cell-derived TNF-α-driven metabolism in modulating these effects on differentiation.

CHAPTER 6: CD4$^+$ T CELL METABOLISM AND FUNCTION IN RHEUMATOID ARTHRITIS

6.1 INTRODUCTION

RA is a chronic inflammatory disease characterised by a significant immune cell infiltrate into the synovial joint and progressive bone and cartilage erosion. TNF-α is a major driver of RA pathogenesis and is produced by a range of cell types including FLS, macrophages, and CD4$^+$ T cells. Indeed, in RA, TNF-α is present in the SF and often at increased levels in the peripheral blood compared to controls (Tetta *et al.*, 1990; Manicourt *et al.*, 2000; Cai *et al.*, 2020). Additionally, RA CD4$^+$ T cells were recently shown to produce more TNF-α than HC (Wu *et al.*, 2021). In the context of RA, TNF-α is reported to be suppressive of Treg function, with anti-TNFα therapy able to rescue this (Valencia *et al.*, 2006; Nie *et al.*, 2013). Yet in other studies, TNF-α signalling is beneficial to Treg differentiation and function (S. Yang *et al.*, 2019; de Kivit *et al.*, 2020). Notably, chronic exposure of CD4$^+$ T cells to TNF-α *in vitro* results in a hyporesponsive state where TCR signalling and CD28 co-stimulation are downregulated in favour of the NFκB pathway to promote survival (Cope *et al.*, 1994; Isomäki *et al.*, 2001; Aspalter *et al.*, 2005). This is in contrast to the observed effect of anti-TNFα driving a hyporesponsive phenotype in CD4$^+$ T cells (Povoleri *et al.*, 2020). One study reported that CD4$^+$ T cells were able to migrate to the inflamed RA synovium down a TNF-α gradient via TNFR1 (Rossol *et al.*, 2013). Our study and others have identified TNF-α signalling to drive a Th17 cell phenotype (Alam *et al.*, 2021; Pesce *et al.*, 2022). However, this effect is yet to be studied in the context of RA pathogenesis. Studies have shown anti-TNFα RA therapies to cause an

increase the numbers of circulating Th1 and Th17 cells, potentially due to their downregulation of chemokine receptors causing reduced ability to migrate to the inflamed tissue (Aerts *et al.*, 2010). The presence of pathogenic Th17 cells in the rheumatoid synovium is important in RA disease progression, mediated through their production of IL-17 and TNF-α (Beringer and Miossec, 2019). Furthermore, Th17.1 cells are a subset of Th17 cells that have undergone plasticity to adopt a Th1-like phenotype (Hirota *et al.*, 2011). They are found to accumulate in RA SF and express increased levels of cytokine compared to Th1 and Th17 cells (Basdeo *et al.*, 2017). However, full mechanisms by which these cells are primed for pathogenic function in RA are not known. Indeed, the effects of TNF-α on the metabolism, fate, and function of Th17 and Th17.1 cell subsets in RA are not well described. Notably, naïve $CD4^+$ T cells from RA patients were observed to have suppressed glycolysis due to a defect in glycolytic enzyme, PFKFB3 (Z. Yang *et al.*, 2013; Yang *et al.*, 2016). A deficiency in NMT1 also prevents AMPK activation leading to unopposed mTOR activity (Z. Wen *et al.*, 2019). In addition, intrinsic defects in the TCA cycle have been reported, resulting in a build-up of acetyl-CoA and mitochondrial aspartate, which cause an invasive phenotype and increased TNF-α production respectively (Wu *et al.*, 2020, 2021). Yet, a full metabolic profile of each $CD4^+$ Th cell subset in RA is has not been described and the drivers of these metabolic perturbations in naïve cells are not fully understood.

Understanding the metabolic perturbations of $CD4^+$ Th cells in RA, the signalling pathways driving them, and how they go on to drive pathogenic cell function will be key in the development of future novel therapeutic targets. In the previous chapters, a role for T cell-derived TNF-α in driving the activation and metabolic reprogramming of naïve $CD4^+$ T cells has been identified, these metabolic effects promoted through PI3K/Akt pathway

activity. TNF-α has also been implicated in driving the differentiation of Th17 cells. However, the relevance of this pathway in RA pathogenesis is unknown.

6.1.1 AIMS

The first aim of this chapter is to develop a flow cytometry panel able to identify multiple $CD4^+$ T cell subsets within PBMCs and then to further characterise expression of cytokines, TFs, phosphorylated signalling molecules, and mitochondrial mass. These flow cytometry panels will be utilised to identify $CD4^+$ T cell subsets in the peripheral blood of RA patients and age- and sex-matched HC and to analyse and compare the metabolism, phenotype, and function of these cells. This approach will test the hypothesis that a TNF-α-mediated PI3K/Akt axis is implicated in the dysregulated metabolism of RA $CD4^+$ T cells.

6.2 RESULTS

6.2.1 Identifying CD4$^+$ T cell subsets by flow cytometry

Peripheral blood samples from RA patients and age- and sex-matched HC were collected and the PBMCs isolated, clinical details of the cohort are presented in Table 6.1. In order to probe the metabolic and functional differences of CD4$^+$ T cell subsets in RA by flow cytometry, a gating strategy was first developed to identify these subsets (Figure 6.1A-B and Figure 6.2A-B). Cells were gated as lymphocytes and single cells, then dead cells were gated out. Having identified a CD4$^+$ cell population, cells were then gated based on a phenotype of CD127^{lo}CD25^{hi} to identify Tregs (Figure 6.1A-B). From those cells remaining outside the Treg gate, CD45RA$^+$ cells were classed as naïve cells and CD45RA$^-$ cells as memory cells. Of note, this gating strategy will not be able to exclude the CD4$^+$ T_{EMRA} population from the CD45RA$^+$ naïve cell gate. Staining for TNFR2 corroborated previous data highlighting the increased levels of the receptor on memory cells compared to naïve cells (Figure 6.1C). A comparatively higher level of TNFR2 expression was present on Tregs.

Using a separate panel, CD4$^+$ Th cell subsets were also identified based on their expression of chemokine receptors CXCR3, CCR4, and CCR6. From these markers, Th1 (CXCR3$^+$CCR4$^-$CCR6$^-$), Th17.1 (CXCR3$^+$CCR4$^-$CCR6$^+$), Th2 (CXCR3$^-$CCR4$^+$CCR6$^-$), and Th17 cells (CXCR3$^-$CCR4$^+$CCR6$^+$) could be distinguished (Gosselin *et al.*, 2010; Yu *et al.*, 2020) (Figure 6.2A-B). To confirm the efficacy of this gating strategy, cells were also stained for characteristic protein markers of Th1 and Th17 cells, specifically cytokines and TFs. Accordingly, Th1 cells expressed IFN-γ with levels in Th2 and Th17 cells essentially undetectable (Figure 6.2C and I). Yet, the highest percentage of IFN-γ$^+$ cells was found to be present in the Th17.1 cell population. This was accompanied by a high expression of T-bet in both Th1 and Th17.1 cells, with relatively lower

levels in Th2 and Th17 cells (Figure 6.2D and J). IL-17A was difficult to detect by flow cytometry with just under 8% of cells positive at the highest point (Figure 6.2E and K). Nonetheless, Th17 cells did express the highest percentage of IL-17A$^+$ cells with little detected in both Th2 and Th1 cell subsets. As described in the literature, Th17.1 cells were able to produce both IFN-γ and IL-17A (Hirota *et al.*, 2011; Basdeo *et al.*, 2017). Indeed, Th17 and Th17.1 cells also recorded the highest expression of RORγt with almost no expression detectable in Th1 and Th2 cells (Figure 6.2F and L). Along with high expression of IFN-γ and IL-17A, Th17.1 cells exhibited the highest percentage of TNF-α$^+$ cells, an average of around 75% (Figure 6.2G and M). Th17 cells had the next highest percentage (around 55%) of TNF-α$^+$ cells with Th1 and Th2 cells on very similar levels of expression, averaging around 40% positive. Furthermore, utilising this gating strategy, the expression of TNFR2 was assessed on each CD4$^+$ Th cell subset (Figure 6.2H). Th1 and Th2 cells exhibited similar levels of TNFR2, but the highest expression was present on both Th17 and Th17.1 cells. These data confirm the effectiveness of the proposed gating strategy at identifying Th1, Th2, Th17, and Th17.1 cell populations. Altogether, these panels enable the identification of multiple CD4$^+$ T cell subsets from within a heterogenous PBMC sample by flow cytometry and allow for further analysis of individual subsets within RA and HC peripheral blood.

Table 6.1 Summary of the RA patient and healthy control cohort

	Healthy controls	RA patients
Number	19	19
Age (years)*	52 (31-87)	55 (29-84)
Sex - % Female	89	89
ACPA positive (>5 U/ml) (n)	N/A	16
RF positive (>30 IU/ml) (n)	N/A	15
CRP (mg/l)*	N/A	5 (<1-39)
ESR (mm/h)*	N/A	22 (2-101)
DAS28 (ESR)*	N/A	4.32 (0.49-7.04)
DAS28 (CRP)*	N/A	4.88 (1.13-7.49)
DMARD use (n)	N/A	15
Methotrexate use (n)	N/A	9
Steroid use (n)	N/A	4
Biologic use (n)	N/A	2

* Median (range). RA=rheumatoid arthritis; ACPA=anti-citrullinated protein antibodies; n=number; RF=rheumatoid factor; CRP=C-reactive protein; ESR=erythrocyte sedimentation rate; DAS28=Disease Activity Score (using 28 joint counts); DMARD=disease-modifying antirheumatic drug.

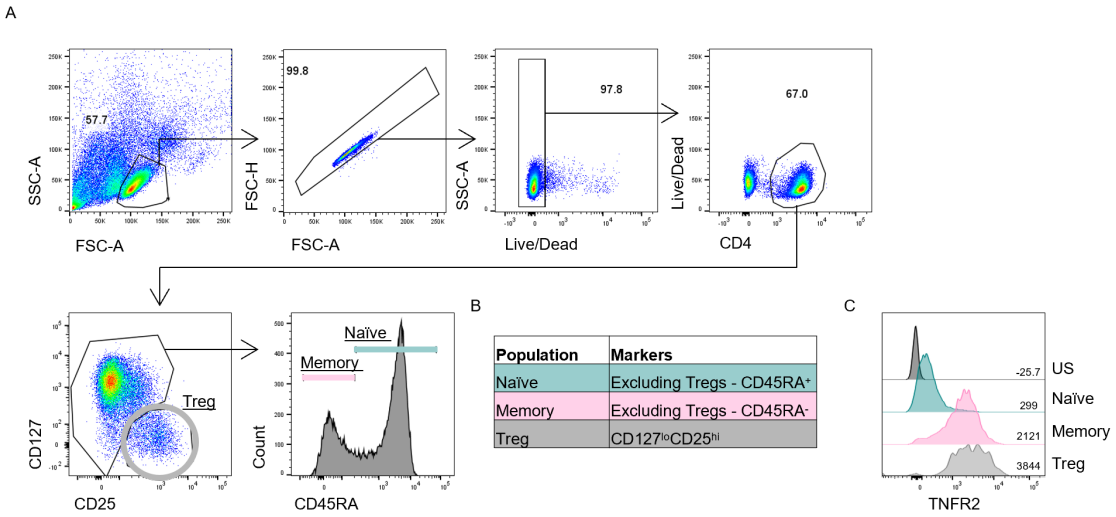

Figure 6.1 Gating strategy for Tregs, naïve, and memory cells in peripheral blood

(**A-C**) PBMCs from healthy controls were thawed and rested overnight before staining for flow cytometry. (**A**) Cells were gated for the removal of debris, doublets, and dead cells. Cells within this gate were then gated on expression of CD4 and cells within the $CD4^+$ T cell gate were then gated as Tregs ($CD127^{lo}CD25^{hi}$). Remaining cells not in the Treg gate were then gated on $CD45RA^+$ (naïve cells) and $CD45RA^-$ (memory cells) (representative plots of n=39 independent donors). (**B**) Markers used to identify naïve, memory, and Treg cells. (**C**) Cells within the naïve, memory, and Treg gates were assessed for expression of TNFR2, US=unstained control (representative plot of n=3 independent donors).

(C) Numbers on the plot indicate mean fluorescence intensity.

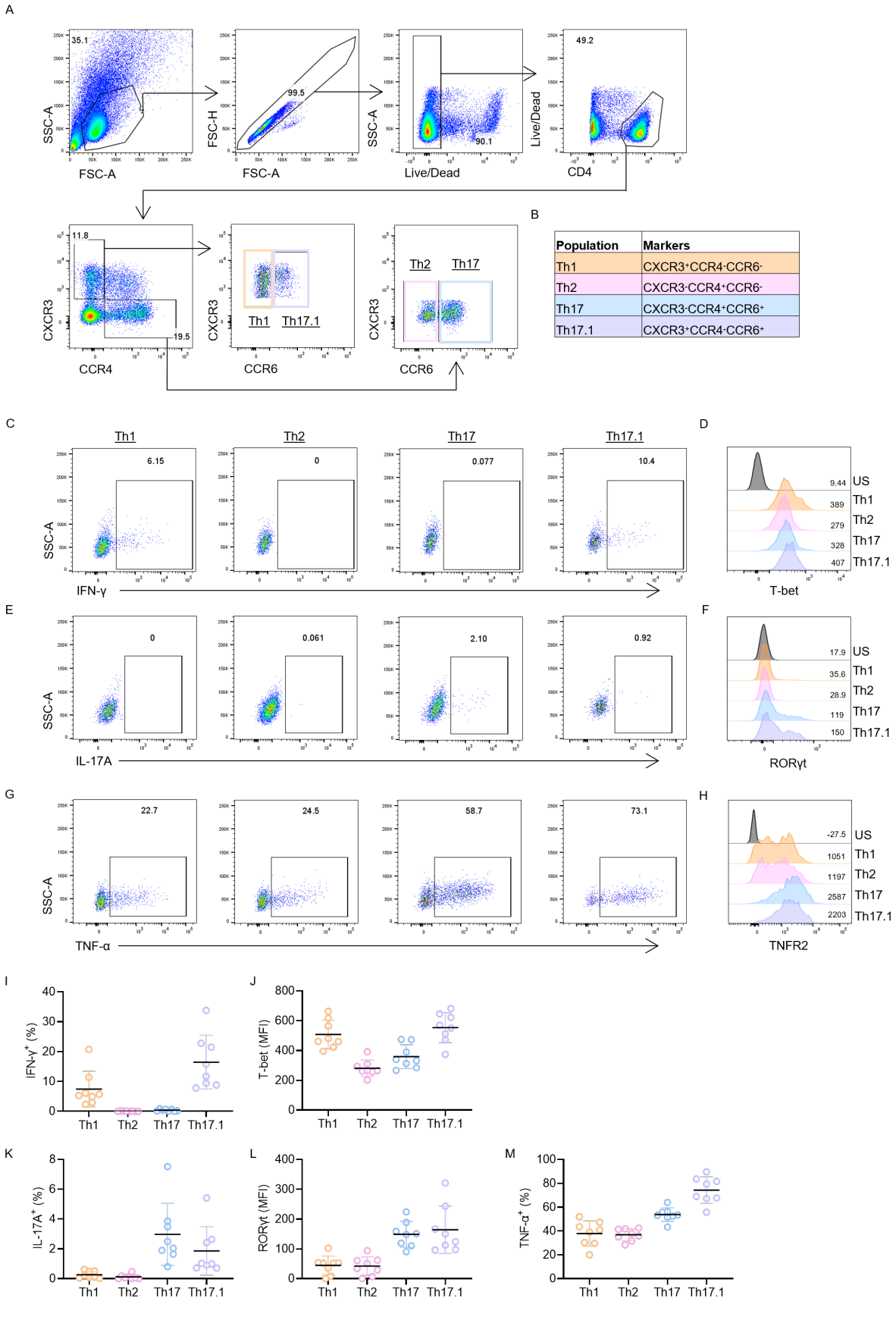
A
35.1
SSC-A
FSC-A
99.5
FSC-H
FSC-A
SSC-A
Live/Dead
90.1
Live/Dead
CD4
49.2
11.8
19.5
CXCR3
CCR4
CXCR3
Th1
Th17.1
CCR6
CXCR3
Th2
Th17
CCR6
B
Population
Markers
Th1
CXCR3+CCR4-CCR6-
Th2
CXCR3-CCR4+CCR6-
Th17
CXCR3-CCR4+CCR6+
Th17.1
CXCR3+CCR4-CCR6+
C
Th1
Th2
Th17
Th17.1
6.15
0
0.077
10.4
SSC-A
IFN-γ
D
9.44
US
389
Th1
279
Th2
328
Th17
407
Th17.1
T-bet
E
0
0.061
2.10
0.92
SSC-A
IL-17A
F
17.9
US
35.6
Th1
28.9
Th2
119
Th17
150
Th17.1
RORγt
G
22.7
24.5
58.7
73.1
SSC-A
TNF-α
H
-27.5
US
1051
Th1
1197
Th2
2587
Th17
2203
Th17.1
TNFR2
I
IFN-γ+ (%)
Th1
Th2
Th17
Th17.1
J
T-bet (MFI)
Th1
Th2
Th17
Th17.1
K
IL-17A+ (%)
Th1
Th2
Th17
Th17.1
L
RORγt (MFI)
Th1
Th2
Th17
Th17.1
M
TNF-α+ (%)
Th1
Th2
Th17
Th17.1

Figure 6.2 Gating strategy for peripheral $CD4^+$ Th cell subsets

(**A**) PBMCs from healthy control (HC) peripheral blood were thawed and rested overnight before staining for flow cytometry. Cells were gated for the removal of debris, doublets, and dead cells. Cells within this gate were then gated on expression of CD4 and cells within the $CD4^+$ T cell gate were then gated as Th1 ($CXCR3^+CCR4^-CCR6^-$), Th2 ($CXCR3^-CCR4^+CCR6^-$), Th17 ($CXCR3^-CCR4^+CCR6^+$), and Th17.1 cells ($CXCR3^+CCR4^-CCR6^-$) (representative plots of n=19 independent donors).

(**B**) Markers used to identify $CD4^+$ Th cell subsets.

(**C-F**) Cells were treated as in (A) with additional stimulation with PMA/ionomycin/brefeldin A for 4 h before staining for flow cytometry. (**C-G**) Cells within the Th1, Th2, Th17, and Th17.1 cell gate were assessed for expression of (**C**) IFN-γ, (**D**) T-bet, (**E**) IL-17A, (**F**) RORγt, and (**G**) TNF-α by flow cytometry, US=unstained control (C-F, representative plots of n=28 independent donors).

(**H**) Cells were treated as in (A) and assessed for the expression of TNFR2, US=unstained control (representative plot of n=3 independent donors).

(**I-M**) Graphs showing (**I**) percentage of IFN-γ^+ cells (**J**) mean fluorescence intensity (MFI) of T-bet (**K**) percentage of IL-$17A^+$ cells (**L**) MFI of RORγt (**M**) percentage of TNF-α^+ cells in each subset (n=8 independent donors).

(D, F, and H) Numbers on the plot indicate MFI. (I-M) Each symbol represents an individual donor and data is presented as the mean ± SD.

6.2.2 Proportions of T cell subsets in RA and healthy control peripheral blood

To begin the comparisons of $CD4^+$ T cells in HC and RA patient peripheral blood, the proportions of each subset were assessed. Firstly, no difference could be seen in the percentage of $CD4^+$ T cells within the lymphocyte gate (Figure 6.3A). Next, using the gating strategies established previously (Figure 6.3B-C), no difference was recorded in the proportion of naïve or memory $CD4^+$ T cells between RA and HC peripheral blood (Figure 6.3D). Moreover, no difference in the proportion of Th1, Th2, Th17, or Th17.1 cells in the $CD4^+$ T cell gate was seen between RA and HC (Figure 6.3E). Notably, Th17.1 cells made up the lowest percentage of $CD4^+$ T cells with the majority exhibiting a Th1 cell phenotype. Tregs were also comparable between HC and RA patients. These data suggest the proportions of $CD4^+$ T cell subsets in peripheral blood remain unchanged in RA.

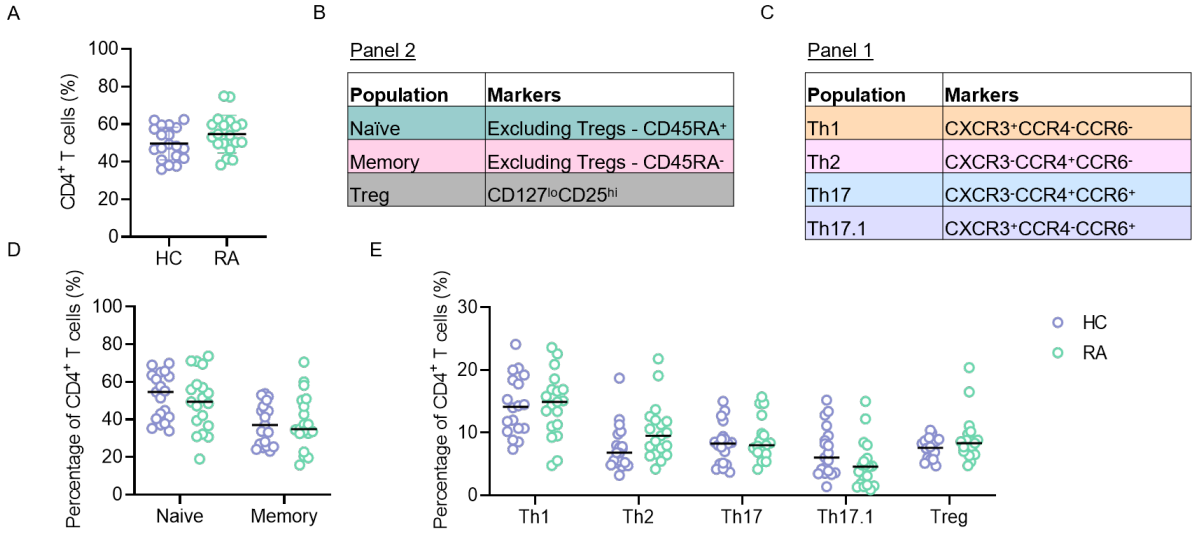

Figure 6.3 No difference in proportions of peripheral CD4⁺ T cell subsets in RA

(**A-E**) PBMCs from rheumatoid arthritis (RA) patients and age- and sex-matched healthy controls (HC) were rested overnight before staining for flow cytometry. Cells were gated as lymphocytes, excluding doublets and dead cells. (**A**) Percentage of cells in the CD4⁺ T cell gate. (**B**) Markers used for identifying Th1, Th2, Th17, and Th17.1 cells. (**C**) Markers used to identify naïve, memory, and Treg cells. (**D-E**) Percentage of (**D**) naïve and memory cells (**E**) Th1, Th2, Th17, Th17.1, and Treg cells in the CD4⁺ T cell gate (A and D-E, n=19 independent donors in each group).

(A and D-E) Each symbol represents an individual donor and data is presented as the (A) mean ± SD (D-E) median. Significance assessed by (A) unpaired t test (D-E) two-way ANOVA with Šídák's multiple comparisons test.

6.2.3 Decreased expression of chemokine receptors on RA $CD4^+$ T cells

Chemokine receptors have a crucial role in inflammation, driving recruitment and trafficking of immune cells to sites of tissue damage (Patel *et al.*, 2001; Hirota *et al.*, 2007). Alongside using the chemokine receptors to identify unique subsets, their expression levels were quantified. On total $CD4^+$ T cells, a lower expression of CXCR3 was seen in RA, with no difference in CCR4 or CCR6 (Figure 6.4A-C). Focusing on specific subsets, Th1 cells which are positive for only CXCR3, expressed much lower levels of the chemokine receptor on the cell surface in RA compared to HC (Figure 6.4D). In accordance with total $CD4^+$ T cell data, Th2 cells which express only CCR4 exhibited no difference in its expression between HC and RA (Figure 6.4E). Again, Th17 cells had comparable levels of CCR4 in both HC and RA but did show a reduction in the expression of CCR6 (Figure 6.4F-G). Contrastingly, Th17.1 cells did not show any difference in CCR6 levels on the surface. However, a decreased expression level of CXCR3 was observed in RA compared to HC (Figure 6.4H-I). Overall, a global decrease in CXCR3 surface expression was seen in RA circulating $CD4^+$ T cells compared to HC, more specifically seen in Th1 and Th17.1 cell subsets. No difference could be seen in CCR4 levels and a reduction in CCR6 was only seen in the Th17 cell population in RA, the subset with the highest CCR6 expression.

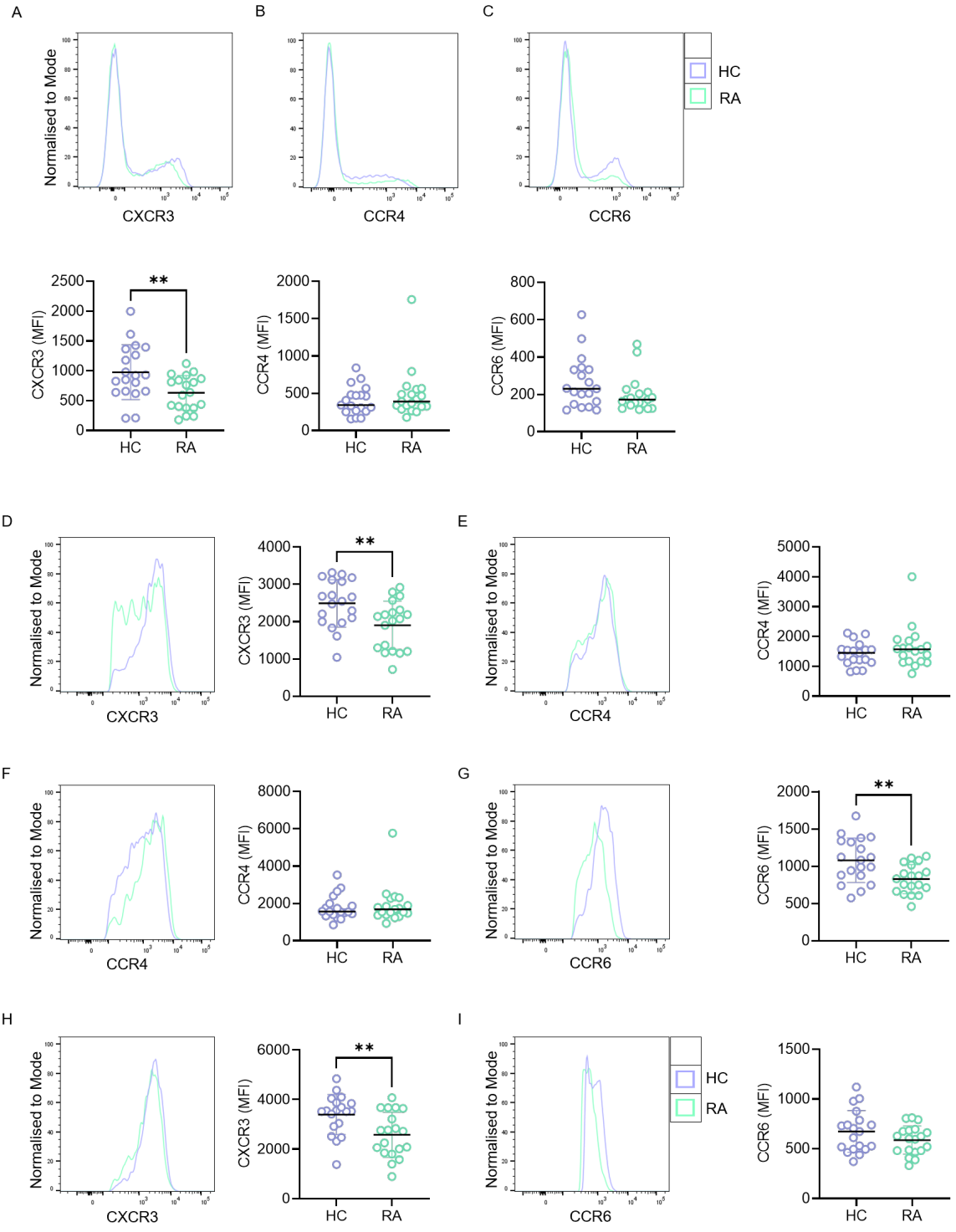
A
B
C
Normalised to Mode
CXCR3
CCR4
CCR6
HC
RA
CXCR3 (MFI)
CCR4 (MFI)
CCR6 (MFI)
**
D
E
F
G
H
I

Figure 6.4 Reduction in chemokine receptors on peripheral $CD4^+$ T cells in RA

(**A-I**) PBMCs from rheumatoid arthritis (RA) patients and age- and sex-matched healthy controls (HC) were rested overnight before staining for flow cytometry. Cells were gated as lymphocytes, excluding doublets and dead cells. (**A-C**) Cells within the $CD4^+$ T cell gate were assessed for expression of (**A**) CXCR3 (**B**) CCR4 (**C**) CCR6. (**D**) Cells within the Th1 cell gate were assessed for CXCR3 expression. (**E**) Cells within the Th2 cell gate were assessed for CCR4 expression. (**F-G**) Cells within the Th17 cell gate were assessed for (**F**) CCR4 (**G**) CCR6 expression. (**H-I**) Cells within the Th17.1 cell gate were assessed for (**H**) CXCR3 (**I**) CCR6 expression, MFI=mean fluorescence intensity (A-I, n=19 independent donors in each group).

(A-I) Each symbol represents an individual donor and data is presented as the (A, D, and G-I) mean ± SD (B-C and E-F) median. Significance assessed by (A, D, and G-I) unpaired t test (B-C and E-FI) Mann-Whitney test, ** $p < 0.01$.

6.2.4 Peripheral CD4$^+$ T cells in RA have increased mitochondrial mass

Next, the aim was to investigate differences in mitochondrial metabolism of CD4$^+$ T cells in RA compared to HC. PBMCs from RA patients and HC were thawed and rested overnight before flow cytometric analysis. Assessing the whole CD4$^+$ T cell population, MVG staining was higher in RA patients compared to HC, suggesting an overall increased mitochondrial mass in RA peripheral CD4$^+$ T cells (Figure 6.5A). In contrast, no difference in mitochondrial activity of the cells, as measured by MSO:MSO+FCCP, was seen between RA and HC (Figure 6.5B). Having assessed differences in the total CD4$^+$ T cell population, naïve and memory cell subsets were probed to understand which specific cell types may be affected. No significant difference in mitochondrial mass was observed in the resting naïve and memory cell subsets (Figure 6.5C). However, a subtle trend towards increased MVG could be seen, in particular in the RA memory cell subset. Extending the analysis to individual Th cell subsets, MVG staining was comparable between Th1, Th2, Th17, and Treg cells in RA and HC (Figure 6.5D). Yet, a difference existed in the Th17.1 cell subset with a considerably higher amount of MVG staining in RA compared to HC. Consistent with total CD4$^+$ T cell data, no difference in mitochondrial activity was seen between HC and RA in naïve or memory cells (Figure 6.5E). Accordingly, mitochondrial activity was largely unaffected between RA and HC peripheral blood CD4$^+$ Th cell subsets, except in the case of Th17.1 cells where a significant increase in the MSO:FCCP ratio was observed in RA (Figure 6.5F). Altogether, these data suggest that peripheral CD4$^+$ T cells, particularly Th17.1 cells, have an increased mitochondrial mass in RA. For Th17.1 cells this was matched with increased mitochondrial activity, both these readouts indicative of heightened OXPHOS.

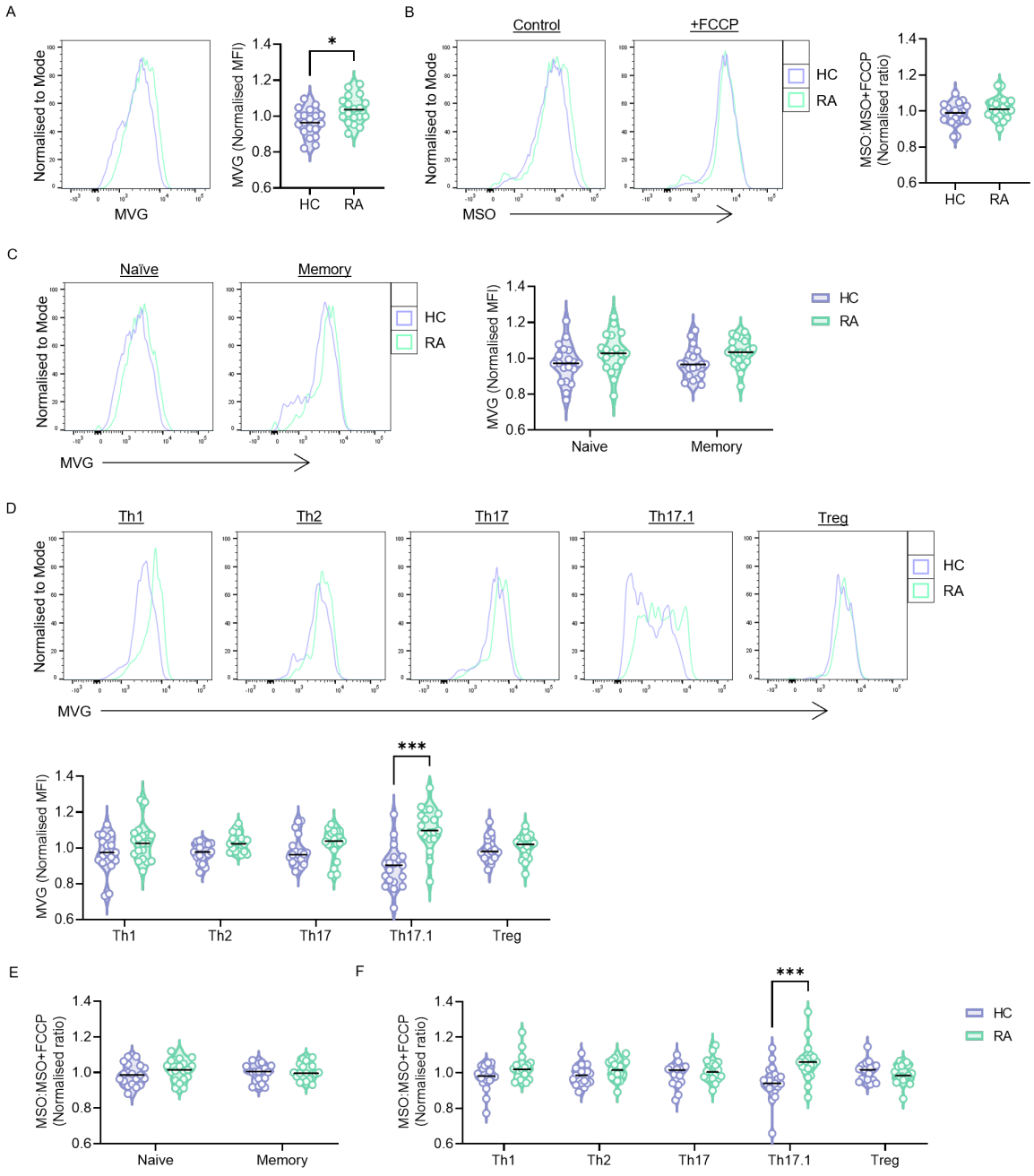
A
Normalised to Mode
MVG
MVG (Normalised MFI)
HC
RA
B
Control
+FCCP
Normalised to Mode
MSO
HC
RA
MSO:MSO+FCCP (Normalised ratio)
C
Naïve
Memory
Normalised to Mode
MVG
HC
RA
MVG (Normalised MFI)
Naive
Memory
D
Th1
Th2
Th17
Th17.1
Treg
Normalised to Mode
MVG
HC
RA
MVG (Normalised MFI)
Th1
Th2
Th17
Th17.1
Treg
E
MSO:MSO+FCCP (Normalised ratio)
Naive
Memory
F
MSO:MSO+FCCP (Normalised ratio)
Th1
Th2
Th17
Th17.1
Treg
HC
RA

Figure 6.5 Increased mitochondrial mass of $CD4^+$ T cells in RA

(**A-G**) PBMCs from rheumatoid arthritis (RA) patients and age- and sex-matched healthy controls (HC) were rested overnight before staining for flow cytometry. Cells were gated as lymphocytes, excluding doublets and dead cells. (**A-B**) Cells within the $CD4^+$ T cell gate were assessed for mean fluorescence intensity (MFI) of (**A**) MVG to measure mitochondrial mass (**B**) ratio of MSO with and without FCCP to measure mitochondrial membrane potential (MSO:MSO+FCCP). (**C-D**) Cells within the (**C**) naïve and memory (**D**) Th1, Th2, Th17, Th17.1 and Treg cell gates were assessed for MFI of MVG. (**E-F**) Cells within the (**E**) naïve and memory (**F**) Th1, Th2, Th17, Th17.1 and Treg cell gates were assessed for MSO:MSO+FCCP (A-F, n=19 independent donors in each group).

(A-F) Each symbol represents an individual donor. Data normalised to the experiment mean for each subset and the median is presented. Significance assessed by two-way ANOVA with Šídák's multiple comparisons test, * $p < 0.05$, *** $p < 0.001$.

6.2.5 Increased levels of Akt phosphorylation in RA CD4$^+$ T cells

Following this identification of an altered metabolic phenotype in RA peripheral CD4$^+$ T cells, cells were analysed for levels of Akt phosphorylation at the T308 residue, phosphorylated specifically by PI3K (Bozulic and Hemmings, 2009). PBMCs were thawed and rested overnight, then activated for 4 h with anti-CD3/28 before staining for analysis by flow cytometry. Due to the technical constraints of a phospho-flow protocol (i.e. immediate fixation required) surface staining was not feasible, instead phenotypic markers had to be stained intracellularly. This limited the analysis to a simpler panel where only naïve and memory CD4$^+$ T cell populations were identified (Figure 6.6A). Cells were gated into a lymphocyte gate, doublets were removed, and a CD4$^+$ T cell gate was clearly defined. From here, cells were gated as naïve (CD45RA$^+$) or memory (CD45RA$^-$). Each population could then be assessed for levels of Akt phosphorylation. Upon activation, naïve cells had a lower level of p-Akt compared to memory cells (Figure 6.6B). These data confirm the validity of this staining panel for use on RA patient samples.

Analysing CD4$^+$ T cells as a whole, those from RA patients exhibited higher levels of p-Akt upon activation compared to HC (Figure 6.6C). Indeed, both naïve and memory cells subsets in RA had significantly increased p-Akt levels after activation compared to matched HC (Figure 6.6D). These data show increased activity of the PI3K/Akt pathway in activated RA peripheral CD4$^+$ T cells.

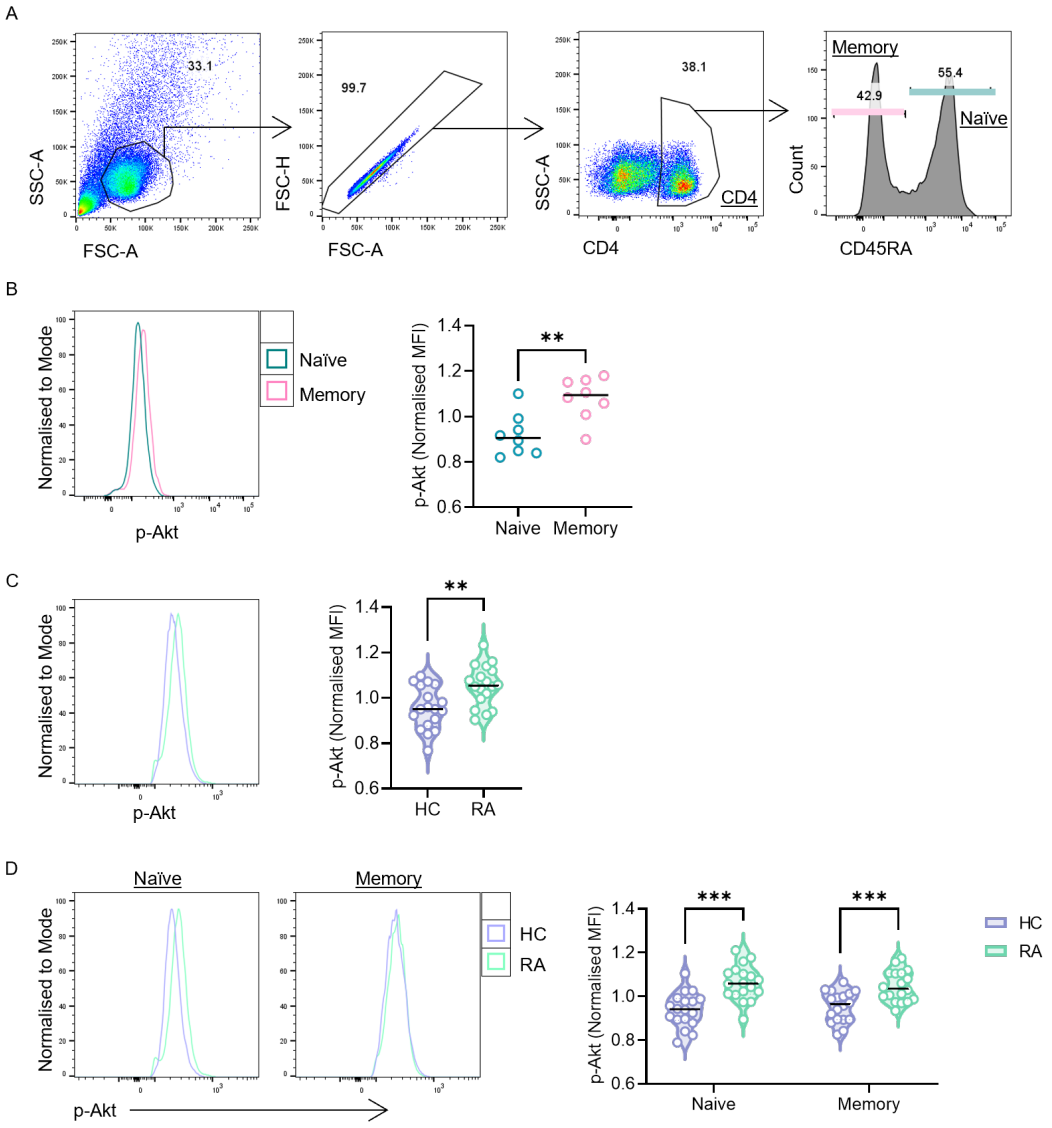

Figure 6.6 Increased levels of phosphorylated Akt in RA peripheral CD4⁺ T cells

(**A-B**) PBMCs from healthy controls (HC) were rested overnight then activated with anti-CD3/28 for 4 h before staining for flow cytometry. (**A**) Cells were gated as lymphocytes and doublets excluded, then a $CD4^+$ cell population was defined. Within the $CD4^+$ T cell gate cells were identified as $CD45RA^+$ (naïve) or $CD45RA^-$ (memory) (representative plots of n=18 independent donors). (**B**) Cells within the naïve and memory cell gates were assessed for mean fluorescence intensity (MFI) of phosphorylated (p)-Akt (n=8 independent donors).

(**C-D**) PBMCs from rheumatoid arthritis (RA) patients and age- and sex-matched HC were treated as in (A-B). Cells within the (**C**) $CD4^+$ (**D**) naïve and memory cell gates were assessed for the MFI of p-Akt (C-F, n=18 independent donors in each group).

(B-D) Each symbol represents an individual donor. Data normalised to the experiment mean (C-D) for each subset and the median is presented. Significance assessed by (B-C) Mann-Whitney test (D) two-way ANOVA with Šídák's multiple comparisons test, ** $p < 0.01$, *** $p < 0.001$.

6.2.6 RA CD4$^+$ T cells have increased expression of membrane-bound TNF-α

It is reported that TNF-α levels are higher in RA. However, most analyses focus on intracellular or soluble levels of TNF-α with little description of levels of mTNF-α (Tetta *et al.*, 1990; Manicourt *et al.*, 2000; Cai *et al.*, 2020; Wu *et al.*, 2021). Here, using a flow cytometry panel to gate on naïve and memory CD4$^+$ T cells, levels of mTNF-α on peripheral CD4$^+$ T cells in RA and HC were assessed. PBMCs were thawed, rested, and activated with anti-CD3/28 for 4 h as before. As described previously, the gating strategy identified a lymphocyte gate, single cells, live cells, then CD4$^+$ T cells (Figure 6.7A). Within the CD4$^+$ T cell gate cells were identified as naïve or memory cells based on CD45RA expression, CD45RA$^+$ and CD45RA$^-$ respectively. Very low levels of mTNF-α were detectable on NA CD4$^+$ T cells, in both RA and HC, but levels did substantially increase upon activation (Figure 6.7B-C). When activated, the percentage of surface TNF-α$^+$ cells was higher among RA peripheral CD4$^+$ T cells than HC (Figure 6.7C). This increase in mTNF-α was also found specifically within the RA memory CD4$^+$ T cell subset (Figure 6.7D). Notably, naïve CD4$^+$ T cells expressed less mTNF-α than memory cells.

Next, to assess the levels of intracellular TNF-α, among other cytokines and TFs, two new flow cytometry panels were employed. Here, the chemokine receptors were again used to separate out Th1, Th2, Th17, and Th17.1 cells, but now used in combination with antibodies to stain intracellular cytokines and TFs (Figure 6.8A-C). To do so, PBMCs were either activated with anti-CD3/28 for 4 h in presence of brefeldin-A to stop the release of cytokines from the cell, or a cocktail of PMA/ionomycin/brefeldin-A. However, activation via PMA/ionomycin caused a substantial reduction in the surface expression of chemokine receptors, which meant that cells could not be gated accurately and readouts for only total CD4$^+$ T cells were reported.

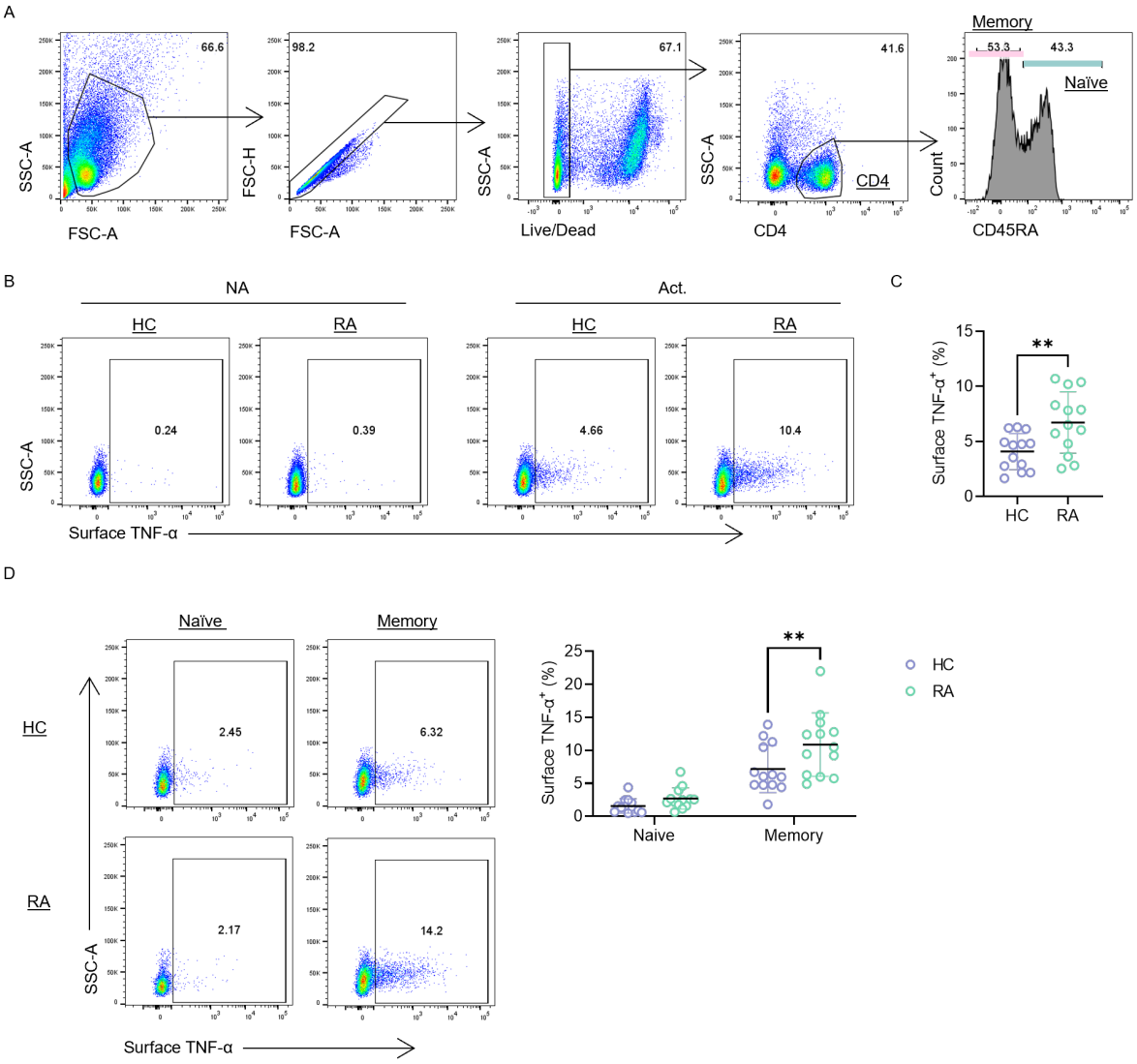

Figure 6.7 Peripheral memory CD4⁺ T cells in RA have increased surface TNF-α

(**A**) PBMCs from rheumatoid arthritis (RA) patients and age- and sex-matched healthy controls (HC) were rested overnight then activated (act.) with anti-CD3/28 for 4 h before staining for flow cytometry. Cells were gated as lymphocytes with doublets and dead cells excluded, then a $CD4^+$ cell population was defined. Within the $CD4^+$ T cell gate cells were identified as $CD45RA^+$ (naïve) or $CD45RA^-$ (memory) (representative plots of n=26 independent donors).

(**B**) $CD4^+$ T cells treated and gated as in (A) with the addition of a non-activated (NA) condition were assessed for levels of surface TNF-α (NA representative plots of n=3 independent donors in each group, Act. representative plots of n=13 independent donors in each group).

(**C-D**) Cells treated and gated as in (A) were assessed for percentage of surface TNF-α in the (**C**) $CD4^+$ T cell (**D**) naïve and memory cell gates (n=13 independent donors in each group).

(C-D) Each symbol represents an individual donor and data is presented as the mean ± SD. Significance assessed by (C) unpaired t test (D) two-way ANOVA with Šídák's multiple comparisons test, ** $p < 0.01$.

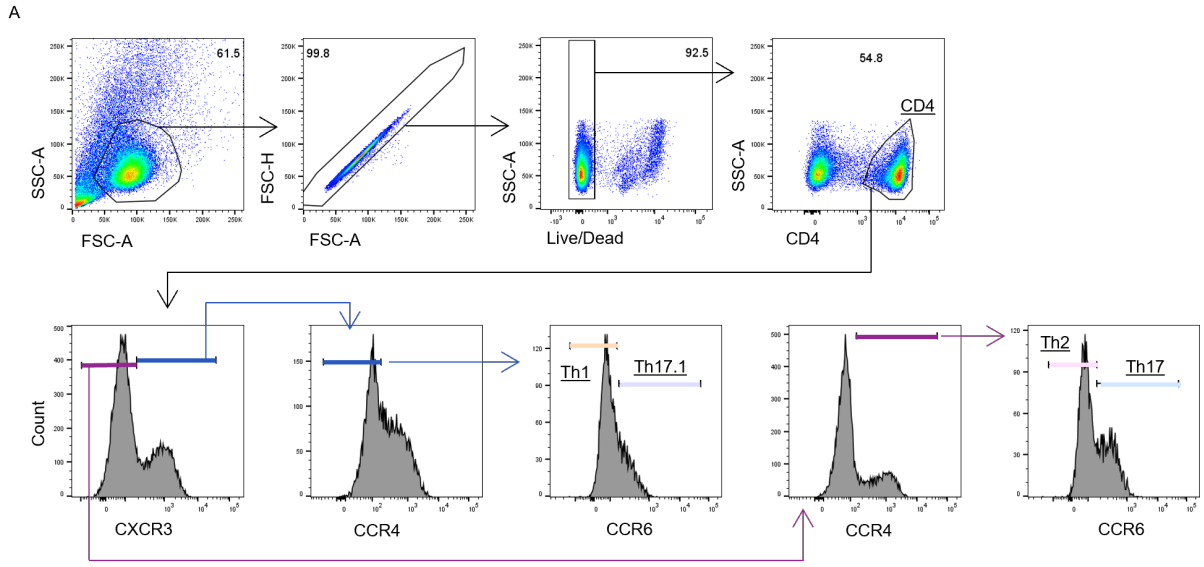

B

Panel 1	Panel 2
Live/Dead	Live/Dead
CD4	CD4
CXCR3	CXCR3
CCR4	CCR4
CCR6	CCR6
RORγt	T-bet
IL-10	IFN-γ
IL-17A	TNF-α
FoxP3	

C

Population	Markers
Th1	$CXCR3^+CCR4^-CCR6^-$
Th2	$CXCR3^-CCR4^+CCR6^-$
Th17	$CXCR3^-CCR4^+CCR6^+$
Th17.1	$CXCR3^+CCR4^-CCR6^+$

Figure 6.8 Gating strategy for intracellular staining of $CD4^+$ Th cell subsets

(**A**) PBMCs from rheumatoid arthritis (RA) patients and age- and sex-matched healthy controls (HC) were rested overnight then activated with anti-CD3/28 for 4 h in presence of brefeldin A before staining for flow cytometry. (**A**) Cells were gated as lymphocytes with doublets and dead cells excluded. Cells within this gate were then gated on expression of CD4 and cells within the $CD4^+$ T cell gate were then gated as Th1 ($CXCR3^+CCR4^-CCR6^-$), Th2 ($CXCR3^-CCR4^+CCR6^-$), Th17 ($CXCR3^-CCR4^+CCR6^+$), and Th17.1 cells ($CXCR3^+CCR4^-CCR6^-$) (representative plots of n=38 independent donors).

(**B**) Two flow cytometry panels utilised for intracellular staining of $CD4^+$ Th cell subsets.

(**C**) Markers used to identify $CD4^+$ Th cell subsets.

In comparison to increased surface TNF-α expression on RA $CD4^+$ T cells, here, no difference in intracellular TNF-α levels were seen between RA and HC total $CD4^+$ T cells when activated by anti-CD3/28 (Figure 6.9A-B). PMA/ionomycin was able to induce considerably higher TNF-α expression in cells but levels were still comparable between RA and HC (Figure 6.9A and C). To delve into this further, each $CD4^+$ Th cell subset was assessed for intracellular TNF-α expression following anti-CD3/28 activation. It could again be seen that Th17.1 cells expressed the highest percentage of TNF-α^+ cells with Th17 cells slightly below (Figure 6.9D). Th1 and Th2 cells had a similar percentage of TNF-α^+ cells but less than both Th17 and Th17.1 cells. No differences in TNF-α expression between RA and HC were seen in any of the subsets. Taken together, these data suggest that levels of intracellular TNF-α in peripheral $CD4^+$ T cells are unchanged in RA compared to HC. In RA, the increased level of surface TNF-α on $CD4^+$ T cells was seen to positively correlate with the percentage of intracellular TNF-α^+ cells (Figure 6.9E). However, no correlation could be seen in the HC group. These data suggest that in RA, peripheral $CD4^+$ T cells express higher amounts of mTNF-α compared to HC. There is also evidence to suggest TNF-α accumulates on the surface of RA $CD4^+$ T cells more so than in HC.

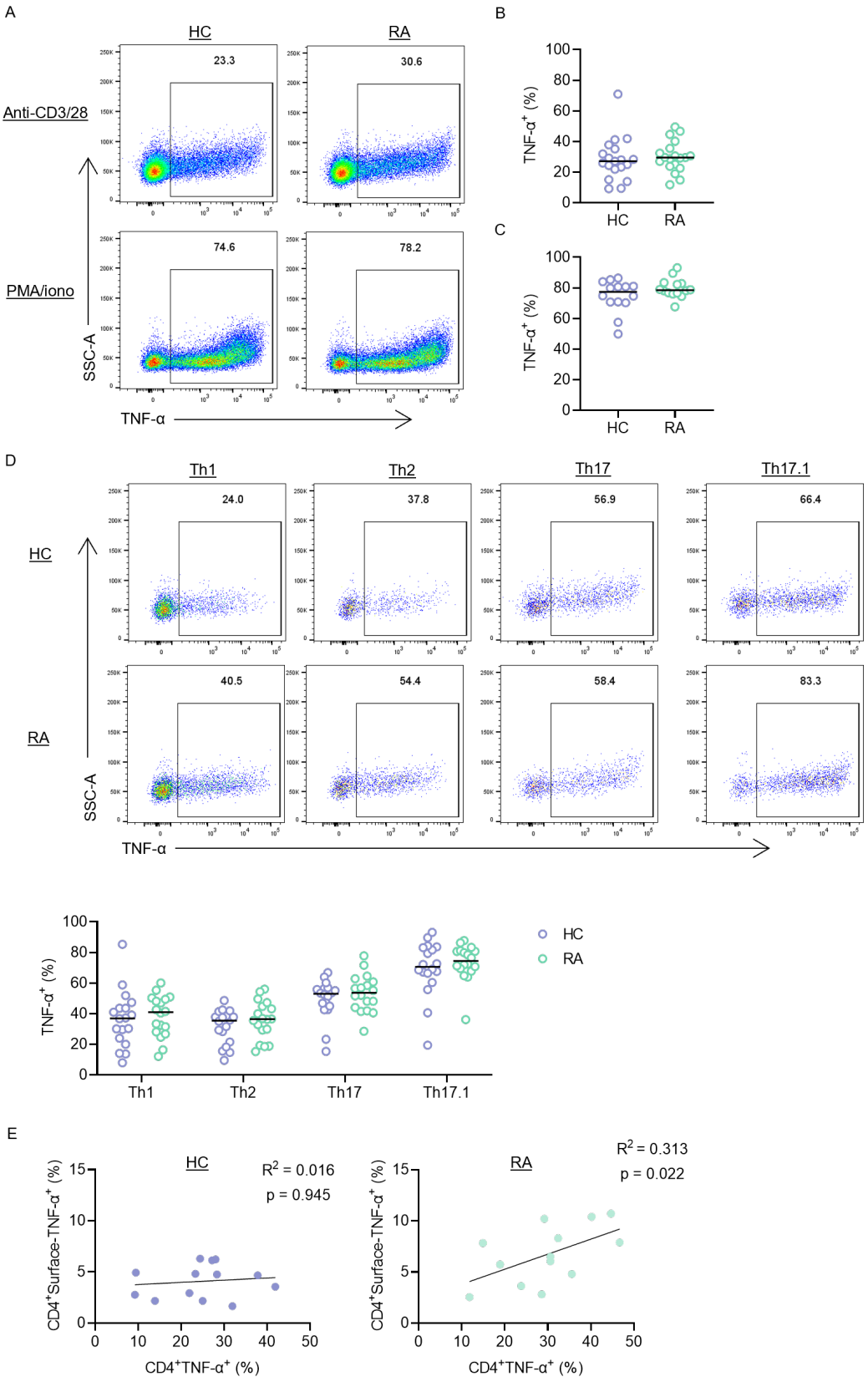
A
HC
RA
Anti-CD3/28
PMA/iono
23.3
30.6
74.6
78.2
SSC-A
TNF-α
B
TNF-α+ (%)
HC
RA
C
D
Th1
Th2
Th17
Th17.1
24.0
37.8
56.9
66.4
40.5
54.4
58.4
83.3
E
CD4+Surface-TNF-α+ (%)
CD4+TNF-α+ (%)
R2 = 0.016
p = 0.945
R2 = 0.313
p = 0.022

Figure 6.9 TNF-α levels in RA and healthy control peripheral blood $CD4^+$ T cells

(**A-C**) PBMCs from rheumatoid arthritis (RA) patients and age- and sex-matched healthy controls (HC) were rested overnight then activated with (**B**) anti-CD3/28 for 4 h in presence of brefeldin A (n=19 independent donors in each group) or (**C**) PMA/ionomycin/brefeldin A for 4 h (n=14 independent donors in each group) before staining for flow cytometry. Cells within the $CD4^+$ T cell gate were assessed for expression of intracellular TNF-α.

(**D**) Cells were treated as in (B) and cells within the Th1, Th2, Th17, and Th17.1 cell gated were assessed for expression of TNF-α (n=18 independent donors in each group).

(**E**) Correlation between levels of surface and intracellular TNF-α in $CD4^+$ T cells in HC and RA.

(B-E) Each symbol represents an individual donor and (B-D) data is presented as the median. Significance assessed by (B-C) Mann-Whitney test (D) two-way ANOVA with Šídák's multiple comparisons test (E) Spearman's correlation coefficient.

6.2.7 Differences in Th1 and Th17 cell function in RA

To extend this analysis of RA and HC peripheral $CD4^+$ T cells, cells were assessed for their expression of characteristic Th1 cell markers, IFN-γ and T-bet. Assessing total $CD4^+$ T cells, no difference in the percentage of IFN-γ^+ cells was seen between RA and HC with either anti-CD3/28 or PMA/ionomycin stimulation (Figure 6.10A-C). In addition, there was no effect on the expression of T-bet in total $CD4^+$ T cells in RA (Figure 6.10D). To probe this further, analysis was focused specifically within Th1 and Th17.1 subsets. There was no difference in RA Th1 cells for levels of IFN-γ^+ cells or T-bet expression (Figure 6.10E-G). This was also true of Th17.1 cells where levels of IFN-γ and T-bet were comparable between RA and HC (Figure 6.10E and H-I). Together, these data suggest no alteration of the Th1 cell phenotype in RA peripheral $CD4^+$ T cells.

Next, phenotypic markers of Th17 cell function were assessed. By anti-CD3/28 stimulation, the percentage of IL-$17A^+$ cells remained very low in a total $CD4^+$ T cell population and were comparable in both RA and HC (Figure 6.11A-B). PMA/ionomycin stimulation was able to boost the percentage positive cells slightly, and in this case RA $CD4^+$ T cells showed a trend towards the increased expression of IL-17A compared to HC $CD4^+$ T cells (Figure 6.11A-C). No difference in RORγt expression was seen between RA and HC $CD4^+$ T cells (Figure 6.11D). Within the Th17 cell population, there was no difference in the percentage of IL-$17A^+$ cells and again no difference in expression of RORγt in RA (Figure 6.11E-G). These observations were also true of the Th17.1 cell population (Figure 6.11E and H-I). Therefore, these data show that RA $CD4^+$ T cells trend towards increased IL-17A production. However, no difference in IL-17A production could be seen within the Th17 or Th17.1 cell subsets and levels of RORγt expression remained comparable with HC.

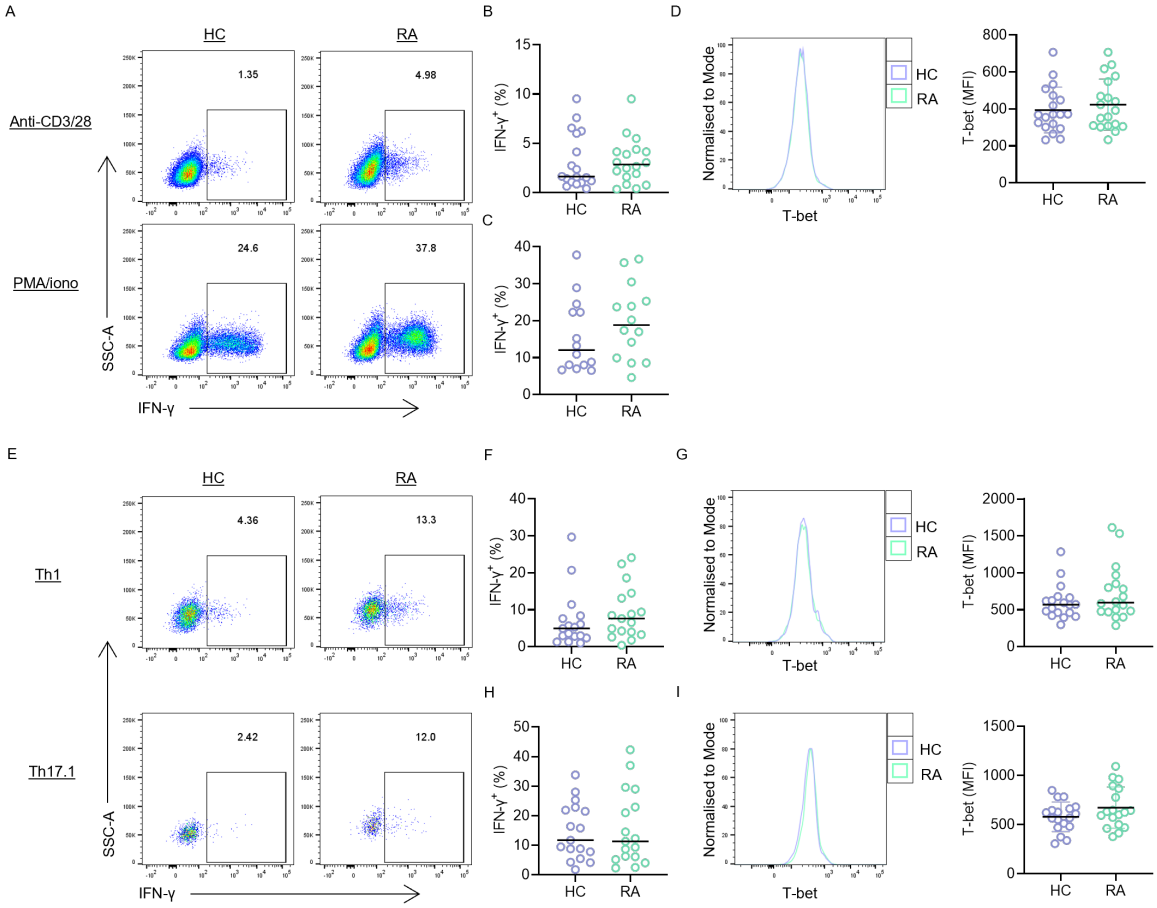

Figure 6.10 No difference in Th1 cells in RA peripheral blood

(**A-C**) PBMCs from rheumatoid arthritis (RA) patients and age- and sex-matched healthy controls (HC) were rested overnight then activated with (**B**) anti-CD3/28 for 4 h in presence of brefeldin A (n=18 independent donors in each group) or (**C**) PMA/ionomycin/brefeldin A (PMA/iono) for 4 h (n=14 independent donors in each group) before staining for flow cytometry. Cells within the $CD4^+$ T cell gate were assessed for expression of intracellular IFN-γ.

(**D**) Cells were treated as in (B) and assessed for expression of T-bet, MFI=mean fluorescence intensity (n=19 independent donors in each group).

(**E-I**) Cells were treated as in (B) and cells in the (**F-G**) Th1 and (**H-I**) Th17.1 cell gates were assessed for the expression of (**E-F and H**) IFN-γ (**G and I**) T-bet (E-I, n=18 independent donors).

(B-I) Each symbol represents an individual donor and data is presented as the (B-C and F-G) median (D and I) mean ± SD. Significance assessed by (B-C and F-G) Mann-Whitney test (D and I) unpaired t test.

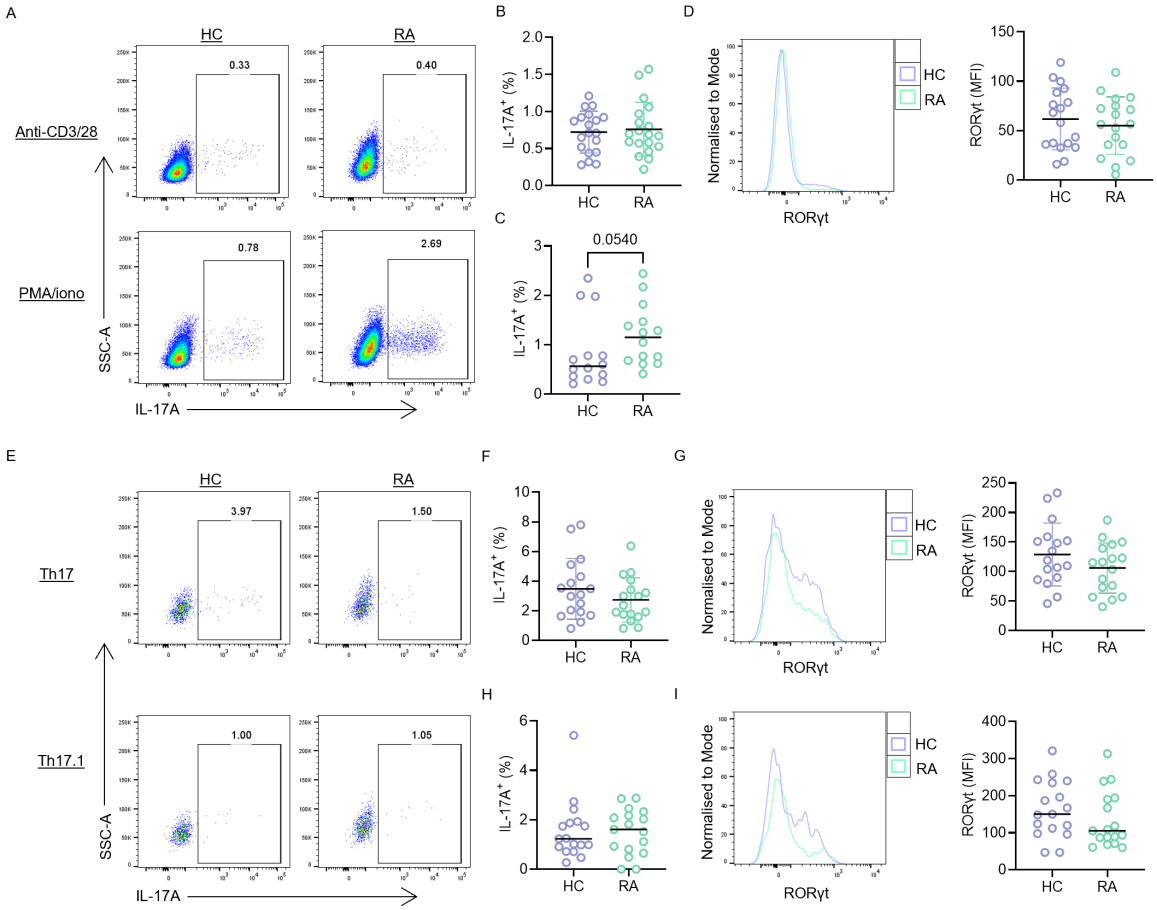

Figure 6.11 RA CD4⁺ T cells trend towards increased IL-17A production

(**A-C**) PBMCs from rheumatoid arthritis (RA) patients and age- and sex-matched healthy controls (HC) were rested overnight then activated with (**B**) anti-CD3/28 for 4 h in presence of brefeldin A (n=19 independent donors in each group) or (**C**) PMA/ionomycin/brefeldin A (PMA/iono) for 4 h (n=14 independent donors in each group) before staining for flow cytometry. Cells within the CD4⁺ T cell gate were assessed for expression of intracellular IL-17A.

(**D**) Cells were treated as in (B) and assessed for expression of RORγt, MFI=mean fluorescence intensity (n=18 independent donors in each group).

(**E-I**) Cells were treated as in (B) and cells in the (**F-G**) Th17 and (**H-I**) Th17.1 cell gates were assessed for the expression of (**E-F and H**) IL-17A (**G and I**) RORγt (E-I, n=17 independent donors).

(B-I) Each symbol represents an individual donor and data is presented as the (B, D and F-G) mean ± SD (C and H-I) median. Significance assessed by (B, D and F-G) unpaired t test (C and H-I) Mann-Whitney test.

6.2.8 Reduced functionality of Tregs in RA

Finally, the regulatory T cell phenotype was assessed. Previously, using cell surface markers CD127 and CD25 to identify Tregs, their proportion in total peripheral $CD4^+$ T cells was seen to be comparable in RA and HC. Here, using FoxP3 staining to identify Tregs, there was again no difference in percentage between RA and HC (Figure 6.12A). However, within the $FoxP3^+$ Treg population, there was a reduced percentage of $IL\text{-}10^+$ cells in RA compared to HC, albeit in general these proportions were small (Figure 6.12B). In total $CD4^+$ T cells, IL-10 became even harder to measure, with <1% positive cells (Figure 6.12C). Nevertheless, there was no difference in IL-10 expression between RA and HC peripheral $CD4^+$ T cells. Together, these data suggest a reduced functionality of Tregs in RA compared to HC, despite their comparable proportion in peripheral blood.

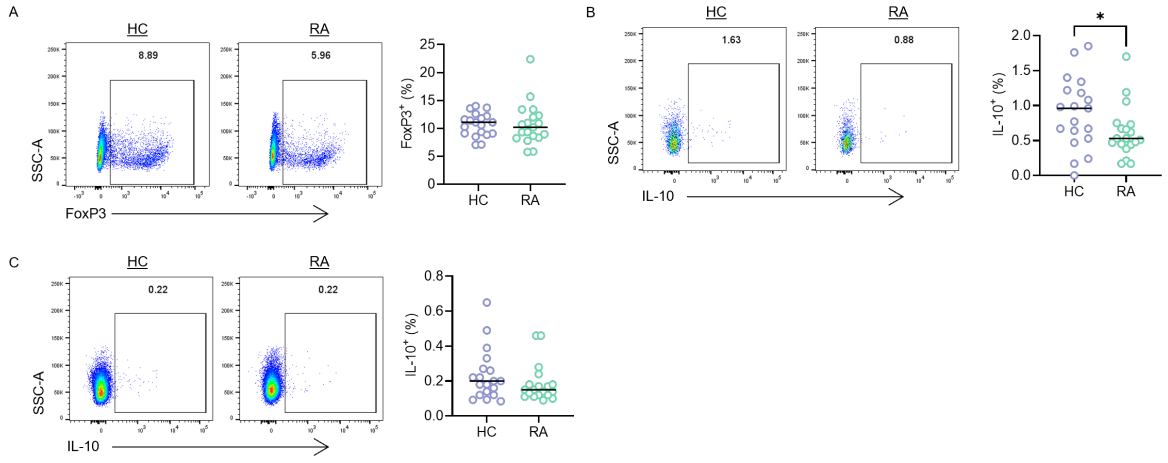

Figure 6.12 Reduced IL-10 production in RA peripheral Tregs

(**A-C**) PBMCs from rheumatoid arthritis (RA) patients and age- and sex-matched healthy controls (HC) were rested overnight then activated with anti-CD3/28 for 4 h in presence of brefeldin A before staining for flow cytometry. (**A**) Cells within the $CD4^+$ T cell gate were assessed for expression of FoxP3. (**B**) Percentage of $FoxP3^+$ cells expressing IL-10. (**C**) Percentage of $CD4^+$ cells expressing IL-10 (A-C, n=19 independent donors).

(A-C) Each symbol represents an individual donor and data is presented as the median. Significance assessed by Mann-Whitney test, * $p < 0.05$.

6.3 DISCUSSION

TNF-α is a leading driver of inflammation and tissue damage in RA, present in the SF and at increased levels in the peripheral blood compared to controls, with RA T cells previously described to over produce TNF-α due to a defect in mitochondrial aspartate production causing expansion of the ER and increased translation (Tetta *et al.*, 1990; Manicourt *et al.*, 2000; Cai *et al.*, 2020; Wu *et al.*, 2021). Anti-TNFα therapies have proven successful in treatment of RA, yet not all patients respond adequately (D.-Y. Chen *et al.*, 2011; Jobanputra *et al.*, 2012; Krieckaert *et al.*, 2012). The complete mechanisms of TNF-α-driven pathogenesis in RA are not understood but will aid in the development of novel therapeutic approaches. In the previous chapters, a TNF-α/PI3K/Akt metabolic axis has been characterised; here, this axis is investigated in the context of RA. Development of a flow cytometry panel using chemokine receptor expression to distinguish $CD4^+$ T cell subsets within PBMCs enabled the assessment of cell phenotype, function, and metabolism in RA compared to HC. No difference in the proportion of $CD4^+$ T cell subsets was observed, but RA peripheral Th1 and Th17.1 cells had a lower expression of CXCR3 and Th17 cells a lower expression of CCR6. Peripheral $CD4^+$ T cells in RA also exhibited increased mitochondrial mass, particularly within the Th17.1 cell subset, increased levels of p-Akt upon activation, and increased levels of surface TNF-α. $CD4^+$ T cells trended towards increased expression of IL-17A and Tregs exhibited reduced IL-10 expression. These data give evidence to implicate the TNF-α/PI3K/Akt metabolic axis in RA pathogenesis.

6.3.1 Circulating $CD4^+$ T cell subsets in RA

In order to analyse the metabolic profile and phenotype of $CD4^+$ T cell subsets in RA a flow cytometry panel, including CD4 and chemokine receptors CXCR3, CCR6, and CCR4, was

designed to identify Th1 ($CD4^+CXCR3^+CCR4^-CCR6^-$), Th17.1 ($CD4^+CXCR3^+CCR4^-CCR6^+$), Th2 ($CD4^+CXCR3^-CCR4^+CCR6^-$), and Th17 cells ($CD4^+CXCR3^-CCR4^+CCR6^+$). In addition, a separate panel used CD127 and CD25 to identify Tregs ($CD4^+CD127^{low}CD25^{high}$) with the remaining cells gated on CD45RA to identify naïve ($CD45RA^+$) and memory cell subsets ($CD45RA^-$). This approach has been utilised by previous studies and its efficacy confirmed by cytokine and TF staining of the identified populations (Gosselin *et al.*, 2010; Yu *et al.*, 2020). These studies are consistent with the data shown here. It was confirmed that Th1 cells expressed IFN-γ and T-bet, Th17 cells expressed IL-17A and RORγt, and Th17.1 cells expressed IFN-γ, IL-17A, T-bet, and RORγt, as has been previously described for these cells (Gosselin *et al.*, 2010; Hirota *et al.*, 2011; Basdeo *et al.*, 2017). Furthermore, the expression of TNFR2 was assessed on these subsets. As reported before (Chen *et al.*, 2008), Tregs had a higher expression of TNFR2 than both naïve and memory non-Treg cells. Also consistent with data from Chapter 3 of the current study, naïve cells had a lower expression of TNFR2 than memory cells. Th17 cells have been reported by another study to have a higher expression of TNFR2 than Th1 cells (Pesce *et al.*, 2022). Indeed, this was confirmed in the data presented here. Moreover, Th17.1 cells expressed similar levels of TNFR2 to Th17 cells. Of note, the study by Pesce *et al.* identified that the percentage of $TNFR1^+$ Th1 and Th17 cells increases in RA with accompanying decreases in $TNFR2^+$ cells. However, another study showed that although $TNFR1^+$ $CD4^+$ T cells increased in RA, no change was detected in $TNFR2^+$ $CD4^+$ T cells (Rossol *et al.*, 2013). TNFR expression was not assessed here in RA patients and HC, yet future studies should test this to understand whether changes in TNFR expression alter the response of $CD4^+$ Th subsets to TNF-α in RA, particularly pathogenic Th17.1 cells which have not been previously looked at.

Results described here show no significant difference in the proportion of $CD4^+$ T cell subsets between HC and RA patients. Previous studies are contradictory in results likely due to the heterogeneity of RA. Compared to HC, some studies have reported increased levels of circulating Th17 cells in RA (D.-Y. Chen *et al.*, 2011; Wang *et al.*, 2012; Pandya *et al.*, 2016), whereas another, similar to the results shown here showed no change (Takeshita *et al.*, 2019). Reports on the proportion of circulating Tregs are also varied, some studies in agreement with the no difference shown here (Liu *et al.*, 2005; Möttönen *et al.*, 2005), whilst others have shown an increase (van Amelsfort *et al.*, 2004; Pandya *et al.*, 2016; Takeshita *et al.*, 2019; Zhang *et al.*, 2022), and decrease (Kawashiri *et al.*, 2011; Niu *et al.*, 2012) in RA patients. Mechanistically, studies have identified that RA naïve $CD4^+$ T cells have impaired activation of the DNA repair protein, ATM, and increased mTOR activity, which both bias differentiation towards Th1 and Th17 cells (Yang *et al.*, 2016; Z. Wen *et al.*, 2019). Several factors may influence the proportion of circulating $CD4^+$ T cell subsets including age, disease stage, use of DMARDs such as methotrexate, and anti-TNFα therapies (D.-Y. Chen *et al.*, 2011; Kremer *et al.*, 2016; Pandya *et al.*, 2016; Ponchel *et al.*, 2020). Although patients and HC were well matched by age and sex, variances here and in other studies, in factors such as treatment and disease stage, may account for the observed disparity in results. Future improvements would better stratify patients based on these variables, however availability of patients to a study does limit this.

RA peripheral $CD4^+$ T cells in the current study expressed lower levels of CXCR3 compared to HC, specifically this decrease was present on Th1 and Th17.1 cells. In addition, CCR6 was decreased on Th17 cells in RA. It is feasible that this decrease is due to the increased release of chemokines from the inflamed synovium, recruiting cells which express high levels of these

chemokine receptors to the synovium and out of the peripheral blood. Indeed, higher expression of CXCL9 and CXCL10 (CXCR3-binding) and CCL20 (CCR6-binding) in RA SF compared to blood plasma has been reported (Ueno *et al.*, 2005; Hirota *et al.*, 2007; Tanida *et al.*, 2009; Pandya *et al.*, 2017; Aldridge *et al.*, 2020). In comparison, CCR4 expression on Th2 and Th17 cells was unaffected. In agreement with this, Aldridge *et al.* reported no difference in the concentration of CCL17 (CCR4-binding) between RA SF and blood plasma. These changes in chemokine receptor expression do not correlate with a change in proportion of circulating cell subsets in the current study, however proportions of cells in SF could not be assessed. Improvements to future work would include analysis of matched SF from RA patients to better understand the reduction in CXCR3 and CCR6 on peripheral $CD4^+$ T cell subsets.

6.3.2 Dysregulated metabolism of RA $CD4^+$ T cells

Several studies have identified dysregulated metabolism of naïve $CD4^+$ T cells in RA, showing them upon 72 h of activation to have lower glycolysis than HC and lower OXPHOS compared to control patients with psoriatic arthritis (Z. Yang *et al.*, 2013; Wu *et al.*, 2020, 2021). In comparison, it was seen here that unstimulated $CD4^+$ T cells in RA had a higher mitochondrial mass than HC $CD4^+$ T cells. There was then a subtle trend observed towards increased MVG staining within the memory cell subset and a significant increase in Th17.1 cells. The majority of the results discussed in previous chapters are based on naïve $CD4^+$ T cell activation. However, the metabolism of the cells in this chapter was assessed directly *ex vivo*, future work should analyse the metabolism of naïve $CD4^+$ T cells from RA patients upon activation. In addition, comparing patients on anti-TNFα therapy or not, or comparing patients prior to and following anti-TNFα therapy. Increased mitochondrial mass in the resting memory but not

naïve cell populations would suggest dysregulated metabolic reprogramming may have occurred during initial priming *in vivo*. Further studies assessing RA naïve $CD4^+$ T cell metabolic reprogramming in the presence of increased TNF-α and anti-TNFα would be able to directly investigate a potential role for T cell-derived TNF-α in mediating this effect. Furthermore, *in vivo* the contribution of TNF-α derived from other cell types, including DCs, FLS, and macrophages, to the observed effects will require further investigation. In comparison, no change was observed in mitochondrial activity as assessed by MSO:MSO+FCCP, these data were consistent with results in Chapter 3 showing minor differences in the ratio. Additional experiments would utilise more sensitive metabolic assays such as Seahorse XF analysis and stable isotope tracing of $^{13}C_6$-glucose and $^{13}C_5$-glutamine to fully characterise the metabolic profile of RA $CD4^+$ T cell subsets and understand the effects on glycolysis, which were not measured here. This would however require isolation of $CD4^+$ T cells from PBMCs and larger numbers of cells and sample volumes not available in this current study. One study has previously assessed changes in metabolite abundance in activated $CD4^+$ T cells after 24 h of infliximab treatment, identifying only trends (Chimenti *et al.*, 2013). Yet, little more is described on the effects on TNF-α on $CD4^+$ Th cell metabolism and function in RA. These data highlight the need for further studies investigating this effect.

Several studies have investigated the metabolism of $CD4^+$ T cells in RA, mostly focusing on bulk $CD4^+$ T cells or naïve $CD4^+$ T cells (Z. Yang *et al.*, 2013; van Loosdregt *et al.*, 2016; Wu *et al.*, 2020, 2021). Consequently, the unique metabolic requirements of individual $CD4^+$ Th cell subsets in RA are well not described. Here, within the $CD4^+$ Th cell subsets, the most striking difference was seen in Th17.1 cells with those in RA exhibiting higher mitochondrial mass and activity. The current study is the first to identify this disparity in Th17.1 cell metabolism in RA.

However, these data are limited by the use of fluorescent mitochondrial probes, it has been previously reported that these probes are exported from the cell via ABC transporter protein 1 (ABCB1) (Dimeloe *et al.*, 2014). Different $CD4^+$ T cell subsets are known to express different levels of this transporter; Tregs lacking expression entirely and Th17.1 cells shown to have significantly higher expression than Th1 or Th17 cells (Ramesh *et al.*, 2014; Koetzier *et al.*, 2020). It has been suggested in one study that PBMCs from patients with active RA expressed increased levels of ABCB1 than those from patients in remission, which in contrast to the data here, would suggest increased levels of fluorescent mitochondrial probe efflux (Atisha-Fregoso *et al.*, 2016). However, it is still possible that RA Th17.1 cells specifically have decreased expression of ABCB1 compared to HC, and therefore reduced efflux of MVG and MSO. Future studies should assess levels of ABCB1 expression in RA and HC peripheral $CD4^+$ Th cell subsets to interrogate this. Additionally, the use of other metabolic assays, such as Seahorse XF and stable isotope tracing as suggested above, would validate the finding that circulating Th17.1 cells in RA exhibit increased mitochondrial metabolism. Th17.1 cells are considered highly inflammatory due to their increased expression of cytokines compared to Th1 and Th17 cells (Basdeo *et al.*, 2017). Indeed, data here show that Th17.1 cells express the highest amount of TNF-α and IFN-γ of the $CD4^+$ Th cell subsets, and similar amounts of IL-17A to Th17 cells. Furthermore, it has been shown that Th17.1 cells accumulate in the SF of RA patients, driving pathogenesis (Basdeo *et al.*, 2017). The effects of TNF-α on Th17.1 cells are not well described. One study demonstrated their loss in a TNFR2 deficient mouse model, along with the loss of Th1 and Th17 cells (Alam *et al.*, 2021). In addition, a recent study highlighted their increased circulating levels in RA to correlate with a good response to anti-TNFα therapy (Millier *et al.*, 2022). A similar observation was made previously on Th17

cells and was suggested to be due to decreased CCR6 expression and impaired recruitment to the rheumatoid joint (Aerts *et al.*, 2010), this mechanism perhaps also relevant to Th17.1 cells. With T cell metabolism so tightly linked to function, it is possible that the increased metabolism of Th17.1 cells in RA drives increased cytokine production. In the current study, under anti-CD3/28 stimulation, RA Th17.1 cells produced comparable levels of TNF-α, IL-17A, and IFN-γ to HC cells. Yet, under PMA/ionomycin stimulation a trend towards increased IL-17A was detected in bulk $CD4^+$ T cells. $CD4^+$ Th cell subsets could not be assessed under PMA/ionomycin stimulation as this method of activation resulted in a loss of chemokine receptor expression making population gating not possible. Further studies would utilise cell sorting (FACS) to first isolate the $CD4^+$ Th cells *ex vivo*, then assess their cytokine production. In addition, the effect of TNF-α on Th17.1 cell metabolism and function could then be assessed.

6.3.3 TNF-α/PI3K/Akt metabolic axis in RA $CD4^+$ T cells

Here, it was seen that RA $CD4^+$ T cells, both naïve and memory cell subsets, had increased levels of Akt phosphorylation than HC counterparts. This observation has not been reported previously but does agree with a previous study reporting dysregulated AMPK and mTOR signalling in RA naïve $CD4^+$ T cells (Z. Wen *et al.*, 2019). This study showed a defect in NMT1 to impair AMPK signalling and result in a persistent activation of mTOR. As has been described in other studies (Delgoffe *et al.*, 2009; Michalek *et al.*, 2011; Chornoguz *et al.*, 2017), it is shown that this aberrant mTOR activity then drives a Th1 and Th17 cell phenotype. The increased p-Akt levels shown here may also contribute to the increased mTOR activity described in RA naïve $CD4^+$ T cells and should be tested in future studies. Indeed, this would

be consistent with the *in vitro* data in Chapter 4, showing TNF-α-driven Akt pathway activity upon naïve $CD4^+$ T cell activation to promote mTOR signalling. Also demonstrated in the current study, TNF-α-driven Akt drives increases in mitochondrial mass in activated naïve $CD4^+$ T cells. Consistent with Akt promoting mTOR activity and mTOR inducing PPARγ, which promotes mitochondrial biogenesis (Angela *et al.*, 2016). Here, RA $CD4^+$ T cells are shown to have increased mitochondrial mass compared to HC, likely linked to the increased Akt signalling activity also seen. However, further studies are required to directly confirm this effect. As shown here in Chapter 3, TNF-α signalling is also required to induce TF c-Myc which is essential for uptake of amino acids such as leucine which then promote mTOR activity (Wang *et al.*, 2011; Marchingo *et al.*, 2020). Controlling amino acid uptake may demonstrate an Akt-independent mechanism by which TNF-α drives mTOR and mitochondrial biogenesis. Although, the anti-TNFα-mediated suppression of amino acid uptake in naïve $CD4^+$ T cells seen here was largely Akt-dependent. Repeating those *in vitro* studies performed here using the Akti and anti-TNFα antibody on isolated RA naïve $CD4^+$ T cells should aid in fully elucidating the mechanisms of TNF-α-driven PI3K/Akt signalling and subsequent metabolic reprogramming in RA.

Previous studies have shown TNF-α to be increased in RA peripheral blood compared to HC (Tetta *et al.*, 1990; Cai *et al.*, 2020). Serum TNF-α concentrations could not be reliably measured in the present study. Future work should aim to perform this analysis to enable correlations between circulating TNF-α and metabolic/functional parameters of RA T cells to be assessed. A recent study used isolated naïve $CD4^+$ T cells activated for 72 h to show that naïve cells from RA patient peripheral blood produced more TNF-α than those from HC (Wu *et al.*, 2021). In the study, this was shown by intracellular flow cytometry and ELISA. In

contrast, intracellular staining of TNF-α here showed no difference between RA and HC in any of the $CD4^+$ T cell subsets analysed. This may be reflective of the heterogeneity of the patient cohort used in the current study, with improved stratification of patients in future work based on factors such as treatment and disease stage able to limit this variability. Assessment of sTNF-α release by $CD4^+$ T cells could not be performed by ELISA as bulk PBMCs were cultured and variability in proportion of $CD4^+$ and $CD8^+$ T cells would affect secreted TNF-α levels. Previous studies have rarely assessed levels of mTNF-α on T cells, so having established a protocol for surface TNF-α staining in Chapter 3, this was applied to activated RA and HC $CD4^+$ T cells. RA memory $CD4^+$ T cells expressed a higher percentage of mTNF-α than HC. These data are in contrast to a previously stated observation that mTNF-α levels are comparable between RA and HC peripheral $CD4^+$ T cells, however these data were not presented in the paper (Rossol *et al.*, 2013). Another study has previously shown that mTNF-α levels are increased on monocytes in RA (Nguyen and Ehrenstein, 2016). In the data presented here, it was also seen that the percentage of mTNF-α^+ $CD4^+$ T cells positively correlated with the percentage of TNF-α^+ $CD4^+$ T cells, as assessed by intracellular staining, in RA but not HC, suggesting that TNF-α may accumulate on the surface of $CD4^+$ T cells in RA. Mechanistically, a study by Wu *et al*. has previously linked increased mitochondrial aspartate production to ER expansion and increased production of TNF-α in RA naïve $CD4^+$ T cells but did not specifically measure mTNF-α levels (Wu *et al.*, 2021). Analysis of TACE levels in RA and HC peripheral blood may provide insight into the regulation of the balance between mTNF-α and sTNF-α. Further work is also required to understand the role of mTNF-α compared to sTNF-α and whether increased levels of mTNF-α on RA $CD4^+$ T cells may contribute to their pathogenic function.

6.3.4 Analysing CD4$^+$ T cell function in RA

A trend towards increased IL-17A expression was seen with PMA/ionomycin stimulation of bulk CD4$^+$ T cells in RA compared to HC. These data are consistent with TNF-α promoting Th17 cell differentiation and increased IL-17 in RA peripheral blood (Penatti *et al.*, 2017; Alam *et al.*, 2021; Pesce *et al.*, 2022). In addition, these data are in accordance with increased Akt/mTOR signalling driving a Th17 cell phenotype (Delgoffe *et al.*, 2009). However, no difference in the proportion of Th17 cells in peripheral blood was observed and RORγt expression was comparable in bulk CD4$^+$ T cells and within Th17 and Th17.1 cell populations. Data here show no effect of anti-TNFα on IL-17 expression in Th17 cells but this is not consistent with other work which suggests TNF-α to promote IL-17 production (Sugita *et al.*, 2012; Ho *et al.*, 2021; Pesce *et al.*, 2022). Further studies are required to understand if the increase in IL-17A in RA CD4$^+$ T cells is linked to TNF-α-mediated effects on metabolism or signalling.

Percentage of Tregs was comparable in RA and HC PBMCs but within the Treg population a lower percentage of cells were IL-10$^+$ in RA patients compared to HC. These data are consistent with previous studies identifying a defect in Treg function in RA (Valencia *et al.*, 2006; Flores-Borja *et al.*, 2008; Nie *et al.*, 2013; Sun *et al.*, 2017). Several of these studies have previously linked TNF-α signalling in RA to the suppression of Treg function, with anti-TNFα treatment able to rescue this effect (Valencia *et al.*, 2006; Nie *et al.*, 2013). In addition, both in the current study and in others, anti-TNFα has been shown to promote IL-10 expression in CD4$^+$ T cells (Evans *et al.*, 2014; Roberts *et al.*, 2017; Povoleri *et al.*, 2020). These data highlight TNF-α as a likely cause of reduced Treg IL-10 production in RA, however further studies are required to directly link this and to understand the mechanism of anti-TNFα-driven IL-10 production. Few other differences in cytokine production and TF expression could be seen

between RA and HC $CD4^+$ T cells, however as mentioned previously, further work is required to fully elucidate this.

6.3.5 Limitations of this work

Data in this chapter are limited by the availability of patient samples. To enable recruitment of enough patients in the time frame, participants were included from any disease stage and type of therapy. Further studies could improve this by applying more stringent selection criteria, particularly regarding the use of anti-TNFα therapies and other treatments which may confound results, including other targeted T cell therapies such as baricitinib. In addition, methotrexate is a first-line treatment for RA and is often used in combination with other therapies. Ensuring the effects of methotrexate on T cell function are controlled for will be important in fully elucidating the role of anti-TNFα. The comparison between those patients on anti-TNFα therapy, and those not, would provide insight into the *in vivo* effects of blocking TNF-α signalling on T cell metabolism in RA. This may also be improved by grouping patients based on their response to anti-TNFα therapy, aiming to understand the mechanisms of anti-TNFα in improving RA. Furthermore, this is a cross-sectional study of patients at one time-point, future work may follow patients before, during, and after anti-TNFα therapy to understand the effects of blocking TNF-α on T cell metabolism and function in RA over time.

PBMCs were isolated on the day of sample collection then stored frozen until use. Cell viability upon thawing and resting overnight was often >90% with good retrieval of cell number. However, the effects of freeze-thawing on cellular metabolism and function cannot be discounted. It is possible that cellular metabolism in particular may be affected by this process due to its sensitivity to environmental stimuli. Previous work in the lab has optimised the

freeze-thawing protocol and shown that the differences in fluorescent mitochondrial probe measurements are comparable between freshly isolated cells and those freeze-thawed then rested at 37°C for a minimum of 6 h.

Throughout this work, multiple flow cytometry markers were analysed by MFI. Variability in human data and fluorescence of mitochondrial dyes or conjugated antibodies on different days meant that the data required normalisation to the experiment mean to be presented. This did limit the data as the true spread of raw values could not be seen, however the effects of treatment on matched pairs could be clearly demonstrated. Analysis of patient samples was particularly affected by this, as only one RA patient sample and age- and sex-matched control could be analysed at a time and had to be normalised to each other. This made it impossible to compare the raw data of samples which had not been run on the same day and restricted the ability to perform any correlations between fluorescent mitochondrial probes or p-Akt and other flow-based readouts. To account for this, all samples would need to be run in parallel, which was not feasible.

The use of a gating strategy based on chemokine receptor expression was able to identify $CD4^+$ T cell subsets under resting and anti-CD3/28 activated conditions. However, PMA/ionomycin stimulation resulted in significant downregulation of chemokine receptors and the loss of distinct populations. This meant that measurements of cytokine expression under PMA/ionomycin stimulation were restricted to bulk $CD4^+$ T cells. Further work would aim to use FACS to separate out the different $CD4^+$ T cell subsets from RA and HC PBMCs and enable the use of PMA/ionomycin stimulation to assess cytokine production. The use of FACS or MACS to purify $CD4^+$ T cell subsets would also enable further cell culture, where *in vitro* treatment of RA $CD4^+$ T cells with an anti-TNFα or isotype control antibody would aid in linking

the effects seen *ex vivo* to increased TNF-α signalling in RA. In addition, the gating strategy utilised for naïve and memory cell used only CD45RA, resulting in the inclusion of the $CD4^+$ T_{EMRA} population in the naïve cell gate and analysis. Although recorded often to be a small percentage of $CD4^+$ T cells, T_{EMRA} cells are driven by chronic antigen stimulation, a process known to be present in environments of chronic inflammatory disease, including RA (Weyand *et al.*, 2014; Burel *et al.*, 2017; Tian *et al.*, 2017). As terminally differentiated memory cells, T_{EMRA} cells are also likely to have different metabolic requirements compared to naïve cells, as well as potentially different responses to TNF-α. It is also known that percentages of $CD4^+$ T_{EMRA} cells can vary substantially between individuals (Burel *et al.*, 2017; Tian *et al.*, 2017). It is possible that their inclusion in the naïve cell gate is confounding the results of MVG staining. Future work would include CCR7 alongside CD45RA in the flow cytometry panel in order to gate on T_{EMRA} ($CD45RA^+CCR7^-$), naïve ($CD45RA^+CCR7^+$), T_{CM} ($CD45RA^-CCR7^+$), and T_{EM} ($CD45RA^-CCR7^-$) (Tian *et al.*, 2017).

Finally, due to peripheral blood sample availability, PBMCs were used in these experiments. This is an approach used by other studies, assessing changes in circulating immune cells, cytokines, and chemokines to provide insight into the systemic inflammatory environment of RA and changes that may occur prior to recruitment to the synovium. However, immune cells present in the SF are of particular interest as this is main site of RA pathogenesis. Additionally, the rheumatoid synovium provides a unique hypoxic and nutrient-deprived environment with substantial levels of cytokines, chemokines, and inflammatory mediators present, all factors able to further alter $CD4^+$ T cell metabolism and function. Future work should collect matched samples of peripheral blood and RA SF to analyse $CD4^+$ T cells both in circulation and at the site of disease.

6.3.6 Conclusion

Firstly, the development of several flow cytometry panels was shown in this chapter enabling the identification of Th1, Th2, Th17, and Th17.1 cells, naïve and memory cells, and Tregs which could then be assessed for expression of surface markers, intracellular cytokines and TFs, and uptake of fluorescent mitochondrial probes. Analysis of PBMCs from RA patients and HC by flow cytometry showed that peripheral $CD4^+$ T cells in RA have heightened levels of mTNF-α, phosphorylation of Akt, and mitochondrial mass compared to HC. These observations consistent with data from the previous chapters identifying a TNF-α-driven PI3K/Akt metabolic axis required for naïve $CD4^+$ T cell activation. RA $CD4^+$ T cells trended towards higher expression of IL-17A and lower expression of IL-10 in the Treg subset compared to HC, although few other differences in $CD4^+$ Th cell subsets were seen. Future studies are required to directly link increased TNF-α in RA to the metabolic dysfunction of $CD4^+$ T cells. Additionally, improved stratification of the patient cohort based on treatment type and disease stage would provide insight into the impact of anti-TNFα therapy on $CD4^+$ T cell metabolism in RA.

CHAPTER 7: GENERAL DISCUSSION

TNF-α is an inflammatory cytokine known to act as a co-stimulatory molecule on $CD4^+$ T cells, promoting cytokine expression and proliferation upon TCR activation. Yet, the role of TNF-α in metabolic reprogramming, which is essential for T cell activation, has not been described. Elucidating the role of TNF-α in driving $CD4^+$ T cell metabolism and function may be crucial in understanding the pathogenesis of RA, where TNF-α is abundant and dysregulated metabolism of $CD4^+$ T cells has been reported. Therefore, this study aimed to use *in vitro* culture of purified human $CD4^+$ T cell subsets treated with an anti-TNFα antibody, isotype control, or increased amounts of TNF-α to assess the effects of TNF-α on $CD4^+$ T cell metabolic reprogramming and the downstream effects on $CD4^+$ T cell fate and function. The aim was to then understand the role of TNF-α in driving these effects in the context of RA. Data presented here have shown, for the first time, that T cell-derived TNF-α is required for the metabolic reprogramming of naïve $CD4^+$ T cells, able to signal through PI3K/Akt/mTOR to promote OXPHOS, glycolysis, and amino acid uptake. TNF-α was also shown to be required for Th1 and Th17 cell differentiation *in vitro*, the suppressive effects on cytokines seen to be partially Akt-dependent. Analysis of $CD4^+$ T cells from RA patients and HC by flow cytometry showed increased levels of mTNF-α, Akt phosphorylation, mitochondrial mass, and a trend towards increased IL-17A expression in RA, highlighting a potential role for this TNF-α/PI3K/Akt metabolic axis in disease pathogenesis (Figure 7.1). Collectively, these data provide further insight into the role of TNF-α in health and chronic inflammatory disease, supporting the development of novel therapeutic targets.

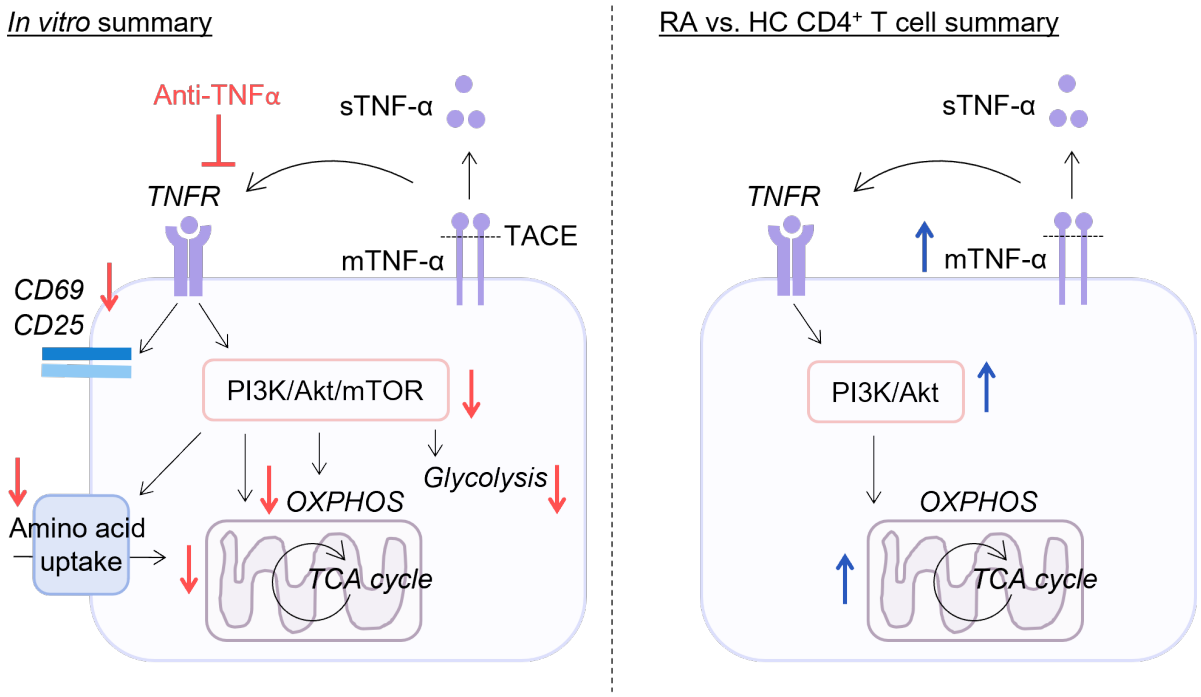

Figure 7.1 Comparison of *in vitro* and RA CD4⁺ T cell findings

Schematic diagram summarising the main findings in this study. TNF-α exists first as a membrane-bound protein (mTNF-α) and is then cleaved by TNF-α converting enzyme (TACE) to its soluble form (sTNF-α). Both these forms are able to bind to TNF receptors (TNFR) on the surface of the cell. With the *in vitro* experiments in Chapters 3 and 4 it was shown that blocking TNF-α with an anti-TNFα antibody suppressed TNF-α signalling through PI3K/Akt/mTOR to suppress the upregulation of oxidative phosphorylation (OXPHOS), glycolysis, amino acid uptake, and mitochondrial biogenesis. Additionally, CD69 and CD25 were decreased by anti-TNFα in an Akt-independent manner. These effects are represented by red arrows. Compared to HC CD4⁺ T cells, RA CD4⁺ T cells exhibited increased mTNF-α, Akt phosphorylation, and mitochondrial mass providing evidence to the role of the TNF-α-driven PI3K/Akt metabolic axis in RA CD4⁺ T cells. These effects are represented by the blue arrows.

7.1 THE ROLE OF TNF-A IN NAÏVE CD4$^+$ T CELL METABOLIC REPROGRAMMING

The work in Chapter 3 identified a novel role for T cell-derived TNF-α in driving metabolic reprogramming of naïve CD4$^+$ T cells upon activation with anti-CD3/28. Blocking TNF-α was first seen to suppress upregulation of activation markers CD69 and CD25, an observation in line with other studies (Aspalter *et al.*, 2003; Povoleri *et al.*, 2020). Having confirmed this effect of anti-TNFα on both naïve and memory cells, it was next sought to assess the metabolic profile of these cells. Fluorescent mitochondrial probes showed activated, anti-TNFα-treated naïve CD4$^+$ T cells to have reduced mitochondrial mass and Seahorse XF analysis showed a decrease in both OXPHOS and glycolysis compared to isotype control-treated cells. In comparison, no effect of blocking TNF-α was seen on memory cells. Reasons for this difference in TNF-α signalling requirements were not elucidated but likely lie in the epigenetic, transcriptional, and metabolic changes induced during naïve cell priming which result in memory cells being able to engage the transcriptional and metabolic programmes required for activation with only anti-CD3/28 signalling.

In the current study, the role of T cell-derived TNF-α was only investigated during the initial activation of naïve CD4$^+$ T cells. It was seen that memory cells do not require this signal, yet it remains unclear whether anti-TNFα-treated naïve CD4$^+$ T cells will be impacted upon restimulation. It is possible that the transcriptional and metabolic suppression induced by blocking the intrinsic TNF-α signal will result in lasting alterations to the cell's ability to respond to TCR/CD28 stimulation. Indeed, it was demonstrated in one study that anti-TNFα treated CD4$^+$ T cells were hyporesponsive upon restimulation, proliferating less and producing reduced amounts of IFN-γ, but also showed that blocking TNF-α did not make the cells anergic or suppressive (Povoleri *et al.*, 2020). However, it was seen in the data presented in the

current study that blocking TNF-α had little effect on the levels of H3K27Ac, suggesting little change to the epigenetics of the cell. Future work should investigate the effects of restimulation on naïve $CD4^+$ T cell metabolism and function after anti-TNFα-treatment, both in the presence and absence of T cell-derived TNF-α to understand the lasting effects of blocking TNF-α during naïve cell activation and whether TNF-α is also required during restimulation.

Investigating this metabolic suppression further, stable isotope tracing experiments showed little change in glucose metabolism through the TCA cycle but an overall reduction in the abundance of TCA cycle intermediates. This prompted the analysis of $^{13}C_5$-glutamine which was reduced in both conversion to glutamate and incorporation into the TCA cycle with the addition of an anti-TNFα antibody. A similar approach has been recently reported by one group, showing that TNFR2 ligation in combination with anti-CD3 stimulation of human naïve $CD4^+$ T cells had no effect on glucose metabolism through the TCA cycle but was able to drive glutamine metabolism (de Kivit *et al.*, 2020; Mensink *et al.*, 2022). In Chapter 4 it was also demonstrated that this suppression by anti-TNFα was present at a transcriptional level, particularly related to genes involved in OXPHOS which failed to upregulate upon activation. The major TF controlling these genes was not identified but c-Myc is a reasonable candidate. C-Myc is known to induce a wide range of metabolic genes upon $CD4^+$ T cell activation including *Ldha* and amino acid transporter *Slc7a5* (Wang *et al.*, 2011; Marchingo *et al.*, 2020), and was shown to be downregulated at both transcript and protein level by anti-TNFα.

It was next tested whether increasing the concentration of TNF-α in the local environment was able to induce the opposite effects to those seen when blocking T cell derived TNF-α. As TNF-α exists in two biologically active forms, it was first tested whether additional sTNF-α

would increase naïve CD4$^+$ T cell metabolism upon activation. The concentration of 50 ng/ml rhTNF-α was used based on previous studies (Valencia *et al.*, 2006; Alam *et al.*, 2021). It is difficult to determine whether this is a physiological representation of local TNF-α concentrations as levels in serum are variable but usually recorded in the range of 1-20 pg/ml in RA (Takeuchi *et al.*, 2011; Schulz *et al.*, 2014; Thilagar *et al.*, 2018). However, the concentration of TNF-α released proximal to the immunological synapse can likely reach a much greater concentration. The addition of sTNF-α had only minor effects on glycolysis and CD25 expression, so a selective increase in mTNF-α was then tested. It is known that mTNF-α has a higher affinity for TNFR2 than sTNF-α and that TNFR2 is the predominant TNFR on CD4$^+$ T cells (Grell *et al.*, 1995; Rossol *et al.*, 2007; Pesce *et al.*, 2022; Su *et al.*, 2022). It is previously reported that the PI3K/Akt/mTOR pathway is downstream of TNFR2 (Aspalter *et al.*, 2003; Kim and Teh, 2004). Several studies also use direct TNFR2 ligation or knockout to investigate the effects of TNF-α signalling on T cells (Chen *et al.*, 2016; de Kivit *et al.*, 2020; Alam *et al.*, 2021; Mensink *et al.*, 2022). Therefore, it was hypothesised that TNFR2 was the receptor mediating the metabolic effects of TNF-α seen in the current study and that levels of mTNF-α would be more important than those of sTNF-α. The increase in mTNF-α driven by TACE inhibitor TAPI-0 was accompanied by a significant loss of T cell-derived sTNF-α and resulted in a reduction in cell metabolism, cell size, and CD25 expression. Reasons for this are unclear and further experiments are required to elucidate the relative requirements of mTNF-α and sTNF-α during naïve CD4$^+$ T cell activation. Previous studies have identified a mechanism of "reverse signalling" by mTNF-α whereby upon its ligation it can instead act as a receptor and activate downstream signalling in the cell (Mitoma *et al.*, 2005; Xin *et al.*, 2006; Rossol *et al.*, 2007; Pallai *et al.*, 2016). This effect has been mainly observed in macrophages and

monocytes, although some evidence exists for its role in T cells, with one study using Jurkats to show mTNF-α reverse signalling to be responsible for IL-10 production (Mitoma *et al.*, 2005). Reverse signalling in macrophages and monocytes has been observed in response to mTNF-α:anti-TNFα interactions, shown to induce TGF-β production and suppress the pro-inflammatory response of the cells (Pallai *et al.*, 2016). It was also shown in one study that overexpression of TNFR2 on $CD4^+$ T cells resulted in increased expression of TNF-α in monocytes (Rossol *et al.*, 2007). Furthermore, the binding of anti-TNFα to monocytes from RA patients was shown to increase mTNF-α levels on the surface and resulted in paradoxical increases in TNF:TNFR2 interactions with Tregs. Although reverse signalling was not identified in this study, it is likely that this is the acting mechanism (Nguyen and Ehrenstein, 2016). The relevance of mTNF-α reverse signalling in naïve $CD4^+$ T cell responses to anti-TNFα was beyond the scope of the work discussed here but should be investigated in future studies.

Following on from the identification of the role of TNF-α in naïve $CD4^+$ T cell activation and metabolic reprogramming, work in Chapter 4 identified a pathway of TNF-α signalling through PI3K/Akt/mTOR. Activation of this pathway was required to drive anti-TNFα-mediated effects on naïve $CD4^+$ T cell metabolism, with suppression of mitochondrial mass, amino acid uptake, and glucose uptake all blunted by the addition of an Akti. In comparison, CD69 and CD25, and c-Myc expression were still suppressed by anti-TNFα in the presence of the Akti, suggesting the involvement of Akt-independent mechanisms. Although no change in NFκB activity with blockade of T cell-derived TNF-α was detected here, contributions of this pathway and others, such as MAPK, to the observed effects of TNF-α on naïve $CD4^+$ T cells requires confirmation in further studies. Collectively, these chapters identified a novel T cell-derived TNF-α/PI3K/Akt axis required for naïve $CD4^+$ T cell metabolic reprogramming upon activation.

7.2 EFFECTS OF TNF-A ON CD4$^+$ T CELL DIFFERENTIATION

Having established a metabolic role for TNF-α in naïve CD4$^+$ T cells, the next aim was to understand the functional impact of T cell-intrinsic TNF-α blockade. To do this, naïve CD4$^+$ T cells were differentiated *in vitro* into Th1 and Th17 cells. In agreement with a previous study, it was established that anti-CD3 only activation is preferred for human Th17 cell differentiation as CD28 ligation is inhibitory of a Th17 cell transcriptional programme and IL-17 production (Revu *et al.*, 2018). Data in this chapter showed that under anti-CD3 only stimulation anti-TNFα was inhibitory of Th1 and Th17 cell differentiation, with the exception of IL-17 production which remained unchanged. For Th1 cells, the addition of CD28 co-stimulation rescued this inhibitory effect, reflecting some level of redundancy between CD28 and TNF-α signalling. An observation that is consistent with previous studies (Aspalter *et al.*, 2003; Kim and Teh, 2004). Although optimal *in vitro*, these conditions of Th1 and Th17 cell polarisation fail to be particularly physiologically relevant. It is likely *in vivo* that varying levels of co-stimulation by APCs and concentrations of a range of cytokines in the local microenvironment would differentially impact naïve CD4$^+$ T cell polarisation. Indeed, studies using mouse models to assess the role of TNF-α in driving Th1 and Th17 cell responses have shown TNF-α to promote Th1 and Th17 cell differentiation (Chen *et al.*, 2016; Alam *et al.*, 2021). Yet, its role in driving pathogenic Th1 and Th17 cell differentiation in human chronic inflammatory disease remains unclear. These experiments were additionally limited by the low percentages of IL-10$^+$ and IL-17A$^+$ CD4$^+$ T cells detectable by intracellular flow cytometry. To improve the sensitivity of cytokine measurements, concentrations in the cell culture supernatants following 6 days of differentiation were also assessed by multiplex cytokine assay. These data showed similar trends to the flow cytometric data but confirmed that low

amounts of IL-10 and IL-17A were produced by Th1 and Th17 cells *in vitro*, often <200 pg/ml and <400 pg/ml respectively, compared to >10,000 pg/ml of IFN-γ. Nevertheless, it was shown that blockade of T cell-derived TNF-α during Th1 and Th17 cell differentiation induced the expression of IL-10, a result consistent with previous studies (Evans *et al.*, 2014; Roberts *et al.*, 2017; Povoleri *et al.*, 2020). Under anti-CD3 only conditions, it was tested whether the effects of anti-TNFα on differentiation were also Akt-dependent. Suppressive effects on IFN-γ in Th1 cells and IL-22 in Th17 cells were partially blunted, as was the induction of IL-10 in Th1 cells. However, anti-TNFα retained the ability to reduce TF expression the Akti condition, suggesting an Akt-independent mechanism. It was also shown that anti-TNFα-treated Th1 and Th17 cells had reduced lactate production compared to isotype control-treated cells, indicative of reduced glycolysis. It remains unclear whether the reduced metabolic capacity of these cells contributes to the functional effects seen and further experiments are required to investigate this.

Throughout the experiments described here, cells were treated in monocultures, this was required to remove additional variables and focus on the role of T cell-derived TNF-α. However, *in vivo* interactions with other cell types and production of TNF-α from multiple sources, including DCs, FLS, and macrophages, must be considered. For naïve $CD4^+$ T cells this is especially relevant of their contact with APCs which provide TCR ligation, co-stimulation, and cytokines. Indeed, it has been previously reported that monocytes in RA express more mTNF-α than HC and that this is increased in the presence of anti-TNFα treatment (Nguyen and Ehrenstein, 2016). Future work should utilise monocyte/$CD4^+$ T cell co-cultures to analyse the effects of external sources of TNF-α and a more physiologically relevant TCR/CD28 signal, an approach that has been used by previous studies (Nguyen and Ehrenstein, 2016; Roberts

et al., 2017). In addition, elucidating the effects of TNF-α on APCs such as macrophages was beyond the scope of the current study, but should be considered in the context of chronic inflammatory disease. Co-culture experiments would address this and aid in investigating the indirect effects of TNF-α on $CD4^+$ T cell metabolism and function through effects on APCs. These co-culture experiments could also be important for further understanding of the functional effects of blocking TNF-α on naïve $CD4^+$ T cells. One previous study has shown that anti-TNFα treated $CD4^+$ T cells had an impaired ability to induce IL-6 and IL-8 production from FLS (Povoleri *et al.*, 2020). These experiments should provide further insight into whether metabolic alterations driven by TNF-α affect the pathogenic functions of $CD4^+$ T cells in RA.

7.3 TNF-A/PI3K/AKT METABOLIC AXIS IN RHEUMATOID ARTHRITIS

Leading on from the work in the previous chapters, Chapter 6 focused on investigating the TNF-α/PI3K/Akt metabolic axis in the context of RA. Using flow cytometric analysis of isolated PBMCs from RA and HC peripheral blood, it was shown that $CD4^+$ T cell subset proportions were comparable in RA and HC. Resting RA $CD4^+$ T cells were shown to have a higher mitochondrial mass than HC and both naïve and memory $CD4^+$ T cells in RA had a higher level of p-Akt upon activation. Although no difference in TNF-α expression was seen by intracellular staining, it was shown that memory $CD4^+$ T cells in RA had a higher percentage of mTNF-α^+ cells than HC. Additionally, there was a trend towards increased $CD4^+$IL-17^+ T cells in RA and a reduction in IL-10 production by Tregs. Collectively, these data provide evidence to suggest that increased levels of mTNF-α may drive PI3K/Akt signalling in RA $CD4^+$ T cells which then promotes mitochondrial biogenesis and inflammatory function. However, these data are not

directly linked, and further studies are needed to understand whether this axis is relevant to RA pathogenesis.

The *in vitro* findings described here have been generated looking at the activation of naïve $CD4^+$ T cells. However, pathogenesis of RA is instead mediated by T_{eff} cells which have already undergone initial naïve $CD4^+$ T cell priming and have migrated to the rheumatoid synovium where they are potentially reactivated by APCs. It is previously described that naïve $CD4^+$ T cells in RA have multiple impairments in metabolism which result in an invasive phenotype, increased TNF-α production, and bias towards Th1 and Th17 cell differentiation (Z. Wen *et al.*, 2019; Wu *et al.*, 2020, 2021). Additional defects in DNA repair have been shown to bias generation of Th1 and Th17 cells and cause premature cellular ageing (Shao *et al.*, 2009; Li *et al.*, 2016; Yang *et al.*, 2016). It is thus reasonably hypothesised that changes to naïve $CD4^+$ T cell activation and metabolic reprogramming will have downstream effects on pathogenic, effector $CD4^+$ T cell function in RA. Further investigation into the effects of TNF-α on Th1 and Th17 cell metabolism and function in RA was beyond the scope of the current study but should be explored in future work.

7.4 FUTURE DIRECTIONS

This study has identified that T cell-derived TNF-α is essential for the metabolic reprogramming of naïve $CD4^+$ T cells upon activation. However, it remains unclear whether these effects are dependent on TNFR1 or TNFR2. Future work should aim to elucidate the contributions of TNFR1 and TNFR2 using blocking antibodies specific to each. In addition, it is not known whether mTNF-α or sTNF-α is more important in mediating these effects, experiments aiming to specifically increase or block mTNF-α will aid in understanding the role

of mTNF-α in modulation of $CD4^+$ T cell metabolism and function. This may be particularly pertinent in RA where it has been seen that both $CD4^+$ T cells and monocytes express increased levels of mTNF-α compared to HC (Nguyen and Ehrenstein, 2016).

The work described here has shown that blocking TNF-α suppresses Th1 and Th17 cell differentiation under anti-CD3 stimulation *in vitro*. However, the mechanisms driving this are unclear. It will be important in future work to link the metabolic suppression mediated through T cell-intrinsic TNF-α blockade with the functional effects seen. This may be tested by re-expression of downregulated metabolic modulators such as c-Myc, which is likely mediating the anti-TNFα-driven metabolic suppression but requires further experiments to be confirmed. Furthermore, it is important to establish the metabolic and functional effects of anti-TNFα on $CD4^+$ T cells in RA. Data presented here provides evidence to suggest a role for the TNF-α/PI3K/Akt metabolic axis in RA $CD4^+$ T cell pathogenic function but further interrogation of this is required. This may be achieved through *in vitro* culture of RA $CD4^+$ T cells in the presence of an anti-TNFα antibody or isotype control with metabolic and functional analysis as performed here in Chapters 3 and 4. In addition, the recruitment of RA patients on anti-TNFα therapy to the study, with RA patients not on anti-TNFα therapy as controls, would allow for the investigation of the *in vivo* effects of anti-TNFα on $CD4^+$ T cell metabolism and function. This would be further improved by the analysis of $CD4^+$ T cells from matched SF, providing insight into how the effects of TNF-α blockade on naïve $CD4^+$ T cell metabolism confer effects on pathogenic function in RA. Understanding this process will aid in the development of novel therapeutic targets for chronic inflammatory disease.

7.5 CONCLUSION

Overall, the data in this study have contributed a novel role for T cell-intrinsic TNF-α in mediating the activation and metabolic reprogramming of naïve $CD4^+$ T cells. It was shown that TNF-α induces activity of the PI3K/Akt/mTOR pathway to mediate these effects on metabolism. These findings aid in understanding the signals required for naïve $CD4^+$ T cell metabolic reprogramming, which is crucial in determining cell fate and function. This may be particularly relevant to inflammatory environments where TNF-α is abundant. It is also shown that blockade of T cell-intrinsic TNF-α during Th1 and Th17 cell differentiation results in reduced expression of IFN-γ and T-bet in Th1 cells and reduced IL-22 and RORγt in Th17 cells. Additionally, both Th1 and Th17 cells exhibited increased IL-10 expression with blockade of TNF-α. The suppressive effects on cytokines and increase in IL-10 in Th1 cells were seen to be partially Akt-dependent, but effects on TFs were mediated through an Akt-independent mechanism. Anti-TNFα treatment of these *in vitro* differentiated cells also conferred a suppression in glycolysis. The relevance of this TNF-α/PI3K/Akt-driven metabolism was then assessed in RA. It was seen that RA $CD4^+$ T cells had higher expression of mTNF-α, p-Akt, and mitochondrial mass, providing evidence to suggest a role for TNF-α in driving PI3K/Akt and metabolic dysregulation in RA $CD4^+$ T cells. This study supports the investigations into the mechanisms of TNF-α-mediated pathogenesis in RA and aids in the work towards development of novel therapeutic targets.

LIST OF REFERENCES

Abboud, G., Choi, S.-C., Kanda, N., Zeumer-Spataro, L., Roopenian, D.C. and Morel, L. (2018) 'Inhibition of Glycolysis Reduces Disease Severity in an Autoimmune Model of Rheumatoid Arthritis', *Frontiers in Immunology*, 9, p. 1973. Available at: https://doi.org/10.3389/fimmu.2018.01973.

Abdallah, M.S., Alarfaj, S.J., Saif, D.S., El-Naggar, M.E., Elsokary, M.A., Elsawah, H.K., Abdelsattar Zaki, S., Wahsh, E.A., Abo Mansour, H.E. and Mosalam, E.M. (2021) 'The AMPK modulator metformin as adjunct to methotrexate in patients with rheumatoid arthritis: A proof-of-concept, randomized, double-blind, placebo-controlled trial', *International Immunopharmacology*, 95, p. 107575. Available at: https://doi.org/10.1016/j.intimp.2021.107575.

Abimannan, T., Peroumal, D., Parida, J.R., Barik, P.K., Padhan, P. and Devadas, S. (2016) 'Oxidative stress modulates the cytokine response of differentiated Th17 and Th1 cells', *Free Radical Biology and Medicine*, 99, pp. 352–363. Available at: https://doi.org/10.1016/j.freeradbiomed.2016.08.026.

Adamopoulos, I.E., Chao, C., Geissler, R., Laface, D., Blumenschein, W., Iwakura, Y., McClanahan, T. and Bowman, E.P. (2010) 'Interleukin-17A upregulates receptor activator of NF-κB on osteoclast precursors', *Arthritis Research & Therapy*, 12(1), p. R29. Available at: https://doi.org/10.1186/ar2936.

Aerts, N.E., De Knop, K.J., Leysen, J., Ebo, D.G., Bridts, C.H., Weyler, J.J., Stevens, W.J. and De Clerck, L.S. (2010) 'Increased IL-17 production by peripheral T helper cells after tumour necrosis factor blockade in rheumatoid arthritis is accompanied by inhibition of migration-associated chemokine receptor expression', *Rheumatology*, 49(12), pp. 2264–2272. Available at: https://doi.org/10.1093/rheumatology/keq224.

Aggarwal, R., Liao, K., Nair, R., Ringold, S. and Costenbader, K.H. (2009) 'Anti-Citrullinated Peptide Antibody (ACPA) Assays and their Role in the Diagnosis of Rheumatoid Arthritis', *Arthritis and rheumatism*, 61(11), pp. 1472–1483. Available at: https://doi.org/10.1002/art.24827.

Alam, M.S., Otsuka, S., Wong, N., Abbasi, A., Gaida, M.M., Fan, Y., Meerzaman, D. and Ashwell, J.D. (2021) 'TNF plays a crucial role in inflammation by signaling via T cell TNFR2', *Proceedings of the National Academy of Sciences of the United States of America*, 118(50), p. e2109972118. Available at: https://doi.org/10.1073/pnas.2109972118.

Al-Azab, M., Qaed, E., Ouyang, X., Elkhider, A., Walana, W., Li, H., Li, W., Tang, Y., Adlat, S., Wei, J., Wang, B. and Li, X. (2020) 'TL1A/TNFR2-mediated mitochondrial dysfunction of fibroblast-like synoviocytes increases inflammatory response in patients with rheumatoid arthritis via reactive oxygen species generation', *The FEBS Journal*, 287(14), pp. 3088–3104. Available at: https://doi.org/10.1111/febs.15181.

Aldridge, J., Ekwall, A.-K.H., Mark, L., Bergström, B., Andersson, K., Gjertsson, I., Lundell, A.-C. and Rudin, A. (2020) 'T helper cells in synovial fluid of patients with rheumatoid arthritis primarily have a Th1 and a CXCR3+Th2 phenotype', *Arthritis Research & Therapy*, 22(1), p. 245. Available at: https://doi.org/10.1186/s13075-020-02349-y.

Alexopoulou, L., Kranidioti, K., Xanthoulea, S., Denis, M., Kotanidou, A., Douni, E., Blackshear, P.J., Kontoyiannis, D.L. and Kollias, G. (2006) 'Transmembrane TNF protects mutant mice against intracellular bacterial infections, chronic inflammation and autoimmunity', *European Journal of Immunology*, 36(10), pp. 2768–2780. Available at: https://doi.org/10.1002/eji.200635921.

Alizadeh, D., Wong, R.A., Yang, X., Wang, D., Pecoraro, J.R., Kuo, C.-F., Aguilar, B., Qi, Y., Ann, D.K., Starr, R., Urak, R., Wang, X., Forman, S.J. and Brown, C.E. (2019) 'IL15 Enhances CAR-T Cell Antitumor Activity by Reducing mTORC1 Activity and Preserving Their Stem Cell Memory Phenotype', *Cancer Immunology Research*, 7(5), pp. 759–772. Available at: https://doi.org/10.1158/2326-6066.CIR-18-0466.

Allison, K.A., Sajti, E., Collier, J.G., Gosselin, D., Troutman, T.D., Stone, E.L., Hedrick, S.M. and Glass, C.K. (2016) 'Affinity and dose of TCR engagement yield proportional enhancer and gene activity in CD4+ T cells', *eLife*, 5, p. e10134. Available at: https://doi.org/10.7554/eLife.10134.

Almutairi, K., Nossent, J., Preen, D., Keen, H. and Inderjeeth, C. (2021) 'The global prevalence of rheumatoid arthritis: a meta-analysis based on a systematic review', *Rheumatology International*, 41(5), pp. 863–877. Available at: https://doi.org/10.1007/s00296-020-04731-0.

van Amelsfort, J.M.R., Jacobs, K.M.G., Bijlsma, J.W.J., Lafeber, F.P.J.G. and Taams, L.S. (2004) 'CD4+CD25+ regulatory T cells in rheumatoid arthritis: Differences in the presence, phenotype, and function between peripheral blood and synovial fluid', *Arthritis & Rheumatism*, 50(9), pp. 2775–2785. Available at: https://doi.org/10.1002/art.20499.

Anders, S., Pyl, P.T. and Huber, W. (2015) 'HTSeq—a Python framework to work with high-throughput sequencing data', *Bioinformatics*, 31(2), pp. 166–169. Available at: https://doi.org/10.1093/bioinformatics/btu638.

Andrews, S. (2010) 'Babraham Bioinformatics - FastQC A Quality Control tool for High Throughput Sequence Data'. (Version 0.11.6) [Computer programme]. Available at: https://www.bioinformatics.babraham.ac.uk/projects/fastqc/.

Angela, M., Endo, Y., Asou, H.K., Yamamoto, T., Tumes, D.J., Tokuyama, H., Yokote, K. and Nakayama, T. (2016) 'Fatty acid metabolic reprogramming via mTOR-mediated inductions of PPARγ directs early activation of T cells', *Nature Communications*, 7, p. 13683. Available at: https://doi.org/10.1038/ncomms13683.

Angelin, A., Gil-de-Gómez, L., Dahiya, S., Jiao, J., Guo, L., Levine, M.H., Wang, Z., Quinn, W., Kopinski, P.K., Wang, L., Akimova, T., Liu, Y., Bhatti, T.R., Han, R., Laskin, B.L., Baur, J.A., Blair, I.A., Wallace, D.C., Hancock, W.W. and Beier, U.H. (2017) 'Foxp3 reprograms T cell metabolism to function in low glucose high lactate environments', *Cell metabolism*, 25(6), pp. 1282-1293.e7. Available at: https://doi.org/10.1016/j.cmet.2016.12.018.

Ardestani, S., Li, B., Deskins, D.L., Wu, H., Massion, P.P. and Young, P.P. (2013) 'Membrane versus soluble isoforms of TNF α exert opposing effects on tumor growth and survival of tumor-associated myeloid cells', *Cancer research*, 73(13), pp. 3938–3950. Available at: https://doi.org/10.1158/0008-5472.CAN-13-0002.

Ashina, K., Tsubosaka, Y., Nakamura, T., Omori, K., Kobayashi, K., Hori, M., Ozaki, H. and Murata, T. (2015) 'Histamine Induces Vascular Hyperpermeability by Increasing Blood Flow and Endothelial Barrier Disruption In Vivo', *PLoS ONE*, 10(7), p. e0132367. Available at: https://doi.org/10.1371/journal.pone.0132367.

Aspalter, R.M., Eibl, M.M. and Wolf, H.M. (2003) 'Regulation of TCR-mediated T cell activation by TNF-RII', *Journal of Leukocyte Biology*, 74(4), pp. 572–582. Available at: https://doi.org/10.1189/jlb.0303112.

Aspalter, R.M., Eibl, M.M. and Wolf, H.M. (2007) 'Defective T-cell activation caused by impairment of the TNF receptor 2 costimulatory pathway in common variable immunodeficiency', *Journal of Allergy and Clinical Immunology*, 120(5), pp. 1193–1200. Available at: https://doi.org/10.1016/j.jaci.2007.07.004.

Aspalter, R.M., Wolf, H.M. and Eibl, M.M. (2005) 'Chronic TNF-α exposure impairs TCR-signaling via TNF-RII but not TNF-RI', *Cellular Immunology*, 237(1), pp. 55–67. Available at: https://doi.org/10.1016/j.cellimm.2005.10.001.

Atisha-Fregoso, Y., Lima, G., Pascual-Ramos, V., Baños-Peláez, M., Fragoso-Loyo, H., Jakez-Ocampo, J., Contreras-Yáñez, I. and Llorente, L. (2016) 'Rheumatoid Arthritis Disease Activity Is Determinant for ABCB1 and ABCG2 Drug-Efflux Transporters Function', *PLOS ONE*, 11(7), p. e0159556. Available at: https://doi.org/10.1371/journal.pone.0159556.

Bailis, W., Shyer, J.A., Zhao, J., Canaveras, J.C.G., Al Khazal, F.J., Qu, R., Steach, H.R., Bielecki, P., Khan, O., Jackson, R., Kluger, Y., Maher, L.J., Rabinowitz, J., Craft, J. and Flavell, R.A. (2019) 'Distinct modes of mitochondrial metabolism uncouple T cell differentiation and function', *Nature*, 571(7765), pp. 403–407. Available at: https://doi.org/10.1038/s41586-019-1311-3.

Bakheet, S.A., Ansari, M.A., Nadeem, A., Attia, S.M., Alhoshani, A.R., Gul, G., Al-Qahtani, Q.H., Albekairi, N.A., Ibrahim, K.E. and Ahmad, S.F. (2019) 'CXCR3 antagonist AMG487 suppresses rheumatoid arthritis pathogenesis and progression by shifting the Th17/Treg cell balance', *Cellular Signalling*, 64, p. 109395. Available at: https://doi.org/10.1016/j.cellsig.2019.109395.

Banerjee, D., Liou, H.-C. and Sen, R. (2005) 'c-Rel-Dependent Priming of Naive T Cells by Inflammatory Cytokines', *Immunity*, 23(4), pp. 445–458. Available at: https://doi.org/10.1016/j.immuni.2005.09.012.

Baron, U., Floess, S., Wieczorek, G., Baumann, K., Grützkau, A., Dong, J., Thiel, A., Boeld, T.J., Hoffmann, P., Edinger, M., Türbachova, I., Hamann, A., Olek, S. and Huehn, J. (2007) 'DNA demethylation in the human FOXP3 locus discriminates regulatory T cells from activated FOXP3+ conventional T cells', *European Journal of Immunology*, 37(9), pp. 2378–2389. Available at: https://doi.org/10.1002/eji.200737594.

Barski, A., Cuddapah, S., Kartashov, A.V., Liu, C., Imamichi, H., Yang, W., Peng, W., Lane, H.C. and Zhao, K. (2017) 'Rapid Recall Ability of Memory T cells is Encoded in their Epigenome', *Scientific Reports*, 7(1), p. 39785. Available at: https://doi.org/10.1038/srep39785.

Basdeo, S.A., Cluxton, D., Sulaimani, J., Moran, B., Canavan, M., Orr, C., Veale, D.J., Fearon, U. and Fletcher, J.M. (2017) 'Ex-Th17 (Nonclassical Th1) Cells Are Functionally Distinct from Classical Th1 and Th17 Cells and Are Not Constrained by Regulatory T Cells', *Journal of Immunology (Baltimore, Md.: 1950)*, 198(6), pp. 2249–2259. Available at: https://doi.org/10.4049/jimmunol.1600737.

Belikan, P., Bühler, U., Wolf, C., Pramanik, G.K., Gollan, R., Zipp, F. and Siffrin, V. (2018) 'CCR7 on CD4+ T Cells Plays a Crucial Role in the Induction of Experimental Autoimmune Encephalomyelitis', *The Journal of Immunology*, 200(8), pp. 2554–2562. Available at: https://doi.org/10.4049/jimmunol.1701419.

Beringer, A. and Miossec, P. (2019) 'Systemic effects of IL-17 in inflammatory arthritis', *Nature Reviews Rheumatology*, 15(8), pp. 491–501. Available at: https://doi.org/10.1038/s41584-019-0243-5.

Bernink, J.H., Krabbendam, L., Germar, K., de Jong, E., Gronke, K., Kofoed-Nielsen, M., Munneke, J.M., Hazenberg, M.D., Villaudy, J., Buskens, C.J., Bemelman, W.A., Diefenbach, A., Blom, B. and Spits, H. (2015) 'Interleukin-12 and -23 Control Plasticity of CD127(+) Group 1 and Group 3 Innate Lymphoid Cells in the Intestinal Lamina Propria', *Immunity*, 43(1), pp. 146–160. Available at: https://doi.org/10.1016/j.immuni.2015.06.019.

Berod, L., Friedrich, C., Nandan, A., Freitag, J., Hagemann, S., Harmrolfs, K., Sandouk, A., Hesse, C., Castro, C.N., Bähre, H., Tschirner, S.K., Gorinski, N., Gohmert, M., Mayer, C.T., Huehn, J., Ponimaskin, E., Abraham, W.-R., Müller, R., Lochner, M. and Sparwasser, T. (2014) 'De novo fatty acid synthesis controls the fate between regulatory T and T helper 17 cells', *Nature Medicine*, 20(11), pp. 1327–1333. Available at: https://doi.org/10.1038/nm.3704.

Beura, L.K., Fares-Frederickson, N.J., Steinert, E.M., Scott, M.C., Thompson, E.A., Fraser, K.A., Schenkel, J.M., Vezys, V. and Masopust, D. (2019) 'CD4+ resident memory T cells dominate immunosurveillance and orchestrate local recall responses', *Journal of Experimental Medicine*, 216(5), pp. 1214–1229. Available at: https://doi.org/10.1084/jem.20181365.

Bevington, S.L., Cauchy, P., Piper, J., Bertrand, E., Lalli, N., Jarvis, R.C., Gilding, L.N., Ott, S., Bonifer, C. and Cockerill, P.N. (2016) 'Inducible chromatin priming is associated with the establishment of immunological memory in T cells', *The EMBO journal*, 35(5), pp. 515–535. Available at: https://doi.org/10.15252/embj.201592534.

Bevington, S.L., Fiancette, R., Gajdasik, D.W., Keane, P., Soley, J.K., Willis, C.M., Coleman, D.J.L., Withers, D.R. and Cockerill, P.N. (2021) 'Stable Epigenetic Programming of Effector and Central Memory CD4 T Cells Occurs Within 7 Days of Antigen Exposure In Vivo', *Frontiers in Immunology*, 12. Available at: https://www.frontiersin.org/articles/10.3389/fimmu.2021.642807.

Bhat, P., Leggatt, G., Waterhouse, N. and Frazer, I.H. (2017) 'Interferon-γ derived from cytotoxic lymphocytes directly enhances their motility and cytotoxicity', *Cell Death & Disease*, 8(6), pp. e2836–e2836. Available at: https://doi.org/10.1038/cddis.2017.67.

Bhattacharyya, N.D. and Feng, C.G. (2020) 'Regulation of T Helper Cell Fate by TCR Signal Strength', *Frontiers in Immunology*, 11. Available at: https://www.frontiersin.org/articles/10.3389/fimmu.2020.00624.

Bishop, E.L., Gudgeon, N. and Dimeloe, S. (2021) 'Control of T Cell Metabolism by Cytokines and Hormones', *Frontiers in Immunology*, 12. Available at: https://www.frontiersin.org/articles/10.3389/fimmu.2021.653605.

Bishop, E.L., Gudgeon, N.H., Mackie, G.M., Chauss, D., Roberts, J., Tennant, D.A., Maslowski, K.M., Afzali, B., Hewison, M. and Dimeloe, S. (2022) '1,25-Dihydroxyvitamin D3 suppresses CD4+ T-cell effector functionality by inhibition of glycolysis', *Immunology*, 166(3), pp. 299–309. Available at: https://doi.org/10.1111/imm.13472.

Blagih, J., Coulombe, F., Vincent, E.E., Dupuy, F., Galicia-Vázquez, G., Yurchenko, E., Raissi, T.C., van der Windt, G.J.W., Viollet, B., Pearce, E.L., Pelletier, J., Piccirillo, C.A., Krawczyk, C.M., Divangahi, M. and Jones, R.G. (2015) 'The Energy Sensor AMPK Regulates T Cell Metabolic Adaptation and Effector Responses In Vivo', *Immunity*, 42(1), pp. 41–54. Available at: https://doi.org/10.1016/j.immuni.2014.12.030.

Blanco, F.J., Möricke, R., Dokoupilova, E., Codding, C., Neal, J., Andersson, M., Rohrer, S. and Richards, H. (2017) 'Secukinumab in Active Rheumatoid Arthritis: A Phase III Randomized, Double-Blind, Active Comparator- and Placebo-Controlled Study', *Arthritis & Rheumatology (Hoboken, N.J.)*, 69(6), pp. 1144–1153. Available at: https://doi.org/10.1002/art.40070.

Boomer, J.S. and Green, J.M. (2010) 'An Enigmatic Tail of CD28 Signaling', *Cold Spring Harbor Perspectives in Biology*, 2(8), p. a002436. Available at: https://doi.org/10.1101/cshperspect.a002436.

Bozulic, L. and Hemmings, B.A. (2009) 'PIKKing on PKB: regulation of PKB activity by phosphorylation', *Current Opinion in Cell Biology*, 21(2), pp. 256–261. Available at: https://doi.org/10.1016/j.ceb.2009.02.002.

Briney, B. and Crowe, J. (2013) 'Secondary mechanisms of diversification in the human antibody repertoire', *Frontiers in Immunology*, 4. Available at: https://www.frontiersin.org/articles/10.3389/fimmu.2013.00042.

van den Broek, T., Borghans, J.A.M. and van Wijk, F. (2018) 'The full spectrum of human naive T cells', *Nature Reviews Immunology*, 18(6), pp. 363–373. Available at: https://doi.org/10.1038/s41577-018-0001-y.

Bryl, E., Vallejo, A.N., Weyand, C.M. and Goronzy, J.J. (2001) 'Down-Regulation of CD28 Expression by TNF-α', *The Journal of Immunology*, 167(6), pp. 3231–3238. Available at: https://doi.org/10.4049/jimmunol.167.6.3231.

Buckler, J.L., Walsh, P.T., Porrett, P.M., Choi, Y. and Turka, L.A. (2006) 'Cutting edge: T cell requirement for CD28 costimulation is due to negative regulation of TCR signals by PTEN', *Journal of Immunology*, 177(7), pp. 4262–4266. Available at: https://doi.org/10.4049/jimmunol.177.7.4262.

Burel, J.G., Qian, Y., Lindestam Arlehamn, C., Weiskopf, D., Zapardiel-Gonzalo, J., Taplitz, R., Gilman, R.H., Saito, M., de Silva, A.D., Vijayanand, P., Scheuermann, R.H., Sette, A. and Peters, B. (2017) 'An Integrated Workflow To Assess Technical and Biological Variability of Cell Population Frequencies in Human Peripheral Blood by Flow Cytometry', *The Journal of Immunology*, 198(4), pp. 1748–1758. Available at: https://doi.org/10.4049/jimmunol.1601750.

Bushnell, B. (2014) 'BBMap: A Fast, Accurate, Splice-Aware Aligner'. (Version 37.99) [Computer programme]. Available at: https://sourceforge.net/projects/bbmap/.

Cai, X.-Y., Zhu, Y., Wang, C., Tang, X.-Y., Han, L., Shu, J.-L., Zhang, X.-Z., Liang, F.-Q., Ge, J.-R., Xu, L., Mei, D., Zhang, L.-L. and Wei, W. (2020) 'Etanercept Inhibits B Cell Differentiation by Regulating TNFRII/TRAF2/NF-κB Signaling Pathway in Rheumatoid Arthritis', *Frontiers in Pharmacology*, 11. Available at: https://www.frontiersin.org/articles/10.3389/fphar.2020.00676.

Callender, L.A., Schroth, J., Carroll, E.C., Garrod-Ketchley, C., Romano, L.E.L., Hendy, E., Kelly, A., Lavender, P., Akbar, A.N., Chapple, J.P. and Henson, S.M. (2021) 'GATA3 induces mitochondrial biogenesis in primary human CD4+ T cells during DNA damage', *Nature Communications*, 12(1), p. 3379. Available at: https://doi.org/10.1038/s41467-021-23715-7.

Cano-Gamez, E., Soskic, B., Roumeliotis, T.I., So, E., Smyth, D.J., Baldrighi, M., Willé, D., Nakic, N., Esparza-Gordillo, J., Larminie, C.G.C., Bronson, P.G., Tough, D.F., Rowan, W.C., Choudhary, J.S. and Trynka, G. (2020) 'Single-cell transcriptomics identifies an effectorness gradient shaping the response of CD4+ T cells to cytokines', *Nature Communications*, 11(1), p. 1801. Available at: https://doi.org/10.1038/s41467-020-15543-y.

Carlson, M. (2019) 'org.Hs.eg.db'. (R package version 3.12.0) [Computer programme]. Available at: http://bioconductor.org/packages/org.Hs.eg.db/.

Carr, E.L., Kelman, A., Wu, G.S., Gopaul, R., Senkevitch, E., Aghvanyan, A., Turay, A.M. and Frauwirth, K.A. (2010) 'Glutamine Uptake and Metabolism Are Coordinately Regulated by ERK/MAPK During T Lymphocyte Activation', *Journal of immunology (Baltimore, Md. : 1950)*, 185(2), pp. 1037–1044. Available at: https://doi.org/10.4049/jimmunol.0903586.

Castellanos, M.C., Muñoz, C., Montoya, M.C., Lara-Pezzi, E., López-Cabrera, M. and de Landázuri, M.O. (1997) 'Expression of the leukocyte early activation antigen CD69 is regulated by the transcription factor AP-1.', *The Journal of Immunology*, 159(11), pp. 5463–5473. Available at: https://doi.org/10.4049/jimmunol.159.11.5463.

Cejka, D., Hayer, S., Niederreiter, B., Sieghart, W., Fuereder, T., Zwerina, J. and Schett, G. (2010) 'Mammalian target of rapamycin signaling is crucial for joint destruction in experimental arthritis and is activated in osteoclasts from patients with rheumatoid arthritis', *Arthritis and Rheumatism*, 62(8), pp. 2294–2302. Available at: https://doi.org/10.1002/art.27504.

Chang, C.-H., Curtis, J.D., Maggi, L.B., Faubert, B., Villarino, A.V., O'Sullivan, D., Huang, S.C.-C., van der Windt, G.J.W., Blagih, J., Qiu, J., Weber, J.D., Pearce, E.J., Jones, R.G. and Pearce, E.L. (2013) 'Posttranscriptional control of T cell effector function by aerobic glycolysis', *Cell*, 153(6), pp. 1239–1251. Available at: https://doi.org/10.1016/j.cell.2013.05.016.

Chang, C.-H., Qiu, J., O'Sullivan, D., Buck, M.D., Noguchi, T., Curtis, J.D., Chen, Q., Gindin, M., Gubin, M.M., van der Windt, G.J.W., Tonc, E., Schreiber, R.D., Pearce, E.J. and Pearce, E.L. (2015) 'Metabolic competition in the tumor microenvironment is a driver of cancer progression', *Cell*, 162(6), pp. 1229–1241. Available at: https://doi.org/10.1016/j.cell.2015.08.016.

Chang, J., Burkett, P.R., Borges, C.M., Kuchroo, V.K., Turka, L.A. and Chang, C.-H. (2013) 'MyD88 is essential to sustain mTOR activation necessary to promote T helper 17 cell proliferation by linking IL-1 and IL-23 signaling', *Proceedings of the National Academy of Sciences of the United States of America*, 110(6), pp. 2270–2275. Available at: https://doi.org/10.1073/pnas.1206048110.

Chang, L., Feng, X. and Gao, W. (2019) 'Proliferation of rheumatoid arthritis fibroblast-like synoviocytes is enhanced by IL-17-mediated autophagy through STAT3 activation', *Connective Tissue Research*, 60(4), pp. 358–366. Available at: https://doi.org/10.1080/03008207.2018.1552266.

Chemin, K., Gerstner, C. and Malmström, V. (2019) 'Effector Functions of CD4+ T Cells at the Site of Local Autoimmune Inflammation—Lessons From Rheumatoid Arthritis', *Frontiers in Immunology*, 10, p. 353. Available at: https://doi.org/10.3389/fimmu.2019.00353.

Chemin, K., Pollastro, S., James, E., Ge, C., Albrecht, I., Herrath, J., Gerstner, C., Tandre, K., Sampaio Rizzi, T., Rönnblom, L., Catrina, A., Holmdahl, R., Klareskog, L., de Vries, N. and Malmström, V. (2016) 'A Novel HLA–DRB1*10:01–Restricted T Cell Epitope From Citrullinated Type II Collagen Relevant to Rheumatoid Arthritis', *Arthritis & Rheumatology*, 68(5), pp. 1124–1135. Available at: https://doi.org/10.1002/art.39553.

Chen, D.-Y., Chen, Y.-M., Chen, H.-H., Hsieh, C.-W., Lin, C.-C. and Lan, J.-L. (2011) 'Increasing levels of circulating Th17 cells and interleukin-17 in rheumatoid arthritis patients with an inadequate response to anti-TNF-α therapy', *Arthritis Research & Therapy*, 13(4), p. R126. Available at: https://doi.org/10.1186/ar3431.

Chen, L. and Flies, D.B. (2013) 'Molecular mechanisms of T cell co-stimulation and co-inhibition', *Nature reviews. Immunology*, 13(4), pp. 227–242. Available at: https://doi.org/10.1038/nri3405.

Chen, Q., Kim, Y.C., Laurence, A., Punkosdy, G.A. and Shevach, E.M. (2011) 'IL-2 Controls the Stability of Foxp3 Expression in TGF-β–Induced Foxp3+ T Cells In Vivo', *The Journal of Immunology*, 186(11), pp. 6329–6337. Available at: https://doi.org/10.4049/jimmunol.1100061.

Chen, X., Nie, Y., Xiao, H., Bian, Z., Scarzello, A.J., Song, N.-Y., Trivett, A.L., Yang, D. and Oppenheim, J.J. (2016) 'TNFR2 expression by CD4 effector T cells is required to induce full-fledged experimental colitis', *Scientific Reports*, 6(1), p. 32834. Available at: https://doi.org/10.1038/srep32834.

Chen, X., Subleski, J.J., Kopf, H., Howard, O.M.Z., Männel, D.N. and Oppenheim, J.J. (2008) 'Expression of TNFR2 defines a maximally suppressive subset of mouse CD4+CD25+FoxP3+ T regulatory cells: applicability to tumor infiltrating T regulatory cells', *Journal of immunology (Baltimore, Md. : 1950)*, 180(10), pp. 6467–6471.

Chen, X., Wu, X., Zhou, Q., Howard, O.M.Z., Netea, M.G. and Oppenheim, J.J. (2013) 'TNFR2 Is Critical for the Stabilization of the CD4+Foxp3+ Regulatory T Cell Phenotype in the Inflammatory Environment', *The Journal of Immunology*, 190(3), pp. 1076–1084. Available at: https://doi.org/10.4049/jimmunol.1202659.

Chimenti, M.S., Tucci, P., Candi, E., Perricone, R., Melino, G. and Willis, A.E. (2013) 'Metabolic profiling of human CD4+ cells following treatment with methotrexate and anti-TNF-α infliximab', *Cell Cycle*, 12(18), pp. 3025–3036. Available at: https://doi.org/10.4161/cc.26067.

Chornoguz, O., Hagan, R.S., Haile, A., Arwood, M.L., Gamper, C.J., Banerjee, A. and Powell, J.D. (2017) 'mTORC1 Promotes T-bet Phosphorylation To Regulate Th1 Differentiation', *The Journal of Immunology*, 198(10), pp. 3939–3948. Available at: https://doi.org/10.4049/jimmunol.1601078.

Church, L.D., Filer, A.D., Hidalgo, E., Howlett, K.A., Thomas, A.M., Rapecki, S., Scheel-Toellner, D., Buckley, C.D. and Raza, K. (2010) 'Rheumatoid synovial fluid interleukin-17-producing CD4 T cells have abundant tumor necrosis factor-alpha co-expression, but little interleukin-22 and interleukin-23R expression', *Arthritis Research & Therapy*, 12(5), p. R184. Available at: https://doi.org/10.1186/ar3152.

Church, L.D., Hessler, G., Goodall, J.E., Rider, D.A., Workman, C.J., Vignali, D.A.A., Bacon, P.A., Gulbins, E. and Young, S.P. (2005) 'TNFR1-induced sphingomyelinase activation modulates TCR signaling by impairing store-operated Ca2+ influx', *Journal of Leukocyte Biology*, 78(1), pp. 266–278. Available at: https://doi.org/10.1189/jlb.1003456.

Clerc, I., Moussa, D.A., Vahlas, Z., Tardito, S., Oburoglu, L., Hope, T.J., Sitbon, M., Dardalhon, V., Mongellaz, C. and Taylor, N. (2019) 'Entry of glucose- and glutamine-derived carbons into the citric acid cycle supports early steps of HIV-1 infection in CD4 T cells', *Nature Metabolism*, 1(7), pp. 717–730. Available at: https://doi.org/10.1038/s42255-019-0084-1.

Cluxton, D., Petrasca, A., Moran, B. and Fletcher, J.M. (2019) 'Differential Regulation of Human Treg and Th17 Cells by Fatty Acid Synthesis and Glycolysis', *Frontiers in Immunology*, 10, p. 115. Available at: https://doi.org/10.3389/fimmu.2019.00115.

Collier, J.L., Weiss, S.A., Pauken, K.E., Sen, D.R. and Sharpe, A.H. (2021) 'Not-so-opposite ends of the spectrum: CD8+ T cell dysfunction across chronic infection, cancer, and autoimmunity', *Nature immunology*, 22(7), pp. 809–819. Available at: https://doi.org/10.1038/s41590-021-00949-7.

Comito, G., Iscaro, A., Bacci, M., Morandi, A., Ippolito, L., Parri, M., Montagnani, I., Raspollini, M.R., Serni, S., Simeoni, L., Giannoni, E. and Chiarugi, P. (2019) 'Lactate modulates CD4+ T-cell polarization and induces an immunosuppressive environment, which sustains prostate carcinoma progression via TLR8/miR21 axis', *Oncogene*, 38(19), pp. 3681–3695. Available at: https://doi.org/10.1038/s41388-019-0688-7.

Conrad, C., Di Domizio, J., Mylonas, A., Belkhodja, C., Demaria, O., Navarini, A.A., Lapointe, A.-K., French, L.E., Vernez, M. and Gilliet, M. (2018) 'TNF blockade induces a dysregulated type I interferon response without autoimmunity in paradoxical psoriasis', *Nature Communications*, 9(1), p. 25. Available at: https://doi.org/10.1038/s41467-017-02466-4.

Cope, A.P., Londei, M., Chu, N.R., Cohen, S.B., Elliott, M.J., Brennan, F.M., Maini, R.N. and Feldmann, M. (1994) 'Chronic exposure to tumor necrosis factor (TNF) in vitro impairs the activation of T cells through the T cell receptor/CD3 complex; reversal in vivo by anti-TNF antibodies in patients with rheumatoid arthritis.', *Journal of Clinical Investigation*, 94(2), pp. 749–760.

Creyghton, M.P., Cheng, A.W., Welstead, G.G., Kooistra, T., Carey, B.W., Steine, E.J., Hanna, J., Lodato, M.A., Frampton, G.M., Sharp, P.A., Boyer, L.A., Young, R.A. and Jaenisch, R. (2010) 'Histone H3K27ac separates active from poised enhancers and predicts developmental state', *Proceedings of the National Academy of Sciences of the United States of America*, 107(50), pp. 21931–21936. Available at: https://doi.org/10.1073/pnas.1016071107.

Crofford, L.J. (2013) 'Use of NSAIDs in treating patients with arthritis', *Arthritis Research & Therapy*, 15(Suppl 3), p. S2. Available at: https://doi.org/10.1186/ar4174.

Cronstein, B.N. and Aune, T.M. (2020) 'Methotrexate and its mechanisms of action in inflammatory arthritis', *Nature Reviews Rheumatology*, 16(3), pp. 145–154. Available at: https://doi.org/10.1038/s41584-020-0373-9.

Crotty, S. (2019) 'T Follicular Helper Cell Biology: A Decade of Discovery and Diseases', *Immunity*, 50(5), pp. 1132–1148. Available at: https://doi.org/10.1016/j.immuni.2019.04.011.

Crowley, T., Buckley, C.D. and Clark, A.R. (2018) 'Stroma: the forgotten cells of innate immune memory', *Clinical and Experimental Immunology*, 193(1), pp. 24–36. Available at: https://doi.org/10.1111/cei.13149.

Cui, G., Staron, M.M., Gray, S.M., Ho, P.-C., Amezquita, R.A., Wu, J. and Kaech, S.M. (2015) 'IL-7-Induced Glycerol Transport and TAG Synthesis Promotes Memory CD8+ T Cell Longevity', *Cell*, 161(4), pp. 750–761. Available at: https://doi.org/10.1016/j.cell.2015.03.021.

Cutolo, M., Sulli, A., Pizzorni, C., Seriolo, B. and Straub, R.H. (2001) 'Anti-inflammatory mechanisms of methotrexate in rheumatoid arthritis', *Annals of the Rheumatic Diseases*, 60(8), pp. 729–735. Available at: https://doi.org/10.1136/ard.60.8.729.

Dang, E.V., Barbi, J., Yang, H.-Y., Jinasena, D., Yu, H., Zheng, Y., Bordman, Z., Fu, J., Kim, Y., Yen, H.-R., Luo, W., Zeller, K., Shimoda, L., Topalian, S.L., Semenza, G.L., Dang, C.V., Pardoll, D.M. and Pan, F. (2011) 'Control of TH17/Treg Balance by Hypoxia-inducible Factor 1', *Cell*, 146(5), pp. 772–784. Available at: https://doi.org/10.1016/j.cell.2011.07.033.

Das, J., Ho, M., Zikherman, J., Govern, C., Yang, M., Weiss, A., Chakraborty, A.K. and Roose, J.P. (2009) 'Digital Signaling and Hysteresis Characterize Ras Activation in Lymphoid Cells', *Cell*, 136(2), pp. 337–351. Available at: https://doi.org/10.1016/j.cell.2008.11.051.

Deason, K., Troutman, T.D., Jain, A., Challa, D.K., Mandraju, R., Brewer, T., Ward, E.S. and Pasare, C. (2018) 'BCAP links IL-1R to the PI3K-mTOR pathway and regulates pathogenic Th17 cell differentiation', *The Journal of Experimental Medicine*, 215(9), pp. 2413–2428. Available at: https://doi.org/10.1084/jem.20171810.

Degboé, Y., Rauwel, B., Baron, M., Boyer, J.-F., Ruyssen-Witrand, A., Constantin, A. and Davignon, J.-L. (2019) 'Polarization of Rheumatoid Macrophages by TNF Targeting Through an IL-10/STAT3 Mechanism', *Frontiers in Immunology*, 10, p. 3. Available at: https://doi.org/10.3389/fimmu.2019.00003.

Delgoffe, G.M., Kole, T.P., Zheng, Y., Zarek, P.E., Matthews, K.L., Xiao, B., Worley, P.F., Kozma, S.C. and Powell, J.D. (2009) 'The mTOR kinase differentially regulates effector and regulatory T cell lineage commitment', *Immunity*, 30(6), pp. 832–844. Available at: https://doi.org/10.1016/j.immuni.2009.04.014.

Delgoffe, G.M., Pollizzi, K.N., Waickman, A.T., Heikamp, E., Meyers, D.J., Horton, M.R., Xiao, B., Worley, P.F. and Powell, J.D. (2011) 'The mammalian Target of Rapamycin (mTOR) regulates T helper cell differentiation through the selective activation of mTORC1 and mTORC2 signaling', *Nature immunology*, 12(4), pp. 295–303. Available at: https://doi.org/10.1038/ni.2005.

Delisle, J.-S., Giroux, M., Boucher, G., Landry, J.-R., Hardy, M.-P., Lemieux, S., Jones, R.G., Wilhelm, B.T. and Perreault, C. (2013) 'The TGF-β-Smad3 pathway inhibits CD28-dependent cell growth and proliferation of CD4 T cells', *Genes & Immunity*, 14(2), pp. 115–126. Available at: https://doi.org/10.1038/gene.2012.63.

Dimeloe, S., Frick, C., Fischer, M., Gubser, P.M., Razik, L., Bantug, G.R., Ravon, M., Langenkamp, A. and Hess, C. (2014) 'Human regulatory T cells lack the cyclophosphamide-extruding transporter ABCB1 and are more susceptible to cyclophosphamide-induced apoptosis', *European Journal of Immunology*, 44(12), pp. 3614–3620. Available at: https://doi.org/10.1002/eji.201444879.

Dimeloe, S., Gubser, P., Loeliger, J., Frick, C., Develioglu, L., Fischer, M., Marquardsen, F., Bantug, G.R., Thommen, D., Lecoultre, Y., Zippelius, A., Langenkamp, A. and Hess, C. (2019) 'Tumor-derived TGF-β inhibits mitochondrial respiration to suppress IFN-γ production by human CD4+ T cells', *Science Signaling*, 12(599), p. eaav3334. Available at: https://doi.org/10.1126/scisignal.aav3334.

Dimeloe, S., Mehling, M., Frick, C., Loeliger, J., Bantug, G.R., Sauder, U., Fischer, M., Belle, R., Develioglu, L., Tay, S., Langenkamp, A. and Hess, C. (2016) 'The Immune-Metabolic Basis of Effector Memory CD4+ T Cell Function under Hypoxic Conditions', *The Journal of Immunology*, 196(1), pp. 106–114. Available at: https://doi.org/10.4049/jimmunol.1501766.

Dobin, A., Davis, C.A., Schlesinger, F., Drenkow, J., Zaleski, C., Jha, S., Batut, P., Chaisson, M. and Gingeras, T.R. (2013) 'STAR: ultrafast universal RNA-seq aligner', *Bioinformatics (Oxford, England)*, 29(1), pp. 15–21. Available at: https://doi.org/10.1093/bioinformatics/bts635.

Domínguez-Andrés, J., Joosten, L.A. and Netea, M.G. (2019) 'Induction of innate immune memory: the role of cellular metabolism', *Current Opinion in Immunology*, 56, pp. 10–16. Available at: https://doi.org/10.1016/j.coi.2018.09.001.

Domm, S., Cinatl, J. and Mrowietz, U. (2008) 'The impact of treatment with tumour necrosis factor-α antagonists on the course of chronic viral infections: a review of the literature', *British Journal of Dermatology*, 159(6), pp. 1217–1228. Available at: https://doi.org/10.1111/j.1365-2133.2008.08851.x.

Dooms, H., Wolslegel, K., Lin, P. and Abbas, A.K. (2007) 'Interleukin-2 enhances CD4+ T cell memory by promoting the generation of IL-7Rα–expressing cells', *The Journal of Experimental Medicine*, 204(3), pp. 547–557. Available at: https://doi.org/10.1084/jem.20062381.

Dulic, S., Vásárhelyi, Z., Sava, F., Berta, L., Szalay, B., Toldi, G., Kovács, L. and Balog, A. (2017) 'T-Cell Subsets in Rheumatoid Arthritis Patients on Long-Term Anti-TNF or IL-6 Receptor Blocker Therapy', *Mediators of Inflammation*, 2017, p. 6894374. Available at: https://doi.org/10.1155/2017/6894374.

Ehrenstein, M.R., Evans, J.G., Singh, A., Moore, S., Warnes, G., Isenberg, D.A. and Mauri, C. (2004) 'Compromised Function of Regulatory T Cells in Rheumatoid Arthritis and Reversal by Anti-TNFα Therapy', *The Journal of Experimental Medicine*, 200(3), pp. 277–285. Available at: https://doi.org/10.1084/jem.20040165.

Elliot, T.A.E., Jennings, E.K., Lecky, D.A.J., Thawait, N., Flores-Langarica, A., Copland, A., Maslowski, K.M., Wraith, D.C. and Bending, D. (2021) 'Antigen and checkpoint receptor engagement recalibrates T cell receptor signal strength', *Immunity*, 54(11), pp. 2481-2496.e6. Available at: https://doi.org/10.1016/j.immuni.2021.08.020.

Emery, P., Burmester, G.R., Bykerk, V.P., Combe, B.G., Furst, D.E., Barré, E., Karyekar, C.S., Wong, D.A. and Huizinga, T.W.J. (2015) 'Evaluating drug-free remission with abatacept in early rheumatoid arthritis: results from the phase 3b, multicentre, randomised, active-controlled AVERT study of 24 months, with a 12-month, double-blind treatment period', *Annals of the Rheumatic Diseases*, 74(1), pp. 19–26. Available at: https://doi.org/10.1136/annrheumdis-2014-206106.

Endo, Y., Asou, H.K., Matsugae, N., Hirahara, K., Shinoda, K., Tumes, D.J., Tokuyama, H., Yokote, K. and Nakayama, T. (2015) 'Obesity Drives Th17 Cell Differentiation by Inducing the Lipid Metabolic Kinase, ACC1', *Cell Reports*, 12(6), pp. 1042–1055. Available at: https://doi.org/10.1016/j.celrep.2015.07.014.

Evangelidou, M., Tseveleki, V., Vamvakas, S.-S. and Probert, L. (2010) 'TNFRI is a positive T-cell costimulatory molecule important for the timing of cytokine responses', *Immunology & Cell Biology*, 88(5), pp. 586–595. Available at: https://doi.org/10.1038/icb.2010.12.

Evans, H.G., Roostalu, U., Walter, G.J., Gullick, N.J., Frederiksen, K.S., Roberts, C.A., Sumner, J., Baeten, D.L., Gerwien, J.G., Cope, A.P., Geissmann, F., Kirkham, B.W. and Taams, L.S. (2014) 'TNF-α blockade induces IL-10 expression in human CD4+ T cells', *Nature Communications*, 5(1), p. 3199. Available at: https://doi.org/10.1038/ncomms4199.

Feldhoff, L.M., Rueda, C.M., Moreno-Fernandez, M.E., Sauer, J., Jackson, C.M., Chougnet, C.A. and Rupp, J. (2017) 'IL-1β induced HIF-1α inhibits the differentiation of human FOXP3+ T cells', *Scientific Reports*, 7, p. 465. Available at: https://doi.org/10.1038/s41598-017-00508-x.

Ferreira, G.B., Gysemans, C.A., Demengeot, J., Cunha, J.P.M.C.M. da, Vanherwegen, A.-S., Overbergh, L., Belle, T.L.V., Pauwels, F., Verstuyf, A., Korf, H. and Mathieu, C. (2014) '1,25-Dihydroxyvitamin D3 Promotes Tolerogenic Dendritic Cells with Functional Migratory Properties in NOD Mice', *The Journal of Immunology*, 192(9), pp. 4210–4220. Available at: https://doi.org/10.4049/jimmunol.1302350.

Feske, S., Giltnane, J., Dolmetsch, R., Staudt, L.M. and Rao, A. (2001) 'Gene regulation mediated by calcium signals in T lymphocytes', *Nature Immunology*, 2(4), pp. 316–324. Available at: https://doi.org/10.1038/86318.

Fields, P.E., Kim, S.T. and Flavell, R.A. (2002) 'Cutting Edge: Changes in Histone Acetylation at the IL-4 and IFN-γ Loci Accompany Th1/Th2 Differentiation', *The Journal of Immunology*, 169(2), pp. 647–650. Available at: https://doi.org/10.4049/jimmunol.169.2.647.

Fischer, R., Marsal, J., Guttà, C., Eisler, S.A., Peters, N., Bethea, J.R., Pfizenmaier, K. and Kontermann, R.E. (2017) 'Novel strategies to mimic transmembrane tumor necrosis factor-dependent activation of tumor necrosis factor receptor 2', *Scientific Reports*, 7(1), p. 6607. Available at: https://doi.org/10.1038/s41598-017-06993-4.

Floess, S., Freyer, J., Siewert, C., Baron, U., Olek, S., Polansky, J., Schlawe, K., Chang, H.-D., Bopp, T., Schmitt, E., Klein-Hessling, S., Serfling, E., Hamann, A. and Huehn, J. (2007) 'Epigenetic Control of the foxp3 Locus in Regulatory T Cells', *PLOS Biology*, 5(2), p. e38. Available at: https://doi.org/10.1371/journal.pbio.0050038.

Flores-Borja, F., Jury, E.C., Mauri, C. and Ehrenstein, M.R. (2008) 'Defects in CTLA-4 are associated with abnormal regulatory T cell function in rheumatoid arthritis', *Proceedings of the National Academy of Sciences of the United States of America*, 105(49), pp. 19396–19401. Available at: https://doi.org/10.1073/pnas.0806855105.

Floudas, A., Neto, N., Orr, C., Canavan, M., Gallagher, P., Hurson, C., Monaghan, M.G., Nagpar, S., Mullan, R.H., Veale, D.J. and Fearon, U. (2022) 'Loss of balance between protective and pro-inflammatory synovial tissue T-cell polyfunctionality predates clinical onset of rheumatoid arthritis', *Annals of the Rheumatic Diseases*, 81(2), pp. 193–205. Available at: https://doi.org/10.1136/annrheumdis-2021-220458.

Fox, R.I. (1993) 'Mechanism of action of hydroxychloroquine as an antirheumatic drug', *Seminars in Arthritis and Rheumatism*, 23(2 Suppl 1), pp. 82–91. Available at: https://doi.org/10.1016/s0049-0172(10)80012-5.

Fox, R.I., Herrmann, M.L., Frangou, C.G., Wahl, G.M., Morris, R.E., Strand, V. and Kirschbaum, B.J. (1999) 'Mechanism of Action for Leflunomide in Rheumatoid Arthritis', *Clinical Immunology*, 93(3), pp. 198–208. Available at: https://doi.org/10.1006/clim.1999.4777.

Fracchia, K.M., Pai, C.Y. and Walsh, C.M. (2013) 'Modulation of T Cell Metabolism and Function through Calcium Signaling', *Frontiers in Immunology*, 4, p. 324. Available at: https://doi.org/10.3389/fimmu.2013.00324.

Frauwirth, K.A., Riley, J.L., Harris, M.H., Parry, R.V., Rathmell, J.C., Plas, D.R., Elstrom, R.L., June, C.H. and Thompson, C.B. (2002) 'The CD28 Signaling Pathway Regulates Glucose Metabolism', *Immunity*, 16(6), pp. 769–777. Available at: https://doi.org/10.1016/S1074-7613(02)00323-0.

Garçon, F., Patton, D.T., Emery, J.L., Hirsch, E., Rottapel, R., Sasaki, T. and Okkenhaug, K. (2008) 'CD28 provides T-cell costimulation and enhances PI3K activity at the immune synapse independently of its capacity to interact with the p85/p110 heterodimer', *Blood*, 111(3), pp. 1464–1471. Available at: https://doi.org/10.1182/blood-2007-08-108050.

Garralda, E., Moreno, V., Alonso, G., Corral, E., Hernandez-Guerrero, T., Ramon, J., Spéville, B.D. de, Martinez, E., Soucek, L., Niewel, M. and Calvo, E. (2022) 'Dose escalation study of OMO-103, a first in class Pan-MYC-Inhibitor in patients (pts) with advanced solid tumors', *European Journal of Cancer*, 174, pp. S5–S6. Available at: https://doi.org/10.1016/S0959-8049(22)00820-6.

Gaud, G., Lesourne, R. and Love, P.E. (2018) 'Regulatory mechanisms in T cell receptor signalling', *Nature Reviews Immunology*, 18(8), pp. 485–497. Available at: https://doi.org/10.1038/s41577-018-0020-8.

Gerriets, V.A., Danzaki, K., Kishton, R.J., Eisner, W., Nichols, A.G., Saucillo, D.C., Shinohara, M.L. and MacIver, N.J. (2016) 'Leptin directly promotes T-cell glycolytic metabolism to drive effector T-cell differentiation in a mouse model of autoimmunity', *European Journal of Immunology*, 46(8), pp. 1970–1983. Available at: https://doi.org/10.1002/eji.201545861.

Gerriets, V.A., Kishton, R.J., Johnson, M.O., Cohen, S., Siska, P.J., Nichols, A.G., Warmoes, M.O., de Cubas, A.A., MacIver, N.J., Locasale, J.W., Turka, L.A., Wells, A.D. and Rathmell, J.C. (2016) 'Foxp3 and Toll-like receptor signaling balance Treg cell anabolic metabolism for suppression', *Nature Immunology*, 17(12), pp. 1459–1466. Available at: https://doi.org/10.1038/ni.3577.

Gerriets, V.A., Kishton, R.J., Nichols, A.G., Macintyre, A.N., Inoue, M., Ilkayeva, O., Winter, P.S., Liu, X., Priyadharshini, B., Slawinska, M.E., Haeberli, L., Huck, C., Turka, L.A., Wood, K.C., Hale, L.P., Smith, P.A., Schneider, M.A., MacIver, N.J., Locasale, J.W., Newgard, C.B., Shinohara, M.L. and Rathmell, J.C. (2015) 'Metabolic programming and PDHK1 control CD4+ T cell subsets and inflammation', *The Journal of Clinical Investigation*, 125(1), pp. 194–207. Available at: https://doi.org/10.1172/JCI76012.

Gerstner, C., Dubnovitsky, A., Sandin, C., Kozhukh, G., Uchtenhagen, H., James, E.A., Rönnelid, J., Ytterberg, A.J., Pieper, J., Reed, E., Tandre, K., Rieck, M., Zubarev, R.A., Rönnblom, L., Sandalova, T., Buckner, J.H., Achour, A. and Malmström, V. (2016) 'Functional and Structural Characterization of a Novel HLA-DRB1*04:01-Restricted α-Enolase T Cell Epitope in Rheumatoid Arthritis', *Frontiers in Immunology*, 7. Available at: https://www.frontiersin.org/articles/10.3389/fimmu.2016.00494.

Gharib, M., Elbaz, W., Darweesh, E., Sabri, N.A. and Shawki, M.A. (2021) 'Efficacy and Safety of Metformin Use in Rheumatoid Arthritis: A Randomized Controlled Study', *Frontiers in Pharmacology*, 12, p. 726490. Available at: https://doi.org/10.3389/fphar.2021.726490.

Glinos, D.A., Soskic, B., Williams, C., Kennedy, A., Jostins, L., Sansom, D.M. and Trynka, G. (2020) 'Genomic profiling of T-cell activation suggests increased sensitivity of memory T cells to CD28 costimulation', *Genes & Immunity*, 21(6), pp. 390–408. Available at: https://doi.org/10.1038/s41435-020-00118-0.

Goldberg, M., Nadiv, O., Luknar-Gabor, N., Koch, P. and Katz, Y. (2008) 'Synergistic Induction of IL-23 Expression in Fibroblast-like Synoviocytes by IL-17 and TNF-Alpha: A Positive Feedback Loop in Rheumatoid Arthritis', *Journal of Allergy and Clinical Immunology*, 121(2), p. S134. Available at: https://doi.org/10.1016/j.jaci.2007.12.534.

Gosselin, A., Monteiro, P., Chomont, N., Diaz-Griffero, F., Said, E.A., Fonseca, S., Wacleche, V., El-Far, M., Boulassel, M.-R., Routy, J.-P., Sekaly, R.-P. and Ancuta, P. (2010) 'Peripheral Blood CCR4+CCR6+ and CXCR3+CCR6+ CD4+ T Cells Are Highly Permissive to HIV-1 Infection', *Journal of immunology (Baltimore, Md. : 1950)*, 184(3), pp. 1604–1616. Available at: https://doi.org/10.4049/jimmunol.0903058.

Goto, Y., Panea, C., Nakato, G., Cebula, A., Lee, C., Diez, M.G., Laufer, T.M., Ignatowicz, L. and Ivanov, I.I. (2014) 'Segmented filamentous bacteria antigens presented by intestinal dendritic cells drive mucosal Th17 cell differentiation', *Immunity*, 40(4), pp. 594–607. Available at: https://doi.org/10.1016/j.immuni.2014.03.005.

Grell, M., Douni, E., Wajant, H., Löhden, M., Clauss, M., Maxeiner, B., Georgopoulos, S., Lesslauer, W., Kollias, G., Pfizenmaier, K. and Scheurich, P. (1995) 'The transmembrane form of tumor necrosis factor is the prime activating ligand of the 80 kDa tumor necrosis factor receptor', *Cell*, 83(5), pp. 793–802. Available at: https://doi.org/10.1016/0092-8674(95)90192-2.

Griffin, G.K., Newton, G., Tarrio, M.L., Bu, D., Maganto-Garcia, E., Azcutia, V., Alcaide, P., Grabie, N., Luscinskas, F.W., Croce, K.J. and Lichtman, A.H. (2012) 'IL-17 and TNFα Sustain Neutrophil Recruitment During Inflammation Through Synergistic Effects on Endothelial Activation', *Journal of Immunology (Baltimore, Md. : 1950)*, 188(12), pp. 6287–6299. Available at: https://doi.org/10.4049/jimmunol.1200385.

Gu, J., Zhou, J., Chen, Q., Xu, X., Gao, J., Li, X., Shao, Q., Zhou, B., Zhou, H., Wei, S., Wang, Q., Liang, Y. and Lu, L. (2022) 'Tumor metabolite lactate promotes tumorigenesis by modulating MOESIN lactylation and enhancing TGF-β signaling in regulatory T cells', *Cell Reports*, 39(12), p. 110986. Available at: https://doi.org/10.1016/j.celrep.2022.110986.

Gudgeon, N., Munford, H., Bishop, E.L., Hill, J., Fulton-Ward, T., Bending, D., Roberts, J., Tennant, D.A. and Dimeloe, S. (2022) 'Succinate uptake by T cells suppresses their effector function via inhibition of mitochondrial glucose oxidation', *Cell Reports*, 40(7), p. 111193. Available at: https://doi.org/10.1016/j.celrep.2022.111193.

Guillot, L., Nathan, N., Tabary, O., Thouvenin, G., Le Rouzic, P., Corvol, H., Amselem, S. and Clement, A. (2013) 'Alveolar epithelial cells: Master regulators of lung homeostasis', *The International Journal of Biochemistry & Cell Biology*, 45(11), pp. 2568–2573. Available at: https://doi.org/10.1016/j.biocel.2013.08.009.

Gulen, M.F., Kang, Z., Bulek, K., Youzhong, W., Kim, T.W., Chen, Y., Altuntas, C.Z., Sass Bak-Jensen, K., McGeachy, M.J., Do, J.-S., Xiao, H., Delgoffe, G.M., Min, B., Powell, J.D., Tuohy, V.K., Cua, D.J. and Li, X. (2010) 'The receptor SIGIRR suppresses Th17 cell proliferation via inhibition of the interleukin-1 receptor pathway and mTOR kinase activation', *Immunity*, 32(1), pp. 54–66. Available at: https://doi.org/10.1016/j.immuni.2009.12.003.

Guo, F., Iclozan, C., Suh, W.-K., Anasetti, C. and Yu, X.-Z. (2008) 'CD28 Controls Differentiation of Regulatory T Cells from Naive CD4 T Cells', *Journal of immunology (Baltimore, Md. : 1950)*, 181(4), pp. 2285–2291.

Gutcher, I. and Becher, B. (2007) 'APC-derived cytokines and T cell polarization in autoimmune inflammation', *The Journal of Clinical Investigation*, 117(5), pp. 1119–1127. Available at: https://doi.org/10.1172/JCI31720.

Gwinn, D.M., Shackelford, D.B., Egan, D.F., Mihaylova, M.M., Mery, A., Vasquez, D.S., Turk, B.E. and Shaw, R.J. (2008) 'AMPK phosphorylation of raptor mediates a metabolic checkpoint', *Molecular cell*, 30(2), pp. 214–226. Available at: https://doi.org/10.1016/j.molcel.2008.03.003.

Haas, R., Smith, J., Rocher-Ros, V., Nadkarni, S., Montero-Melendez, T., D'Acquisto, F., Bland, E.J., Bombardieri, M., Pitzalis, C., Perretti, M., Marelli-Berg, F.M. and Mauro, C. (2015) 'Lactate Regulates Metabolic and Pro-inflammatory Circuits in Control of T Cell Migration and Effector Functions', *PLoS Biology*, 13(7), p. e1002202. Available at: https://doi.org/10.1371/journal.pbio.1002202.

Hafkamp, F.M.J., Taanman-Kueter, E.W.M., van Capel, T.M.M., Kormelink, T.G. and de Jong, E.C. (2022) 'Vitamin D3 Priming of Dendritic Cells Shifts Human Neutrophil-Dependent Th17 Cell Development to Regulatory T Cells', *Frontiers in Immunology*, 13. Available at: https://www.frontiersin.org/articles/10.3389/fimmu.2022.872665.

van Hamburg, J.P., Asmawidjaja, P.S., Davelaar, N., Mus, A.M.C., Colin, E.M., Hazes, J.M.W., Dolhain, R.J.E.M. and Lubberts, E. (2011) 'Th17 cells, but not Th1 cells, from patients with early rheumatoid arthritis are potent inducers of matrix metalloproteinases and proinflammatory cytokines upon synovial fibroblast interaction, including autocrine interleukin-17A production', *Arthritis and Rheumatism*, 63(1), pp. 73–83. Available at: https://doi.org/10.1002/art.30093.

van Hamburg, J.P. and Tas, S.W. (2018) 'Molecular mechanisms underpinning T helper 17 cell heterogeneity and functions in rheumatoid arthritis', *Journal of Autoimmunity*, 87, pp. 69–81. Available at: https://doi.org/10.1016/j.jaut.2017.12.006.

Han, G.M., O'Neil-Andersen, N.J., Zurier, R.B. and Lawrence, D.A. (2008) 'CD4+CD25high T cell numbers are enriched in the peripheral blood of patients with rheumatoid arthritis', *Cellular Immunology*, 253(1), pp. 92–101. Available at: https://doi.org/10.1016/j.cellimm.2008.05.007.

Haney, D., Quigley, M.F., Asher, T.E., Ambrozak, D.R., Gostick, E., Price, D.A., Douek, D.C. and Betts, M.R. (2011) 'Isolation of viable antigen-specific CD8+ T cells based on membrane-bound tumor necrosis factor (TNF)-α expression', *Journal of immunological methods*, 369(1–2), pp. 33–41. Available at: https://doi.org/10.1016/j.jim.2011.04.003.

Hanlon, M.M., Canavan, M., Barker, B.E. and Fearon, U. (2022) 'Metabolites as drivers and targets in rheumatoid arthritis', *Clinical and Experimental Immunology*, 208(2), pp. 167–180. Available at: https://doi.org/10.1093/cei/uxab021.

Harada, Y., Tokushima, M., Matsumoto, Y., Ogawa, S., Otsuka, M., Hayashi, K., Weiss, B.D., June, C.H. and Abe, R. (2001) 'Critical requirement for the membrane-proximal cytosolic tyrosine residue for CD28-mediated costimulation in vivo', *Journal of Immunology (Baltimore, Md.: 1950)*, 166(6), pp. 3797–3803. Available at: https://doi.org/10.4049/jimmunol.166.6.3797.

Harari, A., Vallelian, F. and Pantaleo, G. (2004) 'Phenotypic heterogeneity of antigen-specific CD4 T cells under different conditions of antigen persistence and antigen load', *European Journal of Immunology*, 34(12), pp. 3525–3533. Available at: https://doi.org/10.1002/eji.200425324.

Harrington, L.E., Hatton, R.D., Mangan, P.R., Turner, H., Murphy, T.L., Murphy, K.M. and Weaver, C.T. (2005) 'Interleukin 17-producing CD4+ effector T cells develop via a lineage distinct from the T helper type 1 and 2 lineages', *Nature Immunology*, 6(11), pp. 1123–1132. Available at: https://doi.org/10.1038/ni1254.

Harrington, R., Al Nokhatha, S.A. and Conway, R. (2020) 'JAK Inhibitors in Rheumatoid Arthritis: An Evidence-Based Review on the Emerging Clinical Data', *Journal of Inflammation Research*, 13, pp. 519–531. Available at: https://doi.org/10.2147/JIR.S219586.

Harris-Tryon, T.A. and Grice, E.A. (2022) 'Microbiota and maintenance of skin barrier function', *Science*, 376(6596), pp. 940–945. Available at: https://doi.org/10.1126/science.abo0693.

Hashizume, M., Hayakawa, N. and Mihara, M. (2008) 'IL-6 trans-signalling directly induces RANKL on fibroblast-like synovial cells and is involved in RANKL induction by TNF-α and IL-17', *Rheumatology*, 47(11), pp. 1635–1640. Available at: https://doi.org/10.1093/rheumatology/ken363.

He, S., Wang, L., Miao, L., Wang, T., Du, F., Zhao, L. and Wang, X. (2009) 'Receptor interacting protein kinase-3 determines cellular necrotic response to TNF-alpha', *Cell*, 137(6), pp. 1100–1111. Available at: https://doi.org/10.1016/j.cell.2009.05.021.

Heller, F., Florian, P., Bojarski, C., Richter, J., Christ, M., Hillenbrand, B., Mankertz, J., Gitter, A.H., Bürgel, N., Fromm, M., Zeitz, M., Fuss, I., Strober, W. and Schulzke, J.D. (2005) 'Interleukin-13 Is the Key Effector Th2 Cytokine in Ulcerative Colitis That Affects Epithelial Tight Junctions, Apoptosis, and Cell Restitution', *Gastroenterology*, 129(2), pp. 550–564. Available at: https://doi.org/10.1053/j.gastro.2005.05.002.

Hermans, D., Gautam, S., García-Cañaveras, J.C., Gromer, D., Mitra, S., Spolski, R., Li, P., Christensen, S., Nguyen, R., Lin, J.-X., Oh, J., Du, N., Veenbergen, S., Fioravanti, J., Ebina-Shibuya, R., Bleck, C., Neckers, L.M., Rabinowitz, J.D., Gattinoni, L. and Leonard, W.J. (2020) 'Lactate dehydrogenase inhibition synergizes with IL-21 to promote CD8+ T cell stemness and antitumor immunity', *Proceedings of the National Academy of Sciences of the United States of America*, 117(11), pp. 6047–6055. Available at: https://doi.org/10.1073/pnas.1920413117.

Hill, J.A., Southwood, S., Sette, A., Jevnikar, A.M., Bell, D.A. and Cairns, E. (2003) 'Cutting Edge: The Conversion of Arginine to Citrulline Allows for a High-Affinity Peptide Interaction with the Rheumatoid Arthritis-Associated HLA-DRB1*0401 MHC Class II Molecule1', *The Journal of Immunology*, 171(2), pp. 538–541. Available at: https://doi.org/10.4049/jimmunol.171.2.538.

Hirota, K., Duarte, J.H., Veldhoen, M., Hornsby, E., Li, Y., Cua, D.J., Ahlfors, H., Wilhelm, C., Tolaini, M., Menzel, U., Garefalaki, A., Potocnik, A.J. and Stockinger, B. (2011) 'Fate mapping of IL-17-producing T cells in inflammatory responses', *Nature Immunology*, 12(3), pp. 255–263. Available at: https://doi.org/10.1038/ni.1993.

Hirota, K., Hashimoto, M., Ito, Y., Matsuura, M., Ito, H., Tanaka, M., Watanabe, H., Kondoh, G., Tanaka, A., Yasuda, K., Kopf, M., Potocnik, A.J., Stockinger, B., Sakaguchi, N. and Sakaguchi, S. (2018) 'Autoimmune Th17 Cells Induced Synovial Stromal and Innate Lymphoid Cell Secretion of the Cytokine GM-CSF to Initiate and Augment Autoimmune Arthritis', *Immunity*, 48(6), pp. 1220-1232.e5. Available at: https://doi.org/10.1016/j.immuni.2018.04.009.

Hirota, K., Yoshitomi, H., Hashimoto, M., Maeda, S., Teradaira, S., Sugimoto, N., Yamaguchi, T., Nomura, T., Ito, H., Nakamura, T., Sakaguchi, N. and Sakaguchi, S. (2007) 'Preferential recruitment of CCR6-expressing Th17 cells to inflamed joints via CCL20 in rheumatoid arthritis and its animal model', *The Journal of Experimental Medicine*, 204(12), pp. 2803–2812. Available at: https://doi.org/10.1084/jem.20071397.

Ho, C.-H., Silva, A.A., Tomita, B., Weng, H.-Y. and Ho, I.-C. (2021) 'Differential impacts of TNFα inhibitors on the transcriptome of Th cells', *Arthritis Research & Therapy*, 23(1), p. 199. Available at: https://doi.org/10.1186/s13075-021-02558-z.

Ho, P.-C., Bihuniak, J.D., Macintyre, A.N., Staron, M., Liu, X., Amezquita, R., Tsui, Y.-C., Cui, G., Micevic, G., Perales, J.C., Kleinstein, S.H., Abel, E.D., Insogna, K.L., Feske, S., Locasale, J.W., Bosenberg, M.W., Rathmell, J.C. and Kaech, S.M. (2015) 'Phosphoenolpyruvate Is a Metabolic Checkpoint of Anti-tumor T Cell Responses', *Cell*, 162(6), pp. 1217–1228. Available at: https://doi.org/10.1016/j.cell.2015.08.012.

Howie, D., Cobbold, S.P., Adams, E., Bokum, A.T., Necula, A.S., Zhang, W., Huang, H., Roberts, D.J., Thomas, B., Hester, S.S., Vaux, D.J., Betz, A.G. and Waldmann, H. (2017) 'Foxp3 drives oxidative phosphorylation and protection from lipotoxicity', *JCI Insight*, 2(3). Available at: https://doi.org/10.1172/jci.insight.89160.

Hsieh, C.-S., Macatonia, S.E., Tripp, C.S., Wolf, S.F., O'Garra, A. and Murphy, K.M. (1993) 'Development of TH1 CD4+ T Cells Through IL-12 Produced by Listeria-Induced Macrophages', *Science*, 260(5107), pp. 547–549. Available at: https://doi.org/10.1126/science.8097338.

Huang, J., Fu, X., Chen, X., Li, Z., Huang, Y. and Liang, C. (2021) 'Promising Therapeutic Targets for Treatment of Rheumatoid Arthritis', *Frontiers in Immunology*, 12, p. 686155. Available at: https://doi.org/10.3389/fimmu.2021.686155.

Hwang, J.-R., Byeon, Y., Kim, D. and Park, S.-G. (2020) 'Recent insights of T cell receptor-mediated signaling pathways for T cell activation and development', *Experimental & Molecular Medicine*, 52(5), pp. 750–761. Available at: https://doi.org/10.1038/s12276-020-0435-8.

Ioan-Facsinay, A., Willemze, A., Robinson, D.B., Peschken, C.A., Markland, J., van der Woude, D., Elias, B., Ménard, H.A., Newkirk, M., Fritzler, M.J., Toes, R.E.M., Huizinga, T.W.J. and El-Gabalawy, H.S. (2008) 'Marked differences in fine specificity and isotype usage of the anti-citrullinated protein antibody in health and disease', *Arthritis and Rheumatism*, 58(10), pp. 3000–3008. Available at: https://doi.org/10.1002/art.23763.

Isomäki, P., Panesar, M., Annenkov, A., Clark, J.M., Foxwell, B.M.J., Chernajovsky, Y. and Cope, A.P. (2001) 'Prolonged Exposure of T Cells to TNF Down-Regulates TCRζ and Expression of the TCR/CD3 Complex at the Cell Surface', *The Journal of Immunology*, 166(9), pp. 5495–5507. Available at: https://doi.org/10.4049/jimmunol.166.9.5495.

Ivanov, I.I., Atarashi, K., Manel, N., Brodie, E.L., Shima, T., Karaoz, U., Wei, D., Goldfarb, K.C., Santee, C.A., Lynch, S.V., Tanoue, T., Imaoka, A., Itoh, K., Takeda, K., Umesaki, Y., Honda, K. and Littman, D.R. (2009) 'Induction of Intestinal Th17 Cells by Segmented Filamentous Bacteria', *Cell*, 139(3), pp. 485–498. Available at: https://doi.org/10.1016/j.cell.2009.09.033.

Ivashkiv, L.B. (2018) 'IFNγ: signalling, epigenetics and roles in immunity, metabolism, disease and cancer immunotherapy', *Nature Reviews Immunology*, 18(9), pp. 545–558. Available at: https://doi.org/10.1038/s41577-018-0029-z.

Iwasaki, A. and Medzhitov, R. (2015) 'Control of adaptive immunity by the innate immune system', *Nature immunology*, 16(4), pp. 343–353. Available at: https://doi.org/10.1038/ni.3123.

Jacobs, S.R., Herman, C.E., MacIver, N.J., Wofford, J.A., Wieman, H.L., Hammen, J.J. and Rathmell, J.C. (2008) 'Glucose Uptake Is Limiting in T Cell Activation and Requires CD28-Mediated Akt-Dependent and Independent Pathways', *Journal of immunology (Baltimore, Md. : 1950)*, 180(7), pp. 4476–4486.

Jacobs, S.R., Michalek, R.D. and Rathmell, J.C. (2010) 'IL-7 Is Essential for Homeostatic Control of T Cell Metabolism In Vivo', *Journal of immunology (Baltimore, Md. : 1950)*, 184(7), pp. 3461–3469. Available at: https://doi.org/10.4049/jimmunol.0902593.

James, E.A., Rieck, M., Pieper, J., Gebe, J.A., Yue, B.B., Tatum, M., Peda, M., Sandin, C., Klareskog, L., Malmström, V. and Buckner, J.H. (2014) 'Citrulline-Specific Th1 Cells Are Increased in Rheumatoid Arthritis and Their Frequency Is Influenced by Disease Duration and Therapy', *Arthritis & Rheumatology*, 66(7), pp. 1712–1722. Available at: https://doi.org/10.1002/art.38637.

Janardhan, S.V., Praveen, K., Marks, R. and Gajewski, T.F. (2011) 'Evidence Implicating the Ras Pathway in Multiple CD28 Costimulatory Functions in CD4+ T Cells', *PLoS ONE*, 6(9), p. e24931. Available at: https://doi.org/10.1371/journal.pone.0024931.

Jenkins, M.K., Khoruts, A., Ingulli, E., Mueller, D.L., McSorley, S.J., Reinhardt, R.L., Itano, A. and Pape, K.A. (2001) 'In Vivo Activation of Antigen-Specific CD4 T Cells', *Annual Review of Immunology*, 19(1), pp. 23–45. Available at: https://doi.org/10.1146/annurev.immunol.19.1.23.

Jobanputra, P., Maggs, F., Deeming, A., Carruthers, D., Rankin, E., Jordan, A.C., Faizal, A., Goddard, C., Pugh, M., Bowman, S.J., Brailsford, S. and Nightingale, P. (2012) 'A randomised efficacy and discontinuation study of etanercept versus adalimumab (RED SEA) for rheumatoid arthritis: a pragmatic, unblinded, non-inferiority study of first TNF inhibitor use: outcomes over 2 years', *BMJ Open*, 2(6), p. e001395. Available at: https://doi.org/10.1136/bmjopen-2012-001395.

Johnson, M.O., Wolf, M.M., Madden, M.Z., Andrejeva, G., Sugiura, A., Contreras, D.C., Maseda, D., Liberti, M.V., Paz, K., Kishton, R.J., Johnson, M.E., de Cubas, A.A., Wu, P., Li, G., Zhang, Y., Newcomb, D.C., Wells, A.D., Restifo, N.P., Rathmell, W.K., Locasale, J.W., Davila, M.L., Blazar, B.R. and Rathmell, J.C. (2018) 'Distinct Regulation of Th17 and Th1 Cell Differentiation by Glutaminase-Dependent Metabolism', *Cell*, 175(7), pp. 1780-1795.e19. Available at: https://doi.org/10.1016/j.cell.2018.10.001.

Jones, N., Vincent, E.E., Cronin, J.G., Panetti, S., Chambers, M., Holm, S.R., Owens, S.E., Francis, N.J., Finlay, D.K. and Thornton, C.A. (2019) 'Akt and STAT5 mediate naïve human CD4+ T-cell early metabolic response to TCR stimulation', *Nature Communications*, 10, p. 2042. Available at: https://doi.org/10.1038/s41467-019-10023-4.

de Jong, E., Suddason, T. and Lord, G.M. (2010) 'Translational Mini-Review Series on Th17 Cells: Development of mouse and human T helper 17 cells', *Clinical and Experimental Immunology*, 159(2), pp. 148–158. Available at: https://doi.org/10.1111/j.1365-2249.2009.04041.x.

Jong, E.C. de, Vieira, P.L., Kalinski, P., Schuitemaker, J.H.N., Tanaka, Y., Wierenga, E.A., Yazdanbakhsh, M. and Kapsenberg, M.L. (2002) 'Microbial Compounds Selectively Induce Th1 Cell-Promoting or Th2 Cell-Promoting Dendritic Cells In Vitro with Diverse Th Cell-Polarizing Signals', *The Journal of Immunology*, 168(4), pp. 1704–1709. Available at: https://doi.org/10.4049/jimmunol.168.4.1704.

Jorgovanovic, D., Song, M., Wang, L. and Zhang, Y. (2020) 'Roles of IFN-γ in tumor progression and regression: a review', *Biomarker Research*, 8(1), p. 49. Available at: https://doi.org/10.1186/s40364-020-00228-x.

Kaaij, M.H., van Tok, M.N., Blijdorp, I.C., Ambarus, C.A., Stock, M., Pots, D., Knaup, V.L., Armaka, M., Christodoulou-Vafeiadou, E., van Melsen, T.K., Masdar, H., Eskes, H.J.P.P., Yeremenko, N.G., Kollias, G., Schett, G., Tas, S.W., van Duivenvoorde, L.M. and Baeten, D.L.P. (2020) 'Transmembrane TNF drives osteoproliferative joint inflammation reminiscent of human spondyloarthritis', *Journal of Experimental Medicine*, 217(10), p. e20200288. Available at: https://doi.org/10.1084/jem.20200288.

Kane, L.P., Andres, P.G., Howland, K.C., Abbas, A.K. and Weiss, A. (2001) 'Akt provides the CD28 costimulatory signal for up-regulation of IL-2 and IFN-gamma but not TH2 cytokines', *Nature Immunology*, 2(1), pp. 37–44. Available at: https://doi.org/10.1038/83144.

Kato, R., Sumitomo, S., Tsuchida, Y., Tsuchiya, H., Nakachi, S., Sakurai, K., Hanata, N., Nagafuchi, Y., Kubo, K., Tateishi, S., Kanda, H., Okamura, T., Yamamoto, K. and Fujio, K. (2019) 'CD4+CD25+LAG3+ T Cells With a Feature of Th17 Cells Associated With Systemic Lupus Erythematosus Disease Activity', *Frontiers in Immunology*, 10, p. 1619. Available at: https://doi.org/10.3389/fimmu.2019.01619.

Katsuyama, T., Tsokos, G.C. and Moulton, V.R. (2018) 'Aberrant T Cell Signaling and Subsets in Systemic Lupus Erythematosus', *Frontiers in Immunology*, 9. Available at: https://www.frontiersin.org/articles/10.3389/fimmu.2018.01088.

Kaur, N., Naga, O.S., Norell, H., Al-Khami, A.A., Scheffel, M.J., Chakraborty, N.G., Voelkel-Johnson, C., Mukherji, B. and Mehrotra, S. (2011) 'T cells expanded in presence of IL-15 exhibit increased antioxidant capacity and innate effector molecules', *Cytokine*, 55(2), pp. 307–317. Available at: https://doi.org/10.1016/j.cyto.2011.04.014.

Kawashiri, S.-Y., Kawakami, A., Okada, A., Koga, T., Tamai, M., Yamasaki, S., Nakamura, H., Origuchi, T., Ida, H. and Eguchi, K. (2011) 'CD4+CD25highCD127low/- Treg Cell Frequency from Peripheral Blood Correlates with Disease Activity in Patients with Rheumatoid Arthritis', *The Journal of Rheumatology*, 38(12), pp. 2517–2521. Available at: https://doi.org/10.3899/jrheum.110283.

Kaymak, I., Luda, K.M., Duimstra, L.R., Ma, E.H., Longo, J., Dahabieh, M.S., Faubert, B., Oswald, B.M., Watson, M.J., Kitchen-Goosen, S.M., DeCamp, L.M., Compton, S.E., Fu, Z., DeBerardinis, R.J., Williams, K.S., Sheldon, R.D. and Jones, R.G. (2022) 'Carbon source availability drives nutrient utilization in CD8+ T cells', *Cell Metabolism*, 34(9), pp. 1298-1311.e6. Available at: https://doi.org/10.1016/j.cmet.2022.07.012.

Keck, S., Schmaler, M., Ganter, S., Wyss, L., Oberle, S., Huseby, E.S., Zehn, D. and King, C.G. (2014) 'Antigen affinity and antigen dose exert distinct influences on CD4 T-cell differentiation', *Proceedings of the National Academy of Sciences*, 111(41), pp. 14852–14857. Available at: https://doi.org/10.1073/pnas.1403271111.

Kim, E.K., Kwon, J.-E., Lee, S.-Y., Lee, E.-J., Kim, D.S., Moon, S.-J., Lee, J., Kwok, S.-K., Park, S.-H. and Cho, M.-L. (2018) 'IL-17-mediated mitochondrial dysfunction impairs apoptosis in rheumatoid arthritis synovial fibroblasts through activation of autophagy', *Cell Death & Disease*, 8(1), pp. e2565–e2565. Available at: https://doi.org/10.1038/cddis.2016.490.

Kim, E.Y. and Teh, H.-S. (2001) 'TNF Type 2 Receptor (p75) Lowers the Threshold of T Cell Activation', *The Journal of Immunology*, 167(12), pp. 6812–6820. Available at: https://doi.org/10.4049/jimmunol.167.12.6812.

Kim, E.Y. and Teh, H.-S. (2004) 'Critical Role of TNF Receptor Type-2 (p75) as a Costimulator for IL-2 Induction and T Cell Survival: A Functional Link to CD28', *The Journal of Immunology*, 173(7), pp. 4500–4509. Available at: https://doi.org/10.4049/jimmunol.173.7.4500.

Kim, H.-P. and Leonard, W.J. (2002) 'The basis for TCR-mediated regulation of the IL-2 receptor α chain gene: role of widely separated regulatory elements', *The EMBO Journal*, 21(12), pp. 3051–3059. Available at: https://doi.org/10.1093/emboj/cdf321.

Kim, J., Jung, K.H., Yoo, J., Park, J.H., Yan, H.H., Fang, Z., Lim, J.H., Kwon, S.-R., Kim, M.K., Park, H.-J. and Hong, S.-S. (2020) 'PBT-6, a Novel PI3KC2γ Inhibitor in Rheumatoid Arthritis', *Biomolecules & Therapeutics*, 28(2), pp. 172–183. Available at: https://doi.org/10.4062/biomolther.2019.153.

Kim, Jimyung, M.D, Kang, S., M.D, Kim, Jinhyun, M.D, Kwon, G., M.D, Koo, and S. and M.D (2013) 'Elevated Levels of T Helper 17 Cells Are Associated with Disease Activity in Patients with Rheumatoid Arthritis', *Annals of Laboratory Medicine*, 33(1), pp. 52–59. Available at: https://doi.org/10.3343/alm.2013.33.1.52.

Kim, K.-W., Kim, H.-R., Kim, B.-M., Cho, M.-L. and Lee, S.-H. (2015) 'Th17 Cytokines Regulate Osteoclastogenesis in Rheumatoid Arthritis', *The American Journal of Pathology*, 185(11), pp. 3011–3024. Available at: https://doi.org/10.1016/j.ajpath.2015.07.017.

Kim, S.Y. and Solomon, D.H. (2010) 'Tumor necrosis factor blockade and the risk of viral infection', *Nature Reviews Rheumatology*, 6(3), pp. 165–174. Available at: https://doi.org/10.1038/nrrheum.2009.279.

de Kivit, S., Mensink, M., Hoekstra, A.T., Berlin, I., Derks, R.J.E., Both, D., Aslam, M.A., Amsen, D., Berkers, C.R. and Borst, J. (2020) 'Stable human regulatory T cells switch to glycolysis following TNF receptor 2 costimulation', *Nature Metabolism*, 2(10), pp. 1046–1061. Available at: https://doi.org/10.1038/s42255-020-00271-w.

Klysz, D., Tai, X., Robert, P.A., Craveiro, M., Cretenet, G., Oburoglu, L., Mongellaz, C., Floess, S., Fritz, V., Matias, M.I., Yong, C., Surh, N., Marie, J.C., Huehn, J., Zimmermann, V., Kinet, S., Dardalhon, V. and Taylor, N. (2015) 'Glutamine-dependent α-ketoglutarate production regulates the balance between T helper 1 cell and regulatory T cell generation', *Science Signaling*, 8(396), pp. ra97–ra97. Available at: https://doi.org/10.1126/scisignal.aab2610.

Kobayashi, K., Takahashi, N., Jimi, E., Udagawa, N., Takami, M., Kotake, S., Nakagawa, N., Kinosaki, M., Yamaguchi, K., Shima, N., Yasuda, H., Morinaga, T., Higashio, K., Martin, T.J. and Suda, T. (2000) 'Tumor necrosis factor alpha stimulates osteoclast differentiation by a mechanism independent of the ODF/RANKL-RANK interaction', *The Journal of Experimental Medicine*, 191(2), pp. 275–286. Available at: https://doi.org/10.1084/jem.191.2.275.

Koedderitzsch, K., Zezina, E., Li, L., Herrmann, M. and Biesemann, N. (2021) 'TNF induces glycolytic shift in fibroblast like synoviocytes via GLUT1 and HIF1A', *Scientific Reports*, 11, p. 19385. Available at: https://doi.org/10.1038/s41598-021-98651-z.

Koetzier, S.C., Langelaar, J. van, Blok, K.M., Bosch, T.P.P. van den, Wierenga-Wolf, A.F., Melief, M.-J., Pol, K., Siepman, T.A., Verjans, G.M.G.M., Smolders, J., Lubberts, E., Vries, H.E. de and Luijn, M.M. van (2020) 'Brain-homing CD4+ T cells display glucocorticoid-resistant features in MS', *Neurology - Neuroimmunology Neuroinflammation*, 7(6). Available at: https://doi.org/10.1212/NXI.0000000000000894.

Koga, T., Ichinose, K., Kawakami, A. and Tsokos, G.C. (2021) 'Current Insights and Future Prospects for Targeting IL-17 to Treat Patients With Systemic Lupus Erythematosus', *Frontiers in Immunology*, 11. Available at: https://www.frontiersin.org/articles/10.3389/fimmu.2020.624971.

Kolev, M., Dimeloe, S., Le Friec, G., Navarini, A., Arbore, G., Povoleri, G.A., Fischer, M., Belle, R., Loeliger, J., Develioglu, L., Bantug, G.R., Watson, J., Couzi, L., Afzali, B., Lavender, P., Hess, C. and Kemper, C. (2015) 'Complement Regulates Nutrient Influx and Metabolic Reprogramming during Th1 Cell Responses', *Immunity*, 42(6), pp. 1033–1047. Available at: https://doi.org/10.1016/j.immuni.2015.05.024.

Komatsu, N., Okamoto, K., Sawa, S., Nakashima, T., Oh-hora, M., Kodama, T., Tanaka, S., Bluestone, J.A. and Takayanagi, H. (2014) 'Pathogenic conversion of Foxp3+ T cells into TH17 cells in autoimmune arthritis', *Nature Medicine*, 20(1), pp. 62–68. Available at: https://doi.org/10.1038/nm.3432.

Kondrack, R.M., Harbertson, J., Tan, J.T., McBreen, M.E., Surh, C.D. and Bradley, L.M. (2003) 'Interleukin 7 Regulates the Survival and Generation of Memory CD4 Cells', *The Journal of Experimental Medicine*, 198(12), pp. 1797–1806. Available at: https://doi.org/10.1084/jem.20030735.

Kremer, J.M., Lawrence, D.A., Hamilton, R. and McInnes, I.B. (2016) 'Long-term study of the impact of methotrexate on serum cytokines and lymphocyte subsets in patients with active rheumatoid arthritis: correlation with pharmacokinetic measures', *RMD Open*, 2(1), p. e000287. Available at: https://doi.org/10.1136/rmdopen-2016-000287.

Krieckaert, C.L., Jamnitski, A., Nurmohamed, M.T., Kostense, P.J., Boers, M. and Wolbink, G. (2012) 'Comparison of long-term clinical outcome with etanercept treatment and adalimumab treatment of rheumatoid arthritis with respect to immunogenicity', *Arthritis and Rheumatism*, 64(12), pp. 3850–3855. Available at: https://doi.org/10.1002/art.34680.

Kumar, V., Rosenzweig, R., Asalla, S., Nehra, S., Prabhu, S.D. and Bansal, S.S. (2022) 'TNFR1 Contributes to Activation-Induced Cell Death of Pathological CD4+ T Lymphocytes During Ischemic Heart Failure', *JACC: Basic to Translational Science*, 7(10), pp. 1038–1049. Available at: https://doi.org/10.1016/j.jacbts.2022.05.005.

Kurowska, W., Kuca-Warnawin, E.H., Radzikowska, A. and Maśliński, W. (2017) 'The role of anti-citrullinated protein antibodies (ACPA) in the pathogenesis of rheumatoid arthritis', *Central-European Journal of Immunology*, 42(4), pp. 390–398. Available at: https://doi.org/10.5114/ceji.2017.72807.

Labiano, S., Meléndez-Rodríguez, F., Palazón, A., Teijeira, Á., Garasa, S., Etxeberria, I., Aznar, M.Á., Sánchez-Paulete, A.R., Azpilikueta, A., Bolaños, E., Molina, C., de la Fuente, H., Maiso, P., Sánchez-Madrid, F., de Landázuri, M.O., Aragonés, J. and Melero, I. (2017) 'CD69 is a direct HIF-1α target gene in hypoxia as a mechanism enhancing expression on tumor-infiltrating T lymphocytes', *Oncoimmunology*, 6(4), p. e1283468. Available at: https://doi.org/10.1080/2162402X.2017.1283468.

Lam, J., Takeshita, S., Barker, J.E., Kanagawa, O., Ross, F.P. and Teitelbaum, S.L. (2000) 'TNF-alpha induces osteoclastogenesis by direct stimulation of macrophages exposed to permissive levels of RANK ligand', *The Journal of Clinical Investigation*, 106(12), pp. 1481–1488. Available at: https://doi.org/10.1172/JCI11176.

van Langelaar, J., van der Vuurst de Vries, R.M., Janssen, M., Wierenga-Wolf, A.F., Spilt, I.M., Siepman, T.A., Dankers, W., Verjans, G.M.G.M., de Vries, H.E., Lubberts, E., Hintzen, R.Q. and van Luijn, M.M. (2018) 'T helper 17.1 cells associate with multiple sclerosis disease activity: perspectives for early intervention', *Brain*, 141(5), pp. 1334–1349. Available at: https://doi.org/10.1093/brain/awy069.

Lawson, C.A., Brown, A.K., Bejarano, V., Douglas, S.H., Burgoyne, C.H., Greenstein, A.S., Boylston, A.W., Emery, P., Ponchel, F. and Isaacs, J.D. (2006) 'Early rheumatoid arthritis is associated with a deficit in the CD4 + CD25 high regulatory T cell population in peripheral blood', *Rheumatology*, 45(10), pp. 1210–1217. Available at: https://doi.org/10.1093/rheumatology/kel089.

Leclerc, M., Naserian, S., Pilon, C., Thiolat, A., Martin, G.H., Pouchy, C., Dominique, C., Belkacemi, Y., Charlotte, F., Maury, S., Salomon, B.L. and Cohen, J.L. (2016) 'Control of GVHD by regulatory T cells depends on TNF produced by T cells and TNFR2 expressed by regulatory T cells', *Blood*, 128(12), pp. 1651–1659. Available at: https://doi.org/10.1182/blood-2016-02-700849.

Lee, G.R. (2018) 'The Balance of Th17 versus Treg Cells in Autoimmunity', *International Journal of Molecular Sciences*, 19(3), p. 730. Available at: https://doi.org/10.3390/ijms19030730.

Lee, Jaeseon, Lee, Jennifer, Park, M.-K., Lim, M.-A., Park, E.-M., Kim, E., Yang, E.-J., Lee, S.-Y., Jhun, J.-Y., Park, S.-H., Kim, H.-Y. and Cho, M.-L. (2013) 'Interferon Gamma Suppresses Collagen-Induced Arthritis by Regulation of Th17 through the Induction of Indoleamine-2,3-Deoxygenase', *PLOS ONE*, 8(4), p. e60900. Available at: https://doi.org/10.1371/journal.pone.0060900.

Lee, K., Gudapati, P., Dragovic, S., Spencer, C., Joyce, S., Killeen, N., Magnuson, M.A. and Boothby, M. (2010) 'Mammalian Target of Rapamycin Protein Complex 2 Regulates Differentiation of Th1 and Th2 Cell Subsets via Distinct Signaling Pathways', *Immunity*, 32(6), pp. 743–753. Available at: https://doi.org/10.1016/j.immuni.2010.06.002.

Lee, S.H., Kwon, J. ye, Kim, S.-Y., Jung, K. and Cho, M.-L. (2017) 'Interferon-gamma regulates inflammatory cell death by targeting necroptosis in experimental autoimmune arthritis', *Scientific Reports*, 7(1), p. 10133. Available at: https://doi.org/10.1038/s41598-017-09767-0.

Lee, Y.K., Turner, H., Maynard, C.L., Oliver, J.R., Chen, D., Elson, C.O. and Weaver, C.T. (2009) 'Late developmental plasticity in the T helper 17 lineage', *Immunity*, 30(1), pp. 92–107. Available at: https://doi.org/10.1016/j.immuni.2008.11.005.

León, B. and Ballesteros-Tato, A. (2021) 'Modulating Th2 Cell Immunity for the Treatment of Asthma', *Frontiers in Immunology*, 12. Available at: https://www.frontiersin.org/articles/10.3389/fimmu.2021.637948.

Leung, S., Liu, X., Fang, L., Chen, X., Guo, T. and Zhang, J. (2010) 'The cytokine milieu in the interplay of pathogenic Th1/Th17 cells and regulatory T cells in autoimmune disease', *Cellular & Molecular Immunology*, 7(3), pp. 182–189. Available at: https://doi.org/10.1038/cmi.2010.22.

Li, L., Li, Q., Yan, Z.-X., Sheng, L.-S., Fu, D., Xu, P., Wang, L. and Zhao, W.-L. (2022) 'Transgenic expression of IL-7 regulates CAR-T cell metabolism and enhances in vivo persistence against tumor cells', *Scientific Reports*, 12(1), p. 12506. Available at: https://doi.org/10.1038/s41598-022-16616-2.

Li, X.-F., Sun, Y.-Y., Bao, J., Chen, X., Li, Y.-H., Yang, Y., Zhang, L., Huang, C., Wu, B.-M., Meng, X.-M. and Li, J. (2017) 'Functional role of PPAR-γ on the proliferation and migration of fibroblast-like synoviocytes in rheumatoid arthritis', *Scientific Reports*, 7(1), p. 12671. Available at: https://doi.org/10.1038/s41598-017-12570-6.

Li, Y., Shen, Y., Hohensinner, P., Ju, J., Wen, Z., Goodman, S.B., Zhang, H., Goronzy, J.J. and Weyand, C.M. (2016) 'Deficient activity of the nuclease MRE11A induces T cell aging and promotes arthritogenic effector functions in patients with rheumatoid arthritis', *Immunity*, 45(4), pp. 903–916. Available at: https://doi.org/10.1016/j.immuni.2016.09.013.

Libri, V., Azevedo, R.I., Jackson, S.E., Di Mitri, D., Lachmann, R., Fuhrmann, S., Vukmanovic-Stejic, M., Yong, K., Battistini, L., Kern, F., Soares, M.V.D. and Akbar, A.N. (2011) 'Cytomegalovirus infection induces the accumulation of short-lived, multifunctional CD4+ CD45RA+ CD27− T cells: the potential involvement of interleukin-7 in this process',

Immunology, 132(3), pp. 326–339. Available at: https://doi.org/10.1111/j.1365-2567.2010.03386.x.

Lin, X., Yang, Y., Guo, Y., Liu, H., Jiang, J., Zheng, F. and Wu, B. (2019) 'PTTG1 is involved in TNF-α-related hepatocellular carcinoma via the induction of c-myc', *Cancer Medicine*, 8(12), pp. 5702–5715. Available at: https://doi.org/10.1002/cam4.2473.

Linterman, M.A., Denton, A.E., Divekar, D.P., Zvetkova, I., Kane, L., Ferreira, C., Veldhoen, M., Clare, S., Dougan, G., Espéli, M. and Smith, K.G. (2014) 'CD28 expression is required after T cell priming for helper T cell responses and protective immunity to infection', *eLife*. Edited by F.M. Powrie, 3, p. e03180. Available at: https://doi.org/10.7554/eLife.03180.

Liu, G., Burns, S., Huang, G., Boyd, K., Proia, R.L., Flavell, R.A. and Chi, H. (2009) 'The receptor S1P1 overrides regulatory T cell-mediated immune suppression through Akt-mTOR', *Nature Immunology*, 10(7), pp. 769–777. Available at: https://doi.org/10.1038/ni.1743.

Liu, M.-F., Wang, C.-R., Fung, L.-L., Lin, L.-H. and Tsai, C.-N. (2005) 'The Presence of Cytokine-Suppressive CD4+CD25+ T Cells in the Peripheral Blood and Synovial Fluid of Patients with Rheumatoid Arthritis', *Scandinavian Journal of Immunology*, 62(3), pp. 312–317. Available at: https://doi.org/10.1111/j.1365-3083.2005.01656.x.

Liu, Q., Sun, Z. and Chen, L. (2020) 'Memory T cells: strategies for optimizing tumor immunotherapy', *Protein & Cell*, 11(8), pp. 549–564. Available at: https://doi.org/10.1007/s13238-020-00707-9.

Liu, X., Berry, C.T., Ruthel, G., Madara, J.J., MacGillivray, K., Gray, C.M., Madge, L.A., McCorkell, K.A., Beiting, D.P., Hershberg, U., May, M.J. and Freedman, B.D. (2016) 'T Cell Receptor-induced Nuclear Factor κB (NF-κB) Signaling and Transcriptional Activation Are Regulated by STIM1- and Orai1-mediated Calcium Entry *', *Journal of Biological Chemistry*, 291(16), pp. 8440–8452. Available at: https://doi.org/10.1074/jbc.M115.713008.

Lo, B.C., Shin, S.B., Hernaez, D.C., Refaeli, I., Yu, H.B., Goebeler, V., Cait, A., Mohn, W.W., Vallance, B.A. and McNagny, K.M. (2019) 'IL-22 Preserves Gut Epithelial Integrity and Promotes Disease Remission during Chronic Salmonella Infection', *The Journal of Immunology*, 202(3), pp. 956–965. Available at: https://doi.org/10.4049/jimmunol.1801308.

van Loosdregt, J., Rossetti, M., Spreafico, R., Moshref, M., Olmer, M., Williams, G.W., Venkatanarayanan, H.B., Kumar, P., Copeland, D., Pischel, K., Lotz, M. and Albani, S. (2016) 'Increased autophagy in CD4+ T cells of rheumatoid arthritis patients results in T cell hyperactivation and apoptosis resistance', *European journal of immunology*, 46(12), pp. 2862–2870. Available at: https://doi.org/10.1002/eji.201646375.

Lopez Krol, A., Nehring, H.P., Krause, F.F., Wempe, A., Raifer, H., Nist, A., Stiewe, T., Bertrams, W., Schmeck, B., Luu, M., Leister, H., Chung, H.-R., Bauer, U.-M., Adhikary, T. and Visekruna, A. (2022) 'Lactate induces metabolic and epigenetic reprogramming of pro-inflammatory Th17 cells', *EMBO reports*, 23(12), p. e54685. Available at: https://doi.org/10.15252/embr.202254685.

Loschinski, R., Böttcher, M., Stoll, A., Bruns, H., Mackensen, A. and Mougiakakos, D. (2018) 'IL-21 modulates memory and exhaustion phenotype of T-cells in a fatty acid oxidation-dependent manner', *Oncotarget*, 9(17), pp. 13125–13138. Available at: https://doi.org/10.18632/oncotarget.24442.

Love, M.I., Huber, W. and Anders, S. (2014) 'Moderated estimation of fold change and dispersion for RNA-seq data with DESeq2', *Genome Biology*, 15(12), p. 550. Available at: https://doi.org/10.1186/s13059-014-0550-8.

Loyal, L., Braun, J., Henze, L., Kruse, B., Dingeldey, M., Reimer, U., Kern, F., Schwarz, T., Mangold, M., Unger, C., Dörfler, F., Kadler, S., Rosowski, J., Gürcan, K., Uyar-Aydin, Z., Frentsch, M., Kurth, F., Schnatbaum, K., Eckey, M., Hippenstiel, S., Hocke, A., Müller, M.A., Sawitzki, B., Miltenyi, S., Paul, F., Mall, M.A., Wenschuh, H., Voigt, S., Drosten, C., Lauster, R., Lachman, N., Sander, L.-E., Corman, V.M., Röhmel, J., Meyer-Arndt, L., Thiel, A. and Giesecke-Thiel, C. (2021) 'Cross-reactive CD4+ T cells enhance SARS-CoV-2 immune responses upon infection and vaccination', *Science*, 374(6564), p. eabh1823. Available at: https://doi.org/10.1126/science.abh1823.

Luda, K., Kitchen-Goosen, S., Ma, E., Watson, M., Duimstra, L., Oswald, B., Longo, J., Fu, Z., Madaj, Z., Kupai, A., Dickson, B., Kaymak, I., Lau, K., Compton, S., DeCamp, L., Kelly, D., Puchalska, P., Williams, K., Krawczyk, C., Lévesque, D., Boisvert, F.-M., Sheldon, R., Rothbart, S., Crawford, P. and Jones, R. (2022) 'Ketolysis is a metabolic driver of $CD8^+$ T cell effector function through histone acetylatio'. Available at: https://doi.org/10.1101/2022.08.26.505402.

Luo, P., Wang, P., Xu, J., Hou, W., Xu, P., Xu, K. and Liu, L. (2022) 'Immunomodulatory role of T helper cells in rheumatoid arthritis', *Bone & Joint Research*, 11(7), pp. 426–438. Available at: https://doi.org/10.1302/2046-3758.117.BJR-2021-0594.R1.

Lusty, E., Poznanski, S.M., Kwofie, K., Mandur, T.S., Lee, D.A., Richards, C.D. and Ashkar, A.A. (2017) 'IL-18/IL-15/IL-12 synergy induces elevated and prolonged IFN-γ production by ex vivo expanded NK cells which is not due to enhanced STAT4 activation', *Molecular Immunology*, 88, pp. 138–147. Available at: https://doi.org/10.1016/j.molimm.2017.06.025.

Ma, X. and Xu, S. (2013) 'TNF inhibitor therapy for rheumatoid arthritis', *Biomedical Reports*, 1(2), pp. 177–184. Available at: https://doi.org/10.3892/br.2012.42.

Macintyre, A.N., Gerriets, V.A., Nichols, A.G., Michalek, R.D., Rudolph, M.C., Deoliveira, D., Anderson, S.M., Abel, E.D., Chen, B.J., Hale, L.P. and Rathmell, J.C. (2014) 'The Glucose Transporter Glut1 is Selectively Essential for CD4 T Cell Activation and Effector Function', *Cell metabolism*, 20(1), pp. 61–72. Available at: https://doi.org/10.1016/j.cmet.2014.05.004.

MacLeod, M.K.L., Clambey, E.T., Kappler, J.W. and Marrack, P. (2009) 'CD4 memory T cells: what are they and what can they do?', *Seminars in immunology*, 21(2), pp. 53–61. Available at: https://doi.org/10.1016/j.smim.2009.02.006.

Maeda, S., Osaga, S., Maeda, T., Takeda, N., Tamechika, S., Naniwa, T. and Niimi, A. (2019) 'Circulating Th17.1 cells as candidate for the prediction of therapeutic response to abatacept in patients with rheumatoid arthritis: An exploratory research', *PLOS ONE*, 14(11), p. e0215192. Available at: https://doi.org/10.1371/journal.pone.0215192.

Maekawa, Y., Ishifune, C., Tsukumo, S., Hozumi, K., Yagita, H. and Yasutomo, K. (2015) 'Notch controls the survival of memory CD4+ T cells by regulating glucose uptake', *Nature Medicine*, 21(1), pp. 55–61. Available at: https://doi.org/10.1038/nm.3758.

Manara, M. and Sinigaglia, L. (2015) 'Bone and TNF in rheumatoid arthritis: clinical implications', *RMD Open*, 1(Suppl 1), p. e000065. Available at: https://doi.org/10.1136/rmdopen-2015-000065.

Manel, N., Unutmaz, D. and Littman, D.R. (2008) 'The differentiation of human TH-17 cells requires transforming growth factor-β and induction of the nuclear receptor RORγT', *Nature immunology*, 9(6), pp. 641–649. Available at: https://doi.org/10.1038/ni.1610.

Manicourt, D.H., Poilvache, P., Van Egeren, A., Devogelaer, J.P., Lenz, M.E. and Thonar, E.J. (2000) 'Synovial fluid levels of tumor necrosis factor alpha and oncostatin M correlate with levels of markers of the degradation of crosslinked collagen and cartilage aggrecan in rheumatoid arthritis but not in osteoarthritis', *Arthritis and Rheumatism*, 43(2), pp. 281–288. Available at: https://doi.org/10.1002/1529-0131(200002)43:2<281::AID-ANR7>3.0.CO;2-7.

Marchingo, J.M., Sinclair, L.V., Howden, A.J. and Cantrell, D.A. (2020) 'Quantitative analysis of how Myc controls T cell proteomes and metabolic pathways during T cell activation', *eLife*. Edited by E.A. Robey, T. Taniguchi, E.A. Robey, and J.P. Roose, 9, p. e53725. Available at: https://doi.org/10.7554/eLife.53725.

Martinez, F.O. and Gordon, S. (2014) 'The M1 and M2 paradigm of macrophage activation: time for reassessment', *F1000Prime Reports*, 6, p. 13. Available at: https://doi.org/10.12703/P6-13.

Martínez-Reyes, I. and Chandel, N.S. (2020) 'Mitochondrial TCA cycle metabolites control physiology and disease', *Nature Communications*, 11(1), p. 102. Available at: https://doi.org/10.1038/s41467-019-13668-3.

Matsui, T., Shimada, K., Ozawa, N., Hayakawa, H., Hagiwara, F., Nakayama, H., Sugii, S., Ozawa, Y. and Tohma, S. (2006) 'Diagnostic utility of anti-cyclic citrullinated peptide antibodies for very early rheumatoid arthritis.', *The Journal of Rheumatology*, 33(12), pp. 2390–2397.

Mayer, K.A., Smole, U., Zhu, C., Derdak, S., Minervina, A.A., Salnikova, M., Witzeneder, N., Christamentl, A., Boucheron, N., Waidhofer-Söllner, P., Trauner, M., Hoermann, G., Schmetterer, K.G., Mamedov, I.Z., Bilban, M., Ellmeier, W., Pickl, W.F., Gualdoni, G.A. and Zlabinger, G.J. (2021) 'The energy sensor AMPK orchestrates metabolic and translational adaptation in expanding T helper cells', *The FASEB Journal*, 35(4), p. e21217. Available at: https://doi.org/10.1096/fj.202001763RR.

Medzhitov, R. (2008) 'Origin and physiological roles of inflammation', *Nature*, 454(7203), pp. 428–435. Available at: https://doi.org/10.1038/nature07201.

Mendoza, A., Fang, V., Chen, C., Serasinghe, M., Verma, A., Muller, J., Chaluvadi, V.S., Dustin, M.L., Hla, T., Elemento, O., Chipuk, J.E. and Schwab, S.R. (2017) 'Lymphatic endothelial S1P promotes naïve T cell mitochondrial function and survival', *Nature*, 546(7656), pp. 158–161. Available at: https://doi.org/10.1038/nature22352.

Mensink, M., Tran, T.N.M., Zaal, E.A., Schrama, E., Berkers, C.R., Borst, J. and de Kivit, S. (2022) 'TNFR2 Costimulation Differentially Impacts Regulatory and Conventional CD4+ T-Cell Metabolism', *Frontiers in Immunology*, 13. Available at: https://www.frontiersin.org/articles/10.3389/fimmu.2022.881166.

Michalek, R.D., Gerriets, V.A., Jacobs, S.R., Macintyre, A.N., MacIver, N.J., Mason, E.F., Sullivan, S.A., Nichols, A.G. and Rathmell, J.C. (2011) 'Cutting edge: distinct glycolytic and lipid oxidative metabolic programs are essential for effector and regulatory CD4+ T cell subsets', *Journal of Immunology (Baltimore, Md.: 1950)*, 186(6), pp. 3299–3303. Available at: https://doi.org/10.4049/jimmunol.1003613.

Micheau, O. and Tschopp, J. (2003) 'Induction of TNF receptor I-mediated apoptosis via two sequential signaling complexes', *Cell*, 114(2), pp. 181–190. Available at: https://doi.org/10.1016/s0092-8674(03)00521-x.

Millier, M.J., Fanning, N.C., Frampton, C., Stamp, L.K. and Hessian, P.A. (2022) 'Plasma interleukin-23 and circulating IL-17A+IFNγ+ ex-Th17 cells predict opposing outcomes of anti-TNF therapy in rheumatoid arthritis', *Arthritis Research & Therapy*, 24(1), p. 57. Available at: https://doi.org/10.1186/s13075-022-02748-3.

Mitoma, H., Horiuchi, T., Hatta, N., Tsukamoto, H., Harashima, S.-I., Kikuchi, Y., Otsuka, J., Okamura, S., Fujita, S. and Harada, M. (2005) 'Infliximab induces potent anti-inflammatory responses by outside-to-inside signals through transmembrane TNF-alpha', *Gastroenterology*, 128(2), pp. 376–392. Available at: https://doi.org/10.1053/j.gastro.2004.11.060.

Mittal, N., Mittal, R., Sharma, A., Jose, V., Wanchu, A. and Singh, S. (2012) 'Treatment failure with disease-modifying antirheumatic drugs in rheumatoid arthritis patients', *Singapore Medical Journal*, 53(8), pp. 532–536.

Miyara, M., Gorochov, G., Ehrenstein, M., Musset, L., Sakaguchi, S. and Amoura, Z. (2011) 'Human FoxP3+ regulatory T cells in systemic autoimmune diseases', *Autoimmunity Reviews*, 10(12), pp. 744–755. Available at: https://doi.org/10.1016/j.autrev.2011.05.004.

Moatti, A., Debesset, A., Pilon, C., Beldi-Ferchiou, A., Leclerc, M., Redjoul, R., Charlotte, F., To, N.H., Bak, A., Belkacemi, Y., Salomon, B.L., Issa, F., Michonneau, D., Maury, S., Cohen, J.L. and Thiolat, A. (2022) 'TNFR2 blockade of regulatory T cells unleashes an antitumor immune response after hematopoietic stem-cell transplantation', *Journal for ImmunoTherapy of Cancer*, 10(4), p. e003508. Available at: https://doi.org/10.1136/jitc-2021-003508.

Morinobu, A., Kanno, Y. and O'Shea, J.J. (2004) 'Discrete roles for histone acetylation in human T helper 1 cell-specific gene expression', *The Journal of Biological Chemistry*, 279(39), pp. 40640–40646. Available at: https://doi.org/10.1074/jbc.M407576200.

Mosmann, T.R., Cherwinski, H., Bond, M.W., Giedlin, M.A. and Coffman, R.L. (1986) 'Two types of murine helper T cell clone. I. Definition according to profiles of lymphokine activities and secreted proteins.', *The Journal of Immunology*, 136(7), pp. 2348–2357.

Möttönen, M., Heikkinen, J., Mustonen, L., Isomäki, P., Luukkainen, R. and Lassila, O. (2005) 'CD4+ CD25+ T cells with the phenotypic and functional characteristics of regulatory T cells are enriched in the synovial fluid of patients with rheumatoid arthritis', *Clinical and Experimental Immunology*, 140(2), pp. 360–367. Available at: https://doi.org/10.1111/j.1365-2249.2005.02754.x.

Mu, N., Gu, J., Huang, T., Zhang, C., Shu, Z., Li, M., Hao, Q., Li, W., Zhang, Wangqian, Zhao, J., Zhang, Yong, Huang, L., Wang, S., Jin, X., Xue, X., Zhang, Wei and Zhang, Yingqi (2016) 'A novel NF-κB/YY1/microRNA-10a regulatory circuit in fibroblast-like synoviocytes regulates inflammation in rheumatoid arthritis', *Scientific Reports*, 6(1), p. 20059. Available at: https://doi.org/10.1038/srep20059.

Munford, H. and Dimeloe, S. (2019) 'Intrinsic and Extrinsic Determinants of T Cell Metabolism in Health and Disease', *Frontiers in Molecular Biosciences*, 6, p. 118. Available at: https://doi.org/10.3389/fmolb.2019.00118.

Myers, D.R., Norlin, E., Vercoulen, Y. and Roose, J.P. (2019) 'Active Tonic mTORC1 Signals Shape Baseline Translation in Naive T Cells', *Cell reports*, 27(6), pp. 1858-1874.e6. Available at: https://doi.org/10.1016/j.celrep.2019.04.037.

Nagar, M., Jacob-Hirsch, J., Vernitsky, H., Berkun, Y., Ben-Horin, S., Amariglio, N., Bank, I., Kloog, Y., Rechavi, G. and Goldstein, I. (2010) 'TNF Activates a NF-κB–Regulated Cellular Program in Human CD45RA– Regulatory T Cells that Modulates Their Suppressive Function', *The Journal of Immunology*, 184(7), pp. 3570–3581. Available at: https://doi.org/10.4049/jimmunol.0902070.

Nakaya, M., Xiao, Y., Zhou, X., Chang, J.-H., Chang, M., Cheng, X., Blonska, M., Lin, X. and Sun, S.-C. (2014) 'Inflammatory T cell responses rely on amino acid transporter ASCT2 facilitation of glutamine uptake and mTORC1 kinase activation', *Immunity*, 40(5), pp. 692–705. Available at: https://doi.org/10.1016/j.immuni.2014.04.007.

Ndejembi, M.P., Teijaro, J.R., Patke, D.S., Bingaman, A.W., Chandok, M.R., Azimzadeh, A., Nadler, S.G. and Farber, D.L. (2006) 'Control of memory CD4 T cell recall by the CD28/B7 costimulatory pathway', *Journal of Immunology (Baltimore, Md.: 1950)*, 177(11), pp. 7698–7706. Available at: https://doi.org/10.4049/jimmunol.177.11.7698.

Neefjes, J., Jongsma, M.L.M., Paul, P. and Bakke, O. (2011) 'Towards a systems understanding of MHC class I and MHC class II antigen presentation', *Nature Reviews Immunology*, 11(12), pp. 823–836. Available at: https://doi.org/10.1038/nri3084.

Nemazee, D. (2017) ‘Mechanisms of central tolerance for B cells’, *Nature reviews. Immunology*, 17(5), pp. 281–294. Available at: https://doi.org/10.1038/nri.2017.19.

Németh, T., Nagy, G. and Pap, T. (2022) ‘Synovial fibroblasts as potential drug targets in rheumatoid arthritis, where do we stand and where shall we go?’, *Annals of the Rheumatic Diseases*, 81(8), pp. 1055–1064. Available at: https://doi.org/10.1136/annrheumdis-2021-222021.

Neumann, C., Heinrich, F., Neumann, K., Junghans, V., Mashreghi, M.-F., Ahlers, J., Janke, M., Rudolph, C., Mockel-Tenbrinck, N., Kühl, A.A., Heimesaat, M.M., Esser, C., Im, S.-H., Radbruch, A., Rutz, S. and Scheffold, A. (2014) ‘Role of Blimp-1 in programing Th effector cells into IL-10 producers’, *The Journal of Experimental Medicine*, 211(9), pp. 1807–1819. Available at: https://doi.org/10.1084/jem.20131548.

Newton, K. and Dixit, V.M. (2012) ‘Signaling in Innate Immunity and Inflammation’, *Cold Spring Harbor Perspectives in Biology*, 4(3). Available at: https://doi.org/10.1101/cshperspect.a006049.

Nguyen, D.X. and Ehrenstein, M.R. (2016) ‘Anti-TNF drives regulatory T cell expansion by paradoxically promoting membrane TNF–TNF-RII binding in rheumatoid arthritis’, *The Journal of Experimental Medicine*, 213(7), pp. 1241–1253. Available at: https://doi.org/10.1084/jem.20151255.

Nguyen, Q.P., Deng, T.Z., Witherden, D.A. and Goldrath, A.W. (2019) ‘Origins of CD4+ circulating and tissue-resident memory T-cells’, *Immunology*, 157(1), pp. 3–12. Available at: https://doi.org/10.1111/imm.13059.

Ni, C., Wu, P., Zhu, X., Ye, J., Zhang, Z., Chen, Z., Zhang, Ting, Zhang, Tao, Wang, K., Wu, D., Qiu, F. and Huang, J. (2013) ‘IFN-γ selectively exerts pro-apoptotic effects on tumor-initiating label-retaining colon cancer cells’, *Cancer Letters*, 336(1), pp. 174–184. Available at: https://doi.org/10.1016/j.canlet.2013.04.029.

Nicklin, P., Bergman, P., Zhang, B., Triantafellow, E., Wang, H., Nyfeler, B., Yang, H., Hild, M., Kung, C., Wilson, C., Myer, V.E., MacKeigan, J.P., Porter, J.A., Wang, Y.K., Cantley, L.C., Finan, P.M. and Murphy, L.O. (2009) ‘Bidirectional Transport of Amino Acids Regulates mTOR and Autophagy’, *Cell*, 136(3), pp. 521–534. Available at: https://doi.org/10.1016/j.cell.2008.11.044.

Nie, H., Zheng, Y., Li, R., Guo, T.B., He, D., Fang, L., Liu, X., Xiao, L., Chen, X., Wan, B., Chin, Y.E. and Zhang, J.Z. (2013) ‘Phosphorylation of FOXP3 controls regulatory T cell function and is inhibited by TNF-α in rheumatoid arthritis’, *Nature Medicine*, 19(3), pp. 322–328. Available at: https://doi.org/10.1038/nm.3085.

Niu, Q., Cai, B., Huang, Z., Shi, Y. and Wang, L. (2012) ‘Disturbed Th17/Treg balance in patients with rheumatoid arthritis’, *Rheumatology International*, 32(9), pp. 2731–2736. Available at: https://doi.org/10.1007/s00296-011-1984-x.

Noben-Trauth, N., Hu-Li, J. and Paul, W.E. (2002) 'IL-4 secreted from individual naive CD4+ T cells acts in an autocrine manner to induce Th2 differentiation', *European Journal of Immunology*, 32(5), pp. 1428–1433. Available at: https://doi.org/10.1002/1521-4141(200205)32:5<1428::AID-IMMU1428>3.0.CO;2-0.

Ohshima, Y., Yang, L.-P., Avice, M.-N., Kurimoto, M., Nakajima, T., Sergerie, M., Demeure, C.E., Sarfati, M. and Delespesse, G. (1999) 'Naive Human CD4+ T Cells Are a Major Source of Lymphotoxin α', *The Journal of Immunology*, 162(7), pp. 3790–3794. Available at: https://doi.org/10.4049/jimmunol.162.7.3790.

Oliveros, J.C. (2007) *Venny 2.1.0*. Available at: https://bioinfogp.cnb.csic.es/tools/venny/ (Accessed: 12 August 2022).

Ormseth, M.J., Oeser, A.M., Cunningham, A., Bian, A., Shintani, A., Solus, J., Tanner, S. and Stein, C.M. (2013) 'Peroxisome proliferator-activated receptor γ agonist effect on rheumatoid arthritis: a randomized controlled trial', *Arthritis Research & Therapy*, 15(5), p. R110. Available at: https://doi.org/10.1186/ar4290.

Ouyang, W. and Valdez, P. (2008) 'IL-22 in mucosal immunity', *Mucosal Immunology*, 1(5), pp. 335–338. Available at: https://doi.org/10.1038/mi.2008.26.

Pallai, A., Kiss, B., Vereb, G., Armaka, M., Kollias, G., Szekanecz, Z. and Szondy, Z. (2016) 'Transmembrane TNF-α Reverse Signaling Inhibits Lipopolysaccharide-Induced Proinflammatory Cytokine Formation in Macrophages by Inducing TGF-β: Therapeutic Implications', *Journal of Immunology (Baltimore, Md.: 1950)*, 196(3), pp. 1146–1157. Available at: https://doi.org/10.4049/jimmunol.1501573.

Paludan, S.R., Pradeu, T., Masters, S.L. and Mogensen, T.H. (2021) 'Constitutive immune mechanisms: mediators of host defence and immune regulation', *Nature Reviews Immunology*, 21(3), pp. 137–150. Available at: https://doi.org/10.1038/s41577-020-0391-5.

Pandya, J.M., Lundell, A.-C., Andersson, K., Nordström, I., Theander, E. and Rudin, A. (2017) 'Blood chemokine profile in untreated early rheumatoid arthritis: CXCL10 as a disease activity marker', *Arthritis Research & Therapy*, 19(1), p. 20. Available at: https://doi.org/10.1186/s13075-017-1224-1.

Pandya, J.M., Lundell, A.-C., Hallström, M., Andersson, K., Nordström, I. and Rudin, A. (2016) 'Circulating T helper and T regulatory subsets in untreated early rheumatoid arthritis and healthy control subjects', *Journal of Leukocyte Biology*, 100(4), pp. 823–833. Available at: https://doi.org/10.1189/jlb.5A0116-025R.

Park, H., Li, Z., Yang, X.O., Chang, S.H., Nurieva, R., Wang, Y.-H., Wang, Y., Hood, L., Zhu, Z., Tian, Q. and Dong, C. (2005) 'A distinct lineage of CD4 T cells regulates tissue inflammation by producing interleukin 17', *Nature Immunology*, 6(11), pp. 1133–1141. Available at: https://doi.org/10.1038/ni1261.

Patel, D.D., Zachariah, J.P. and Whichard, L.P. (2001) 'CXCR3 and CCR5 Ligands in Rheumatoid Arthritis Synovium', *Clinical Immunology*, 98(1), pp. 39–45. Available at: https://doi.org/10.1006/clim.2000.4957.

PDL BioPharma, Inc. (2008) *A Phase 2 Study to Evaluate the Safety, Tolerability, and Activity of Fontolizumab in Subjects With Active Rheumatoid Arthritis*. Clinical trial registration NCT00281294. clinicaltrials.gov. Available at: https://clinicaltrials.gov/ct2/show/NCT00281294.

Pearce, E.L. (2010) 'Metabolism in T cell activation and differentiation', *Current opinion in immunology*, 22(3), pp. 314–320. Available at: https://doi.org/10.1016/j.coi.2010.01.018.

Pelletier, M., Maggi, L., Micheletti, A., Lazzeri, E., Tamassia, N., Costantini, C., Cosmi, L., Lunardi, C., Annunziato, F., Romagnani, S. and Cassatella, M.A. (2010) 'Evidence for a cross-talk between human neutrophils and Th17 cells', *Blood*, 115(2), pp. 335–343. Available at: https://doi.org/10.1182/blood-2009-04-216085.

Penatti, A., Facciotti, F., De Matteis, R., Larghi, P., Paroni, M., Murgo, A., De Lucia, O., Pagani, M., Pierannunzii, L., Truzzi, M., Ioan-Facsinay, A., Abrignani, S., Geginat, J. and Meroni, P.L. (2017) 'Differences in serum and synovial CD4+ T cells and cytokine profiles to stratify patients with inflammatory osteoarthritis and rheumatoid arthritis', *Arthritis Research & Therapy*, 19(1), p. 103. Available at: https://doi.org/10.1186/s13075-017-1305-1.

Peng, M., Yin, N., Chhangawala, S., Xu, K., Leslie, C.S. and Li, M.O. (2016) 'Aerobic glycolysis promotes T helper 1 cell differentiation through an epigenetic mechanism', *Science (New York, N.Y.)*, 354(6311), pp. 481–484. Available at: https://doi.org/10.1126/science.aaf6284.

Perucha, E., Melchiotti, R., Bibby, J.A., Wu, W., Frederiksen, K.S., Roberts, C.A., Hall, Z., LeFriec, G., Robertson, K.A., Lavender, P., Gerwien, J.G., Taams, L.S., Griffin, J.L., de Rinaldis, E., van Baarsen, L.G.M., Kemper, C., Ghazal, P. and Cope, A.P. (2019) 'The cholesterol biosynthesis pathway regulates IL-10 expression in human Th1 cells', *Nature Communications*, 10(1), p. 498. Available at: https://doi.org/10.1038/s41467-019-08332-9.

Pesce, B., Ribeiro, C.H., Larrondo, M., Ramos, V., Soto, L., Catalán, D. and Aguillón, J.C. (2022) 'TNF-α Affects Signature Cytokines of Th1 and Th17 T Cell Subsets through Differential Actions on TNFR1 and TNFR2', *International Journal of Molecular Sciences*, 23(16), p. 9306. Available at: https://doi.org/10.3390/ijms23169306.

Pickens, S.R., Volin, M.V., Mandelin, A.M., II, Kolls, J.K., Pope, R.M. and Shahrara, S. (2010) 'IL-17 Contributes to Angiogenesis in Rheumatoid Arthritis', *The Journal of Immunology*, 184(6), pp. 3233–3241. Available at: https://doi.org/10.4049/jimmunol.0903271.

Ponchel, F., Burska, A.N., Hunt, L., Gul, H., Rabin, T., Parmar, R., Buch, M.H., Conaghan, P.G. and Emery, P. (2020) 'T-cell subset abnormalities predict progression along the Inflammatory Arthritis disease continuum: implications for management', *Scientific Reports*, 10(1), p. 3669. Available at: https://doi.org/10.1038/s41598-020-60314-w.

Povoleri, G.A.M., Lalnunhlimi, S., Steel, K.J.A., Agrawal, S., O'Byrne, A.M., Ridley, M., Kordasti, S., Frederiksen, K.S., Roberts, C.A. and Taams, L.S. (2020) 'Anti-TNF treatment negatively regulates human CD4+ T-cell activation and maturation in vitro, but does not confer an anergic or suppressive phenotype', *European Journal of Immunology*, 50(3), pp. 445–458. Available at: https://doi.org/10.1002/eji.201948190.

Preston, G.C., Sinclair, L.V., Kaskar, A., Hukelmann, J.L., Navarro, M.N., Ferrero, I., MacDonald, H.R., Cowling, V.H. and Cantrell, D.A. (2015) 'Single cell tuning of Myc expression by antigen receptor signal strength and interleukin-2 in T lymphocytes', *The EMBO Journal*, 34(15), pp. 2008–2024. Available at: https://doi.org/10.15252/embj.201490252.

Previte, D.M., O'Connor, E.C., Novak, E.A., Martins, C.P., Mollen, K.P. and Piganelli, J.D. (2017) 'Reactive oxygen species are required for driving efficient and sustained aerobic glycolysis during CD4+ T cell activation', *PLOS ONE*, 12(4), p. e0175549. Available at: https://doi.org/10.1371/journal.pone.0175549.

Priyadharshini, B., Loschi, M., Newton, R.H., Zhang, J.-W., Finn, K.K., Gerriets, V.A., Huynh, A., Rathmell, J.C., Blazar, B.R. and Turka, L.A. (2018) 'TGF-β and PI3K Signals Modulate Distinct Metabolism of Treg Subsets', *Journal of immunology (Baltimore, Md. : 1950)*, 201(8), pp. 2215–2219. Available at: https://doi.org/10.4049/jimmunol.1800311.

Priyadharshini, B., Welsh, R.M., Greiner, D.L., Gerstein, R.M. and Brehm, M.A. (2010) 'Maturation-dependent licensing of naive T cells for rapid TNF production', *PloS One*, 5(11), p. e15038. Available at: https://doi.org/10.1371/journal.pone.0015038.

Pucino, V., Certo, M., Bulusu, V., Cucchi, D., Goldmann, K., Pontarini, E., Haas, R., Smith, J., Headland, S.E., Blighe, K., Ruscica, M., Humby, F., Lewis, M.J., Kamphorst, J.J., Bombardieri, M., Pitzalis, C. and Mauro, C. (2019) 'Lactate Buildup at the Site of Chronic Inflammation Promotes Disease by Inducing CD4+ T Cell Metabolic Rewiring', *Cell Metabolism*, 30(6), pp. 1055-1074.e8. Available at: https://doi.org/10.1016/j.cmet.2019.10.004.

Quinn, W.J., Jiao, J., TeSlaa, T., Stadanlick, J., Wang, Z., Wang, L., Akimova, T., Angelin, A., Schäfer, P.M., Cully, M.D., Perry, C., Kopinski, P.K., Guo, L., Blair, I.A., Ghanem, L.R., Leibowitz, M.S., Hancock, W.W., Moon, E.K., Levine, M.H., Eruslanov, E.B., Wallace, D.C., Baur, J.A. and Beier, U.H. (2020) 'Lactate Limits T Cell Proliferation via the NAD(H) Redox State', *Cell reports*, 33(11), p. 108500. Available at: https://doi.org/10.1016/j.celrep.2020.108500.

Rajan, S., Ye, J., Bai, S., Huang, F. and Guo, Y.-L. (2008) 'NF-κB, but not p38 MAP Kinase, is required for TNF-α-induced expression of cell adhesion molecules in endothelial cells', *Journal of Cellular Biochemistry*, 105(2), pp. 477–486. Available at: https://doi.org/10.1002/jcb.21845.

Ramesh, R., Kozhaya, L., McKevitt, K., Djuretic, I.M., Carlson, T.J., Quintero, M.A., McCauley, J.L., Abreu, M.T., Unutmaz, D. and Sundrud, M.S. (2014) 'Pro-inflammatory human Th17 cells selectively express P-glycoprotein and are refractory to glucocorticoids', *The Journal of Experimental Medicine*, 211(1), pp. 89–104. Available at: https://doi.org/10.1084/jem.20130301.

Raskov, H., Orhan, A., Christensen, J.P. and Gögenur, I. (2021) 'Cytotoxic CD8+ T cells in cancer and cancer immunotherapy', *British Journal of Cancer*, 124(2), pp. 359–367. Available at: https://doi.org/10.1038/s41416-020-01048-4.

Rathmell, J.C., Elstrom, R.L., Cinalli, R.M. and Thompson, C.B. (2003) 'Activated Akt promotes increased resting T cell size, CD28-independent T cell growth, and development of autoimmunity and lymphoma', *European Journal of Immunology*, 33(8), pp. 2223–2232. Available at: https://doi.org/10.1002/eji.200324048.

Raud, B., McGuire, P.J., Jones, R.G., Sparwasser, T. and Berod, L. (2018) 'Fatty acid metabolism in CD8+ T cell memory: challenging current concepts', *Immunological reviews*, 283(1), pp. 213–231. Available at: https://doi.org/10.1111/imr.12655.

Ray, J.P., Staron, M.M., Shyer, J.A., Ho, P.-C., Marshall, H.D., Gray, S.M., Laidlaw, B.J., Araki, K., Ahmed, R., Kaech, S.M. and Craft, J. (2015) 'The Interleukin-2-mTORc1 Axis Defines the Reciprocal Signaling, Differentiation, and Metabolism of T Helper 1 and Follicular B Helper T Cells', *Immunity*, 43(4), pp. 690–702. Available at: https://doi.org/10.1016/j.immuni.2015.08.017.

Raza, K., Falciani, F., Curnow, S.J., Ross, E.J., Lee, C.-Y., Akbar, A.N., Lord, J.M., Gordon, C., Buckley, C.D. and Salmon, M. (2005) 'Early rheumatoid arthritis is characterized by a distinct and transient synovial fluid cytokine profile of T cell and stromal cell origin', *Arthritis Research & Therapy*, 7(4), pp. R784–R795. Available at: https://doi.org/10.1186/ar1733.

Renaude, E., Kroemer, M., Loyon, R., Binda, D., Borg, C., Guittaut, M., Hervouet, E. and Peixoto, P. (2020) 'The Fate of Th17 Cells is Shaped by Epigenetic Modifications and Remodeled by the Tumor Microenvironment', *International Journal of Molecular Sciences*, 21(5), p. 1673. Available at: https://doi.org/10.3390/ijms21051673.

Revu, S., Wu, J., Henkel, M., Rittenhouse, N., Menk, A., Delgoffe, G.M., Poholek, A.C. and McGeachy, M.J. (2018) 'IL-23 and IL-1β Drive Human Th17 Cell Differentiation and Metabolic Reprogramming in Absence of CD28 Costimulation', *Cell reports*, 22(10), pp. 2642–2653. Available at: https://doi.org/10.1016/j.celrep.2018.02.044.

Richer, M.J., Pewe, L.L., Hancox, L.S., Hartwig, S.M., Varga, S.M. and Harty, J.T. (2015) 'Inflammatory IL-15 is required for optimal memory T cell responses', *The Journal of Clinical Investigation*, 125(9), pp. 3477–3490. Available at: https://doi.org/10.1172/JCI81261.

Ripoll, J.G., Giraldo, N.A., Bolaños, N.I., Roa, N., Rosas, F., Cuéllar, A., Puerta, C.J. and González, J.M. (2018) 'T cells responding to Trypanosoma cruzi detected by membrane TNF-α and CD154 in chagasic patients', *Immunity, Inflammation and Disease*, 6(1), pp. 47–57. Available at: https://doi.org/10.1002/iid3.197.

Roberts, C.A., Durham, L.E., Fleskens, V., Evans, H.G. and Taams, L.S. (2017) 'TNF Blockade Maintains an IL-10+ Phenotype in Human Effector CD4+ and CD8+ T Cells', *Frontiers in Immunology*, 8. Available at: https://www.frontiersin.org/articles/10.3389/fimmu.2017.00157.

van Roon, J.A.G., Hartgring, S.A.Y., van der Wurff-Jacobs, K.M.G., Bijlsma, J.W.J. and Lafeber, F.P.J.G. (2010) 'Numbers of CD25+Foxp3+ T cells that lack the IL-7 receptor are increased intra-articularly and have impaired suppressive function in RA patients', *Rheumatology*, 49(11), pp. 2084–2089. Available at: https://doi.org/10.1093/rheumatology/keq237.

Ross, S.H. and Cantrell, D.A. (2018) 'Signaling and Function of Interleukin-2 in T Lymphocytes', *Annual review of immunology*, 36, pp. 411–433. Available at: https://doi.org/10.1146/annurev-immunol-042617-053352.

Rossol, M., Meusch, U., Pierer, M., Kaltenhäuser, S., Häntzschel, H., Hauschildt, S. and Wagner, U. (2007) 'Interaction between Transmembrane TNF and TNFR1/2 Mediates the Activation of Monocytes by Contact with T Cells1', *The Journal of Immunology*, 179(6), pp. 4239–4248. Available at: https://doi.org/10.4049/jimmunol.179.6.4239.

Rossol, M., Schubert, K., Meusch, U., Schulz, A., Biedermann, B., Grosche, J., Pierer, M., Scholz, R., Baerwald, C., Thiel, A., Hagen, S. and Wagner, U. (2013) 'Tumor Necrosis Factor Receptor Type I Expression of CD4+ T Cells in Rheumatoid Arthritis Enables Them to Follow Tumor Necrosis Factor Gradients Into the Rheumatoid Synovium', *Arthritis & Rheumatism*, 65(6), pp. 1468–1476. Available at: https://doi.org/10.1002/art.37927.

Rostamian, H., Fallah-Mehrjardi, K., Khakpoor-Koosheh, M., Pawelek, J.M., Hadjati, J., Brown, C.E. and Mirzaei, H.R. (2021) 'A metabolic switch to memory CAR T cells: Implications for cancer treatment', *Cancer Letters*, 500, pp. 107–118. Available at: https://doi.org/10.1016/j.canlet.2020.12.004.

Ruan, Q., Kameswaran, V., Zhang, Y., Zheng, S., Sun, J., Wang, J., DeVirgiliis, J., Liou, H.-C., Beg, A.A. and Chen, Y.H. (2011) 'The Th17 immune response is controlled by the Rel–RORγ–RORγT transcriptional axis', *The Journal of Experimental Medicine*, 208(11), pp. 2321–2333. Available at: https://doi.org/10.1084/jem.20110462.

Saad, M.I., Rose-John, S. and Jenkins, B.J. (2019) 'ADAM17: An Emerging Therapeutic Target for Lung Cancer', *Cancers*, 11(9), p. 1218. Available at: https://doi.org/10.3390/cancers11091218.

Sallusto, F., Lenig, D., Förster, R., Lipp, M. and Lanzavecchia, A. (1999) 'Two subsets of memory T lymphocytes with distinct homing potentials and effector functions', *Nature*, 401(6754), pp. 708–712. Available at: https://doi.org/10.1038/44385.

Salmond, R.J. (2018) 'mTOR Regulation of Glycolytic Metabolism in T Cells', *Frontiers in Cell and Developmental Biology*, 6, p. 122. Available at: https://doi.org/10.3389/fcell.2018.00122.

Salomon, B., Lenschow, D.J., Rhee, L., Ashourian, N., Singh, B., Sharpe, A. and Bluestone, J.A. (2000) 'B7/CD28 Costimulation Is Essential for the Homeostasis of the CD4+CD25+ Immunoregulatory T Cells that Control Autoimmune Diabetes', *Immunity*, 12(4), pp. 431–440. Available at: https://doi.org/10.1016/S1074-7613(00)80195-8.

Saraiva, M., Christensen, J.R., Veldhoen, M., Murphy, T.L., Murphy, K.M. and O'Garra, A. (2009) 'Interleukin-10 production by Th1 cells requires interleukin-12-induced STAT4 transcription factor and ERK MAP kinase activation by high antigen dose', *Immunity*, 31(2), pp. 209–219. Available at: https://doi.org/10.1016/j.immuni.2009.05.012.

Saxena, V., Li, L., Paluskievicz, C., Kasinath, V., Bean, A., Abdi, R., Jewell, C.M. and Bromberg, J.S. (2019) 'Role of Lymph Node Stroma and Microenvironment in T Cell Tolerance', *Immunological reviews*, 292(1), pp. 9–23. Available at: https://doi.org/10.1111/imr.12799.

Scally, S.W., Petersen, J., Law, S.C., Dudek, N.L., Nel, H.J., Loh, K.L., Wijeyewickrema, L.C., Eckle, S.B.G., van Heemst, J., Pike, R.N., McCluskey, J., Toes, R.E., La Gruta, N.L., Purcell, A.W., Reid, H.H., Thomas, R. and Rossjohn, J. (2013) 'A molecular basis for the association of the HLA-DRB1 locus, citrullination, and rheumatoid arthritis', *Journal of Experimental Medicine*, 210(12), pp. 2569–2582. Available at: https://doi.org/10.1084/jem.20131241.

Scharping, N.E., Rivadeneira, D.B., Menk, A.V., Vignali, P.D.A., Ford, B.R., Rittenhouse, N.L., Peralta, R., Wang, Yiyang, Wang, Yupeng, DePeaux, K., Poholek, A.C. and Delgoffe, G.M. (2021) 'Mitochondrial stress induced by continuous stimulation under hypoxia rapidly drives T cell exhaustion', *Nature Immunology*, 22(2), pp. 205–215. Available at: https://doi.org/10.1038/s41590-020-00834-9.

Schieke, S.M., Phillips, D., McCoy, J.P., Aponte, A.M., Shen, R.-F., Balaban, R.S. and Finkel, T. (2006) 'The Mammalian Target of Rapamycin (mTOR) Pathway Regulates Mitochondrial Oxygen Consumption and Oxidative Capacity*', *Journal of Biological Chemistry*, 281(37), pp. 27643–27652. Available at: https://doi.org/10.1074/jbc.M603536200.

Schmidt, A., Oberle, N. and Krammer, P.H. (2012) 'Molecular Mechanisms of Treg-Mediated T Cell Suppression', *Frontiers in Immunology*, 3, p. 51. Available at: https://doi.org/10.3389/fimmu.2012.00051.

Schmitt, E. and Williams, C. (2013) 'Generation and Function of Induced Regulatory T Cells', *Frontiers in Immunology*, 4. Available at: https://www.frontiersin.org/articles/10.3389/fimmu.2013.00152.

Schrezenmeier, E. and Dörner, T. (2020) 'Mechanisms of action of hydroxychloroquine and chloroquine: implications for rheumatology', *Nature Reviews. Rheumatology*, 16(3), pp. 155–166. Available at: https://doi.org/10.1038/s41584-020-0372-x.

Schuh, K., Twardzik, T., Kneitz, B., Heyer, J., Schimpl, A. and Serfling, E. (1998) 'The Interleukin 2 Receptor α Chain/CD25 Promoter Is a Target for Nuclear Factor of Activated T Cells', *Journal of Experimental Medicine*, 188(7), pp. 1369–1373. Available at: https://doi.org/10.1084/jem.188.7.1369.

Schulz, M., Dotzlaw, H. and Neeck, G. (2014) 'Ankylosing Spondylitis and Rheumatoid Arthritis: Serum Levels of TNF-alpha and Its Soluble Receptors during the Course of Therapy with Etanercept and Infliximab', *BioMed Research International*, 2014, p. e675108. Available at: https://doi.org/10.1155/2014/675108.

Schwindling, C., Quintana, A., Krause, E. and Hoth, M. (2010) 'Mitochondria positioning controls local calcium influx in T cells', *Journal of Immunology (Baltimore, Md.: 1950)*, 184(1), pp. 184–190. Available at: https://doi.org/10.4049/jimmunol.0902872.

Sckisel, G.D., Bouchlaka, M.N., Monjazeb, A.M., Crittenden, M., Curti, B.D., Wilkins, D.E.C., Alderson, K.A., Sungur, C.M., Ames, E., Mirsoian, A., Reddy, A., Alexander, W., Soulika, A., Blazar, B.R., Longo, D.L., Wiltrout, R.H. and Murphy, W.J. (2015) 'Out-of-Sequence Signal 3 Paralyzes Primary CD4+ T-Cell-Dependent Immunity', *Immunity*, 43(2), pp. 240–250. Available at: https://doi.org/10.1016/j.immuni.2015.06.023.

Sena, L.A., Li, S., Jairaman, A., Prakriya, M., Ezponda, T., Hildeman, D.A., Wang, C.-R., Schumacker, P.T., Licht, J.D., Perlman, H., Bryce, P.J. and Chandel, N.S. (2013) 'Mitochondria are required for antigen-specific T cell activation through reactive oxygen species signaling', *Immunity*, 38(2), pp. 225–236. Available at: https://doi.org/10.1016/j.immuni.2012.10.020.

Shao, L., Fujii, H., Colmegna, I., Oishi, H., Goronzy, J.J. and Weyand, C.M. (2009) 'Deficiency of the DNA repair enzyme ATM in rheumatoid arthritis', *The Journal of Experimental Medicine*, 206(6), pp. 1435–1449. Available at: https://doi.org/10.1084/jem.20082251.

Shen, H., Goodall, J.C. and Hill Gaston, J.S. (2009) 'Frequency and phenotype of peripheral blood Th17 cells in ankylosing spondylitis and rheumatoid arthritis', *Arthritis and Rheumatism*, 60(6), pp. 1647–1656. Available at: https://doi.org/10.1002/art.24568.

Shevyrev, D., Tereshchenko, V., Kozlov, V., Sizikov, A., Chumasova, O. and Koksharova, V. (2021) 'T-regulatory cells from patients with rheumatoid arthritis retain suppressor functions in vitro', *Experimental and Therapeutic Medicine*, 21(3), pp. 1–1. Available at: https://doi.org/10.3892/etm.2021.9641.

Shi, C. and Pamer, E.G. (2011) 'Monocyte recruitment during infection and inflammation', *Nature reviews. Immunology*, 11(11), pp. 762–774. Available at: https://doi.org/10.1038/nri3070.

Shi, H., Chapman, N.M., Wen, J., Guy, C., Long, L., Dhungana, Y., Rankin, S., Pelletier, S., Vogel, P., Wang, H., Peng, J., Guan, K.-L. and Chi, H. (2019) 'Amino Acids License Kinase mTORC1 Activity and Treg Cell Function via Small G Proteins Rag and Rheb', *Immunity*, 51(6), pp. 1012-1027.e7. Available at: https://doi.org/10.1016/j.immuni.2019.10.001.

Shi, J.-H. and Sun, S.-C. (2018) 'Tumor Necrosis Factor Receptor-Associated Factor Regulation of Nuclear Factor κB and Mitogen-Activated Protein Kinase Pathways', *Frontiers in Immunology*, 9. Available at: https://www.frontiersin.org/articles/10.3389/fimmu.2018.01849.

Shi, L.Z., Wang, R., Huang, G., Vogel, P., Neale, G., Green, D.R. and Chi, H. (2011) 'HIF1α–dependent glycolytic pathway orchestrates a metabolic checkpoint for the differentiation of TH17 and Treg cells', *The Journal of Experimental Medicine*, 208(7), pp. 1367–1376. Available at: https://doi.org/10.1084/jem.20110278.

Shibuya, H., Yoshitomi, H., Murata, K., Kobayashi, S., Furu, M., Ishikawa, M., Fujii, T., Ito, H. and Matsuda, S. (2015) 'TNFα, PDGF, and TGFβ synergistically induce synovial lining hyperplasia via inducible PI3Kδ', *Modern Rheumatology*, 25(1), pp. 72–78. Available at: https://doi.org/10.3109/14397595.2014.900847.

Shyer, J.A., Flavell, R.A. and Bailis, W. (2020) 'Metabolic signaling in T cells', *Cell Research*, 30(8), pp. 649–659. Available at: https://doi.org/10.1038/s41422-020-0379-5.

Sikorska, D., Rutkowski, R., Łuczak, J., Samborski, W. and Witowski, J. (2018) 'No effect of anti-TNF-α treatment on serum IL-17 in patients with rheumatoid arthritis', *Central-European Journal of Immunology*, 43(3), pp. 270–275. Available at: https://doi.org/10.5114/ceji.2018.80045.

Sinclair, L.V., Neyens, D., Ramsay, G., Taylor, P.M. and Cantrell, D.A. (2018) 'Single cell analysis of kynurenine and System L amino acid transport in T cells', *Nature Communications*, 9(1), p. 1981. Available at: https://doi.org/10.1038/s41467-018-04366-7.

Sinclair, L.V., Rolf, J., Emslie, E., Shi, Y.-B., Taylor, P.M. and Cantrell, D.A. (2013) 'Antigen receptor control of amino acid transport coordinates the metabolic re-programming that is essential for T cell differentiation', *Nature immunology*, 14(5), pp. 500–508. Available at: https://doi.org/10.1038/ni.2556.

Smeltz, R.B., Chen, J., Ehrhardt, R. and Shevach, E.M. (2002) 'Role of IFN-γ in Th1 Differentiation: IFN-γ Regulates IL-18Rα Expression by Preventing the Negative Effects of IL-4 and by Inducing/Maintaining IL-12 Receptor β2 Expression', *The Journal of Immunology*, 168(12), pp. 6165–6172. Available at: https://doi.org/10.4049/jimmunol.168.12.6165.

Snook, J.P., Kim, C. and Williams, M.A. (2018) 'TCR signal strength controls the differentiation of CD4+ effector and memory T cells', *Science immunology*, 3(25), p. eaas9103. Available at: https://doi.org/10.1126/sciimmunol.aas9103.

Soroosh, P., Ine, S., Sugamura, K. and Ishii, N. (2007) 'Differential requirements for OX40 signals on generation of effector and central memory CD4+ T cells', *Journal of Immunology (Baltimore, Md.: 1950)*, 179(8), pp. 5014–5023. Available at: https://doi.org/10.4049/jimmunol.179.8.5014.

Steyers, C.M. and Miller, F.J. (2014) 'Endothelial Dysfunction in Chronic Inflammatory Diseases', *International Journal of Molecular Sciences*, 15(7), pp. 11324–11349. Available at: https://doi.org/10.3390/ijms150711324.

Stritesky, G.L., Yeh, N. and Kaplan, M.H. (2008) 'IL-23 promotes maintenance but not commitment to the Th17 lineage', *Journal of immunology (Baltimore, Md. : 1950)*, 181(9), pp. 5948–5955.

Su, Z., Dhusia, K. and Wu, Y. (2022) 'Understanding the functional role of membrane confinements in TNF-mediated signaling by multiscale simulations', *Communications Biology*, 5(1), pp. 1–11. Available at: https://doi.org/10.1038/s42003-022-03179-1.

Sugita, S., Kawazoe, Y., Imai, A., Yamada, Y., Horie, S. and Mochizuki, M. (2012) 'Inhibition of Th17 differentiation by anti-TNF-alpha therapy in uveitis patients with Behçet's disease', *Arthritis Research & Therapy*, 14(3), p. R99. Available at: https://doi.org/10.1186/ar3824.

Sun, H., Gao, W., Pan, W., Zhang, Q., Wang, G., Feng, D., Geng, X., Yan, X. and Li, S. (2017) 'Tim3+Foxp3+ Treg Cells Are Potent Inhibitors of Effector T Cells and Are Suppressed in Rheumatoid Arthritis', *Inflammation*, 40(4), pp. 1342–1350. Available at: https://doi.org/10.1007/s10753-017-0577-6.

Surendar, J., Frohberger, S.J., Karunakaran, I., Schmitt, V., Stamminger, W., Neumann, A.-L., Wilhelm, C., Hoerauf, A. and Hübner, M.P. (2019) 'Adiponectin Limits IFN-γ and IL-17 Producing CD4 T Cells in Obesity by Restraining Cell Intrinsic Glycolysis', *Frontiers in Immunology*, 10, p. 2555. Available at: https://doi.org/10.3389/fimmu.2019.02555.

Suto, T., Tosevska, A., Dalwigk, K., Kugler, M., Dellinger, M., Stanic, I., Platzer, A., Niederreiter, B., Sevelda, F., Bonelli, M., Pap, T., Kiener, H., Okamura, K., Chikuda, H., Aletaha, D., Heinz, L.X. and Karonitsch, T. (2022) 'TNFR2 is critical for TNF-induced rheumatoid arthritis fibroblast-like synoviocyte inflammation', *Rheumatology (Oxford, England)*, 61(11), pp. 4535–4546. Available at: https://doi.org/10.1093/rheumatology/keac124.

Szabo, S.J., Kim, S.T., Costa, G.L., Zhang, X., Fathman, C.G. and Glimcher, L.H. (2000) 'A novel transcription factor, T-bet, directs Th1 lineage commitment', *Cell*, 100(6). Available at: https://doi.org/10.1016/s0092-8674(00)80702-3.

Szekanecz, Z., McInnes, I.B., Schett, G., Szamosi, S., Benkő, S. and Szűcs, G. (2021) 'Autoinflammation and autoimmunity across rheumatic and musculoskeletal diseases', *Nature Reviews Rheumatology*, 17(10), pp. 585–595. Available at: https://doi.org/10.1038/s41584-021-00652-9.

Taams, L.S. (2020) 'Interleukin-17 in rheumatoid arthritis: Trials and tribulations', *Journal of Experimental Medicine*, 217(3), p. e20192048. Available at: https://doi.org/10.1084/jem.20192048.

Tai, X., Cowan, M., Feigenbaum, L. and Singer, A. (2005) 'CD28 costimulation of developing thymocytes induces Foxp3 expression and regulatory T cell differentiation independently of interleukin 2', *Nature Immunology*, 6(2), pp. 152–162. Available at: https://doi.org/10.1038/ni1160.

Tai, Y., Wang, Q., Korner, H., Zhang, L. and Wei, W. (2018) 'Molecular Mechanisms of T Cells Activation by Dendritic Cells in Autoimmune Diseases', *Frontiers in Pharmacology*, 9. Available at: https://www.frontiersin.org/articles/10.3389/fphar.2018.00642.

Takaba, H. and Takayanagi, H. (2017) 'The Mechanisms of T Cell Selection in the Thymus', *Trends in Immunology*, 38(11), pp. 805–816. Available at: https://doi.org/10.1016/j.it.2017.07.010.

Takahashi, S., Saegusa, J., Sendo, S., Okano, T., Akashi, K., Irino, Y. and Morinobu, A. (2017) 'Glutaminase 1 plays a key role in the cell growth of fibroblast-like synoviocytes in rheumatoid arthritis', *Arthritis Research & Therapy*, 19(1), p. 76. Available at: https://doi.org/10.1186/s13075-017-1283-3.

Takeshita, M., Suzuki, K., Kondo, Y., Morita, R., Okuzono, Y., Koga, K., Kassai, Y., Gamo, K., Takiguchi, M., Kurisu, R., Mototani, H., Ebisuno, Y., Yoshimura, A. and Takeuchi, T. (2019) 'Multi-dimensional analysis identified rheumatoid arthritis-driving pathway in human T cell', *Annals of the Rheumatic Diseases*, 78(10), pp. 1346–1356. Available at: https://doi.org/10.1136/annrheumdis-2018-214885.

Takeuchi, T., Miyasaka, N., Tatsuki, Y., Yano, T., Yoshinari, T., Abe, T. and Koike, T. (2011) 'Baseline tumour necrosis factor alpha levels predict the necessity for dose escalation of infliximab therapy in patients with rheumatoid arthritis', *Annals of the Rheumatic Diseases*, 70(7), pp. 1208–1215. Available at: https://doi.org/10.1136/ard.2011.153023.

Takiishi, T., Fenero, C.I.M. and Câmara, N.O.S. (2017) 'Intestinal barrier and gut microbiota: Shaping our immune responses throughout life', *Tissue Barriers*, 5(4), p. e1373208. Available at: https://doi.org/10.1080/21688370.2017.1373208.

Tamir, A., Granot, Y. and Isakov, N. (1996) 'Inhibition of T lymphocyte activation by cAMP is associated with down-regulation of two parallel mitogen-activated protein kinase pathways, the extracellular signal-related kinase and c-Jun N-terminal kinase', *Journal of Immunology*, 157(4), pp. 1514–1522.

Tang, C.-Y. and Mauro, C. (2017) 'Similarities in the Metabolic Reprogramming of Immune System and Endothelium', *Frontiers in Immunology*, 8. Available at: https://www.frontiersin.org/articles/10.3389/fimmu.2017.00837.

Tanida, S., Yoshitomi, H., Nishitani, K., Ishikawa, M., Kitaori, T., Ito, H. and Nakamura, T. (2009) 'CCL20 produced in the cytokine network of rheumatoid arthritis recruits CCR6+ mononuclear cells and enhances the production of IL-6', *Cytokine*, 47(2), pp. 112–118. Available at: https://doi.org/10.1016/j.cyto.2009.05.009.

Tanimine, N., Germana, S.K., Fan, M., Hippen, K., Blazar, B.R., Markmann, J.F., Turka, L.A. and Priyadharshini, B. (2019) 'Differential effects of 2-deoxy-D-glucose on in vitro expanded human regulatory T cell subsets', *PLoS ONE*, 14(6), p. e0217761. Available at: https://doi.org/10.1371/journal.pone.0217761.

Tartaglia, L.A., Goeddel, D.V., Reynolds, C., Figari, I.S., Weber, R.F., Fendly, B.M. and Palladino, M.A. (1993) 'Stimulation of human T-cell proliferation by specific activation of the 75-kDa tumor necrosis factor receptor.', *The Journal of Immunology*, 151(9), pp. 4637–4641.

Tartaglia, L.A., Weber, R.F., Figari, I.S., Reynolds, C., Palladino, M.A. and Goeddel, D.V. (1991) 'The two different receptors for tumor necrosis factor mediate distinct cellular responses.', *Proceedings of the National Academy of Sciences*, 88(20), pp. 9292–9296. Available at: https://doi.org/10.1073/pnas.88.20.9292.

Tetta, C., Camussi, G., Modena, V., Di Vittorio, C. and Baglioni, C. (1990) 'Tumour necrosis factor in serum and synovial fluid of patients with active and severe rheumatoid arthritis.', *Annals of the Rheumatic Diseases*, 49(9), pp. 665–667.

Thilagar, S., Theyagarajan, R., Sudhakar, U., Suresh, S., Saketharaman, P. and Ahamed, N. (2018) 'Comparison of serum tumor necrosis factor-α levels in rheumatoid arthritis individuals with and without chronic periodontitis: A biochemical study', *Journal of Indian Society of Periodontology*, 22(2), pp. 116–121. Available at: https://doi.org/10.4103/jisp.jisp_362_17.

Tian, Y., Babor, M., Lane, J., Schulten, V., Patil, V.S., Seumois, G., Rosales, S.L., Fu, Z., Picarda, G., Burel, J., Zapardiel-Gonzalo, J., Tennekoon, R.N., De Silva, A.D., Premawansa, S., Premawansa, G., Wijewickrama, A., Greenbaum, J.A., Vijayanand, P., Weiskopf, D., Sette, A. and Peters, B. (2017) 'Unique phenotypes and clonal expansions of human CD4 effector memory T cells re-expressing CD45RA', *Nature Communications*, 8(1), p. 1473. Available at: https://doi.org/10.1038/s41467-017-01728-5.

Tokura, Y., Phadungsaksawasdi, P. and Ito, T. (2018) 'Atopic dermatitis as Th2 disease revisited', *Journal of Cutaneous Immunology and Allergy*, 1(5), pp. 158–164. Available at: https://doi.org/10.1002/cia2.12033.

Trebak, M. and Kinet, J.-P. (2019) 'Calcium signalling in T cells', *Nature Reviews Immunology*, 19(3), pp. 154–169. Available at: https://doi.org/10.1038/s41577-018-0110-7.

Trefzer, A., Kadam, P., Wang, S.-H., Pennavaria, S., Lober, B., Akçabozan, B., Kranich, J., Brocker, T., Nakano, N., Irmler, M., Beckers, J., Straub, T. and Obst, R. (2021) 'Dynamic adoption of anergy by antigen-exhausted CD4+ T cells', *Cell Reports*, 34(6), p. 108748. Available at: https://doi.org/10.1016/j.celrep.2021.108748.

Tseng, W.-Y., Huang, Y.-S., Clanchy, F., McNamee, K., Perocheau, D., Ogbechi, J., Luo, S.-F., Feldmann, M., McCann, F.E. and Williams, R.O. (2019) 'TNF receptor 2 signaling prevents DNA methylation at the Foxp3 promoter and prevents pathogenic conversion of regulatory T

cells', *Proceedings of the National Academy of Sciences*, 116(43), pp. 21666–21672. Available at: https://doi.org/10.1073/pnas.1909687116.

Ueda, Y., Saegusa, J., Okano, T., Sendo, S., Yamada, H., Nishimura, K. and Morinobu, A. (2019) 'Additive effects of inhibiting both mTOR and glutamine metabolism on the arthritis in SKG mice', *Scientific Reports*, 9, p. 6374. Available at: https://doi.org/10.1038/s41598-019-42932-1.

Ueno, A., Yamamura, M., Iwahashi, M., Okamoto, A., Aita, T., Ogawa, N. and Makino, H. (2005) 'The production of CXCR3-agonistic chemokines by synovial fibroblasts from patients with rheumatoid arthritis', *Rheumatology International*, 25(5), pp. 361–367. Available at: https://doi.org/10.1007/s00296-004-0449-x.

Valencia, X., Stephens, G., Goldbach-Mansky, R., Wilson, M., Shevach, E.M. and Lipsky, P.E. (2006) 'TNF downmodulates the function of human CD4+CD25hi T-regulatory cells', *Blood*, 108(1), pp. 253–261. Available at: https://doi.org/10.1182/blood-2005-11-4567.

Vander Heiden, M.G., Cantley, L.C. and Thompson, C.B. (2009) 'Understanding the Warburg Effect: The Metabolic Requirements of Cell Proliferation', *Science (New York, N.Y.)*, 324(5930), pp. 1029–1033. Available at: https://doi.org/10.1126/science.1160809.

Volpe, E., Servant, N., Zollinger, R., Bogiatzi, S.I., Hupé, P., Barillot, E. and Soumelis, V. (2008) 'A critical function for transforming growth factor-β, interleukin 23 and proinflammatory cytokines in driving and modulating human TH-17 responses', *Nature Immunology*, 9(6), pp. 650–657. Available at: https://doi.org/10.1038/ni.1613.

Wajant, H. and Siegmund, D. (2019) 'TNFR1 and TNFR2 in the Control of the Life and Death Balance of Macrophages', *Frontiers in Cell and Developmental Biology*, 7. Available at: https://www.frontiersin.org/articles/10.3389/fcell.2019.00091.

Wang, F., Zhang, S., Jeon, R., Vuckovic, I., Jiang, X., Lerman, A., Folmes, C.D., Dzeja, P.D. and Herrmann, J. (2018) 'Interferon Gamma Induces Reversible Metabolic Reprogramming of M1 Macrophages to Sustain Cell Viability and Pro-Inflammatory Activity', *EBioMedicine*, 30, pp. 303–316. Available at: https://doi.org/10.1016/j.ebiom.2018.02.009.

Wang, R., Dillon, C.P., Shi, L.Z., Milasta, S., Carter, R., Finkelstein, D., McCormick, L.L., Fitzgerald, P., Chi, H., Munger, J. and Green, D.R. (2011) 'The Transcription Factor Myc Controls Metabolic Reprogramming upon T Lymphocyte Activation', *Immunity*, 35(6), pp. 871–882. Available at: https://doi.org/10.1016/j.immuni.2011.09.021.

Wang, T., Sun, X., Zhao, J., Zhang, J., Zhu, H., Li, C., Gao, N., Jia, Y., Xu, D., Huang, F.-P., Li, N., Lu, L. and Li, Z.-G. (2015) 'Regulatory T cells in rheumatoid arthritis showed increased plasticity toward Th17 but retained suppressive function in peripheral blood', *Annals of the Rheumatic Diseases*, 74(6), pp. 1293–1301. Available at: https://doi.org/10.1136/annrheumdis-2013-204228.

Wang, W., Shao, S., Jiao, Z., Guo, M., Xu, H. and Wang, S. (2012) 'The Th17/Treg imbalance and cytokine environment in peripheral blood of patients with rheumatoid arthritis', *Rheumatology International*, 32(4), pp. 887–893. Available at: https://doi.org/10.1007/s00296-010-1710-0.

Warnes, G.R., Bolker, B., Bonebakker, L., Gentleman, R., Huber, W., Liaw, A., Lumley, T., Maechler, M., Magnusson, A., Moeller, S., Schwartz, M., Venables, B. and Galili, T. (2015) 'gplots: Various R Programming Tools for Plotting Data'. (R package version 3.1.1) [Computer programme]. Available at: https://CRAN.R-project.org/package=gplots.

Watson, M.J., Vignali, P.D.A., Mullett, S.J., Overacre-Delgoffe, A.E., Peralta, R.M., Grebinoski, S., Menk, A.V., Rittenhouse, N.L., DePeaux, K., Whetstone, R.D., Vignali, D.A.A., Hand, T.W., Poholek, A.C., Morrison, B.M., Rothstein, J.D., Wendell, S.G. and Delgoffe, G.M. (2021) 'Metabolic support of tumor-infiltrating regulatory T cells by lactic acid', *Nature*, 591(7851), pp. 645–651. Available at: https://doi.org/10.1038/s41586-020-03045-2.

Weiskopf, D., Bangs, D.J., Sidney, J., Kolla, R.V., De Silva, A.D., de Silva, A.M., Crotty, S., Peters, B. and Sette, A. (2015) 'Dengue virus infection elicits highly polarized CX3CR1+ cytotoxic CD4+ T cells associated with protective immunity', *Proceedings of the National Academy of Sciences*, 112(31), pp. E4256–E4263. Available at: https://doi.org/10.1073/pnas.1505956112.

Wen, H.-Y., Wang, J., Zhang, S.-X., Luo, J., Zhao, X.-C., Zhang, C., Wang, C.-H., Hu, F.-Y., Zheng, X.-J., Cheng, T., Niu, H.-Q., Liu, G.-Y., Yang, W.-X., Yu, N.-N., Ru, J.-L., Chen, Q.-X., Lu, X.-C., He, P.-F., Gao, C. and Li, X.-F. (2019) 'Low-Dose Sirolimus Immunoregulation Therapy in Patients with Active Rheumatoid Arthritis: A 24-Week Follow-Up of the Randomized, Open-Label, Parallel-Controlled Trial', *Journal of Immunology Research*, 2019, p. 7684352. Available at: https://doi.org/10.1155/2019/7684352.

Wen, Z., Jin, K., Shen, Y., Yang, Z., Li, Y., Wu, B., Tian, L., Shoor, S., Roche, N.E., Goronzy, J.J. and Weyand, C.M. (2019) 'N-myristoyltransferase deficiency impairs AMPK activation and promotes synovial tissue inflammation', *Nature immunology*, 20(3), pp. 313–325. Available at: https://doi.org/10.1038/s41590-018-0296-7.

Weyand, C.M. and Goronzy, J.J. (2021) 'The Immunology of Rheumatoid Arthritis', *Nature immunology*, 22(1), pp. 10–18. Available at: https://doi.org/10.1038/s41590-020-00816-x.

Weyand, C.M., Yang, Z. and Goronzy, J.J. (2014) 'T Cell Aging in Rheumatoid Arthritis', *Current opinion in rheumatology*, 26(1), pp. 93–100. Available at: https://doi.org/10.1097/BOR.0000000000000011.

Wickham, H., Chang, W., Henry, L., Pedersen, T.L., Takahashi, K., Wilke, C., Woo, K., Yutani, H. and Dunnington, D. (2016) 'ggplot2: Create Elegant Data Visualisations Using the Grammar of Graphics'. (R package version 3.3.5) [Computer programme]. Available at: https://CRAN.R-project.org/package=ggplot2.

Wieczorek, M., Abualrous, E.T., Sticht, J., Álvaro-Benito, M., Stolzenberg, S., Noé, F. and Freund, C. (2017) 'Major Histocompatibility Complex (MHC) Class I and MHC Class II Proteins: Conformational Plasticity in Antigen Presentation', *Frontiers in Immunology*, 8. Available at: https://www.frontiersin.org/articles/10.3389/fimmu.2017.00292.

van der Windt, G.J.W., Everts, B., Chang, C.-H., Curtis, J.D., Freitas, T.C., Amiel, E., Pearce, E.J. and Pearce, E.L. (2012) 'Mitochondrial respiratory capacity is a critical regulator of CD8+ T cell memory development', *Immunity*, 36(1), pp. 68–78. Available at: https://doi.org/10.1016/j.immuni.2011.12.007.

Wofford, J.A., Wieman, H.L., Jacobs, S.R., Zhao, Y. and Rathmell, J.C. (2008) 'IL-7 promotes Glut1 trafficking and glucose uptake via STAT5-mediated activation of Akt to support T-cell survival', *Blood*, 111(4), pp. 2101–2111. Available at: https://doi.org/10.1182/blood-2007-06-096297.

Wolfson, R.L., Chantranupong, L., Saxton, R.A., Shen, K., Scaria, S.M., Cantor, J.R. and Sabatini, D.M. (2016) 'Sestrin2 is a leucine sensor for the mTORC1 pathway', *Science*, 351(6268), pp. 43–48. Available at: https://doi.org/10.1126/science.aab2674.

Wu, B., Qiu, J., Zhao, T.V., Wang, Y., Maeda, T., Goronzy, I.N., Akiyama, M., Ohtsuki, S., Jin, K., Tian, L., Goronzy, J.J. and Weyand, C.M. (2020) 'Succinyl-CoA Ligase Deficiency in Pro-inflammatory and Tissue-Invasive T Cells', *Cell Metabolism*, 32(6), pp. 967-980.e5. Available at: https://doi.org/10.1016/j.cmet.2020.10.025.

Wu, B., Zhao, T.V., Jin, K., Hu, Z., Abdel, M.P., Warrington, K.J., Goronzy, J.J. and Weyand, C.M. (2021) 'Mitochondrial aspartate regulates TNF biogenesis and autoimmune tissue inflammation', *Nature Immunology*, 22(12), pp. 1551–1562. Available at: https://doi.org/10.1038/s41590-021-01065-2.

Xia, F., Qian, C.-R., Xun, Z., Hamon, Y., Sartre, A.-M., Formisano, A., Mailfert, S., Phelipot, M.-C., Billaudeau, C., Jaeger, S., Nunès, J.A., Guo, X.-J. and He, H.-T. (2018) 'TCR and CD28 Concomitant Stimulation Elicits a Distinctive Calcium Response in Naive T Cells', *Frontiers in Immunology*, 9. Available at: https://www.frontiersin.org/articles/10.3389/fimmu.2018.02864.

Xin, L., Wang, J., Zhang, H., Shi, W., Yu, M., Li, Q., Jiang, X., Gong, F., Gardner, K., Li, Q.Q. and Li, Z. (2006) 'Dual regulation of soluble tumor necrosis factor-alpha induced activation of human monocytic cells via modulating transmembrane TNF-alpha-mediated "reverse signaling"', *International Journal of Molecular Medicine*, 18(5), pp. 885–892.

Yago, T., Nanke, Y., Ichikawa, N., Kobashigawa, T., Mogi, M., Kamatani, N. and Kotake, S. (2009) 'IL-17 induces osteoclastogenesis from human monocytes alone in the absence of osteoblasts, which is potently inhibited by anti-TNF-alpha antibody: a novel mechanism of osteoclastogenesis by IL-17', *Journal of Cellular Biochemistry*, 108(4), pp. 947–955. Available at: https://doi.org/10.1002/jcb.22326.

Yang, K., Shrestha, S., Zeng, H., Karmaus, P.W.F., Neale, G., Vogel, P., Guertin, D.A., Lamb, R.F. and Chi, H. (2013) 'T cell exit from quiescence and differentiation into Th2 cells depend on Raptor-mTORC1-mediated metabolic programming', *Immunity*, 39(6), pp. 1043–1056. Available at: https://doi.org/10.1016/j.immuni.2013.09.015.

Yang, P., Qian, F.-Y., Zhang, M.-F., Xu, A.-L., Wang, X., Jiang, B.-P. and Zhou, L.-L. (2019) 'Th17 cell pathogenicity and plasticity in rheumatoid arthritis', *Journal of Leukocyte Biology*, 106(6), pp. 1233–1240. Available at: https://doi.org/10.1002/JLB.4RU0619-197R.

Yang, S., Liu, F., Wang, Q.J., Rosenberg, S.A. and Morgan, R.A. (2011) 'The Shedding of CD62L (L-Selectin) Regulates the Acquisition of Lytic Activity in Human Tumor Reactive T Lymphocytes', *PLoS ONE*, 6(7), p. e22560. Available at: https://doi.org/10.1371/journal.pone.0022560.

Yang, S., Wang, J., Brand, D.D. and Zheng, S.G. (2018) 'Role of TNF–TNF Receptor 2 Signal in Regulatory T Cells and Its Therapeutic Implications', *Frontiers in Immunology*, 9. Available at: https://www.frontiersin.org/articles/10.3389/fimmu.2018.00784.

Yang, S., Xie, C., Chen, Y., Wang, J., Chen, X., Lu, Z., June, R.R. and Zheng, S.G. (2019) 'Differential roles of TNFα-TNFR1 and TNFα-TNFR2 in the differentiation and function of CD4+Foxp3+ induced Treg cells in vitro and in vivo periphery in autoimmune diseases', *Cell Death & Disease*, 10(1), pp. 1–13. Available at: https://doi.org/10.1038/s41419-018-1266-6.

Yang, X.Y., Zheng, K.D., Lin, K., Zheng, G., Zou, H., Wang, J.M., Lin, Y.Y., Chuka, C.M., Ge, R.S., Zhai, W. and Wang, J.G. (2015) 'Energy Metabolism Disorder as a Contributing Factor of Rheumatoid Arthritis: A Comparative Proteomic and Metabolomic Study', *PLOS ONE*, 10(7), p. e0132695. Available at: https://doi.org/10.1371/journal.pone.0132695.

Yang, Z., Fujii, H., Mohan, S.V., Goronzy, J.J. and Weyand, C.M. (2013) 'Phosphofructokinase deficiency impairs ATP generation, autophagy, and redox balance in rheumatoid arthritis T cells', *The Journal of Experimental Medicine*, 210(10), pp. 2119–2134. Available at: https://doi.org/10.1084/jem.20130252.

Yang, Z., Shen, Y., Oishi, H., Matteson, E.L., Tian, L., Goronzy, J.J. and Weyand, C.M. (2016) 'Restoring oxidant signaling suppresses pro-arthritogenic T-cell effector functions in rheumatoid arthritis', *Science translational medicine*, 8(331), p. 331ra38. Available at: https://doi.org/10.1126/scitranslmed.aad7151.

Yao, Y., Xu, X.-H. and Jin, L. (2019) 'Macrophage Polarization in Physiological and Pathological Pregnancy', *Frontiers in Immunology*, 10. Available at: https://www.frontiersin.org/articles/10.3389/fimmu.2019.00792.

Yap, H.-Y., Tee, S.Z.-Y., Wong, M.M.-T., Chow, S.-K., Peh, S.-C. and Teow, S.-Y. (2018) 'Pathogenic Role of Immune Cells in Rheumatoid Arthritis: Implications in Clinical Treatment and Biomarker Development', *Cells*, 7(10), p. 161. Available at: https://doi.org/10.3390/cells7100161.

Yarilina, A., Xu, K., Chen, J. and Ivashkiv, L.B. (2011) 'TNF activates calcium-nuclear factor of activated T cells (NFAT)c1 signaling pathways in human macrophages', *Proceedings of the National Academy of Sciences of the United States of America*, 108(4), pp. 1573–1578. Available at: https://doi.org/10.1073/pnas.1010030108.

Yarosz, E.L. and Chang, C.-H. (2018) 'The Role of Reactive Oxygen Species in Regulating T Cell-mediated Immunity and Disease', *Immune Network*, 18(1), p. e14. Available at: https://doi.org/10.4110/in.2018.18.e14.

Yokota, S., Geppert, T.D. and Lipsky, P.E. (1988) 'Enhancement of antigen- and mitogen-induced human T lymphocyte proliferation by tumor necrosis factor-alpha.', *The Journal of Immunology*, 140(2), pp. 531–536.

Young, K.E., Flaherty, S., Woodman, K.M., Sharma-Walia, N. and Reynolds, J.M. (2017) 'Fatty acid synthase regulates the pathogenicity of Th17 cells', *Journal of Leukocyte Biology*, 102(5), pp. 1229–1235. Available at: https://doi.org/10.1189/jlb.3AB0417-159RR.

Yu, F.-Y., Xie, C.-Q., Jiang, C.-L., Sun, J.-T. and Huang, X.-W. (2018) 'TNF-α increases inflammatory factor expression in synovial fibroblasts through the toll-like receptor-3-mediated ERK/AKT signaling pathway in a mouse model of rheumatoid arthritis', *Molecular Medicine Reports*, 17(6), pp. 8475–8483. Available at: https://doi.org/10.3892/mmr.2018.8897.

Yu, G., Wang, L.-G., Han, Y. and He, Q.-Y. (2012) 'clusterProfiler: an R package for comparing biological themes among gene clusters', *Omics: A Journal of Integrative Biology*, 16(5), pp. 284–287. Available at: https://doi.org/10.1089/omi.2011.0118.

Yu, X., Wang, M. and Cao, Z. (2020) 'Reduced CD4+T Cell CXCR3 Expression in Patients With Allergic Rhinitis', *Frontiers in Immunology*, 11. Available at: https://www.frontiersin.org/articles/10.3389/fimmu.2020.581180.

Zanin-Zhorov, A., Ding, Y., Kumari, S., Attur, M., Hippen, K.L., Brown, M., Blazar, B.R., Abramson, S.B., Lafaille, J.J. and Dustin, M.L. (2010) 'Protein Kinase C-θ Mediates Negative Feedback on Regulatory T Cell Function', *Science*, 328(5976), pp. 372–376. Available at: https://doi.org/10.1126/science.1186068.

Zaragoza, B., Chen, X., Oppenheim, J.J., Baeyens, A., Gregoire, S., Chader, D., Gorochov, G., Miyara, M. and Salomon, B.L. (2016) 'Suppressive activity of human regulatory T cells is maintained in the presence of TNF', *Nature Medicine*, 22(1), pp. 16–17. Available at: https://doi.org/10.1038/nm.4019.

Zhang, H. and Xiao, W. (2017) 'TNFR1 and TNFR2 differentially mediate TNF-α-induced inflammatory responses in rheumatoid arthritis fibroblast-like synoviocytes', *Cell Biology International*, 41(4), pp. 415–422. Available at: https://doi.org/10.1002/cbin.10735.

Zhang, Q., Cui, F., Fang, L., Hong, J., Zheng, B. and Zhang, J.Z. (2013) 'TNF-α impairs differentiation and function of TGF-β-induced Treg cells in autoimmune diseases through Akt and Smad3 signaling pathway', *Journal of Molecular Cell Biology*, 5(2), pp. 85–98. Available at: https://doi.org/10.1093/jmcb/mjs063.

Zhang, R., Miao, J., Zhang, K., Zhang, B., Luo, X., Sun, H., Zheng, Z. and Zhu, P. (2022) 'Th1-Like Treg Cells Are Increased But Deficient in Function in Rheumatoid Arthritis', *Frontiers in Immunology*, 13, p. 863753. Available at: https://doi.org/10.3389/fimmu.2022.863753.

Zhong, X., Lee, H.-N. and Surh, Y.-J. (2018) 'RvD1 inhibits TNFα-induced c-Myc expression in normal intestinal epithelial cells and destabilizes hyper-expressed c-Myc in colon cancer cells', *Biochemical and Biophysical Research Communications*, 496(2), pp. 316–323. Available at: https://doi.org/10.1016/j.bbrc.2017.12.171.

Zhu, J., Min, B., Hu-Li, J., Watson, C.J., Grinberg, A., Wang, Q., Killeen, N., Urban, J.F., Guo, L. and Paul, W.E. (2004) 'Conditional deletion of Gata3 shows its essential function in TH1-TH2 responses', *Nature Immunology*, 5(11), pp. 1157–1165. Available at: https://doi.org/10.1038/ni1128.

Zhu, J. and Paul, W.E. (2010) 'Heterogeneity and plasticity of T helper cells', *Cell research*, 20(1), pp. 4–12. Available at: https://doi.org/10.1038/cr.2009.138.

Zizzo, G., De Santis, M., Bosello, S.L., Fedele, A.L., Peluso, G., Gremese, E., Tolusso, B. and Ferraccioli, G. (2011) 'Synovial fluid-derived T helper 17 cells correlate with inflammatory activity in arthritis, irrespectively of diagnosis', *Clinical Immunology*, 138(1), pp. 107–116. Available at: https://doi.org/10.1016/j.clim.2010.10.002.

Zuo, J., Tang, J., Lu, M., Zhou, Z., Li, Y., Tian, H., Liu, E., Gao, B., Liu, T. and Shao, P. (2021) 'Glycolysis Rate-Limiting Enzymes: Novel Potential Regulators of Rheumatoid Arthritis Pathogenesis', *Frontiers in Immunology*, 12. Available at: https://www.frontiersin.org/articles/10.3389/fimmu.2021.779787.

Zygmunt, B.M., Węgrzyn, A., Gajska, W., Yevsa, T., Chodaczek, G. and Guzmán, C.A. (2018) 'Mannose Metabolism Is Essential for Th1 Cell Differentiation and IFN-γ Production', *The Journal of Immunology*, 201(5), pp. 1400–1411. Available at: https://doi.org/10.4049/jimmunol.1700042.